A Study of the properties of

Click evoked otoacoustic emissions and ~~the~~ development of a clinical otoacoustic hearing test instrument.

A thesis submitted for the degree of

Doctor of Philosophy

of the

University of London.

Peter John Bray

Institute of Laryngology and Otology,

University College and Middlesex School of Medicine,

London.

June 1989.

Abstract.

The study of otoacoustic emissions (OAE) from the human ear is introduced with special reference to their clinical applicability. The need for a new instrument is demonstrated, which is capable of measuring click evoked OAEs in the clinical environment. Preparatory to the specification and construction of such an instrument, a thorough examination of the transient acoustic response of the ear canal, and the physical properties of the OAE was undertaken. An outcome of this research was the development of a technique which efficiently extracts the cochlear response component from that of the ear canal and middle ear. Various implementations of possible clinical OAE test systems were developed using a minicomputer prototype OAE instrument.

A dedicated clinical OAE measurement instrument was designed and constructed to implement the findings of the above. This comprised 2 digital circuit boards and an extensive suite of software based around an IBM PC. Evaluation of the instrument was undertaken during the testing of patients attending the premises for auditory investigations. Operator experience of instrument function are discussed and used for further refinements.

The instrument was placed in routine clinical service. Results for patients with a variety of hearing pathologies are discussed. The practical evaluation of the instrument highlighted two areas for further research. Experimental studies were undertaken to establish the role of the middle ear and the value of latency analysis on the OAE.

The instrument developed during this project has been introduced into clinical/laboratory service internationally. A discussion of possible further developments of the instrument/technique are given.

Contents

List of tables and illustrations.

Acknowledgements.

My thanks to my supervisor David Kemp for his help and guidance during the period of this work.

To Siobhan Ryan for her valuable feedback on the practical aspects of the instrument operation, and her clinical testing expertise.

And to David Brass for his help during the construction of the analogue circuits, and his knowledge on matters technical.

Finally thanks to my family and friends for tolerating my neglect of them during the preparation of this document.

Introduction to otoacoustic emissions and their clinical applications.

This thesis details research based on the phenomenon of sound re-emission from the human ear canal. Evoked acoustic emissions are reported to be dependent upon normal functioning of the inner ear, which implies a clinical applicability of this phenomenon.

Landmarks in the developments of the biophysics of hearing.

The ear consists of an external 'sound collecting' appendage called the pinna, leading to an ear canal. The ear canal is terminated by the ear drum which is connected to a series of three small bones. These bones convey the sound vibration from the ear canal to the cochlea, which is the sensory organ. The cochlea converts sound waves to nerve impulses which go to the brain along the auditory nerve. This basic understanding of the ear was assumed 200 years ago. However the precise basis of the function of the inner ear in response to sound is still not clear.

Early theories of the mechanism of hearing drew parallels between musical instruments and the inner workings of the ear. The inner ear, or cochlea, is helically shaped like a shell. This led people to believe that it behaved as a simple resonator (e.g. like an organ pipe). Cotugno, in 1760, made the first discovery which contradicted the 'passive resonance' theory. He proved that the living cochlea was in fact full of fluid. Up until this point is was assumed that fluid found in the cochlea was in fact an artefact caused by death.

By the 19th century, the mathematical analysis of vibrations and harmonics was well developed. In 1851, Corti discovered the intricate nature of the cochlea using the light microscope. This enabled Helmholtz in 1863 to postulate that the structures of

the 'organ of Corti' were in fact the resonant elements that were necessary to perform this frequency analysis of the incoming sound. Helmholtz suggested that each area of the basilar membrane resonated at different frequencies, thus enabling it to perform frequency analysis of the incoming sound.

Such instruments as the harp have obvious parallels with Helmholtz's theory of the ear. With each harp string having a different resonant frequency, it can therefore act as a form of passive frequency analyser. However, no one provided a satisfactory explanation of how the ear overcomes the damping of the resonant vibration in the fluid filled cochlea (akin to playing a harp underwater).

By 1870, the telephone had been invented leading to new theories which suggested that the ear worked as a non-resonant electromechanical transducer. These theories proposed that the ear converted sound energy to electrical nerve impulses which were then decoded by the brain.

In 1930, Wever & Bray[42] discovered the cochlear microphonic (CM) signal. The CM is an electrical potential which can be measured in the region of the cochlea, and is an exact electrical replica of the incident sound waves. This obviously substantiated the theory of the ear acting as a non-resonant electromechanical transducer.

However, it was soon discovered that the CM was not in fact a neural signal. Due to the refractory period after a nerve impulse, the auditory nerve, in common with all nerves, cannot convey neural impulses at frequencies much above 1KHz. In response to this, the 'volley theory' was proposed by Wever[44] which suggested that the neural response to high frequency sound was temporally separated and shared amongst many nerve fibres, thus enabling complete conveyance of even high frequency sound waves to the brain.

In 1940, Békésy was observing the mechanical displacement of the basilar membrane in response to sound input. His method involved cutting a small window into

the cochlea of a cadaver and observing the basilar membrane motion using a microscope and stroboscopic illumination. This enabled him to see the resonant behaviour of the membrane. In addition, he observed a travelling wave which propagated from the base of the cochlear along the basilar membrane. As a result of these findings, Békésy and many others since have attempted to model the basilar membrane travelling wave using mathematical and physical models. Békésy found that the travelling wave could only propagate from the base of the cochlea to the apex.

In 1948, Gold[14] estimated the 'Q' value of the membrane resonance from psychoacoustic measurements of his own hearing. He reasoned that, in order to achieve such a high degree of subjective frequency discrimination, the Q factor of the membrane resonance must be very high (i.e. 200-300). He postulated that, in order to overcome the damping of the basilar membrane motion inside the fluid filled cochlea, and therefore achieve such sharp resonances, some active mechanical process must be involved. He likened the mechanism to that of a regenerative radio receiver, where the frequency selectivity is enhanced by feeding back a proportion of the amplified radio frequency signal to the tuned circuit. He extended the analogy by suggesting that the input signal (i.e. incident sound) controlled the output of some biological energy store, similar to the way in which the base current of a transistor controls the much larger collector current from a battery. He suggested that the CM in fact drove some electromechanical biological system situated inside the cochlea which provided amplification to the travelling wave. He also went as far as to suggest that as a by-product of this active amplification process there was a possibility of sound emissions from the ear. His suggestions, however, were largely ignored because his Q factor calculations were felt to be erroneous, and no biological evidence existed as to the presence of the active mechanism. It must be noted though that all the competing evidence for the Q values of the basilar membrane resonance was obtained from dead ears (Békésy etc.).

Direct measurements of the basilar membrane motion in response to incident sound are almost impossible to obtain in the living animal without some disturbance of the normal hearing process. This is because the organ of Corti exists within a bony case, is very small, and is filled with two fluids which must not mix. By necessity, methods of measurement of the vibration of the basilar membrane have evolved which cause less 'insult' to the organ of Corti, and which are more sensitive thereby enabling measurements to be made at more 'normal' sound levels.

In 1967, Johnstone & Boyle[22] pioneered the Mössbauer technique to measure the motion of the basilar membrane. The Mössbauer technique involves placing a minute radioactive source (0.1μg Gamma emitter) onto the basilar membrane, and then measuring the velocity of vibration of the basilar membrane by the doppler shift of the gamma radiation. This technique could measure velocities down to 0.2mm/s. Although this is 70dB above the basilar mebrane motion at the threshold of hearing, it is still considerably more sensitive than Békésy's observations which were at 145dB.

Rhode[36] used the same Mössbauer technique on the ears of living squirrel monkeys, and measured the vibration at various places along the basilar membrane in response to sound stimulation. His findings showed very sharp tuning along the basilar membrane, and a 'nonlinearity' such that the tuning was much sharper at low levels of stimulation.

Although the work of Rhode demonstrated sharper tuning in the basilar membrane than previously shown by any other worker, it was still assumed that the mechanics of the membrane motion provided a poor degree of tuning and that some additional tuning mechanism existed. Kiang et al[29], in 1965, had shown that a single nerve fibre of the auditory nerve exhibited very sharp tuning. This led to the proposal of a 'second filter' which was a property of the auditory nerve[11]. This was supported by the observation that the iso-amplitude neural tuning curve becomes 'detuned' when the cochlea becomes anoxic or is metabolically inhibited.

In 1972, it was shown that 90% of all of the afferent fibres emanated from the inner hair cells (IHCs) (there are 3 times as many outer hair cells (OHCs) as IHCs). This work was achieved by carefully tracing the routes of the innervation to the hair cells in the organ of Corti[40]. It was therefore realised that the IHCs had the major sensory role. The OHCs have both afferent and efferent innervation. It was suggested that the OHCs were responsible for permitting the ear to work over such a large (120dB) dynamic range (i.e. the IHCs and OHCs having staggered operating ranges of sensitivity to sound intensities).

Russell & Sellick[37] in 1977 showed that the high degree of frequency selectivity in the cochlea occurred 'before' the auditory nerve. They measured the electrical potentials in the nerve fibre and in the cell body of the IHCs to sound stimulation. They compared the iso-amplitude tuning curves of both the nerve fibre and the IHC and found that they were the same, thus indicating that the tuning occurred at or before the IHC.

In summary, by 1977, more elaborate techniques had developed for measuring the mechanical and neural behaviour of the cochlea, with these causing less disturbance to the system. This permitted measurements of the system in response to lower levels of sound input, resulting in the observation that the cochlea exhibited extremely sharp tuning to sound input. It was not agreed whether this tuning existed solely in the motion of the basilar membrane or was augmented by the function of the IHCs. It was not clear what role the OHCs played, and exactly how this fine tuning occurred.

Discovery of the otoacoustic emission.

The discovery of the existence of an acoustic emission from the human ear in 1977 followed work by Kemp on the fine structure of the audiogram. Elliot[11] had found that a "ripple" existed in the audiogram. This suggested a high Q system (similar to the membrane resonance proposed by Gold). The sustained tone then interferes with the incoming tone producing an enhanced or suppressed threshold. This threshold

increase or decrease is a function of frequency, and therefore produces a ripple in the audiogram. Kemp however explained the 'ripple effect' as due to a standing wave effect within the cochlea.

To test this hypothesis, Kemp proposed that after an acoustic impulse was applied to the ear canal a series of acoustic reflections would occur in the cochlea leading to an acoustic re-emission. He found that an acoustic emission could be evoked by an acoustic click stimulus, and that it was possible to measure this using a microphone sealed in the ear canal. The emission was delayed by 5-15ms, hence the name 'cochlear echo', and is termed an 'Otoacoustic Emission' (OAE).

He proposed that the long travel times in and out of the cochlea are consistent with a reflection of the travelling wave with much of the damping removed. Furthermore the point of reflection might be associated with the activity responsible for removing the damping (this was supported by the observations of cochlear nonlinearity and the absence of OAEs with cochlear deafness).

The 'Active' process.

Kemp suggested that these sounds were emitted from within the cochlea as a by-product of some active nonlinear mechanical feedback process. This was supported by the work of Kim et al[30] who suggested that distortion products were produced by nonlinearities in the basilar membrane mechanics (as shown by Rhode[36]), and were actually propagated along the basilar membrane.

Kemp & Chum[25] calculated that the energy output of the cochlea could be greater, in some cases, than the energy in the stimulus. In addition, spontaneous emissions could be recorded in some ears[45], just as Gold had predicted 30 years previously.

The idea that an active process existed within the cochlea was received with considerable scepticism, similar to when it was first postulated by Gold in 1948. Furthermore, the concept of sound emission from within the cochlea requires a transmission mechanism to propagate the sound out of the cochlea. This was contrary to Békésy's findings which suggested that the travelling wave could only travel in one direction, from base to apex. Therefore, either a reverse travelling wave existed[23], or another method of propagation was occurring, such as direct sound transmission through the cochlear fluid[46]. Many workers have designed mathematical models to simulate the sound propogation along the cochlear partition in an attempt to model the phenomenon of otoacoustic re-emission.

Active, nonlinear mechanical processes present within the cochlea, inferred by the existence of OAEs, stimulated further research into the function of the OHCs. The OHCs, with their efferent innervation, became the focus of attention for the source of mechanical energy. It had been well established that the IHCs were detectors of movement in the organ of Corti, directly stimulating the audi ory nerve. Actin and myosin filaments, which are often associated with a contractile function, were discovered in the OHCs[12,50]. More recently, isolated single OHCs have been demonstrated to contract as a result of electrical stimulation[7] and altering the ionic enviroment of the bathing solution[51].

The IHCs are therefore considered to be the primary 'sensory' cells of the cochlea, whereas the OHCs are termed 'effectors', applying a mechanical input to the basilar membrane motion. It is currently believed that the OHCs are capable of contributing energy to the travelling wave, as it propagates along the basilar membrane, so as to amplify the membrane displacement. As a result, the sensitivity to sound input would be increased. Furthermore, this energy input, by overcoming the damping of the membrane motion, sharpens the resonance-like behaviour of the basilar membrane, thus increasing the frequency selectivity of the ear. This process is highly nonlinear, having greater significance at lower levels of sound input.

Although the idea of an active mechanical input to the basilar membrane motion being provided by the OHCs is still unproven, the evidence supporting this idea is now very strong. Work by Khanna & Leonnard[28] and Sellick et al[39], using laser interferometry and Mössbauer techniques respectively, showed mechanical tuning of the basilar membrane similar to the very selective tuning found in the auditory nerve. Such sharp tuning is indicative of a low loss system, and since the cochlear partition is filled with fluid, some active mechanical input to the membrane must be involved to overcome the damping.

The otoacoustic emission is believed to be a by-product of this active process. The findings of Kemp & Chum,[25] that the emission can have greater energy than the stimulating signal, support this hypothesis. In addition, the same factors which decrease the sharpness of the frequency selectivity also decrease or eradicate the emission (e.g. ototoxic drugs, noise and pathological conditions). Otoacoustic emissions can therefore perform as an indicator of the physiological condition of the basilar membrane mechanics.

Classification of OAE types.

The phenomena of acoustic emissions can be observed by various methods. Below is a list of the four categories of otoacoustic emissions, which are differentiated by the method of evocation.

Transient Evoked Otoacoustic Emissions (TEOAE). Kemp used a transient excitation to measure the OAE. He found that after 5ms post stimulus (pst) the original excitation had decayed to a negligible level, but a "slowly decaying response component was present" between 5 and 20ms pst. This OAE has been termed the transient evoked OAE, or delayed OAE, and is commonly referred to as the 'cochlear echo'.

Stimulus Frequency Otoacoustic Emissions (SFOAE). In addition to transient evoked OAEs, emissions can be evoked at the stimulus frequency by a continuous

tone. In this method of observation the detailed amplitude and phase variations of the sound in the ear canal are monitored in relation to the swept frequency stimulus. The ear canal sound level has a series of peaks and troughs as a function of frequency which corresponds with the subjective threshold measurements of Elliot. This is caused by the emission interacting with the stimulus, producing cancellation and addition with the stimulus tone. Wilson[45] used a lock-in analyser to measure the stimulus frequency OAEs from several subjects, and concluded, from measurements of the emission delay, that it must be a function of the cochlea.

Distortion Product Otoacoustic Emissions (DPOAE). When OAEs are evoked by two tone stimulation, emissions contain 'distortion products' of the two stimulation tones, as well as the stimulus tones. That is, the emission has components at a frequency which is not present in the stimulation. The strongest emission distortion component is usually at the frequency of 2F1-F2, where F1 and F2 are the frequencies of stimulation.

Spontaneous Otoacoustic Emissions (SOAE). Gold[14], in 1948, hypothesised that the same active mechanism in the ear which overcame the damping of the membrane resonance could result in a spontaneous emission if the 'positive feedback' was too high. Such emissions have been found to exist. Several investigators[35,45] have shown the presence of spontaneous emissions in 30-40% of normal ears.

Prevalence of OAEs.

From the first reports of OAEs it was found that they were present in normal ears but were absent in cases of deafness. For the presence of otoacoustic emissions to be an effective indicator of 'normal' cochlear physiology, emissions must be measurable from almost all normal ears. Kemp[23] found that emissions occurred in all the subjects he tested with "otologically normal" ears. The table below summarises the results of investigations into the presence of OAEs in normal ears by many of the other workers.

Investigator	Year	No. ears	%OAE
Kemp	1978	37	100%
Johnsen & Elberling	1982	10	100%
Probst et al	1986	28	100%
Bonfils et al	1986	131	100%
Wit & Ritsma	1979	9	100%
Stevens & Ip	1988	38	97%
Rutten	1980	29	90%
Grandori	1983	12	90%
Horst et al	1983	8	75%
Zwicker	1983	21	70%
vanDijk & Wit	1987	210	40%

table 1.1

From the table, it is apparent that most workers found a high OAE prevalence (≥90%). But not all the researchers were able to measure emissions in all normal subjects. For example, van Dijk & Wit[8] found emissions present in only 85 of the 210 normal subjects tested. Although all of these studies used transient stimuli to evoke the emission, there were many differences in the methods employed. It is therefore suggested that it is this lack of uniformity in measurement techniques, that accounts for the range of results, rather than the absence of emissions in up to 60% of normally hearing subjects. For example, the paper by van Dijk & Wit[8] fails to report the noise conditions under which the emission measurements were performed. In addition, it was suggested[5] that the equipment used in this study (Peters AP200) provides insufficient information to the operator to enable a reliable measurement of the OAE to be performed.

In summary, the literature suggests that OAEs occur in all normally functioning ears, and that the percentage measured is a reflection of the technique used rather than the actual prevalence of emissions. As a result, great emphasis should be placed on developing the most reliable measurement technique.

The effect of ear pathology on the presence of OAEs.

As well as studies of the presence or absence of OAEs in normal ears, much research has been performed on the occurrence of OAEs in 'abnormal' ears. Kemp[23] found no emissions in subjects who had a best threshold of greater than 30dB HL. Rutten[38] found that if an OAE was present at a given frequency, then the audiogram threshold at this same frequency was better than 15dBHL.

Kemp also found that subjects with conductive losses, due to diseased middle ears had no measurable OAEs. This has been confirmed by other workers[5]. Even though the cochlea may well have been functioning normally, the poor transmission of the emission, from the cochlea to the ear drum, resulted in the emission being immeasurably small. In addition, the stimulus is also attenuated as it is propagated from the ear canal to the cochlea, and as a result the cochlea receives less stimulation.

Stevens & Ip[41] measured the OAEs from 18 normal and 19 hearing impaired subjects, in order to establish the suitability of the OAE test as a detector of hearing impairment. They concluded that by using careful recording techniques no subject with "impaired cochlear function over a wide range of frequencies will be missed" using the OAE test.

Bonfils et al[4] conducted a large study on the effect of presbycusis on the presence of OAEs. They found a 100% incidence of emissions in subjects less than 60 years of age. However, this incidence fell to an average of only 35% for subjects of over 60 years of age, although "it is noteworthy that OAEs could be recorded in old subjects (over 60 years) with relative preservation of hearing".

Many workers have taken a different approach to testing the OAE technique as an indicator of cochlear function. Rather than measure the emissions from ears with known cochlear impairment, they have subjected normal cochleae to insults at such a level as to cause temporary threshold shift (TTS) effects.

Kemp[24] investigated the effect on the OAE after the cochlea had received a noise insult sufficient to cause a TTS. He found that after a 12 minute exposure to a 625Hz tone at 105dB HL the emission intensity was 7.5dB smaller at 1 minute post-exposure time than the pre-exposure intensity. Kemp suggested that the stability of the OAE is "high enough to permit long term cochlear monitoring and this would be of value in hearing conservation programmes". He also suggested that by monitoring the emission intensity immediately following modest noise exposure "might give a quick, safe and objective indicator of an individuals sensitivity to noise induced cochlear strain".

Anderson & Kemp[2], and Johnsen & Elberling[19] have both investigated the effect of ototoxic drugs on the OAE. Johnsen & Elberling induced a flat sensorineural hearing loss of 25-30dB HL using serum salicyate. They found that the emission "virtually disappeared", however, after 2 days complete recovery of the emission had occurred. Anderson & Kemp used injections of both furosemide and etacrylic acid in laboratory primates to study the effect on the emission caused by these drugs. They found that administration of each drug caused a substantial reduction of the emission intensity (within minutes) followed by some degree of recovery (within hours).

The importance of objective tests of cochlear function.

By definition an objective test of cochlear function requires no response from the subject. There are several groups of subjects where it is essential that testing be carried out by objective means. For example, the mentally impaired and very young cannot be relied upon to produce correct subjective responses to sound stimuli. In addition, there are other groups that cannot be totally relied upon to make correct subjective

responses. For example, patients with so called inorganic hearing losses (IOHL) and patients requesting compensation for noise induced hearing losses (NIHL).

In the case of the mentally impaired and infants, the majority of patients presenting for test have normal cochlear function[1]. A quick and reliable screening test of cochlear function is all that is required. Whereas, in the latter two groups a more precise measure of auditory threshold is necessary.

Objective tests of cochlear function measure physiologically generated signals which originate in the cochlea. These include the electro-cochleagraph (ECoG) test which measures the cochlear microphonic signal, and the brain stem electric response (BSER) which measures the collective auditory nerve response as it travels 'up' the brainstem. Both of these tests require electrical contact with the patient. In the case of BSER, this involves placing 3 or 4 electrodes on the head of the subject and measuring the potential difference across two of the electrodes. The electrical response is averaged to thousands of stimuli to overcome the background myogenic activity.

In the case of the ECoG, the measuring electrode is positioned so as to measure the CM response at the base of the cochlea. This is normally achieved using a trans-tympanic electrode which passes through the ear drum and rests near the round window of the cochlea. An alternative electrode placement is at the end of the ear canal near the ear drum. However, this placement produces a lower signal to noise ratio and therefore longer averaging times are required.

Both of the techniques described above fall under the title of evoked response audiometry (ERA). They can both establish the threshold of the response by repeating the measurements at different levels of stimulation. By using data collected from

1 The incidence of severe hearing impairment at birth is approximately 1:1000 (Martin[32])

normal ears, it is possible, from the determined threshold of either response, to calculate the psychophysical auditory threshold.

The OAE is another type of physiological, cochlear-originating evoked response. The presence of the emission is dependent upon 'normal' (i.e. better than 20dB HL) auditory thresholds. Unlike ECoG and BSER the OAE "cannot be used to estimate psychoacoustic thresholds"[41]. However, the application of the test as a screening test for normal cochlear function is widely accepted[5,9,41].

The role of OAEs in neonatal hearing screening.

A successful hearing screening programme for the neonatal population group has yet to be implemented. At present, the accepted method of screening for hearing impairment involves administering the 'distraction test' method when the infant reaches an age of 8 months. This test is conducted by the Health Visitor service. Recent research has shown grave inadequacies of this method in efficiently detecting hearing impairment. In a study conducted in the Greater Manchester area, Newton[34] reported that, of all the confirmed cases of sensorineural deafness, 45% passed the health visitor screening test at 8 months. This is further illustrated by the work of Martin[32] which showed that in the European Community 50% of all children who had an average hearing loss of 50dB or worse (in the better ear) had reached 3 years of age before detection of the impairment.

Johnsen et al[21] first investigated the possibility of using the OAE test as a means of neonatal hearing screening. They stated the requirements of a suitable hearing screening test as being "fast, non-invasive and easy to perform" as well as having a "high sensitivity and specificity, yielding a very low rate of false-positive errors and virtually no false-negative errors". Their investigations showed that emissions were recorded in all of the 20 neonates' ears tested.

Stevens et al[42] published a study of the comparison of BSER and OAE tests on a population of 346 neonates. The neonates were mainly tested whilst inpatients of a neonatal intensive care unit. 97% of the babies were followed up and tested at 8 months using distraction testing and typanometry.

Stevens et al found the mean total time taken for the OAE test to be 12.1 minutes compared with 21 minutes for the BSER test (these times are measured from entering the test room until departure). Much of the difference in time is accounted for by the electrode placement for the BSER test.

Stevens et al succeeded in measuring OAEs bilaterally from 79% of all the neonates tested. Those babies that failed the BSER test were subsequently retested using BSER. Of the 21 surviving neonates who failed the BSER test, 20 of them failed the one OAE test. Stevens et al conclude that "the OAE test would make a good first screen to be followed by the BSER if no OAE was present".

Other roles.

The role of the OAE test in a neonatal screening capacity has been outlined above. Various workers suggest that the OAE test has other clinical applications.

- Rutten[38] concluded that the "physiological vulnerablity" ..of the OAE.. "seems important for early detection of progressive hearing losses".
- Kemp[26] suggests that a "potential application of OAEs is the registration of detailed otoacoustic parameters of the patient for future use indicating early changes in that ear, whether caused by disease, noise exposure or some drug treatment".
- The OAE test has a possible application in screening the hearing of patients with other handicaps, such as the children in special schools. Foulkes[13] reported that at a special school the "pilot study showed only 6% of children able to co-operate in sweep frequency hearing tests as usually practised in

mainstream schools". The need for an objective hearing test in such circumstances is apparent. However, many of these children would require a general anaesthetic (with the associated risk) in order to perform either BSER or ECoG tests. The use of the OAE test as a first level screen of cochlear function for these children has many advantages over the alternatives.

In summary, there is general agreement, by the workers in OAE application research, that the OAE test could play a useful role as a cochlear function indicator in the clinical test enviroment. The emission is particularly useful for the screening of normal cochlear function because it has been found that it is generally absent in ears which have a hearing loss of 20dB or more.

1.8 The suitability of various OAE measurement techniques.

Kemp et al[26] suggested that "an acoustic transient provides the most appropriate excitation of the ear canal to elicit cochlear echoes for clinical purposes". Many of the other studies of OAEs have employed 'transient evoked' methods of excitation of the ear canal. However other methods are used, namely two tone (to measure the distortion products) and tone burst stimulation (to measure the delayed stimulus frequency emission). Both of these excitation methods result in emissions of limited frequency content. To obtain the frequency information contained in the transient evoked OAE requires many measurements at different frequencies using these other methods. The time penalty imposed by this accounts for the popularity of the transient evoked technique.

All of the studies of OAEs have utilised laboratory-type research equipment rather than purpose built clinical measurement equipment (many originate from adapted ERA equipment). As a result, in some cases this does not allow a full investigation of the measurement technique which is most appropriate to otoacoustic emission measurement.

The published evidence shows the inadequacies of some of the currently used emission measurement and interpretation techniques. This emphasises the need for the OAE test method to be thoroughly investigated to establish the optimum signal capturing and identification techniques before it can be evaluated for its clinical performance (i.e. as a screening test).

Elberling et al[9] point to a problematic area of OAE measurement, namely the difficulty encountered in successfully separating the influence of the middle ear response to the evoking acoustic transient from the cochlear re-emission. They conclude that "counter measures to avoid or overcome"... "the stimulus induced artefact (tail of the acoustic stimulation)"... "should be taken before recording of stimulated evoked emissions can be launched and used in a clinical test battery", because in some cases it was found that the artefact in "ears with no emissions could be wrongly taken for responses". Thorough investigations into the most appropriate techniques to alleviate this problem must be undertaken, leading to a technique which can be used to reliably measure the OAE completely immune to middle ear response contamination.

1.9 Conclusion.

The major aim of this study is to specify, design and build an OAE instrument for clinical application of the OAE measurement technique. However before a suitable instrument specification can be formulated it is necessary to evaluate a range of methods for measuring the emission response to ensure that the most appropriate method is employed. This evaluation involves carefully investigating the physical properties of the transient evoked OAE. Once the best technique has been established, it should ideally be incorporated into a portable, rugged and clinically orientated instrument. This would permit the evaluation of the OAE technique to progress into a true clinical enviroment, enabling the practical diagnostic value of the OAE phenomenon to be fully established.

The acoustic response of the human ear canal to transient acoustic excitation.

Abstract.

A thorough examination of the acoustic properties of the ear canal during transient excitation was undertaken as a preparation for the specification of a suitable instrument design for the measurement of OAEs evoked by transient stimulation.

Introduction.

The purpose of the tympanic membrane is to collect incident sound energy and transmit it along the ossicular chain to the cochlea. The acoustic impedance of the ear drum is important for auditory function as it determines the energy available for absorption by the cochlea, and therefore the hearing sensitivity. The acoustic impedance of the ear drum is determined by the physical properties of the drum, such as the tension of the membrane, and its mass per unit area. In addition, there are influences upon the ear drum impedance due to the ossicular chain, the enclosed cavities of the middle ear, and the complex input impedance of the cochlea. For the purposes of this chapter we need to understand the response of the ear canal to transient excitation.

2.1 Approaches to computation of the ear canal transient response.

The adult human ear canal can be compared to a tube approximately 2cm in length, and 6mm in diameter, terminated by a thin membrane representing the ear drum. This seals the end of the ear canal, separating the outer ear from the middle ear. The acoustic response of the ear canal is determined by the impedance of the canal and ear drum in combination. At low frequencies the wavelength of sound is much greater than the dimensions of the ear canal (at 1KHz, $\lambda = 33$cm). If the dimensions of the ear canal and the impedance of the drum were known to sufficient accuracy at low

frequencies, it would be possible to treat the system as a lumped impedance and compute the transient response.

Zwislocki[53] and others have described various analogues of the interrelationship and absolute quantities of the complex impedances of the components in the auditory system. The Zwislocki model of the middle ear consists of five resonant elements representing various anatomical features of the middle ear system (fig.2.1). This diagram has an additional component representing the volume of the ear canal. This latter component has been included as it relates to the specific case of acoustic impedance measurements of the ear drum performed using an acoustic probe sealed in the ear canal.

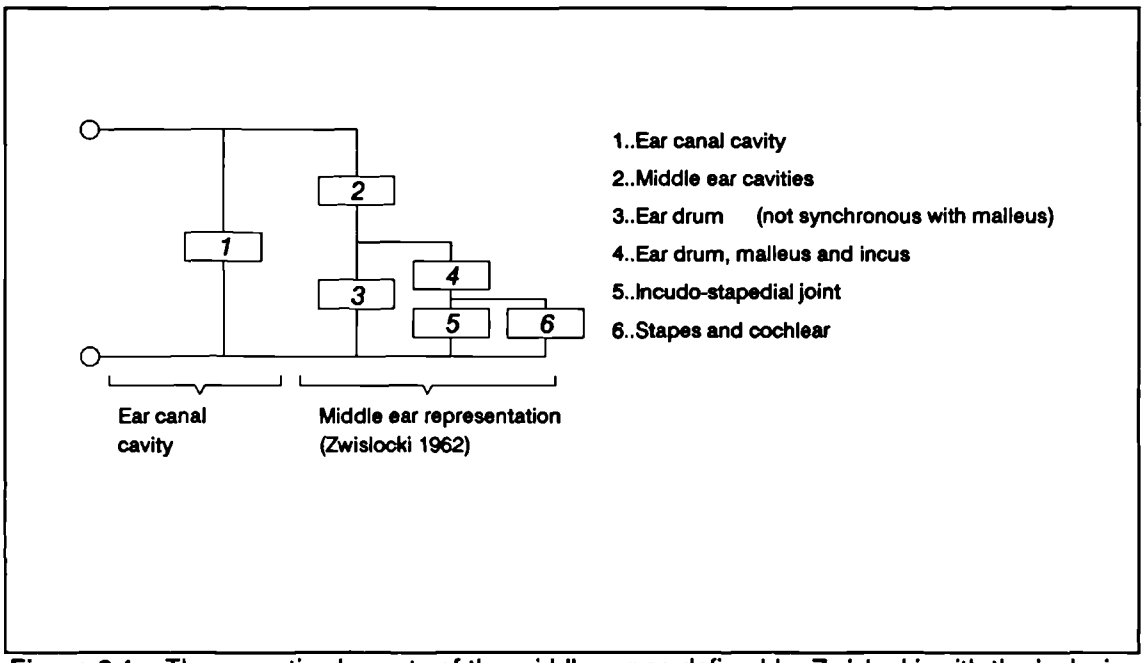

Figure 2.1 The acoustic elements of the middle ear as defined by Zwislocki, with the inclusion of a component for the volume of the ear canal.

Electrical modelling of acoustic systems can be performed with voltage and current being used as analogies to pressure and volume velocity, respectively. These analogies require that the volume of a cavity is represented by a capacitor, acoustic resistance by electrical resistance, and the inertance of a mass of air by inductance. Various electrical analogues of the middle ear system have been published. Using such a model, it is possible to simulate the response of the sealed ear canal under transient

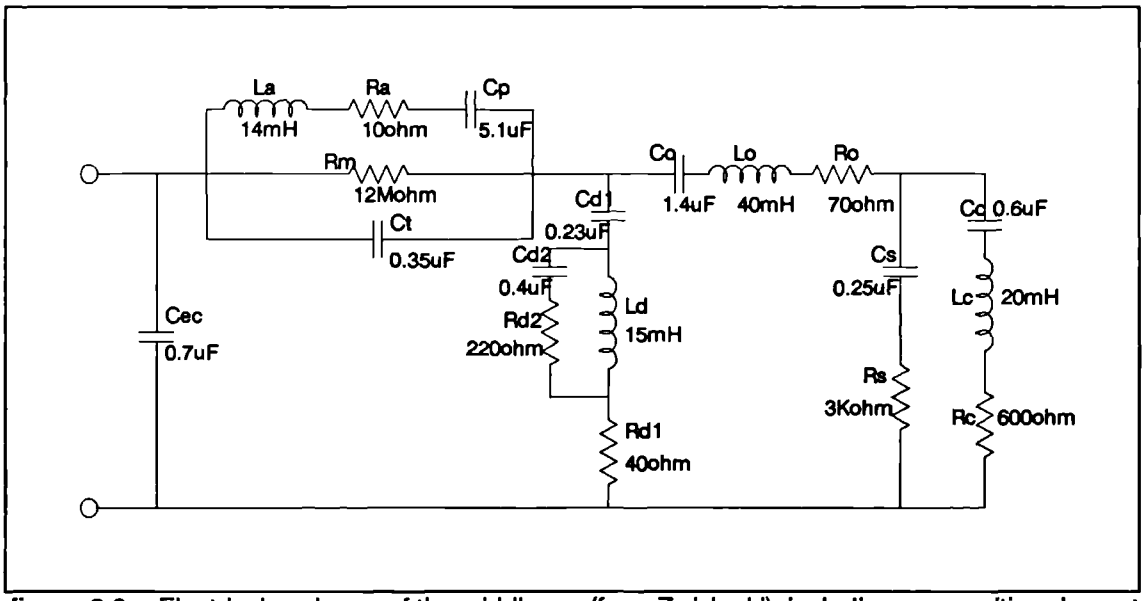

figure 2.2 Electrical analogue of the middle ear (from Zwislocki), including a capacitive element for the volume of the ear canal

acoustic stimulation. The Zwislocki model (one of the earliest published models) was selected because of its relative simplicity (see fig.2.2).

In addition to the components of the middle ear model, a capacitor was added to represent the compliance of the sealed ear canal. To completely replicate the practical acoustic situation, a further impedance should be in parallel with the ear canal capacitor which represents cavities in the probe itself, and any leaks around the edge of the probe to 'free space'.

For higher frequencies (i.e. when the wavelength is less than the dimensions of the ear canal) the lumped impedance model is inadequate and the system is best considered as a transmission line. At and above this frequency the ear canal exhibits standing wave resonant characteristics. The frequency and damping of the resonance in the ear canal is determined by the length of the tube, the terminating impedance of the ear drum and the acoustic radiation at the open end, collectively. Open and closed tubes have different modes of resonance. In the case of the open adult human ear canal, the fundamental mode of resonance occurs at approximately 3.3KHz. When the ear canal is closed due to the insertion of a probe (i.e. during OAE measurement)

the fundamental resonance occurs at approximately 5.5KHz. The literature shows that the transient evoked OAE occurs below this frequency and therefore it is appropriate to consider the ear as a lumped impedance rather than a transmission line.

2.2.1 Direct measurements - Frequency domain.

Ear drum impedance is measured in clinical situations by a test instrument called a tympanometer. This is achieved by reducing the mobility (i.e. increasing the stiffness) of the ear drum by the application of external pneumatic pressure (of about 200mm water pressure i.e.2000Pa), thus allowing an acoustic impedance measurement that approximates to that of the ear canal only. With reference to the analogue model (fig.2.1), this is equivalent to increasing the impedance of the network containing the drum impedances such that its influence upon the impedance measured at the terminals is negligible, therefore allowing direct measurement of the ear canal volume. A further measurement is taken at ambient pressure. As the two impedances act in parallel, a simple calculation yields the acoustic impedance of the ear drum at the test frequency. This is generally restricted to 220Hz. In laboratory studies, measurements of ear drum impedance have been performed over a wide frequency range, and they have been used to examine the input efficiency of the ear drum.

At higher frequencies the transmission line effect is taken into account. For example, J.Allen[(1)] showed the acoustic impedance of the ear drum in a normally functioning ear to be comparable to that of air (approximately 400 Rayls) over the frequency range 200Hz to 33KHz. The technique employed by Allen involved an acoustic transmission line which was perfectly matched to the stimulating transducer. Upon insertion of this probe into the ear it was possible to establish the terminating impedance by determining the reflection coefficient of the ear drum.

Impedance data can be used to ascertain the transient acoustic response of the ear canal, even including components due to the cochlea. It would involve establishing the complex impedance of the ear canal at all frequencies. An inverse Fourier

transform technique could then be employed in order to compute the transient response waveform. In practice, the accuracy of this technique is limited by the accuracy of the response data available, more specifically, the frequency resolution and the measurement precision. Any fine structure in the amplitude and phase response measurements with respect to frequency corresponds to small, delayed components in the transient response waveform. For example, to predict features in the transient response once it has decayed to a signal level 60dB below the initial response amplitude (a typical OAE) requires that measurements of complex amplitude be accurate to at least 0.01dB. Although it is conceivable that measurements to this degree of precision could be performed upon physical systems, such measurements upon the human ear canal are beyond practical feasibility. Time domain measurements were investigated as a more practical method of determining the transient response of the ear canal.

2.2.2 Direct measurements - Time domain.

Békésy[3] used an optical method to directly measure the transient response of the ear drum. This was achieved by the use of optically reflective material attached to the ear drum. This method has the advantage over acoustic methods of measuring directly the transient response of the ear drum, without the need to separate the complex impedance components due to the ear canal (see fig.2.3a).

Despite the apparent advantage of performing direct measures upon the ear drum, in 1978, Kemp[23] used an acoustic technique to measure the transient response of the ear canal. This measurement technique was modelled using the electrical model described earlier (see fig.2.2). In the case of acoustic stimulation, the loudspeaker transducer generates a volume velocity stimulus pulse. Therefore, to represent this in the model a high impedance electrical pulse must be used (i.e. a current pulse). The response of the model is measured as a voltage developed across the ear canal capacitor (i.e. the pressure developed in the ear canal). The electrical pulse was also

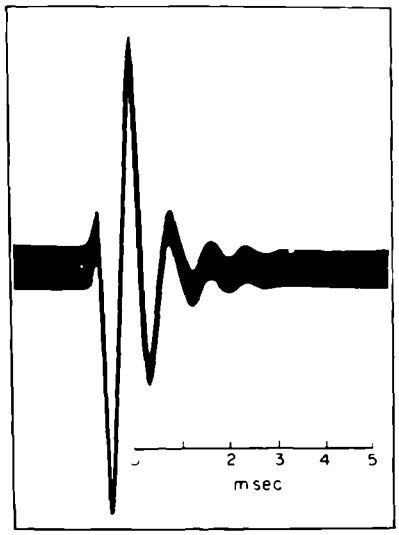

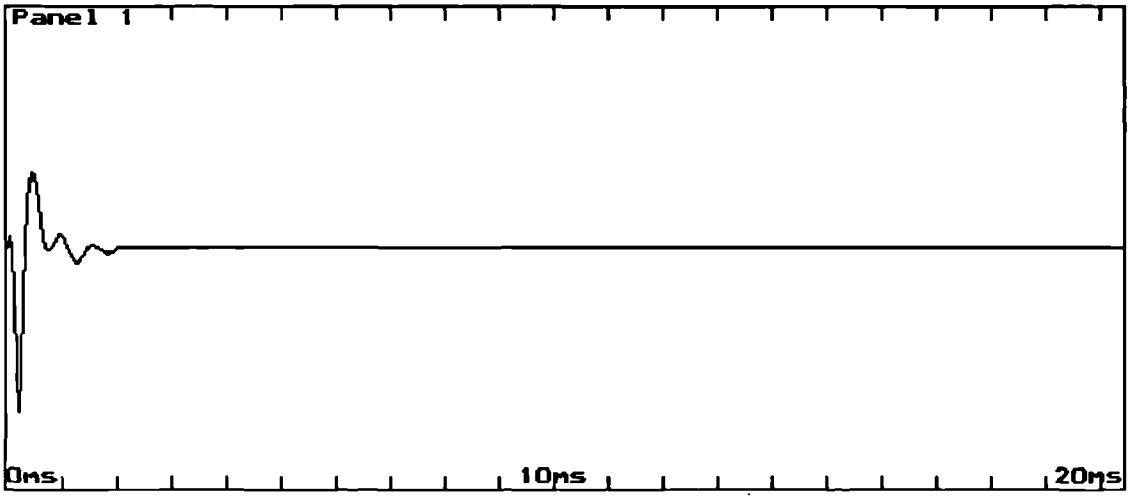

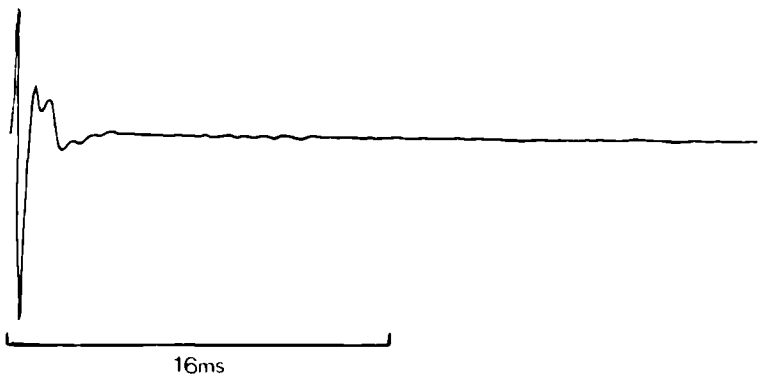

figure 2.3(a,b,c) Fig.2.3(a) is a reproduction of the transient response of the ear canal recorded using an optical method from the work of Békésy. Fig.2.3(b) is an electrical measurement of the transient response of the Zwislocki electrical analogue (shown in fig.2.2). Fig.2.3(c) is a reproduction of the transient response of the ear canal recorded using an acoustic method and averaging, from the work of Kemp.

low pass filtered to limit the frequency content of the stimulation to fall within the operational bandwidth of the model (2KHz). This model predicts the transient response (see fig.2.3c) to be like that observed by Békésy (see fig.2.3b) and the first 5ms of the response measured acoustically by Kemp (see fig.2.3c).

Due to the high sensitivity of the acoustic technique, Kemp demonstrated that the response was in fact long and complex. The key to the sensitivity of this technique was the use of a sensitive microphone sealed in the ear canal, and the use of averaging (approximately 1000 averages). A schematic representation of the equipment configuration that Kemp employed in his work is illustrated in fig.2.4. The sensitivity of this technique permitted measurements of acoustic signals as small as 0dBspl (the microphone noise floor of 30dBspl was reduced to 0dBspl by the averaging). This can be shown to be equivalent to a motion of the ear drum of just 2 Angström, which is many times below the limit of resolution of any optical measurement previously made.

For these investigations, it was decided to employ an acoustic method of transient response measurement using a microphone sealed in the ear canal, as this provided the highest degree of sensitivity.

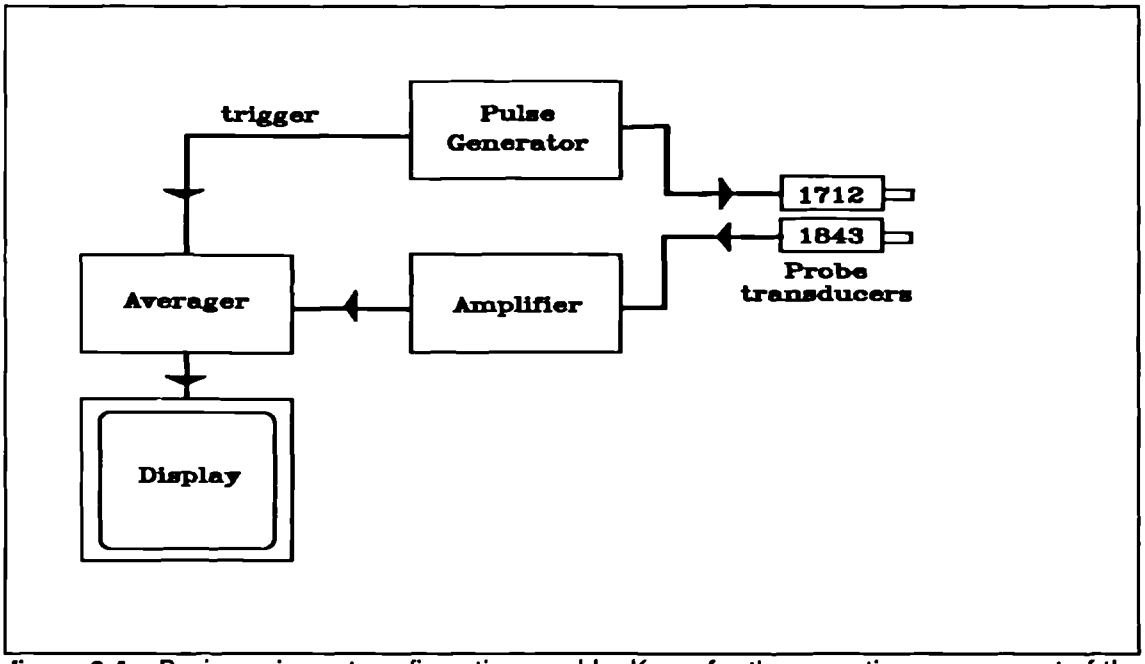

figure 2.4 Basic equipment configuration used by Kemp for the acoustic measurement of the response of the human ear canal to transient acoustic stimulation

2.3 Probe development and construction.

Having decided to employ an acoustic method to measure the transient response of the ear canal, an acoustic probe must be designed. This needs to perform the dual task of providing transient stimulation and measurement of the fine detail present in the acoustic response. To achieve this, the probe must have a high microphone sensitivity (and low intrinsic noise), and both the stimulating and microphone transducers must have broad, flat frequency spectra, to ensure that the measured transient acoustic response of the ear canal is minimally modified by the combined transfer functions of the elements of the measuring system.

The relationship of the microphone output to middle ear dynamics depends on the coupling between the ear drum and the microphone transducer. In the electrical analogue, the ear canal capacitor shunts the middle ear and probe. This coupling is comprised of the volume of the canal, shunted by any additional components, due to, for example, free space if the probe is not well sealed in the canal. This coupling can be increased by reducing the effective volume with which the ear drum communicates and eliminating any leaks. The effective volume is minimised by designing a probe which fits into the ear canal, and has a high acoustic resistance from the ear canal to the surrounding air. A small 'leak' (high acoustic resistance) to free space decreases the sensitivity to low frequencies. Therefore, to achieve the highest sensitivity and a broad bandwidth, the probe must achieve a seal with the ear canal.

Knowles miniature transducers were selected (these were gratefully received free of charge from Knowles). Their small size enabled the entire assembly of transducers, electrical and acoustic connections (see fig.2.6) to be contained within a plastic speculum tip designed to fit snugly in the human ear canal.

A test cavity was constructed for the purpose of examining the probe frequency characteristics and sensitivity. This cavity was designed to function as a useful approximation to the average adult ear canal (e.g. volume and shape). The cavity was a plastic

cylinder of length 1.3cm that had a volume of $1cm^3$. A rubber plug was fitted to the end of the tube which has a hole that allows an air-tight, accurate location of the speculum into the cavity. At the opposite, closed end of the tube, a small piece of open cell foam was fixed to the wall of the tube. This results in a more realistic behaviour of the test cavity, as the foam approximately replicates the resistive loss of the ear drum. A small hole was drilled in the side of the cavity, and the probe tip of a Brüel and Kjær (B&K) 1/4 inch microphone glued and sealed into position. This microphone was connected to a B&K measuring amplifier for the purpose of measuring the frequency characteristics of the assembled acoustic probe.

By experimenting with different lengths and diameters of tubing, the coupling between the stimulating transducer (Knowles BP1712) and the test cavity was adjusted to achieve the widest and flattest frequency response. A peak existed in the response at approximately 2KHz, due to a primary pipe resonance of the 2mm internal diameter (ID) coupling tube, and this was reduced with the addition of a sintered metal acoustic resistance of 2200Ω(cgs), positioned 4mm from the port of the transducer. The resulting sound field into the test cavity was flat within ±5dB from 120Hz to 4.6KHz. This response is shown in fig.2.5a.

The Knowles EA1843 miniature microphone was selected to measure the response, as it is small in size and has a wide frequency response (125Hz to 9KHz ±5dB). The EA1843 is an electret microphone with an internal FET amplifier. Due to tapering of the end of the speculum tip, the port of the microphone was positioned 6mm back from the tip, and a length of 1.5mm ID plastic tubing was used to couple to the microphone. Fig.2.5b shows the frequency response of the microphone in the test cavity to a constant sound pressure level.

Both of the transducers were embedded in the plastic speculum tip using epoxy resin. Each transducer was connected to separately screened miniature cable to minimise the possibility of crosstalk. Care was taken to disperse the stress at the point

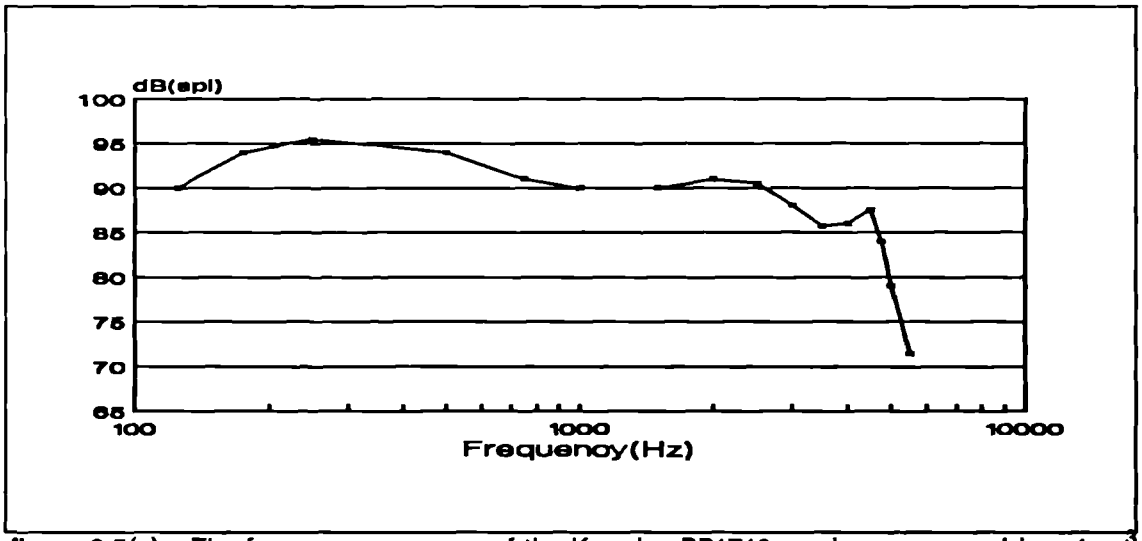

figure 2.5(a) The frequency response of the Knowles BP1712 receiver, measured in a 1cm^3 cavity using a B&K microphone and measuring amplifier. The electrical input was a 0.1V peak sine wave.

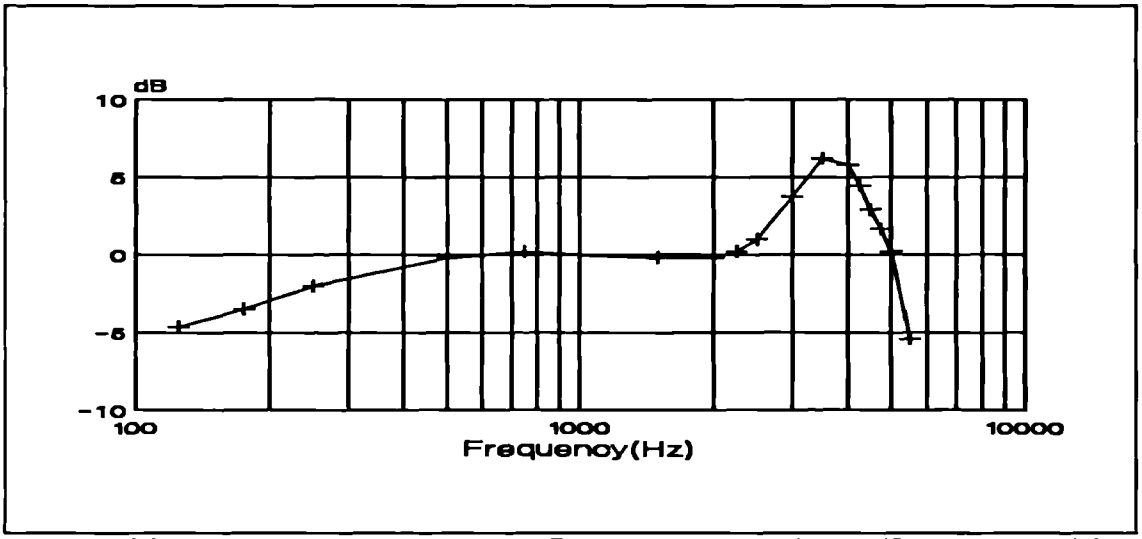

figure 2.5(b) The sensitivity of the Knowles EA1843 microphone in a 88dBspl sound field. The dB scale is relative to 20mV peak to peak output from the microphone.

where the wire emerges from the probe. This was achieved by using rubber sleeving fitted over the wire at the point of exit. A third tube of 0.5mm ID communicated from the tip to the back of the probe, thus allowing equalisation of the sealed ear canal to ambient pressure once the probe is inserted. This tube extended beyond the back of the probe to permit the application of pneumatic pressure for use in later experiments. The layout of the components within the speculum tip is illustrated in fig.2.6.

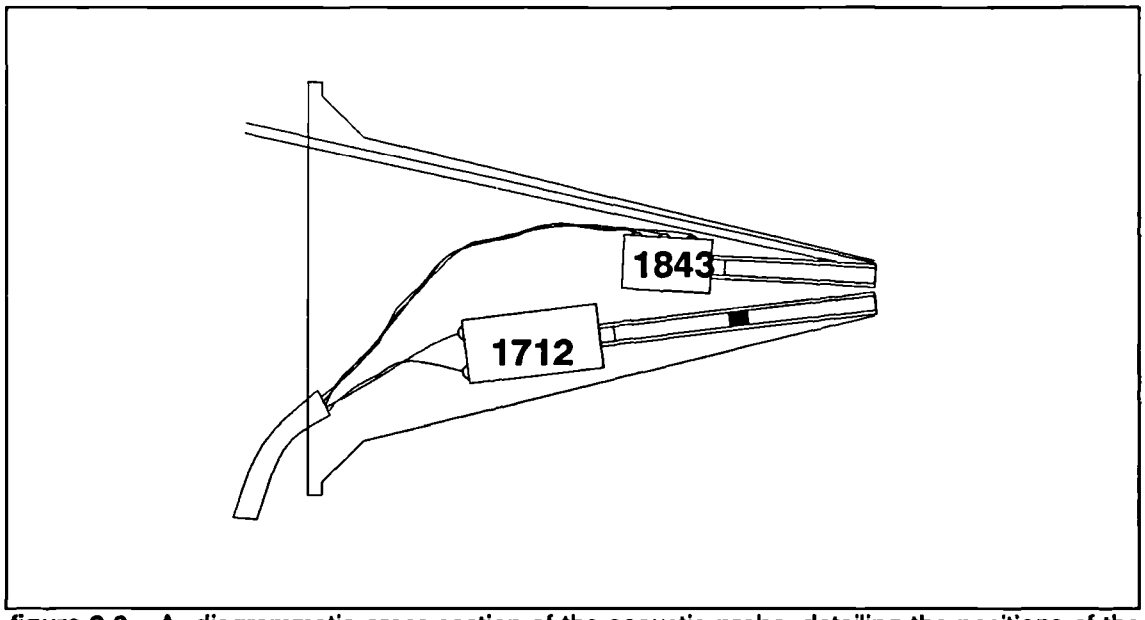

figure 2.6 A diagrammatic cross-section of the acoustic probe, detailing the positions of the various components within the plastic speculum tip.

Probe performance.

Fig.2.5(a&b) illustrates the frequency characteristics of the stimulating and microphone transducers, measured in the test cavity using sinusoidal stimulation and the B&K measurement system described above.

The transient behaviour of the probe was also measured. For transient excitation a unipolar 80 microsecond electrical pulse was applied to the stimulating transducer. This pulse contains practically equal amplitudes of all frequencies up to and above the frequency limit of the stimulating transducer (this is illustrated in fig.2.7, which is the frequency spectrum of the 80 microsecond unipolar pulse). The transient response in the test cavity is shown in fig.2.8a, and the frequency spectrum of the response is shown in fig.2.8b. The response is measured by the Knowles microphone in the speculum tip, and therefore is affected by the transfer function of the microphone (illustrated above in fig.2.5b).

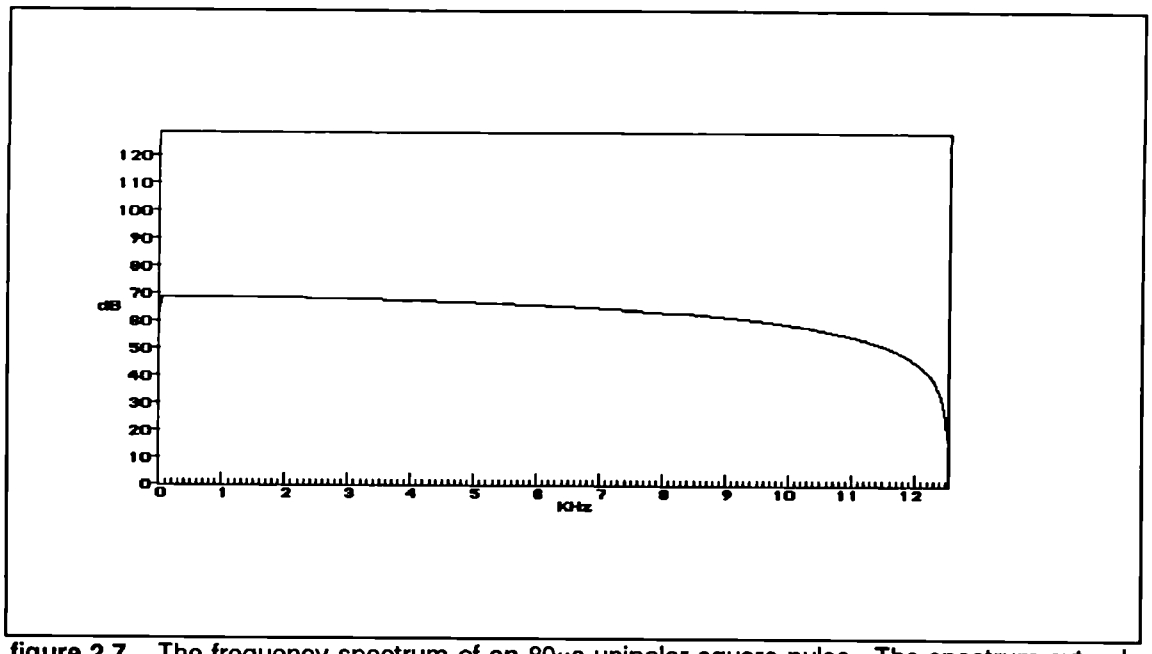

figure 2.7 The frequency spectrum of an 80μs unipolar square pulse. The spectrum extends beyond 12.5KHz (as this is the first null in the spectrum), but is not shown.

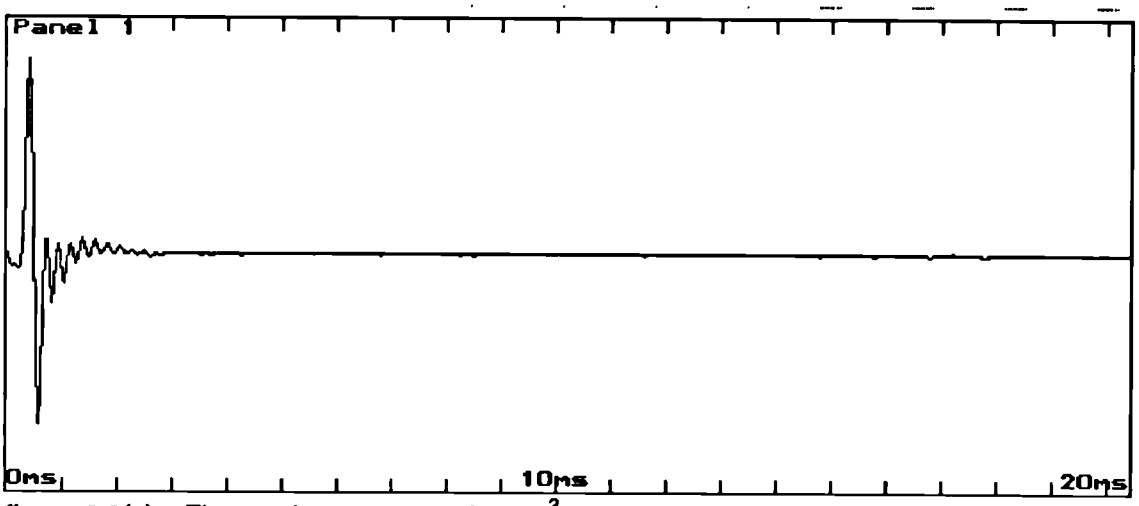

figure 2.8(a) The transient response of a 1cm^3 test cavity (see text), measured using the acoustic probe.

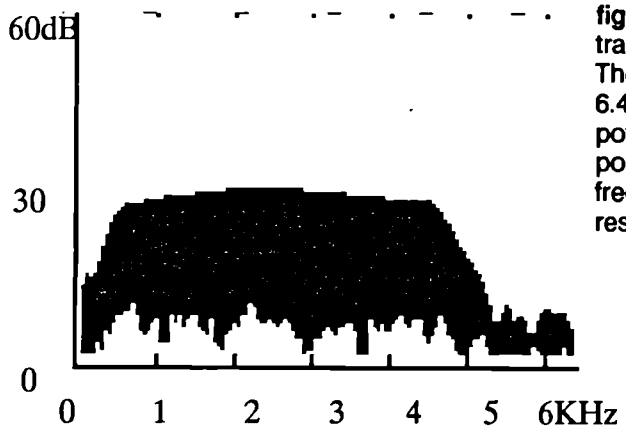

figure 2.8(b) The frequency spectrum of the transient response of the test cavity (fig.8a). The X-axis displays the frequency from 0 to 6.4KHz and the Y-axis displays the spectral power over a range of 60dB. The unshaded portion at the bottom of the spectrum is the frequency spectrum of the noise in the transient response measurement.

2.4 Measurement of the transient acoustic response of the human ear canal.

The transient response of the human ear canal was measured using the acoustic probe discussed above. Using one of the many commercially available rubber probe tips (as employed for tympanometry), positioned on the end of the speculum, a comfortable and sealed fit in the ear canal can be achieved in almost all subjects over the age of 3 years.

Fig.2.9 is an example of the transient acoustic response of the ear canal recorded from a young adult male subject. A 1mV transient electrical stimulus was applied to the loudspeaker in the probe as previously, and the response waveform was measured with the probe's own microphone. The peak pressure of the transient response was 4 milli Pascals.

The transient response of this ear canal can be compared to the transient response of the test cavity (fig.2.8a). The responses are similar. This indicates that, to a first approximation, the complex impedance of the test cavity and the ear canal are comparable. The transient response of the human ear canal, shown in fig.2.9 can also be compared with the optical measurements of Békésy, the acoustic measurements of Kemp, and the predictive measurements on the Zwislocki model (see fig.2.4).

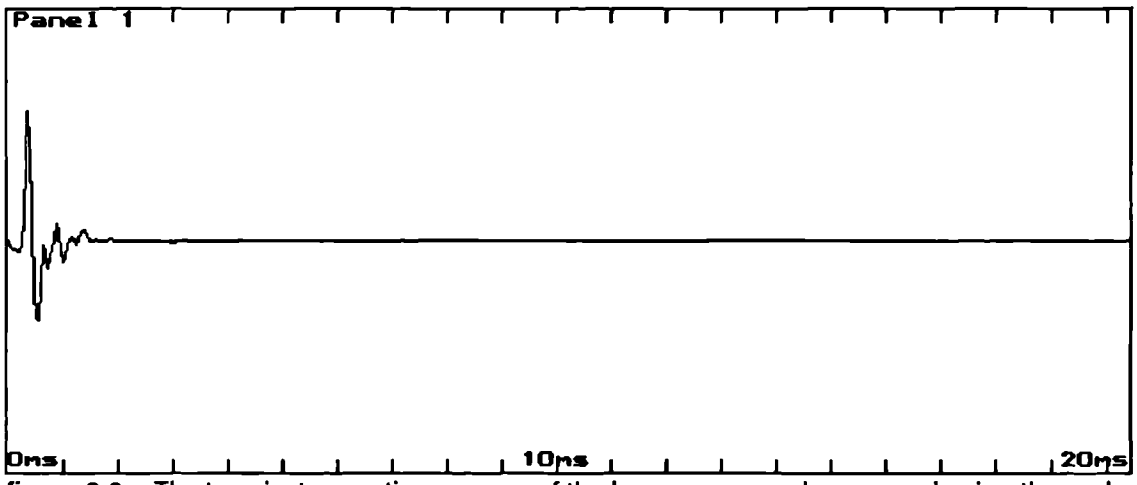

figure 2.9 The transient acoustic response of the human ear canal, measured using the probe and excitation pulse described in the text

Fig.2.10a illustrates exactly the same response data as that shown in fig.2.9, but with an amplification of 32 times. A much smaller, delayed component in the response is observed between 4 and 12ms. This is the part of the transient acoustic response that Kemp showed to be of cochlear origin, and is named the Otoacoustic Emission (OAE). In this example the peak sound pressure in the ear canal at about 8ms (in the centre of the delayed response) is 60μPa. Fig.2.10b shows the transient response of the test cavity under the same amplification as the ear canal data, and exhibits no delayed response. This serves to illustrate that the delayed component (after 4ms) is only present in the ear.

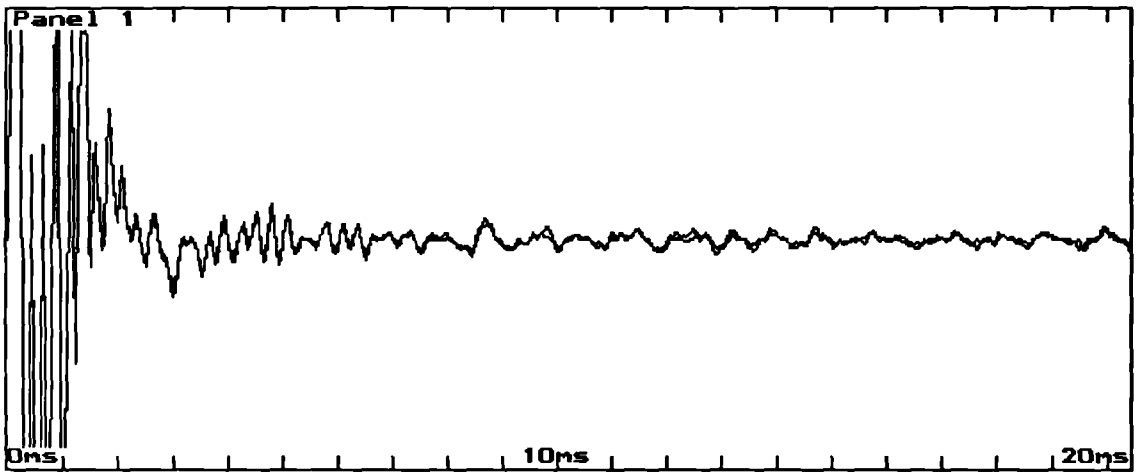

figure 2.10(a) The transient acoustic response of the human ear canal (same data as fig.2.9), under 32 times higher amplification. Two measurements are superimposed to illustrate the reliability of the measurements

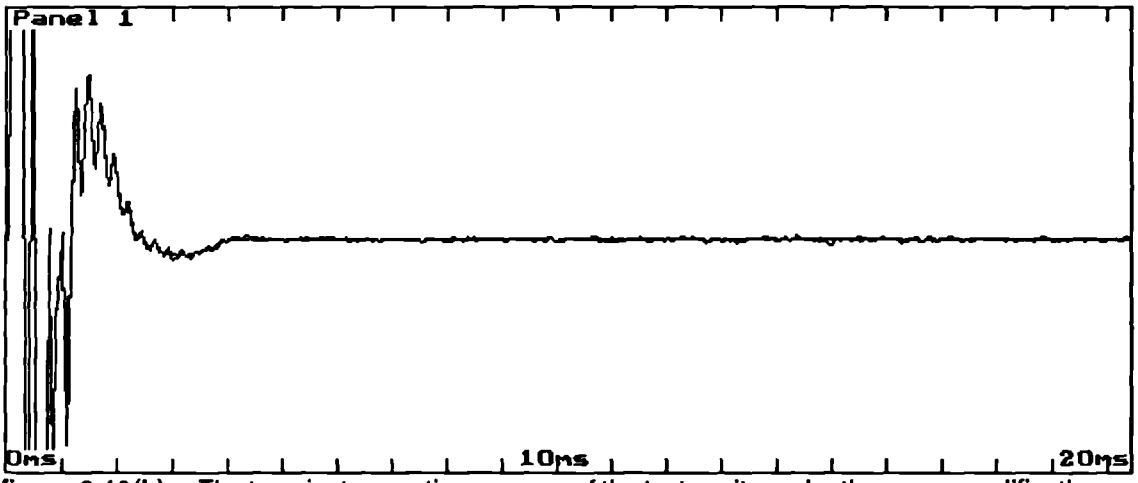

figure 2.10(b) The transient acoustic response of the test cavity under the same amplification as the above figure. Notice the absence of any delayed (beyond 4ms) response.

In Zwislocki's model, the middle ear and cochlea are represented by a set of resonant elements. Early attempts to explain the observed delayed response, referred to the resonant elements within the model[23]. For any resonant element to have a long transient response decay constant, the bandwidth of resonance must be narrow. Furthermore, for an electrical analogue (such as a transmission line) to reproduce a wide band delayed response (e.g. for 10ms up to 3KHz, as in the OAE) it must consist of many reactive elements (e.g. approximately 20 second order elements are required to achieve up to a 2KHz bandwidth). The Zwislocki model, containing only 5 elements, cannot produce a response of this delay and bandwidth.

Furthermore, the decay constants of the initial and delayed transient responses observed in the ear canal are dissimilar. The initial transient decays with a time constant of approximately 1ms, whereas the delayed response has a time constant in the order of 10ms. It is possible to devise an electrical analogue which has an increasing time constant, with time, but the circuit would have to contain a highly resonant element which is lightly coupled (i.e. through a high impedance) to a more highly damped resonant element. No such highly resonant, lightly coupled elements exist in the middle ear.

2.5 A method for separating the ear canal and cochlear contributions of the transient acoustic response.

The initial response, in the example shown in fig.2.9, is a fast decaying oscillatory ring, attributable to the middle ear, whereas the delayed response emanating from the cochlea, shown in fig.2.10a (same data amplified), is a sustained waveform containing many different wavelengths (i.e. a wide bandwidth). The initial transient response is well understood (as illustrated by its accurate prediction by the Zwislocki model), but the complex, wide band, delayed response originating from the cochlea was not measured until 1978 by Kemp, and is not predicted by Zwislocki's model.

In order that the acoustic properties of this delayed response from the cochlea can be studied, a separation of the initial ear canal response, and the delayed cochlear response needs to be performed. One approach to this problem is to separate the two responses in time. This is performed by choosing a time at which the initial ear canal response has decayed to below the level of the cochlear contribution (a suitable time being 4 or 5ms). This method, used by Kemp and others, has two major setbacks. Firstly, the initial response of the ear canal can vary considerably with different fittings of the probe in the ear canal, leading to difficulties in predicting the end of the ear canal transient response. Secondly, the delayed response from the cochlea could conceivably start before the end of the initial response of the ear canal, resulting in either contamination of the separated cochlear response, or some loss of the response by later separation.

A more rigorous approach to separating the ear canal and cochlear contributions would be to distinguish the cochlear component by ascertaining a unique property of the delayed component. This possibility emerged from the study of the relationship between the excitation input and the response size. If the OAE is in fact of physiological origin, then it would be expected to exhibit non-linear growth in response to increasing excitation. This property would offer an effective means of separation of the two components. In order to exploit this, a careful study of the growth of the response to increasing excitation must be performed.

By varying the intensity of the signal delivered to the loudspeaker in the probe, a study was performed on the relationship between excitation intensity and the amplitude of the delayed response. A series of transient responses were taken from the same ear, with the stimulus intensity as the only variable. The intensity of the excitation pulse ranged from the predetermined operational maximum of the loudspeaker in the probe, in 6dB steps, down to a level at which the delayed response was no longer discernible amongst the background noise of the measuring equipment, allowing a range of measurements of almost 50dB. The excitation intensity in the ear canal was

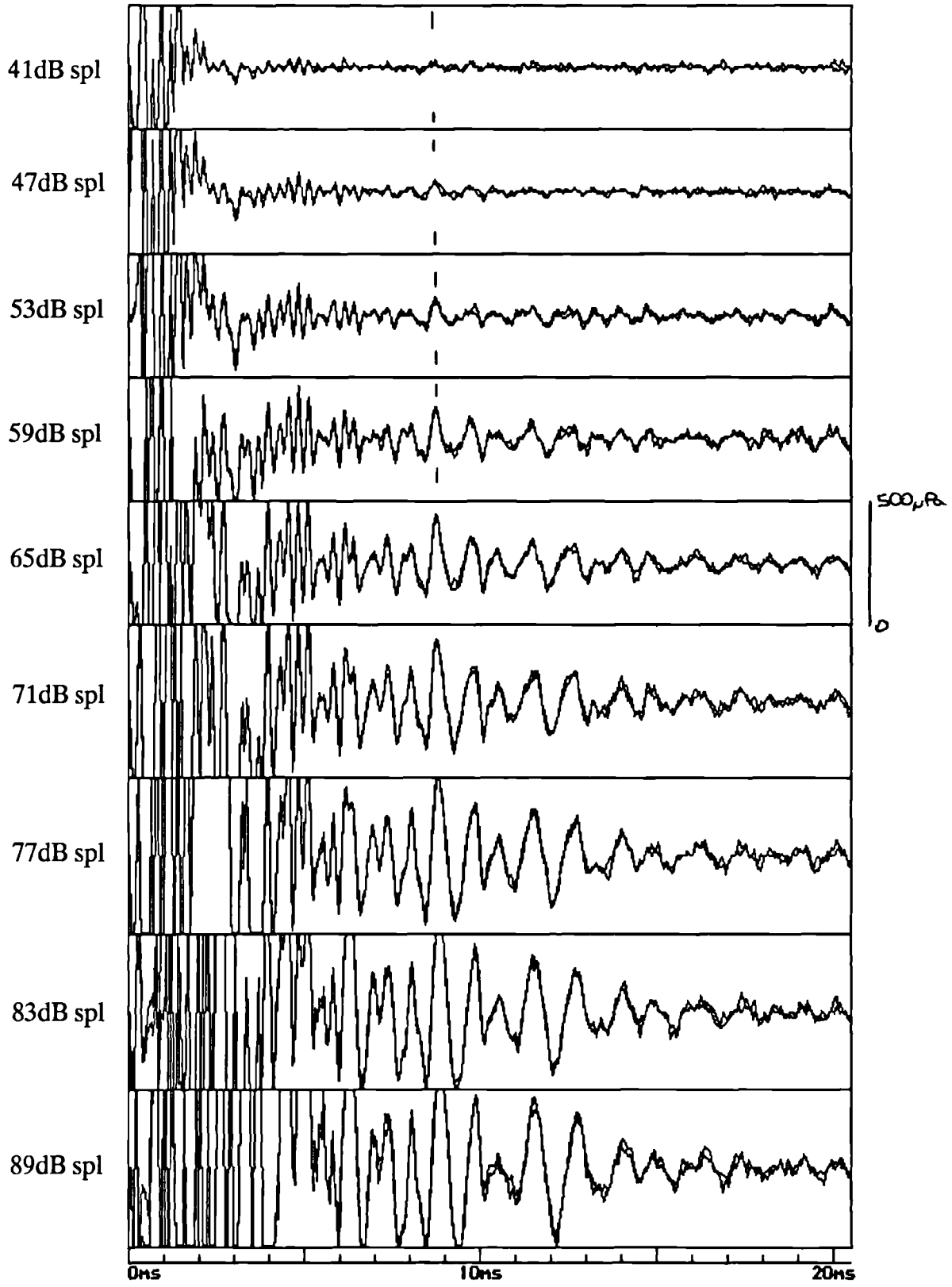

figure 2.11 This figure shows a series of transient acoustic responses recorded from the same ear canal. The excitation pulse was increased in size by 6dB between each recording. The figures at the left hand edge of the data indicates the actual peak size of the excitation pulse in dBspl. All the responses are displayed under the same amplification, permitting a visual analysis of the growth rate of the delayed response to increasing excitation.

measured for each level by the microphone in the probe, and expressed in dBspl of the peak pressure excursion of the transient. Measured in this way, the resulting excitation intensities ranged from 41 to 89dBspl.

The initial section (i.e. 0-3ms) of the transient response, which is the response of the middle ear and ear canal, grew in a linear manner (this is not represented on fig.2.11 due to limited space) that is for each 6dB increase in excitation applied to the ear, the initial response doubles in size. Fig.2.11 shows the measured responses, after the initial transient, at the various levels of excitation. The data is amplified to show the detail of the delayed response. The delayed response clearly increases with increasing excitation, and most features of the response waveform can be seen to correspond with the responses at the other excitation intensities.

Examination of the delayed responses reveals less than linear growth. The quantitative description of this nonlinearity requires selection of appropriate descriptive parameters. As the middle ear transient response is a simple, fast decaying waveform which behaves in a predictable, linear manner, it is acceptable to quantify the initial response in terms of the peak pressure excursion (this holds for any set of transient measurements performed on the ear canal if the excitation intensity is the only variable). Fig.2.12 illustrates the study of the growth of a single peak in the delayed response (at 8.7ms delay), versus the stimulus intensity (this peak is illustrated on fig.2.11). A line respresenting a linear growth (i.e. like the stimulus) is drawn on to the graph. The delayed response, when represented by a single peak, clearly departs from linearity as a result of increasing stimulation. This nonlinearity takes the form of a saturation of the response at higher intensity stimulation.

The delayed response is, however, a more complex waveform with no obvious single feature with which it could be represented. A waveform peak can be chosen, but until the delayed response is proven to behave in a linear and predictable manner, this may well prove to be unrepresentative of the response.

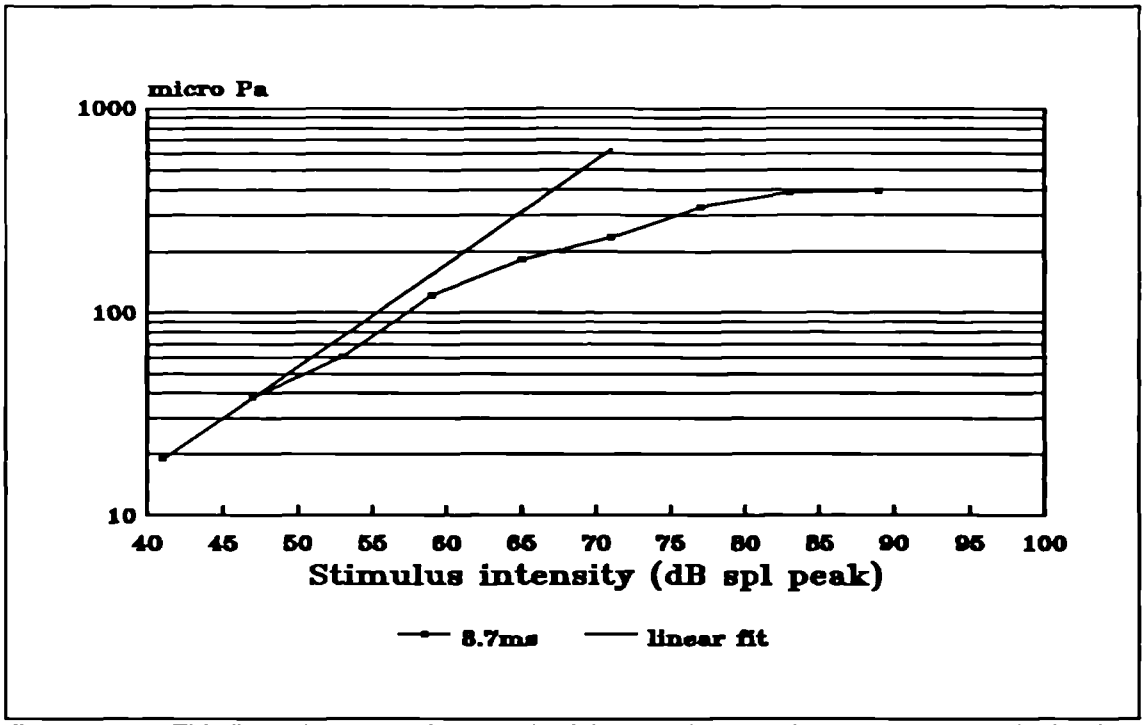

figure 2.12 This figure illustrates the growth of the waveform peak present at 8.7ms in the data shown in fig.2.11 as a result of increasing the excitation pulse. A straight line has been added to the graph to permit a comparison with linear growth.

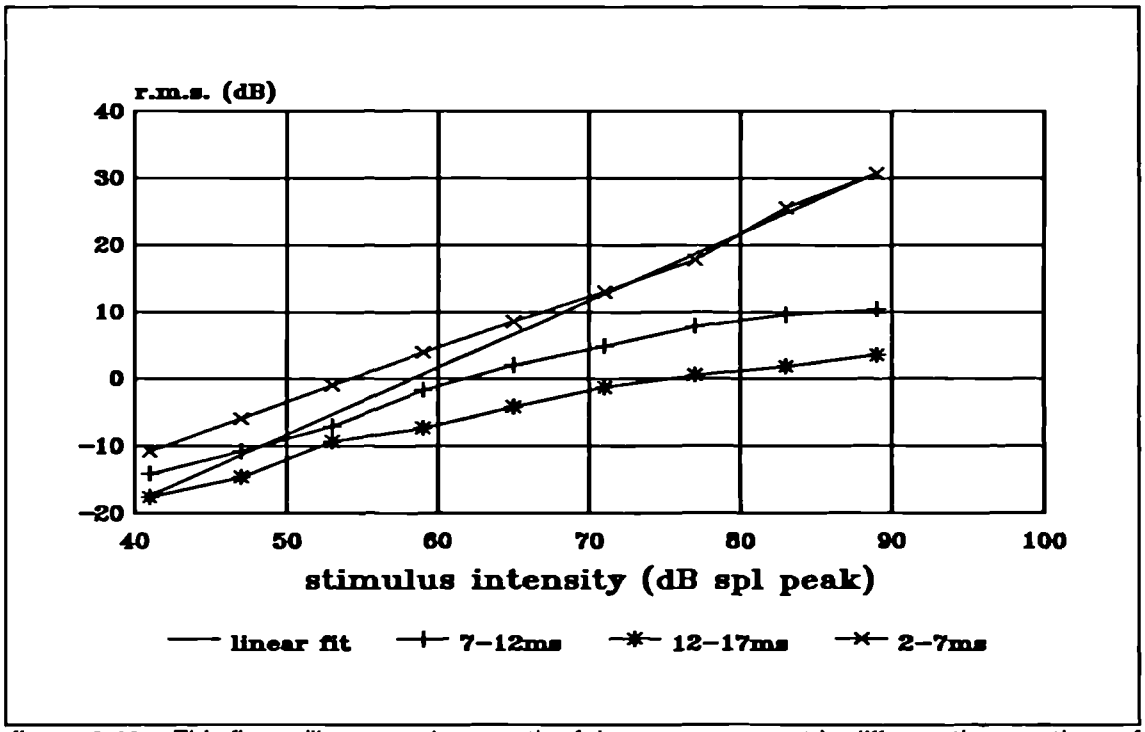

figure 2.13 This figure illustrates the growth of the energy present in different time sections of the response waveforms (shown in fig.2.11) as a function of increased excitation. A straight line has been added to illustrate linear growth.

A more rigorous analysis was performed. Using rms calculations on sections of the response waveform, the relative growths of the various sections to increasing stimulation could be studied. Three sections of the response were chosen (2-7ms, 7-12ms and 12-17ms). The rms of each section, expressed in dB, was plotted versus the stimulus intensity (see fig.2.13). Again, a line representing linear growth to the stimulus was added to the graph. The growth of the two later sections both exhibited saturating nonlinearity similar to that which is illustrated in fig.2.12. The rms of the earliest section of the response (2-7ms) exhibited nonlinearity to low level stimulation, but at the higher levels the rms grows linearly (i.e. in the same way as the stimulus input). This is due to the 'tail' of the initial transient response encroaching into the 2-7ms section at higher intensities of stimulation.

Definition of the 'derived nonlinear response'.

As the data in fig.2.13 shows, the delayed section of the transient response can be distinguished from the early section by its departure from linearity to increasing levels of excitation. This characteristic of the delayed response provides the more rigorous method of separation of the two components of the response. We will define a 'derived nonlinear response' as the component of the response which departs from linearity (to excitation level). This derived nonlinear response contains the delayed components and none of the initial linear response.

2.6 The derived nonlinear measurement technique.

Because the initial transient response grows in a linear manner, it is possible to perform a measurement at any given level of excitation and predict the response at any other level of excitation by calculation. At all levels of excitation the initial transient response is greater in amplitude than the delayed response, and due to the saturating nonlinear growth of the delayed component, this becomes more extreme at higher levels. Therefore, a measurement of the transient response at a high level of excitation allows detail of the initial response to be most accurately estimated. If a

second measurement of the whole transient response is then taken at a substantially lower level of excitation, the initial response can be predicted from the original measurement at high excitation based on a linear growth assumption. Upon subtraction of the predicted initial low level response (i.e scaled by calculation) from the actual low level measured response, all the linear response is perfectly cancelled. However, the response measured at the lower level of excitation contains proportionally more of the nonlinear delayed response, and therefore, upon subtraction, a residual delayed response remains. The amplitude of the residual delayed response is a function of the saturating nonlinearity of the delayed response. This component is the 'derived nonlinear response', obtained by a method of scaled subtraction.

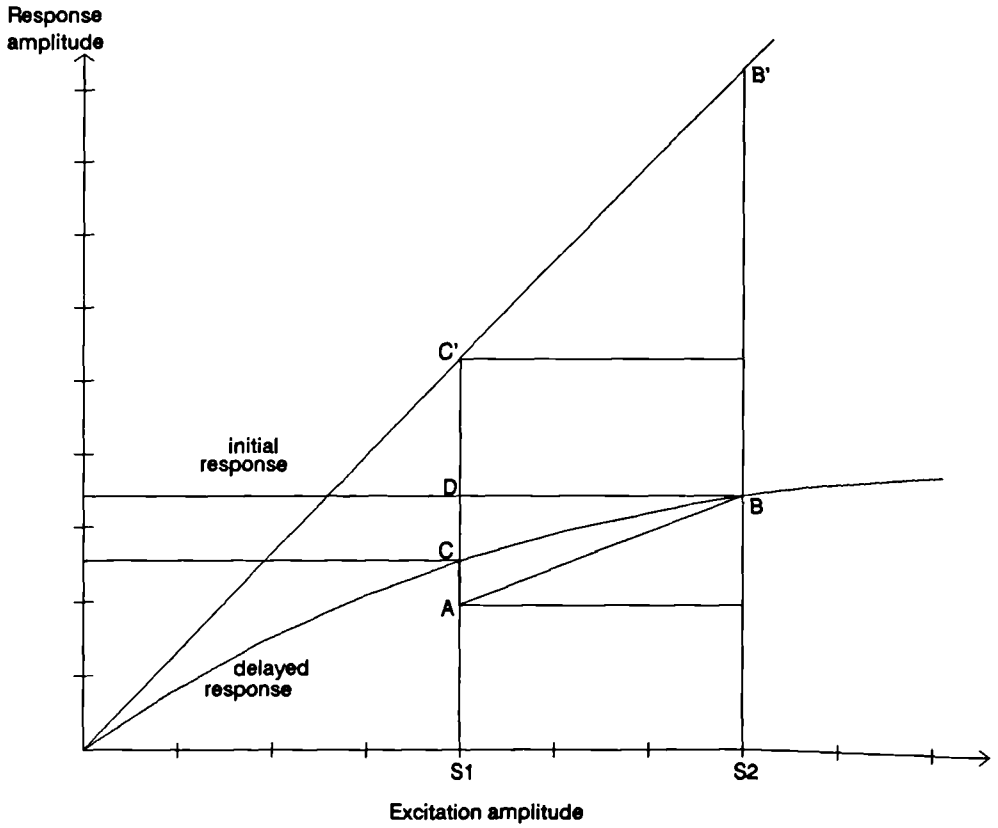

figure 2.14 Theoretical amplitude growth of the initial and delayed components of the transient acoustic response of the ear canal. The initial response, passing through the origin, C' and B', is completely linear, whereas the delayed response (origin, C, B) is tending towards saturation at the higher levels of excitation.

This technique of scaled subtraction can be further illustrated and developed with the aid of a diagrammatic example of the amplitude of the initial and delayed response plotted versus the excitation input (see fig.2.14). Drawn onto the graph are the amplitude values of the initial response (C' and B') and delayed response (C and B), as a result of the two levels of excitation (S1 and S2). As the initial response is linear, we can measure the initial response at any level (say S2 yielding B') and exactly predict the initial response at any other level (say S1 yielding C'), by scaling according to the relationship of S2 to S1. The straight line (from B to A) through the value of the delayed response (B) at the higher level of excitation (S2) represents the hypothetical decrease of the amplitude of the delayed response if it too had been linear, and the same scaling process had been applied. The predicted amplitude of the delayed response to lower excitation can be calculated (A). However, the measured amplitude (C) of the response at the lower level of excitation yields a value above the predicted one.

Therefore, after the application of the scaled subtraction technique to the two transient response measurements, the initial linear response is entirely cancelled, and a residual response remains which has an amplitude of AC. As the figure shows, the length of the quantity AC depends upon the nature of the departure from linearity, and which excitation intensities are chosen. Clearly, if S1 and S2 are equal then the derived nonlinear response is zero. Also, as S2 is increased to very high levels, the derived nonlinear response becomes a more accurate measure of the true nonlinear response. In practice, the use of high levels of excitation is limited by the probe transducers, and out of respect for the ears of the test subject. For any reasonable and different levels of excitation (S1 and S2), the derived nonlinear response will contain a substantial proportion of the signal of interest, the amount being dependent upon S1 and S2.

As the residual response of the scaled subtraction technique is dependent on the levels of excitation (S1 and S2), further consideration must be given to the selection

of suitable values. If the delayed response amplitude was completely saturated (i.e. the response amplitude was always the same level, independent of the excitation used), then irrespective of the chosen levels of excitation (S1 and S2), the amplitude of the derived nonlinear response would be dependent only upon the difference in excitation levels, and could be described by the equation AC = C(1-(S1/S2)). Therefore, the largest derived nonlinear response is obtained when S2 is much greater than S1. However, as the real data in fig.2.13 shows, the curve is closer to linearity at low levels of excitation, and at the higher levels a greater departure from linearity occurs. Therefore, to obtain the largest derived nonlinear response, the two measurements must be performed at higher levels of excitation. Therefore, both S1 and S2 must be high.

This nonlinear measurement technique has the advantage of completely eliminating any components of the transient response which are not affected by any nonlinear physiological processes. However, in the case of real data, the response is not completely saturated as excitation is increased, and therefore in the process of cancelling the linear response, part of the cochlear response is also eliminated. With reference to fig.2.14, the amplitude of the discarded portion of the response is represented by the quantity CD.

2.7 Implementation of the scaled subtraction technique.

A practical implementation of the scaled subtraction technique involves measuring the transient response of the ear canal at two different levels of excitation. In the real world of data collection the signal to noise ratio is not infinite. The need to observe the fine detail present in the transient response obviates the use of averaging to increase the signal to noise ratio. However, the measured noise for any given instrument conditions present in the transient response is independent of excitation level (although we do not know if the intrinsic noise of the cochlea is independent of excitation level). The signal to noise ratio of the averaged response is dependent upon

the noise level and the number of averaged responses. Because the measured noise is constant with excitation, and the response size is a function of excitation level, the signal to noise ratio is also a function of the excitation level.

However, the scaled subtraction technique introduces another influence upon the signal to noise ratio of the resulting averaged response. More specifically, due to the scaling of the data before subtraction, the signal to noise ratio of the derived nonlinear response is affected by the ratio of the number of averages at each level of excitation. An investigation into this effect, and a theoretical assessment of the optimum choice of excitation levels is necessary to achieve the highest quality of derived nonlinear response.

2.8 Optimisation of the scaled subtraction technique.

The signal to noise ratio of the averaged derived nonlinear response can be theoretically investigated, and from this investigation conclude an optimum relationship between the two levels of excitation and the optimum ratio of measurements taken at these two levels. The outcome of this optimisation is to acquire the highest quality of response measurement in a given amount of time or, conversely, to obtain the necessary quality of response measurement in the shortest time.

By deriving a general expression for the signal to noise ratio of the derived nonlinear response, it is possible to determine the effect of changing the relative sizes of the two excitation levels and the relative numbers of measurements taken at each level. Certain assumptions were made to facilitate the derivation of the equation. For example, the noise level in each measurement is assumed to be independent of the excitation level.

Consider two levels of excitation S1 and S2. The number of responses measured at these two levels are NS1 and NS2 respectively. Each measurement contains a part of the response (SL) which behaves linearly to excitation level, a part of the response

which does not behave linearly (R), and a quantity of noise (N). If we assume that SL is the linear component at the level of excitation S1, then the linear component in the response at the excitation level S2 is given by SL*S2/S1. Also if we assume for this calculation that the nonlinear component (R) is totally saturated, then both R and N are independent of the excitation.

Therefore after summing NS1 responses at the excitation level of S1, the entire summed response contains the following quantities of components.

$$NS1*SL + NS1*R + (NS1)^{1/2}*N$$

Similarly, after NS2 sums of the response at excitation level S2, the summed response is described by,

$$NS2*(S2/S1)*SL + NS2*R + (NS2)^{1/2}*N$$

The technique of scaled subtraction involves scaling the summed response at one level of excitation so that the linear components at both levels equate. Therefore a scaling factor must be applied to one of the above equations so that the linear component SL can be equated. Thus,

$NS2*(S2/S1)*SL = NS1*SL*K$ where K is the scaling factor.

Therefore $K = (NS2/NS1)*(S2/S1)$

The scaling factor K is used to multiply the summed response to excitation level S1, and the various components are subtracted. As a result the linear component SL cancels, leaving the quantities represented by the equation below.

$$\underbrace{(NS2*R - K*NS1*R)}_{\text{Signal}} + \underbrace{(\sqrt{NS2}*N - \sqrt{NS1}*N*K)}_{\text{Noise}}$$

This leaves a residual component which has a proportion of the nonlinear response R and a quantity of summated noise. Therefore, if we divide the residual terms

containing R by those containing N, we have defined the signal to noise ratio. Furthermore we can define a term NT which is the total number of measurements (i.e. NS1 + NS2). The equation is generated and reduced in the steps below.

$$\frac{\text{Signal}}{\text{Noise}} = \frac{NS2*R - K*NS1*R}{\sqrt{NS2}*N - \sqrt{NS1}*N*K}$$

$$= \frac{R*NS2*(1-\frac{S2}{S1})}{\sqrt{NS2*N^2 + NS1*N^2*\frac{NS2^2}{NS1^2}*\frac{S2^2}{S1^2}}}$$

$$= \frac{R*NS2*(1-\frac{S2}{S1})}{N*\sqrt{NS2*(1+\frac{NS2}{NS1}*\frac{S2^2}{S1^2})}}$$

$$\propto \frac{NS2*(1-\frac{S2}{S1})}{\sqrt{NS2*(1+\frac{NS2}{NT-NS2}*\frac{S2^2}{S1^2})}}$$

Using this equation we can investigate the effect of varying the proportion of NS2 to the total NT for any ratio of excitation levels. Fig.2.15 shows a series of curves for a ratio of excitation levels of 3:1, generated by a Pascal programme which implements the above equation. The series of curves are produced by varying the total number of measurements (NT). The tick on the X axis is the point at which the ratio of NS2 to NS1 equates to the ratio of S1 to S2. This point coincides with the maximum of the signal to noise ratio for each curve, and although not shown, this is generally the case for any ratio of excitation levels (similar families of curves can be produced for different ratios of excitation level). Therefore, **the optimum ratio of measurements at each level of excitation is inversely related to the ratio of the excitation levels.** For example, if the ratio of excitation levels is 10 to 1, then the maximum signal to noise ratio is achieved when the ratio of the number of measurements added at these two levels is 1 to 10 (and therefore no scaling of the responses is required before subtraction).

Fig.2.16(a) shows a series of curves generated by the same equation, but with a fixed total number NT (i.e. fixed total measurement time), and the ratio of the two

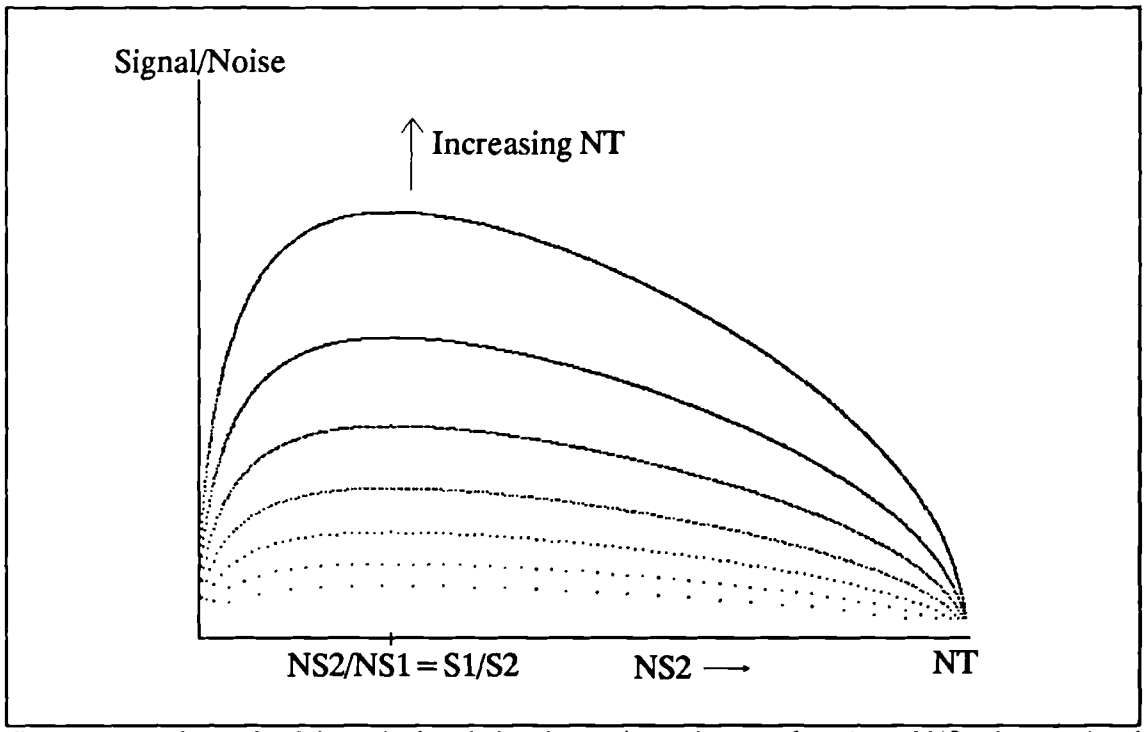

figure 2.15 A graph of the calculated signal to noise ratio, as a function of NS2, for a ratio of stimuli levels of 3 to 1. The peak in the curve occurs at the point where the ratio of NS2 to NS1 is equal to the ratio of S1 to S2.

excitation levels as the variable. In this particular figure the ratio varies from 1:12 to 12:1. The locus of the maximum points of the curves is drawn in fig.2.16(b). This indicates that the signal to noise ratio is greater when the difference between the two levels of excitation is greatest. This would suggest that a very high and very low level of excitation would best be employed. However, in the case of the real data shown in fig.2.11 and fig.2.12, it has already been discussed that the use of a low excitation level yields less derived nonlinear response (due to the increased linearity at lower levels). Therefore, the equation must be modified to include a more realistic growth behaviour of the nonlinear component (rather than the previous assumption of complete saturation), in order that the optimum excitation ratio can be more realistically predicted.

A simplistic representation of a saturating nonlinear response is given by the equation $R = (S)^n$, where n is between 0 and 1. With reference to the data shown in fig.2.13, the function approximates to $R = (S)^{0.5}$. Therefore if R1 and R2 are the

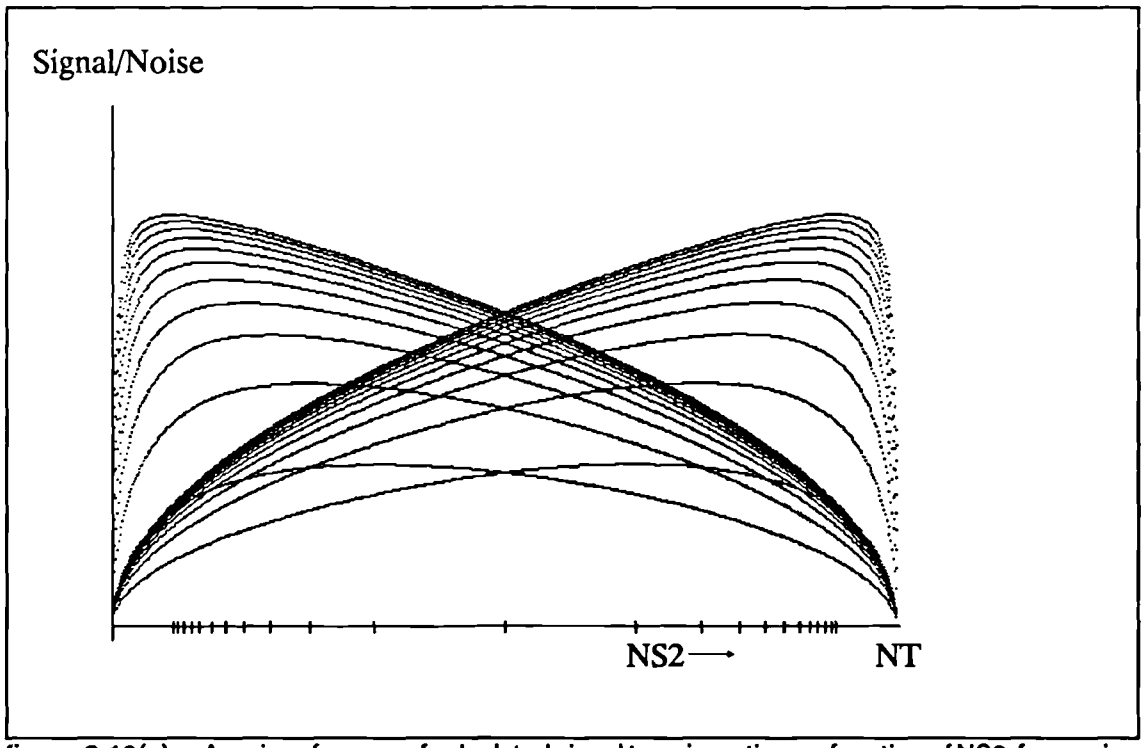

figure 2.16(a) A series of curves of calculated signal to noise ratio as a function of NS2, for varying ratios of excitation level (S2 to S1). The total number of averages (NT) is the same for each curve. The ticks on the x-axis are the x-values for the maximum of each curve, as described in the previous figure.

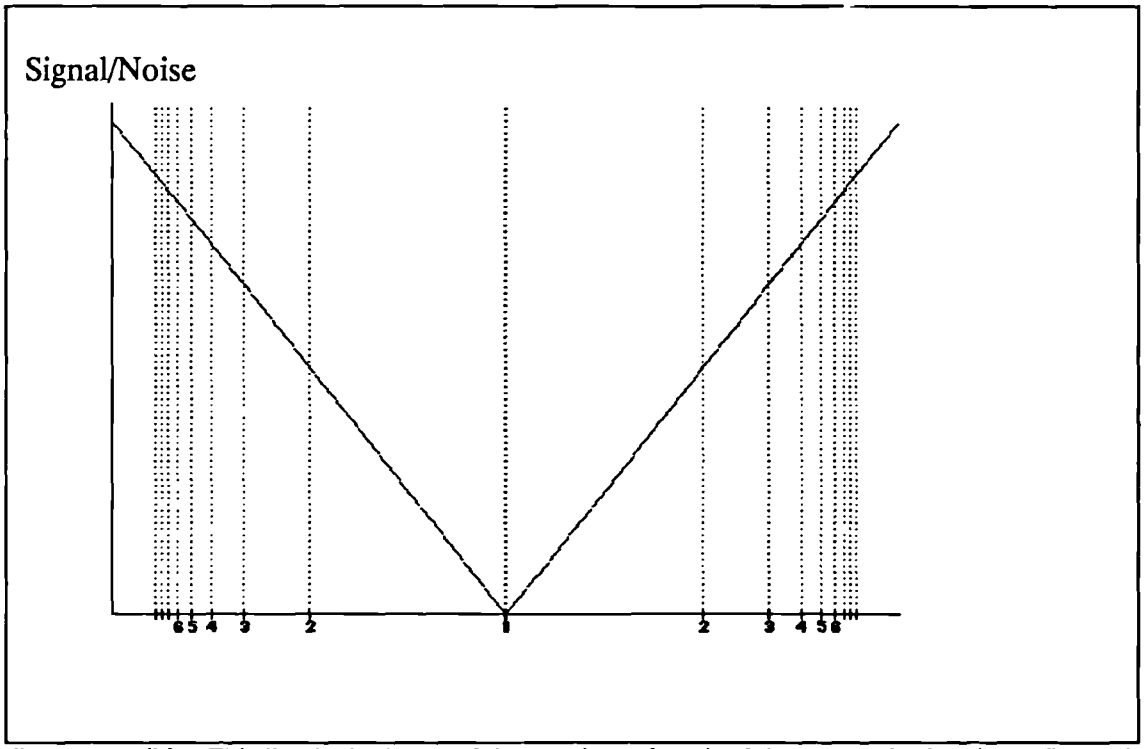

figure 2.16(b) This line is the locus of the maxima of each of the curves in the above figure. It therefore indicates the maximum signal to noise ratio for a given NT, as the ratio of excitation levels is varied. The x-axis is the ratio of S2 to S1 and extends from 30:1 to 1:30.

nonlinear responses at excitation levels S1 and S2, then $R2 = R1*(S2/S1)^{0.5}$. This elaboration can be included in the signal to noise equation, which then takes the form,

$$\frac{\text{Signal}}{\text{Noise}} \propto \frac{NS2\left(\sqrt{\frac{S2}{S1}} - \frac{S2}{S1}\right)}{\sqrt{NS2*\left(1+\frac{NS2}{NT-NS2}*\frac{S2^2}{S1^2}\right)}}$$

This equation still yields a maximum in the signal to noise ratio when the ratio of the number of samples at each level of excitation is the inverse of the ratio of excitation levels. The plot of the locus of the maximum of each curve, for different levels of excitation, is shown in fig.2.17.

The curve shown in fig.2.17 has several features requiring careful examination. This graph has been derived in the same way as fig.2.16, by plotting the maximum of each curve of the signal to noise (for a fixed total number of averages NT), as the ratio of excitation levels is varied. The X-axis is the ratio of S2 to S1 as it ranges from 1/600 to 600. At unity (in the centre) the curve shows that the signal to noise ratio is zero as expected (due to the fact that if the two levels of excitation are the same then the derived nonlinear response does not exist). The reason that the curve is not symmetrical about this point is due to the original derivation of the equation and the variables chosen. Effectively S1 is fixed and S2 is varied. As can be seen from the curve, for very high ratios of S2 to S1, (i.e. the right hand end of the curve, when S2 is much greater than S1) the signal to noise ratio is high. This is because the nonlinear component of the response is a more saturated function at higher levels (as defined by the equation $R = (S)^{0.5}$). Therefore at very high levels of S2, the curve approaches that of the one in fig.2.16(b), when the response was assumed completely saturated. On the opposite side of unity (i.e. when S2 is smaller than S1), the level of S2 tends towards zero. As S2 becomes smaller, the gradient of the curve $R = (S)^{0.5}$ becomes steeper, thus for a given decrease in S the decrease in R is greater than at higher levels of S. As a result of this, the derived nonlinear component decreases in size as lower levels of excitation are used. As can be seen from the fig.2.17, the signal to noise ratio has a peak value

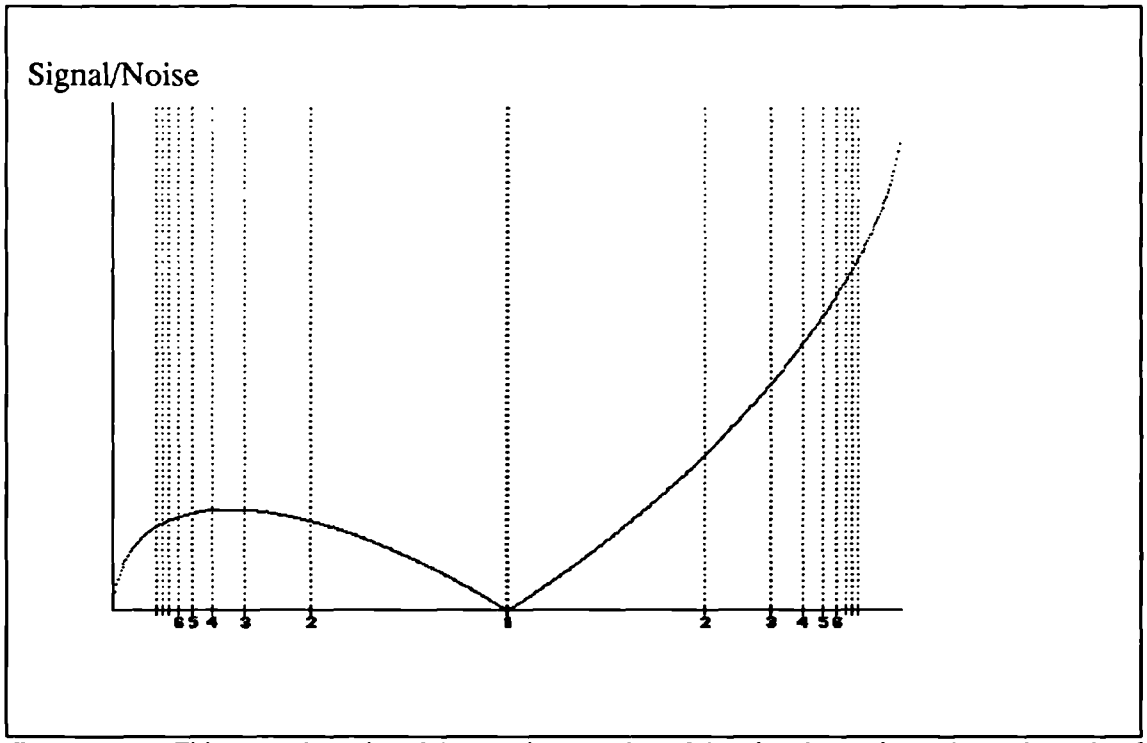

figure 2.17 This curve is a plot of the maximum value of the signal to noise ratio as the ratio of S2 to S1 is varied from 1:600 to 600:1. This curve is derived in the same way as that in fig.2.16(b) except that the equation has a more realistic growth of the delayed response(see text).

and then decreases as S2 gets smaller. The right hand side of the curve shows that the higher signal to noise ratios are obtained by selecting higher levels of excitation. The left hand side of the curve shows that having selected the upper excitation level, there is an optimum selection for the level of the lower excitation level. The upper level of excitation is limited by the constraints of the transducers and the comfort of the subject, and therefore the low level of excitation has to be chosen which yields the maximum signal to noise ratio. From the data shown in fig.2.17 this ratio is approximately 3.5:1. This value obviously depends upon the relationship of R to S.

In conclusion, this analysis indicates that the optimum signal to noise ratio is obtained when the ratio of measurements at the high and low levels of excitation is the inverse of the ratio of the excitation levels. In addition, when an approximation of the behaviour of the real growth rate of the nonlinear component is included in the equation, the maximum signal to noise ratio is obtained when the ratio of excitation levels is 3.5 to 1.

2.9 A practical example of the scaled subtraction technique.

As an illustrative example of the scaled subtraction technique, the transient response of the human ear canal has been measured at two different levels. The ratio between the two levels of excitation is 3:1. Fig.2.18 shows the process of nonlinear response derivation using the scaled subtraction technique. The upper trace (a) shows the transient response at the higher level of excitation (68dBspl peak). Trace (b) is the transient response to the lower level of excitation (58.5dB spl peak). As the analysis above indicates, the optimum signal to noise is achieved when the ratio of measurements is the inverse of the excitation ratio. Therefore, three times as many summations of the transient response at the lower level of excitation need to be performed. Trace (c) is the transient response at the lower level of excitation after

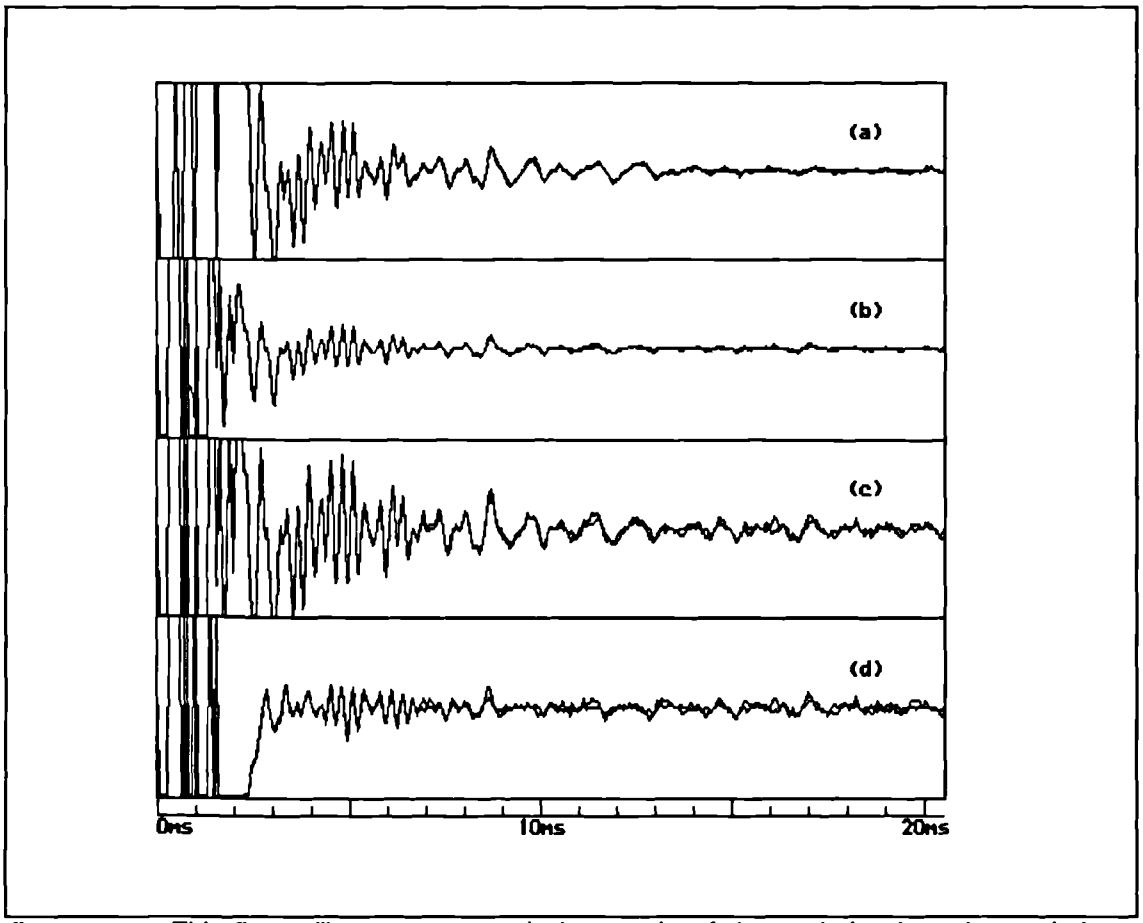

figure 2.18 This figure illustrates a practical example of the scaled subtraction technique. Waveforms (a) and (b) are two transient responses due to two levels of excitation 9.5dB different in intensity (i.e. a 3:1 ratio). Waveform (c) is the average of 3 responses to the smaller stimulus. The difference between (c) and (a) is calculated and displayed as waveform (d). Waveform (d) only contains components of the transient response which do not grow linearly to increased excitation.

three times as many averages. Trace (d) is the residual response after trace (a) has been subtracted from trace (c). This is the nonlinear derived response.

In addition to the residual delayed nonlinear response, the figure illustrates that a nonlinearity is present during the first 2-3ms. This is an artefact which is present due to the dynamic range limit of the measuring system. During the transient response measurement, the amplified signal from the microphone of the probe is digitised using a 12 bit ADC. At the high levels of excitation required (so that the delayed response is more saturated), the dynamic range of the 12 bit ADC is insufficient to accurately measure the small delayed response as well as the much larger initial transient. Therefore, the ADC becomes a source of extreme saturating nonlinearity to large signal levels, resulting in the large derived nonlinear signal exhibited at the early section of trace (d). This overload effect is easily predicted by monitoring when the range of the ADC is exceeded. To remove this artefact the residual response is multiplied by a window which has a gain of zero at the region where an overload of the ADC has occurred, and a gain of unity elsewhere, with a smooth transition between these two states. In practice, this window consists of a blank region for the first 2 or 3ms, and is unity for the rest of the response. After the response has been multiplied by this window the remaining nonlinear response (3 to 20ms) contains a proportion of the signal which originates from within the cochlea.

Properties of the nonlinear Otoacoustic Emission.

3.1 Introduction.

The evoked otoacoustic emission (OAE) is defined as an acoustic signal that can be measured in the ear canal and which originates in the cochlea. As detailed in chapter 2, the use of transient excitation resulted in only partial temporal separation of the excitation signal and the OAE. Complex processing is required to fully separate the response of the middle ear to the excitation signal from the response elicited from the cochlea. In order to achieve this complete separation, a technique was developed based on the nonlinear growth of the cochlear response component to increasing excitation level. This technique requires that measurements be made of the transient response at two different levels of excitation. All the linear components (i.e. the middle ear response) of the transient response are removed by scaled subtraction of the two measurements. The residual derived nonlinear response is a substantial proportion of the true cochlear transient evoked OAE and is specifically engineered to contain no 'contamination' from the middle ear response to the excitation transient.

The derived nonlinear technique allows a study of the properties of the transient response signal component which is of cochlear origin only.[1] Therefore this technique provided a very practical way to study the OAE without continual regard for the problem of differentiating the response of the middle ear from that of the cochlea.

1 As this separation method is based on the nonlinear property of the cochlear component, care was taken not to exceed the operational limits of the measurement system and transducers, as this would have introduced additional nonlinearities.

This chapter details a series of specific investigations of the properties of the transient evoked derived nonlinear OAE. Such an understanding of the derived nonlinear OAE is necessary before specifying an instrument design suitable for the measurement of the OAE signal in the clinical and research environment. A further purpose of this study was to confirm that the derived nonlinear OAE exhibits similar properties to the 'whole' OAE.

General method.

Unless otherwise stated, the OAE responses which are shown and processed are all derived nonlinear responses, obtained by the method of scaled subtraction (chapter 2). This was done to ensure that the studies were performed on the cochlear response, uncontaminated by any components of the response due to the middle ear.

The practical implementation of the scaled subtraction technique used two excitation levels at an amplitude ratio of 3:1 based on the analysis detailed in chapter 2. The optimum ratio of measurements at these two levels is 1:3 (see fig.2.17). Therefore a stimulus 'package' was designed, consisting of 3 stimuli of one size, and 1 stimulus of three times the size. Care was taken during the data collection process to always collect an integral number of stimulus 'package' subaverages. This ensures that the linear components are completely cancelled.

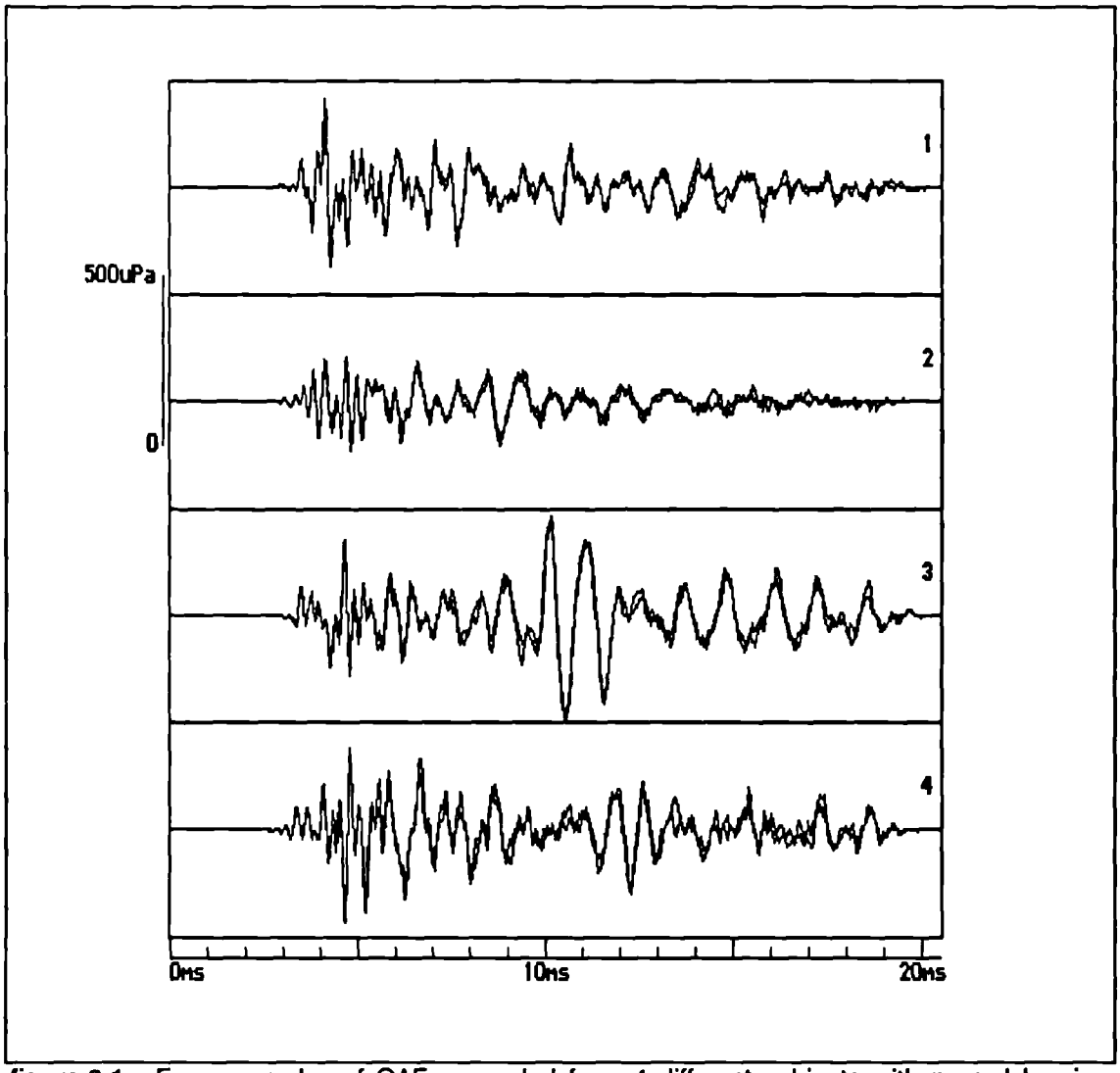

figure 3.1 Four examples of OAEs recorded from 4 different subjects with normal hearing. Although gross features of the waveforms are similar, they each contain unique detail.

General features of the derived nonlinear OAE waveform.

Fig.3.1 shows the OAEs present in 4 ears from 4 audiometrically normal adult subjects. In each case the response is displayed between 3 and 20ms.[2]

2 The residual nonlinearity caused by exceeding the measurement range of the ADC during excitation has been removed by the windowing technique described in chapter 2.

The peak level of the excitation transient in the four examples given was 79dBspl ±2dB.[3] Responses 1 and 2 have the majority of the energy between 4 and 10ms, and have decayed to zero by approximately 18ms. The energy in responses 3 and 4 is more evenly distributed over the whole 3 to 20ms period. The intensity of the four responses is 7.7, 5.2, 11.9 and 9.5dBspl respectively.

In all the examples shown the waveforms contain a range of frequencies. This range can be estimated with reference to the time scale as being between 1 and 4KHz.

In the case of the data shown in Fig.3.1, (and all other acoustic responses in this thesis unless otherwise stated), each response waveform consists of two repeat measurements superimposed. This allows a visual check of the reliability of the measurement proving that the signal is intrinsically stable and repeatable.

Frequency analysis of OAEs.

Fig.3.2 shows the cross power spectra of the OAE waveforms which were illustrated in fig.3.1. Each spectrum contains energy distributed between 500Hz and 5KHz. The spectra have broadly similar energy distributions (i.e. if each spectrum was averaged into 1KHz bands, the spectral densities in each example would be roughly comparable). However, the individual fine details of both the spectra and the waveforms are distinctly different.

The cross power spectrum was obtained by multiplying the two complex frequency spectra of the OAE waveforms. No smoothing was applied to the spectra.

The range of frequencies in these OAE spectra is greater than the spectra of OAEs from normal ears published by other authors[20,35]. There are two possible reasons for this. The frequency response of the acoustic probe used for these measurements

3 The figure quoted for the excitation level is the peak pressure excursion (expressed in dBspl) of the smaller stimulus, as measured by the probe's microphone.

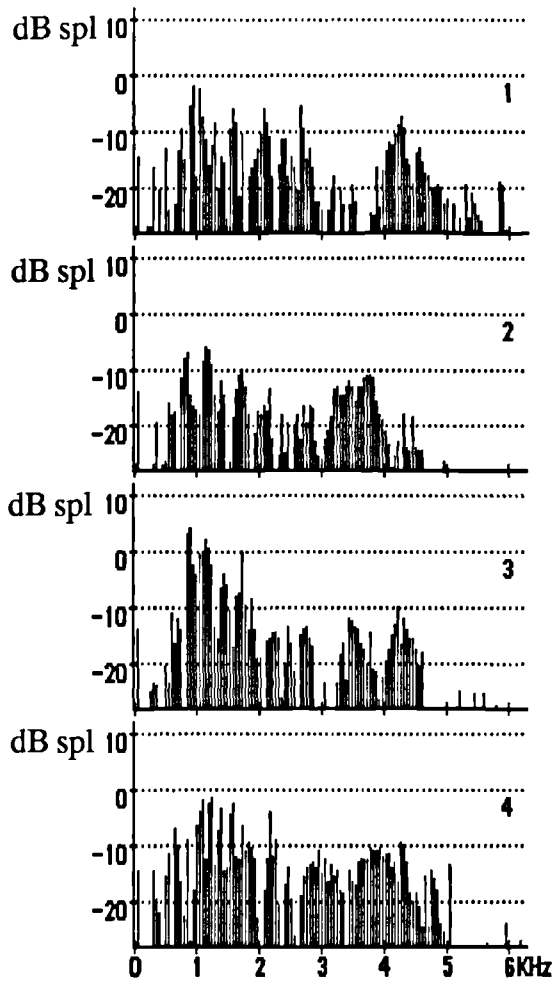

figure 3.2 The cross power frequency spectra of the OAE waveforms shown in fig 3.1.

possibly extended above that of the others. The other explanation relates to the observation that the higher frequency components of the OAE appear to be present at a short pst (see section 3.3). Therefore the nonlinear extraction technique has enabled measurement of these high frequency components of the emission which temporal separation of the whole transient response would not have allowed.

3.2 The effect of excitation intensity upon the nonlinear OAE waveform and frequency spectrum.

3.2.1 Waveform.

There are two advantages of studying the effect of excitation level on the derived nonlinear OAE. Firstly, the derived nonlinear technique allows a study of the whole OAE waveform, including 3-7ms pst which would otherwise be contaminated by the initial transient response of the middle ear, up to a higher level of excitation. Previously reported studies of the growth of the OAE in relation to excitation level relied upon temporal separation of the cochlear and middle ear responses to the excitation. At high levels of excitation the middle ear response can continue for as long as 8ms. Therefore the studies of OAE growth had to be on measurements of the OAE after 8ms.

Secondly, it is also possible to calculate the growth of the whole cochlear component of the transient response from the derived nonlinear OAE based on the assumption of OAE saturation at the highest excitation level.

A series of OAE measurements were taken at different levels of excitation. Fig.3.3 shows the OAE data collected from one ear of an audiometrically normal young adult. The level of excitation ranged from 53dB to 89dBspl (peak) in steps of 6dB[4]. The OAE is just visibly discernible at the lowest level of excitation (trace 1). The size of the OAE response grew more rapidly to increasing stimulation at the lower levels (traces 2, 3 and 4) than at the higher levels, where the response tends towards saturation.

4 The auditory threshold of the stimulus click was at 42dBspl (peak). Therefore the range of excitation was 11 to 47dBSL

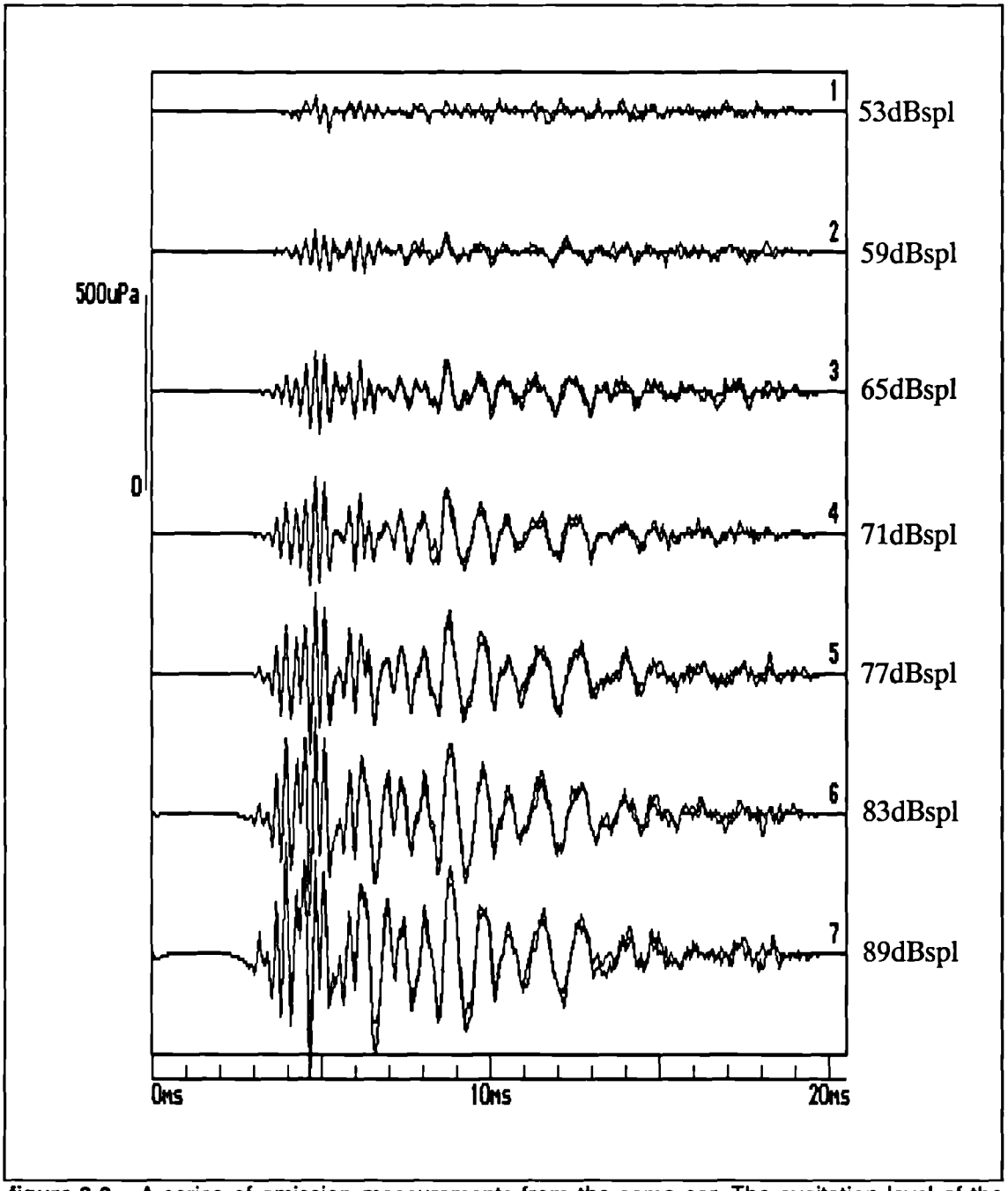

figure 3.3 A series of emission measurements from the same ear. The excitation level of the smaller stimulus ranged from 53 to 89dBspl peak, in steps of 6dB.

The lower trace in fig.3.4 is the growth of the derived nonlinear OAE to increasing excitation. The curve was derived from the data shown in fig.3.3. The size of the OAE is expressed as an intensity by calculating the 'root mean square' (rms) of the waveform

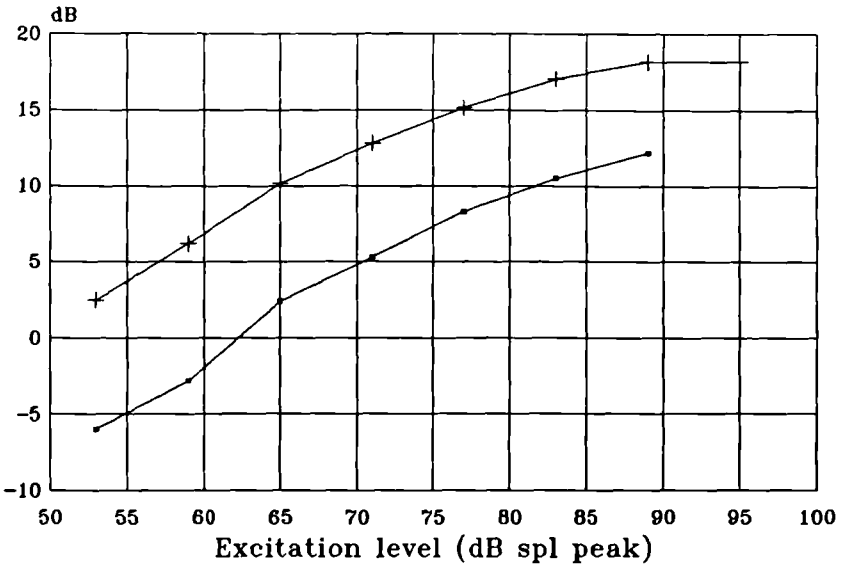

figure 3.4 The lower curve demonstrates the growth of the intensity of the derived nonlinear emission, as a function of excitation level. The top curve is the calculated intensity of the whole cochlear emission (see text).

and converting to dBspl.[5] As observed from fig.3.3, the rate of increase of the size of the response decreased at higher levels of excitation. At all levels the response increased less than the increase in excitation. In the middle of the curve, for every 6dB increase in excitation, the response grew by 3dB (the intensity of the OAE was therefore related to the square root of the excitation intensity). However, at the highest levels of excitation the increase in response was only 2dB for each 6dB (i.e. the response level was related to the cube root of the excitation level).

Although the size of the derived nonlinear OAE is determined by the difference of two measurements of the whole OAE, it is possible to establish the growth of the whole OAE by calculation from the derived nonlinear OAE data. All that is required to complete the information necessary to calculate the amplitude growth of the whole OAE is a measure of the amplitude of the whole OAE at one level of excitation. This

5 The calibration of this spl quantity was achieved by assuming that the OAE is completely saturated.

can be achieved by two methods. Firstly, by measuring the amplitude of the entire transient response at a pst where the response of the middle ear has decayed to insignificant proportions (i.e. at a pst greater than 10ms). This latter section of the transient response can then by matched to the latter section of the derived nonlinear OAE enabling an estimate of the size of the entire cochlear component of the transient response. Secondly, because of the scaling and subtraction of the two transient response measurements, by assuming that the OAE is completely saturated at the highest levels of excitation the derived nonlinear OAE becomes a known proportion of the whole cochlear component of the transient response. Since the OAE does exhibit almost complete saturation at the higher levels of excitation, this latter method was selected.

In this particular implementation of the derived nonlinear technique the nonlinear OAE is derived by adding three responses at one level of excitation and subtracting one response at a level of excitation three times greater.[6] Therefore, if the cochlear response was completely saturated, after performing this averaging process the residual nonlinear response would be half the size of the whole OAE. Assuming that the OAE is saturated, and applying this theory to the data shown in fig.3.4, the intensity of the whole OAE at a level of excitation of 89dB and 95dB was 18.2dB (i.e. 12.2dB + 6dB). By working down in intensity from this known value the whole OAE intensity at all levels was calculated. This calculation was performed by using the equation above in a rearranged form. The intensity of the whole OAE, calculated by this method, is shown in fig.3.4 as the upper curve.

The growth of the whole OAE as calculated by the above method is similar to the plots of the growth of the delayed component of the entire transient response shown in chapter 2 (i.e. as the level of excitation is increased, the cochlear component of the transient response tends towards saturation). As a result of this decrease in OAE

6 E.g. $OAE(nonlinear) = \Sigma 3 * OAE^{(small\ stim)} - OAE^{(big\ stim)}$

saturation at lower excitation intensities, the difference between the whole OAE and the derived nonlinear OAE widens. At the lowest excitation level the difference between the whole and derived nonlinear OAE is 8.5dB as opposed to 6dB at the highest level. This suggests that when measuring OAEs at low levels of excitation (i.e. in a quiet test environment) because of the decreased OAE saturation and the reduction of the contamination from the middle ear response, the advantage of using the derived nonlinear technique is reduced. Temporal separation of the cochlear and middle ear responses results in an 8.5dB larger OAE signal.

3.2.2 Frequency spectrum.

The growth of the OAE to increasing excitation intensity was also observed in the frequency domain. Fig.3.5 shows the cross power frequency spectra of the same series of OAE responses illustrated in fig.3.3. The frequency spectrum of the OAE grew to increasing stimulation, as expected, and all the spectra have similar underlying features. An analysis of the growth of two frequency points within the spectrum was performed. The frequencies 1.1KHz and 3.8KHz were chosen as they represented peaks in the OAE frequency spectrum and therefore could be measured accurately at the low levels of excitation. Fig.3.6 shows the graph of the growth of these spectral points. The growth rates of these two frequency components compares to the previous analyses of the growth characteristics of the OAE.

In summary, the **average** growth of the derived nonlinear OAE is approximately 3dB for each 6dB increase in excitation. But at the higher levels of excitation, the growth of the OAE tends towards saturation. In fig.3.6, the 3.8KHz curve increases less than 1dB for a 6dB increase in excitation at the highest level of excitation.

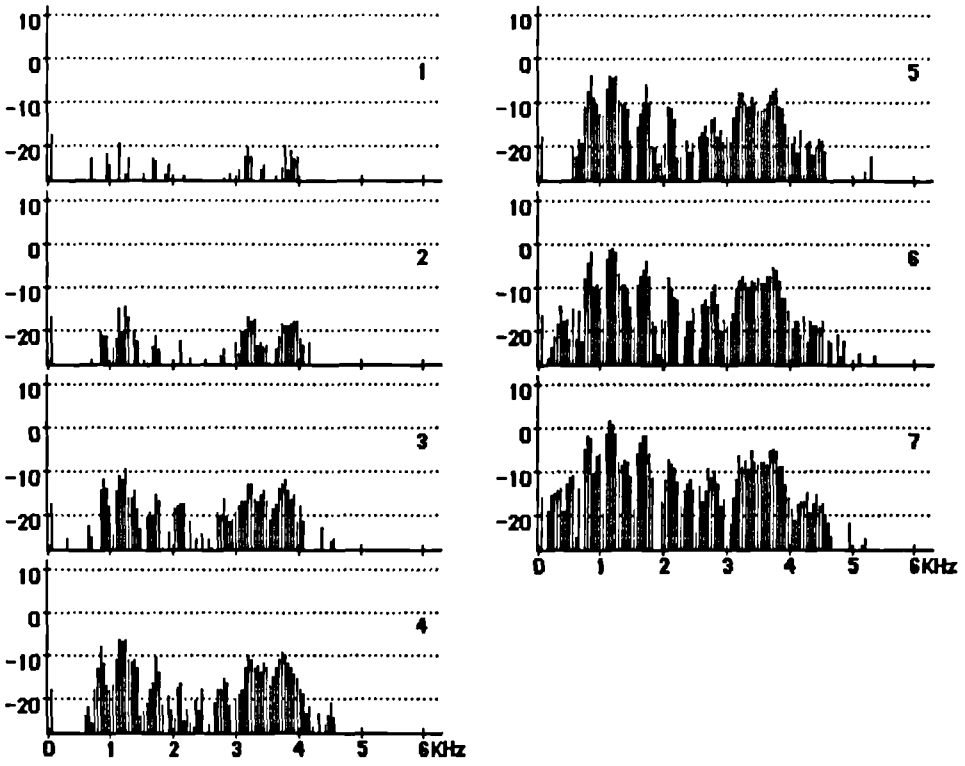

figure 3.5 The seven cross power spectra in this figure are calculated from the emission waveforms displayed in fig.3.3 (i.e. the stimulus increase between each measurement is 6dB).

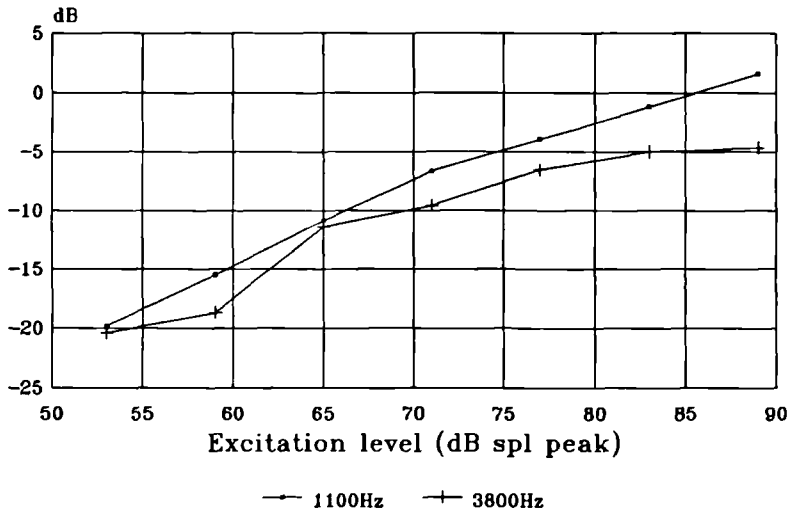

figure 3.6 The growth of the 1.1KHz and 3.8KHz frequency spectrum peaks displayed in fig.3.5 as a function of excitation level.

3.3 The characteristic group latencies of different frequencies within OAE waveforms.

Typically, the OAE from a normal ear contains a range of frequencies which usually extends from around 600Hz up to and above 4KHz. A pattern in the distribution of these different wavelengths is often observed in the OAE waveform. A typical example of this distribution is illustrated in fig.3.7, which is an OAE recorded from a normal adult ear. It can be observed that the predominant frequency in the region of 4 to 6ms is of a much shorter wavelength than that in the region of 10ms.

A study of this 'dispersive' phenomenom of the different frequency components was undertaken to establish the normal distribution of different wavelengths within the OAE. This would provide a further distinguishing feature of the OAE thereby enabling more specific data processing of the OAE to be implemented (thus increasing the signal to noise ratio of the processed data).

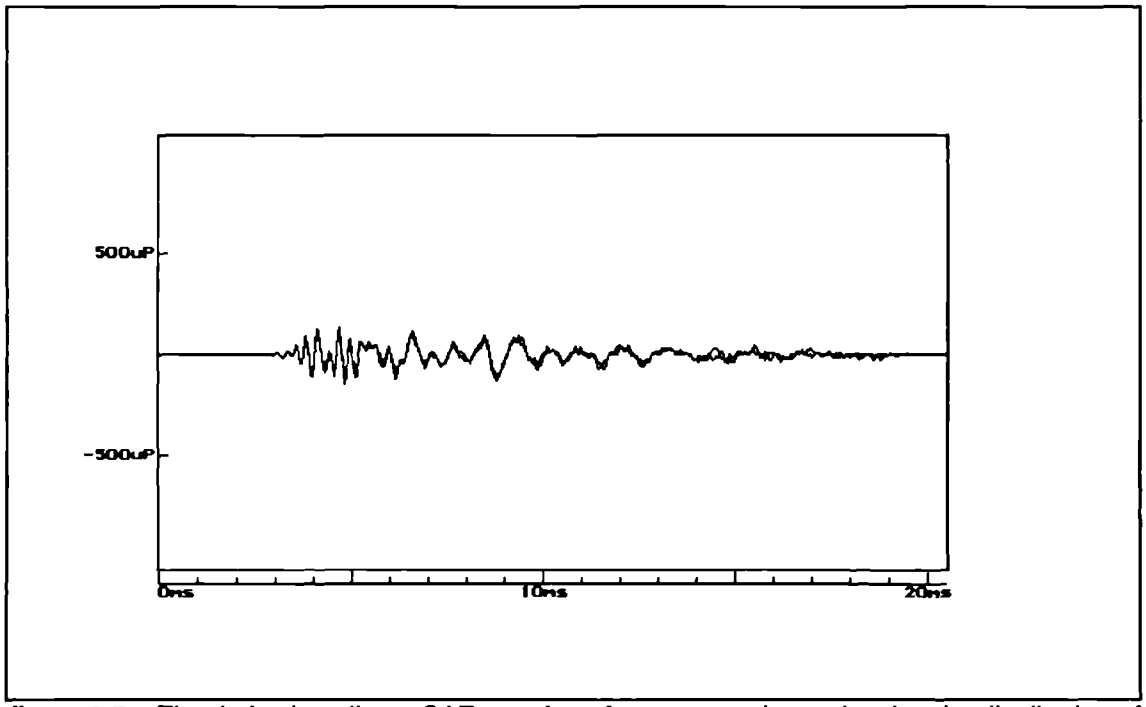

figure 3.7 The derived nonlinear OAE waveform from a normal ear, showing the distribution of different wavelengths along the waveform.

The study consisted of three different methods of investigation.

1. The click evoked OAEs of 24 normal ears were each bandpass filtered 'around' peaks that existed in their frequency spectra. The latency of the envelope of the filtered response was then plotted versus the centre frequency of the filter.

2. The frequency spectra of 27 segments of the OAE waveform were plotted as a function of pst. In addition this 'spectrograph' result was averaged for the same 24 OAEs, as above, to produce an average frequency distribution.

3. Tone pulse stimuli waveforms were used to evoke OAEs of limited bandwidth. The envelope delay of the narrow band response was then noted.

3.3.1 Time domain study of bandpass filtered responses.

Fig.3.8 shows the result of the application of a bandpass filter upon the same OAE response shown in fig.3.7 at two dominant frequencies. The centre frequency of the filter is 3.8KHz for the top panel and 1.1KHz for the lower. In this example, these two frequency components within the emission occur only within distinct time intervals, and exhibit a well defined amplitude envelope. It was observed that the amplitude envelope for the lower frequency components (below 1.5KHz) was often less distinct, and a group latency could not be attributed to the response at that frequency. At 3.8KHz the group latency of the filtered response (i.e. the pst of the centre of the amplitude envelope of the filtered response) is far less than in the case of the lower frequency filter.

It was noted that often a distinct envelope in the filtered response occurred when the centre frequency of the filter was positioned at a peak in the frequency spectrum of the emission. As a result of this observation, a technique was developed which allowed filtering of the response around these peaks in the spectra. The cross power spectrum of the OAE was calculated and displayed. Then, using a specifically written Pascal analysis programme, the peaks in the spectrum were identified and marked

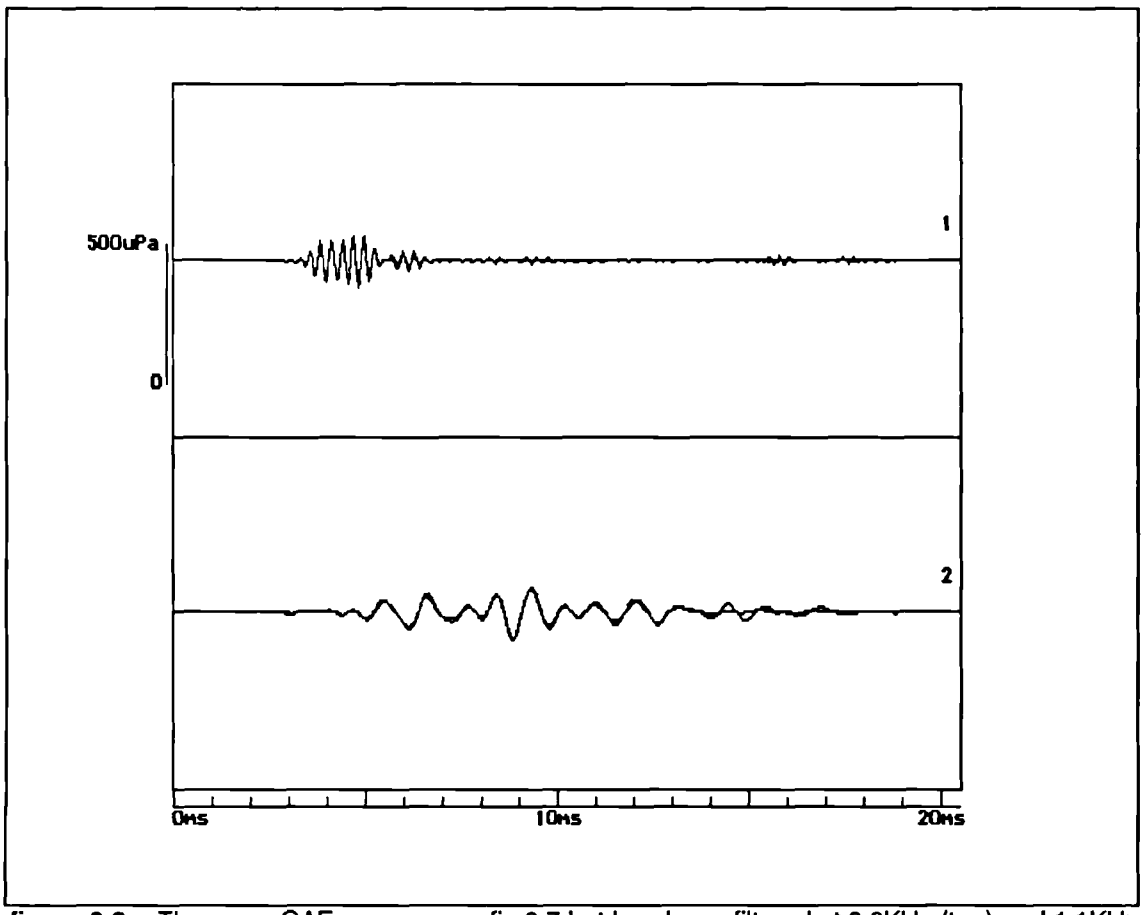

figure 3.8 The same OAE response as fig.3.7 but bandpass filtered at 3.8KHz (top) and 1.1KHz (bottom).

using the cursor control keys. The complex spectra of the OAE responses were then multiplied by a window function, centred around the peak, which represents an 8th order Butterworth bandpass filter. The resulting data was then inverse Fourier transformed to reconstruct the waveform of the filtered response.

A study of the latency of the amplitude envelopes of filtered responses as a function of frequency was then undertaken. The subjects for this study were 12 normally hearing adults in the age range of 20 to 30 years. Satisfactory recordings of emissions were obtained from all the 24 ears to the normal level of transient stimulation (approximately 75 dBspl peak), and the data was then analysed using the analysis programme.

For each of the 24 emission responses various peaks in the spectra were isolated using the cursor keys and the low and high cut frequencies for filtering were then calculated from the cursor positions. After the processing if a distinct burst of response was present in the filtered waveform, then the latency of the envelope peak was saved to a disk file along with the centre frequency of the filter. This was done for all of the peaks in the spectrum that resulted in clearly defined envelopes in the response waveform.

Fig.3.9 is a plot of the filter frequency versus envelope pst data for all the 24 emissions combined. This plot shows a clear decrease in envelope latency as a function of frequency, with very few points falling outside of the general trend. This graph has been re-plotted in fig.3.10 with the frequency axis drawn logarithmically. An estimate of the envelope latency with respect to frequency can be obtained by a best line fit to the data in this logarithmic plot.

From this investigation it has been shown that the envelope latency increases as the frequency of the emission decreases. From fig.3.10 it can be observed that typically the 1KHz component of the emission is present at about 10ms pst, whereas emissions at 3KHz are present at 5ms pst.

There are, however, a few data points that do err from the line considerably. There are two factors in the measurement method that could cause these deviations. Firstly, to ensure that the otoacoustic emission response is completely free from stimulus 'tail' artefact (due to exceeding the range of the ADC), the response is windowed with a raised cosine function, that has a zero section of 2.5ms at the beginning. For estimates of latency at frequencies above 3KHz, the envelope of the burst of response at this frequency becomes affected by the window envelope. Consequently, accurate estimation of the centre of the response burst at these frequencies becomes more difficult. Secondly, at frequencies below about 1.5KHz, the filtered response often has a very

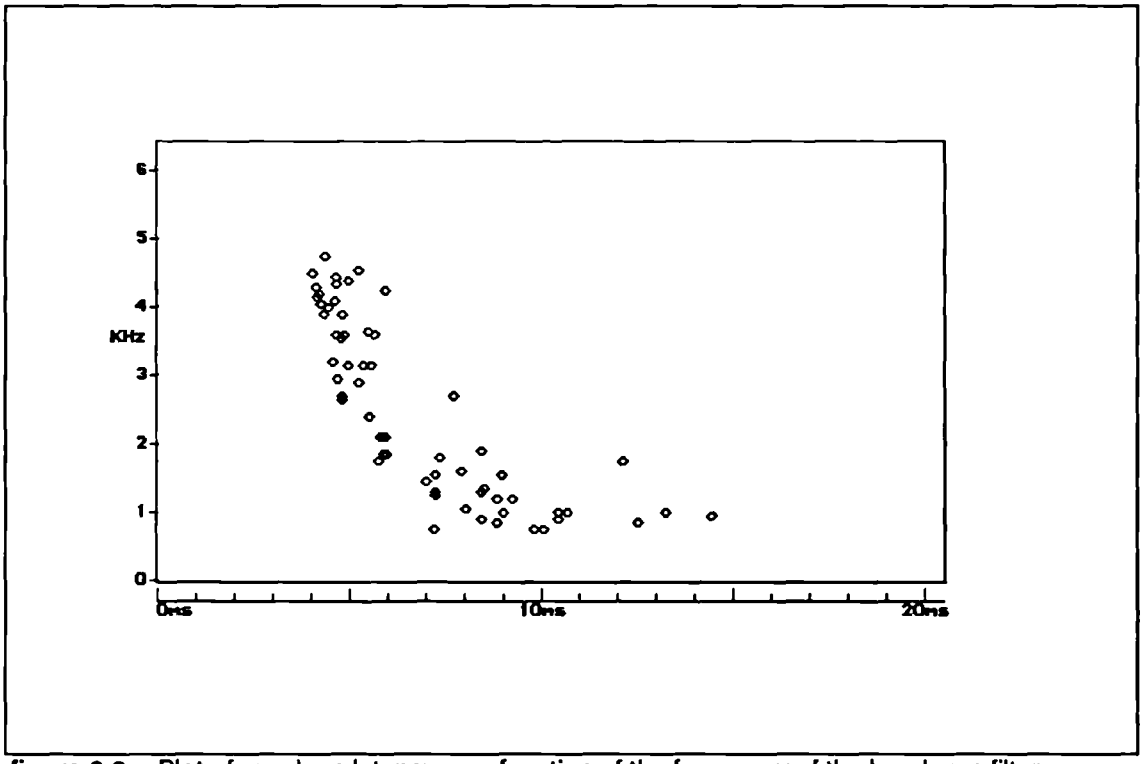

figure 3.9 Plot of envelope latency as a function of the frequency of the bandpass filter.

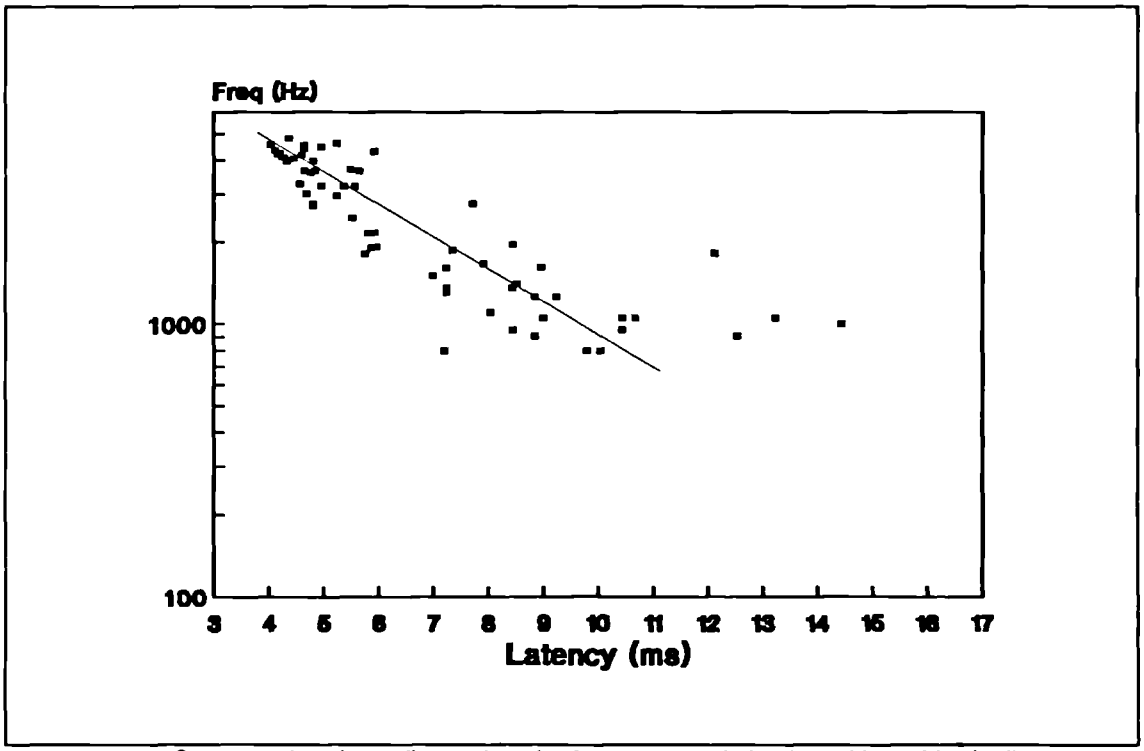

figure 3.10 Same as the above figure, but the frequency axis is plotted logarithmically enabling a line of best fit to be included.

broad amplitude envelope. This introduces errors in estimation of the centre of the envelope.

It was noted that in some cases two bursts of the filtered response were present. The criterion that was applied involved estimating the latency from the first burst, and ignoring the second. This criterion is correct if the second burst is due to a multiple reflection of the emission within the cochlea. However, if it is due to destructive interference of the response waveform by two adjacent frequencies, then the estimates of latency will be incorrect.

3.3.2 Frequency analysis of segmented OAE response waveforms.

The above method relied upon identifying distinct amplitude envelopes within the bandpass filtered emission waveform. These 'packets' of different frequencies within the emission were present commonly, but in some cases identification of a distinct envelope was difficult. A second study was undertaken using spectral analysis of short subsections of the entire response waveform. The resulting series of spectra were then displayed so that any patterns in the distribution of the various frequencies as a function of pst could be observed. The Pascal analysis programme was elaborated to fulfil this task.

The analysis was achieved by calculating the cross power spectra of short sections of the two responses which were created by multiplying the responses by a raised cosine window function. The window was advanced along the responses in order to study the frequency components of each section. The window had rise and fall times of 2.5ms, and was advanced 0.64ms for each cross power spectrum calculation.

The resulting 27 cross power spectra were then displayed on the VDU, one at a time in quick succession. The left and right cursor keys controlled this function. This was done so that the 'grey' scale of the final display could be adjusted to suit the

dynamic range of the data (the up and down cursor keys set the upper and lower limits of the grey scale). Finally, the 'spectrograph' output was displayed.

This analysis was applied to the same data from the 24 normal ears, as the above described filtering technique. Fig.3.11 shows the result of this analysis on one of the emissions. As can be seen from the figure, the elected display format takes the form of a computerised spectrograph, with time on the X-axis and frequency on the Y-axis. The cross spectral power is represented by the size of the dot. A clear pattern is evident in this figure, showing a decreasing frequency content of the waveform with an increase in the pst.

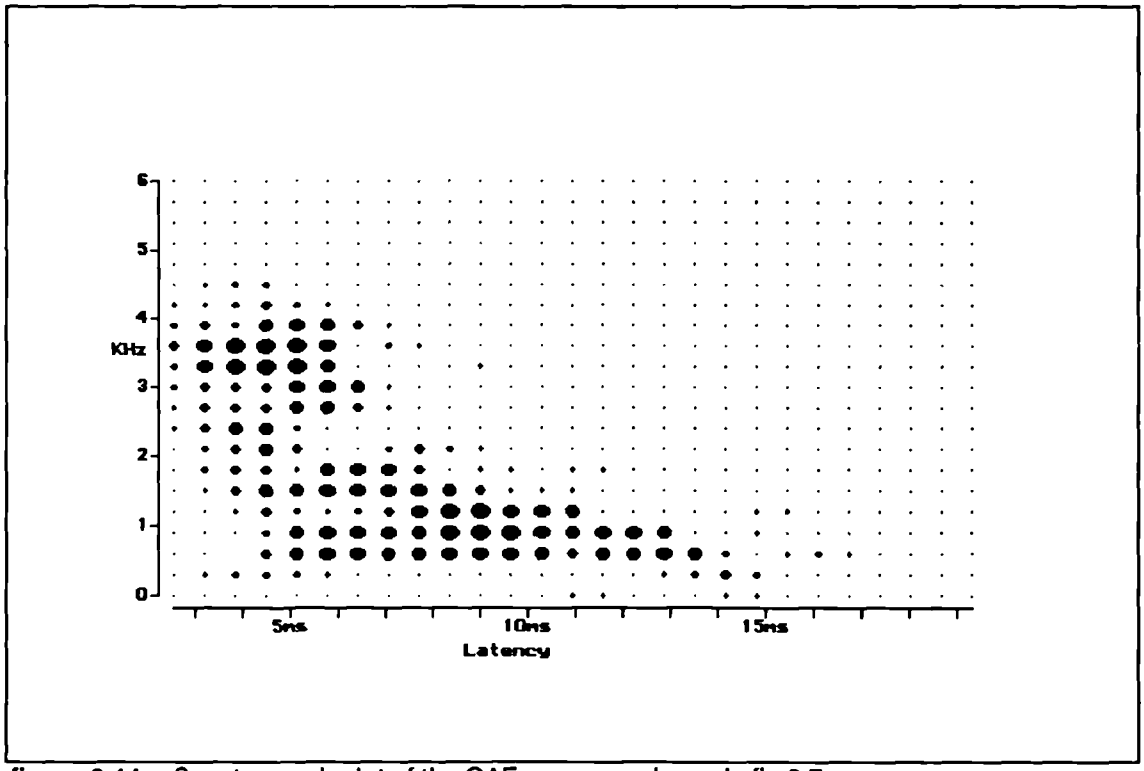

figure 3.11 Spectrograph plot of the OAE response shown in fig.3.7.

This technique was further extended to permit the averaging of the spectrograph data from the 24 ears. The spectrograph data for each ear was accumulated to a disk file by averaging the complex spectral data for each response. The resulting file was then loaded and scaled accordingly. This averaged data is displayed as Fig.3.12.

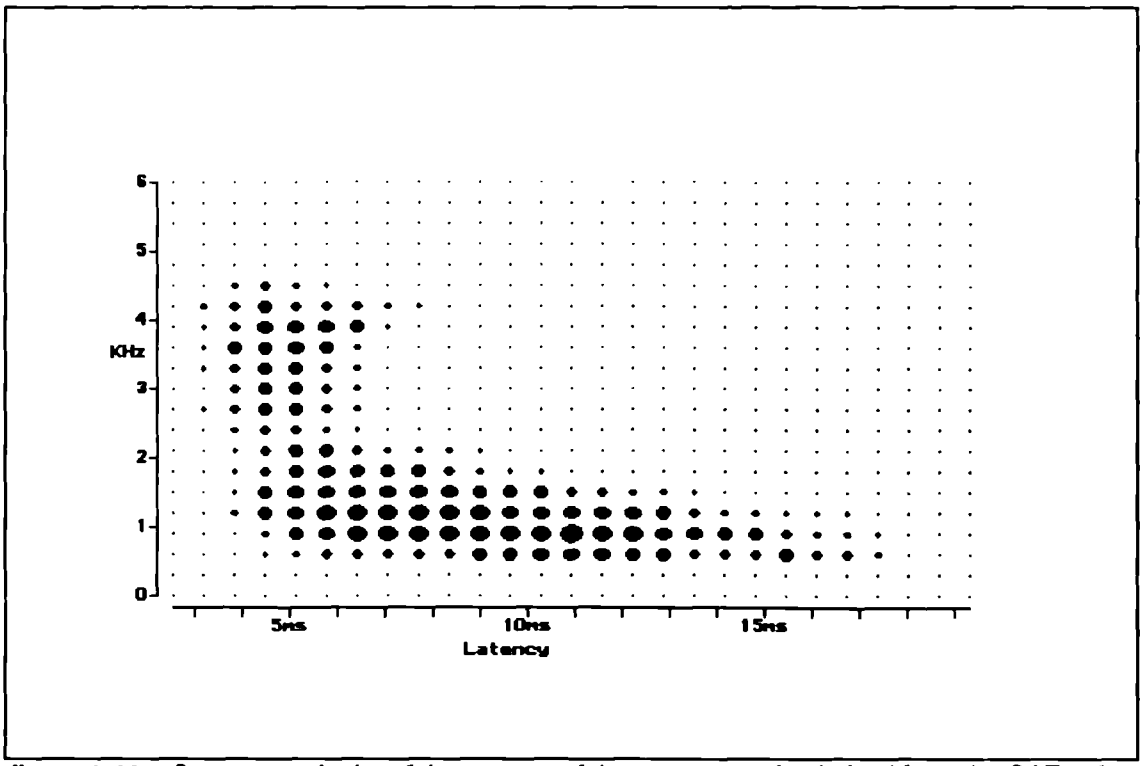

figure 3.12 Spectrograph plot of the average of the spectrographs derived from the OAEs of 24 normal ears.

The data in fig.3.12 exhibits the same general trend of a decrease in frequency as the pst increases. However, for the lower frequency components there is a far greater range of pst than at the higher frequencies. This is due to the fact that all of the data is included by the nature of this technique, whereas in the previous filtering technique the data was only added to the pool of points if a distinct envelope was evident in the filtered response waveform.

3.3.3 Study of OAE using narrow band stimulation.

In this investigation narrow band stimuli were used to evoke responses of minimal frequency spread. The group delay of the response at these frequencies was then ascertained from the amplitude envelope of this narrow band response.

Previous workers, including Wilson[45] and Probst[35], have shown that the OAE contains only the frequencies present in the stimulus. Therefore the use of tone burst excitation allows the study of narrow band emission responses.

The stimuli were created using an 'in house' utility program for the generation of complex stimuli. In all cases a sine wave of fixed frequency was multiplied by a raised cosine window, resulting in a burst of stimulus, which had a rise and fall time of 1.28ms. The same 3 + 1 linearly balanced stimulus protocol was used to ensure measurement of only the cochlear response. Fig.3.13 shows the spectrum of this type of stimulus, with the centre frequency at 1KHz.

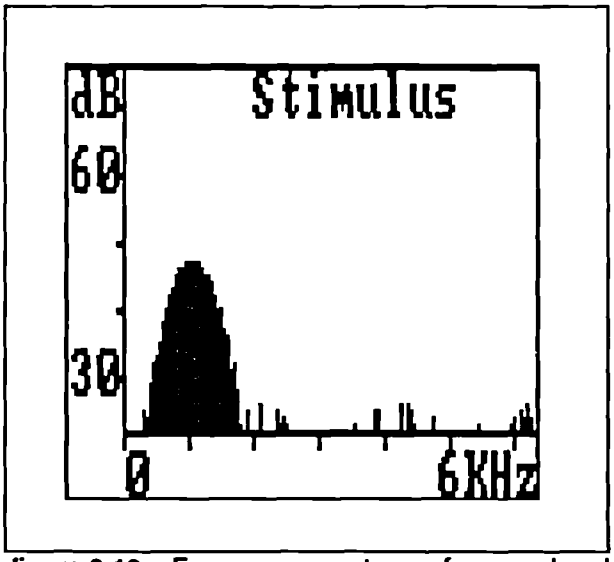

figure 3.13 Frequency spectrum of narrow band tone burst stimulus centred at 1KHz.

In Fig.3.14 the OAE responses of one ear to tone burst stimulation centred at 1KHz and 4KHz is shown. This figure can be compared to fig.3.8 which shows the click evoked emission waveform, from the same ear, filtered at two frequencies similar to the centre frequencies of the narrow band stimuli used to evoke the emissions shown in fig.3.14.

Agreement with the results of the previous two studies was achieved. The pst of the 1KHz response was approximately 10ms, and 4ms for the 4KHz response. One method used to describe the pst of the response is the 'wave delay'. For example, the 1KHz emission envelope has a maximum at 10ms, and therefore can be expressed as a 10 wave delay. Similarly the 4KHz emission at 4ms is a 16 wave delay. However, if the envelope of the stimulus is also taken into account (which has a peak amplitude at 1.28ms), the results for 1 and 4KHz are adjusted to 9 and 11 waves respectively.

Summary.

The results from all three of these different investigations are in agreement. There is an apparent general relationship between the pst and the presence of different

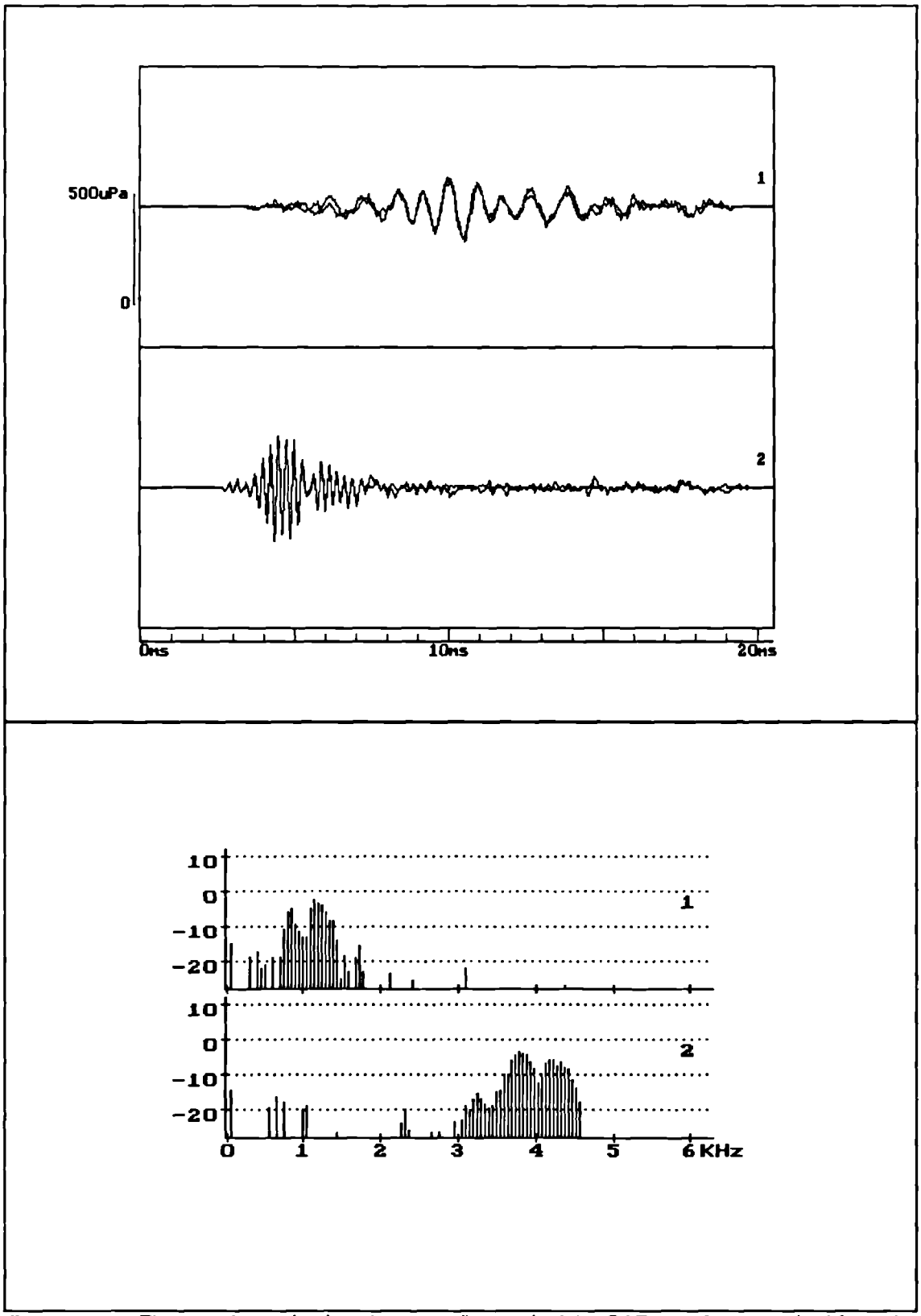

figure 3.14 The waveforms (top) and spectra (bottom) of the OAE waveforms evoked from the same ear using tone pulse stimuli at 1KHz and 4KHz.

frequency components within the emission waveform. The data shown in fig.3.12, created by averaging the 'spectrographs' from the 24 responses, can be used to design a 'template' for response recognition, thereby permitting more elaborate data processing of the emission signal. This template procedure is further discussed and implemented in chapter 6.

3.4 Conclusions.

The growth of the derived nonlinear OAE component was found to be similar to the growth of the temporally separated OAE shown in chapter 2. This is consistent with steadily increasing saturation of the OAE response to increasing excitation levels.

A study of the growth of the cross power spectrum of the nonlinear OAE to increasing excitation levels revealed similar saturated growth of the different frequency components.

Frequency dispersion of the nonlinear OAE was investigated. Three methods of frequency dispersion analysis were developed. The average pattern of OAE frequency dispersion for 24 normal ears was established.

The design of a clinical OAE measurement instrument.

4.1 Towards a clinical OAE instrument specification.

The general aims.

An instrument which indicates the cochlear status by measuring the OAE has a role in clinical audiology (chapter 1). Chapters 2 and 3 discussed the techniques by which the cochlear component can be completely separated from the transient response of the ear canal. Such techniques are essential for a clinical instrument which must eliminate all components of the signal other than that originating in the cochlea, so that the cochlear function can be ascertained. However, a clinical instrument must fulfil many more criteria than are necessary in the laboratory context. In order to achieve this, the instrument must have the following additional characteristics:-

- It must complete the test in the shortest possible time. In the clinical environment the patient often attends for many tests and therefore the time taken for each test must be kept to a minimum. A short test time is also most important when testing young children as the 'quiet' period is often very short.

- The software must be 'user friendly', enabling an unfamiliar operator to perform emission measurements with the minimum of training (i.e. each decision point in the software must be explained on the screen).

- It must be able to differentiate between the required emission response and any unwanted noise contamination of the response. In the clinical test environment, the noise conditions are often less ideal than in the laboratory.

For this reason the instrument must be very efficient at noise recognition and rejection.

- During testing it must report to the operator various essential information such as the quality of probe fit in the ear canal, the current noise level in the ear canal, and the quality of response data so far obtained. This allows the operator to decide what action to take (i.e. whether an early termination of the test is possible, or whether the test should be abandoned and re-started).
- At the end of the test it must report to the operator all the information necessary to judge the outcome of the emission measurement, and the conditions under which the measurement was obtained.
- Finally, for practical reasons, the instrument must be easily transportable (to facilitate movement between clinics and field trials at other establishments) and easy to operate. For the purpose of this study, this feature allows the instrument design to be assessed in many environments and by operators who are less familiar with the instrument.

This chapter details the design and development, by the author, of an instrument which fulfils each of these criteria.

Special requirements of a clinical OAE instrument.

The operational requirements of the clinical OAE instrument were evolved. The following factors influenced the final instrument specification:-

1. The existing minicomputer-based OAE instrument design, and the later developments to this instrument.

2. The experiences gained whilst testing many patients on an experimental minicomputer emission measurement system.

3. Investigations into the emission properties detailed in the previous chapters.

4. The above design aims.

The resulting operational requirements of the clinical OAE instrument are listed below:-

- In order that the test time be decreased to a minimum, all the data processing and display functions should be implemented in 'real time'.
- Transient excitation should be repetitively delivered to the sealed ear canal (a repetition rate of about 50Hz allows sufficient time for the full range of frequencies to be emitted from the cochlea and keeps the total measurement time to a minimum).
- Excitation should take place at two different levels, permitting the derivation of a nonlinear emission response component. A study of the optimum choice of levels resulted in the use of a 3 to 1 ratio (see chapter 2).
- The instrument should be capable of detecting and rejecting responses contaminated by an undue level of noise. If an efficient noise rejection scheme were to be implemented, then the time to obtain a satisfactory emission measurement from the ear would be reduced, thereby resulting in a shorter test time.
- In order to indicate to the operator the certainty of a successful emission measurement, the response waveform data should be averaged alternately into two 'averaging pools'. Correlation of these two averaged waveforms is an indicator of the quality of the data obtained (i.e. the signal to noise ratio of the data). In addition, this allows early termination of the test whilst still retaining two independent repeat measurements of the emission.
- The instrument should implement frequency analysis and cross correlation of the measured emission responses (see chapter 3), as part of the response data analysis at the end of the test.

- Measurement of the initial transient response should be retained as this provides valuable information of the probe placement in the ear canal. Correct probe fit is important for ensuring adequate delivery of the sound stimulation, for efficient recovery of the emission response, and for reducing the contamination of the response from ambient sound sources.

The evolution of the detailed instrument design specification.

The system used to measure the OAE, during the preparatory work for this chapter, was based around a Computer Automation minicomputer. A considerable amount of additional hardware was required to process and interface the emission signal to the computer, such as amplifiers, analogue interfaces and a plotter for hard copies of the data. This system was initially specified and commissioned by David Kemp.

It was originally envisaged that this minicomputer system configuration, performing OAE measurements, could fulfil a clinical role, and indeed several hundred patients with various audiological impairments were tested by the author and others. Fig.4.1 shows a photograph of the minicomputer and associated peripheral equipment.

During this work, many of the ideas incorporated into the new instrument design were tested and implemented on the minicomputer system. For example, over a period of use, it became apparent which information and analyses of the response data needed to be output to the plotter and which saved on disk. Many of the techniques which were employed in the data processing methods are discussed in published papers[5,26,27]. Fig.4.2 shows the plotted output of a normal OAE measured using this system.

Unfortunately, as experience mounted, several disadvantages of the system became apparent:-

figure 4.1 Photograph of the minicomputer based experimental OAE measurement instrument. The main components are a 16bit minicomputer, a Cambridge Electronic Design analogue interface and an 80MByte winchester disk.

- The large size of the equipment necessary to perform the OAE measurement precluded many suitable patients. It was impractical to move the patients (who often attend the hospital for many tests) to the part of the building where the equipment was sited, and the equipment was too heavy to move. This problem led to considerable logistic difficulties when experi-

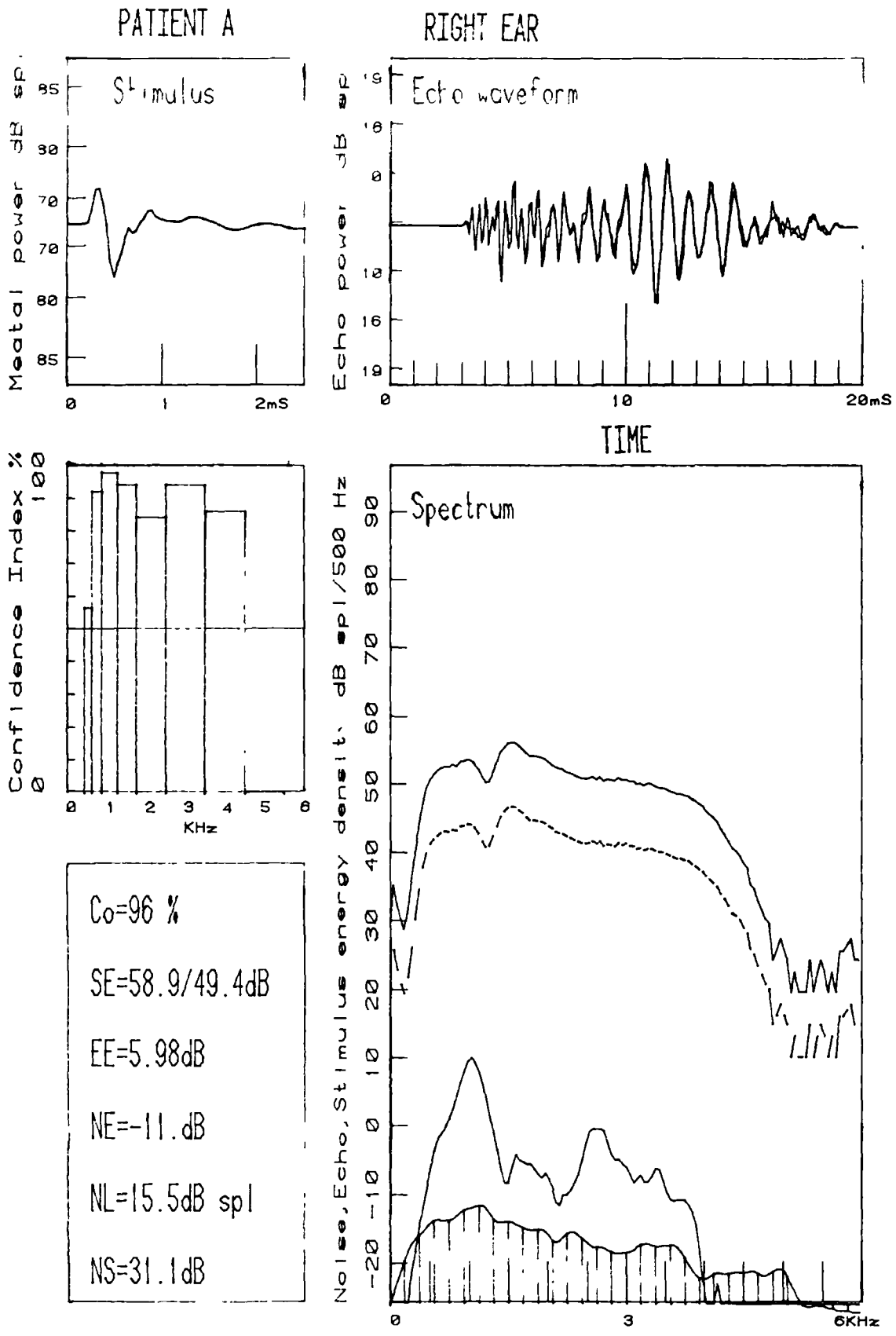

figure 4.2 The output format of an emission measurement from a normal ear, performed with the minicomputer system. This consists of stimulus and response waveform displays, and frequency spectra of the stimulus, response and noise.

menting with various new techniques of signal processing for emission data obtained from infants, as the infant clinic was in a different building on the hospital site.

- As more complex techniques for signal processing were developed (specifically to tackle the extra problems of measuring OAEs from young children and infants), the minicomputer system became overburdened with data processing subroutines to the point where it could no longer work in real time. As a result of this, the raw emission data was recorded directly onto a fast winchester disk for 'off line' processing and analysis. This has the major disadvantage of not allowing any operator feedback as to the quality of the data collected up to that point and therefore whether the test should be terminated or not.

As the system was extended for use on young children and infants, it became apparent that a more 'efficient' instrument was required which could make 'optimum' use of the patient's time. Often when testing children of 1 to 3 years of age, the 'quiet' time available for successful emission measurement is in the order of 1 minute, and it is therefore essential that none of this time be wasted.

As mentioned above, the lack of mobility of the minicomputer measurement system became a severe limitation of its applicability. It therefore became apparent that the instrument would need to be small and portable.

Despite the many disadvantages detailed above, the minicomputer system provided an excellent means of experimenting with, and optimising the various signal processing techniques. The raw emission waveform data was stored on the winchester disk and many different noise rejection/acceptance criteria were applied to the same data. This permitted an objective comparison of the techniques. The outcome of this study was a practical and efficient means of data collection[5,26], which was then implemented in the new instrument.

Having specified data collection methods from the experiences gained when using the minicomputer system, it remained to devise a hardware system on which they could be implemented. Unless a very high speed computer is used, the problem of real time data processing requires dedicated signal processing hardware.

There were two options for the instrument design. Either a dedicated 'stand alone' instrument, or a design based around an existing computer. A dedicated instrument has the advantage of being more portable as only the components essential to the required task are included in the design. However, it was considered that the flexibility permitted by a design based around an existing computer outweighed any disadvantages.

Reasons for the implementation of the instrument on an IBM PC.

It was decided to use the IBM Personal Computer (PC) as the 'host' of the measurement system. This computer was chosen for the following reasons:-

- There is a considerable amount of literature available on the internal architecture and the bus interfacing requirements of the IBM PC.
- There are a great number of software packages available, including compilers and signal processing libraries.
- The bus design of the IBM PC, XT and AT allows sufficient compatibility between the models for the interface boards to be interchangeable. This allows the instrument design to function in many different sizes and speeds of machine (from a cheap, battery powered portable PC to a high speed AT).
- The IBM PC, XT and AT are becoming common in hospitals and universities, allowing the dedicated hardware to be transported to the site, and plugged into a computer on the premises. This facilitates field trials of the instrument.

A grant was obtained from the Medical Research Council (MRC) for the construction and evaluation the OAE instrument[33]. An IBM AT clone made by Ferranti was purchased for the development of the instrument. This computer uses an Intel 80286 microprocessor. Other IBM clones belonging to the Institute of Laryngology and Otology were used to check the compatibility of the instrument hardware. Various other items of test equipment essential to the development were also made available courtesy of the Hearing Research Trust (such as a 16 channel, 20MHz logic analyser, and a digital storage oscilloscope).

The digital section of the instrument was developed on IBM PC prototyping expansion boards, and the analogue circuits were developed on copper strip-board. After completion of the prototype, and much testing, the design was transferred to a printed circuit board. This was achieved using a computer-aided design (CAD) package, called VUTRAX, in collaboration with the medical physics department of University College Hospital.

4.2 Technical description of the OAE measurement instrument.

Overview.

The chosen method for implementing the instrument design uses two dedicated signal processing interface cards fitted into the host computer. One of these cards is dedicated to stimulus production, the other to signal capture and conditioning. Fig.4.3 shows a schematic diagram of the basic host computer and interface cards.

Both of the interface cards have random access memory situated on the boards. This memory is configured in such a way as to allow access to and from the memory by either the host computer or the on-board logic. This type of memory configuration is termed 'dual-ported memory'. In the case of the stimulus generation board this allows any stimulus waveform to be loaded onto the board before the measurement commences. Therefore unless the stimulus needs to be changed in the middle of an emission measurement, the card requires little further servicing. This has the advantage of freeing the host computer to pursue other tasks. Also, on the signal capture card, the dual-ported memory stores the response until the host computer is free to

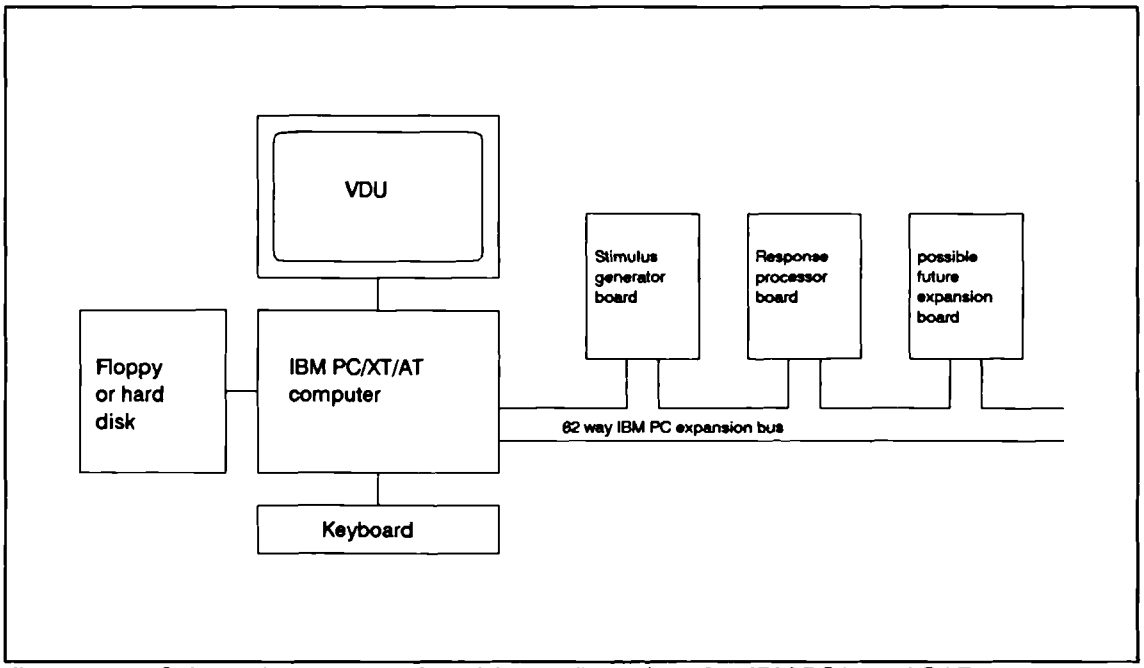

figure 4.3 Schematic representation of the configuration of an IBM PC based OAE measurement instrument.

read it into normal memory. Again this allows considerably more efficient software to be written. The alternative would be to have the host computer servicing the signal input and output functions almost continuously.

By including all the necessary control logic on the interface cards, the stimulus production and response data collection can continue independently until the memory on the response collection card has been filled. At this point the data must be read from the dual-ported memory on the card, and the data collection process initiated again.

4.2.1 Stimulus generator board- functional description.

One of the two interface cards of the measurement instrument is dedicated to producing a stimulus waveform used for evoking the OAE. The board can be broken down into functional sub-units. The interaction of these sub-units is shown in fig.4.4. The board contains sufficient static random access memory (RAM) to store a stimulus waveform of 4096 words (each word is 12 bits of data). This on-board memory is dual-ported. It can be written to by the host, therefore enabling various waveforms to be stored. In addition, the stored waveform can be read by the on-board circuitry and converted to an analogue waveform by the Digital to Analogue converter (DAC).

A crystal oscillator, present on the board, generates the clock signal which determines the time interval between each point of the stimulus waveform. The clock runs at ten times the data sample speed, and is divided down by a decade decoder (see fig.4.5). This enables the production of 20 timing pulses (half clock cycles) within each data point interval which are used to control the timing of the memory read cycle and data latching of the DAC. The fundamental frequency of the crystal clock can be controlled by the software via one of the 8 bit control ports.

Three 8 bit ports are provided for the control of the measurement hardware. All are sited on the stimulus generator board, and are 'hard wired' into the port address space at consecutive addresses. One of the ports is dedicated to the control of the measurement system functions (i.e. the clock frequency, and whether the dual-ported memory is under host or local control). The second port is solely responsible for the control of a digitally controlled attenuator, (which determines the voltage applied to the probe transducer for a given size of the stimulus waveform). The third port is for returning the current operational status of the instrument hardware to the host computer.

An address generator is used to cyclically address the on-board memory. This generator is derived from the divided clock signal, and consists of two seven stage

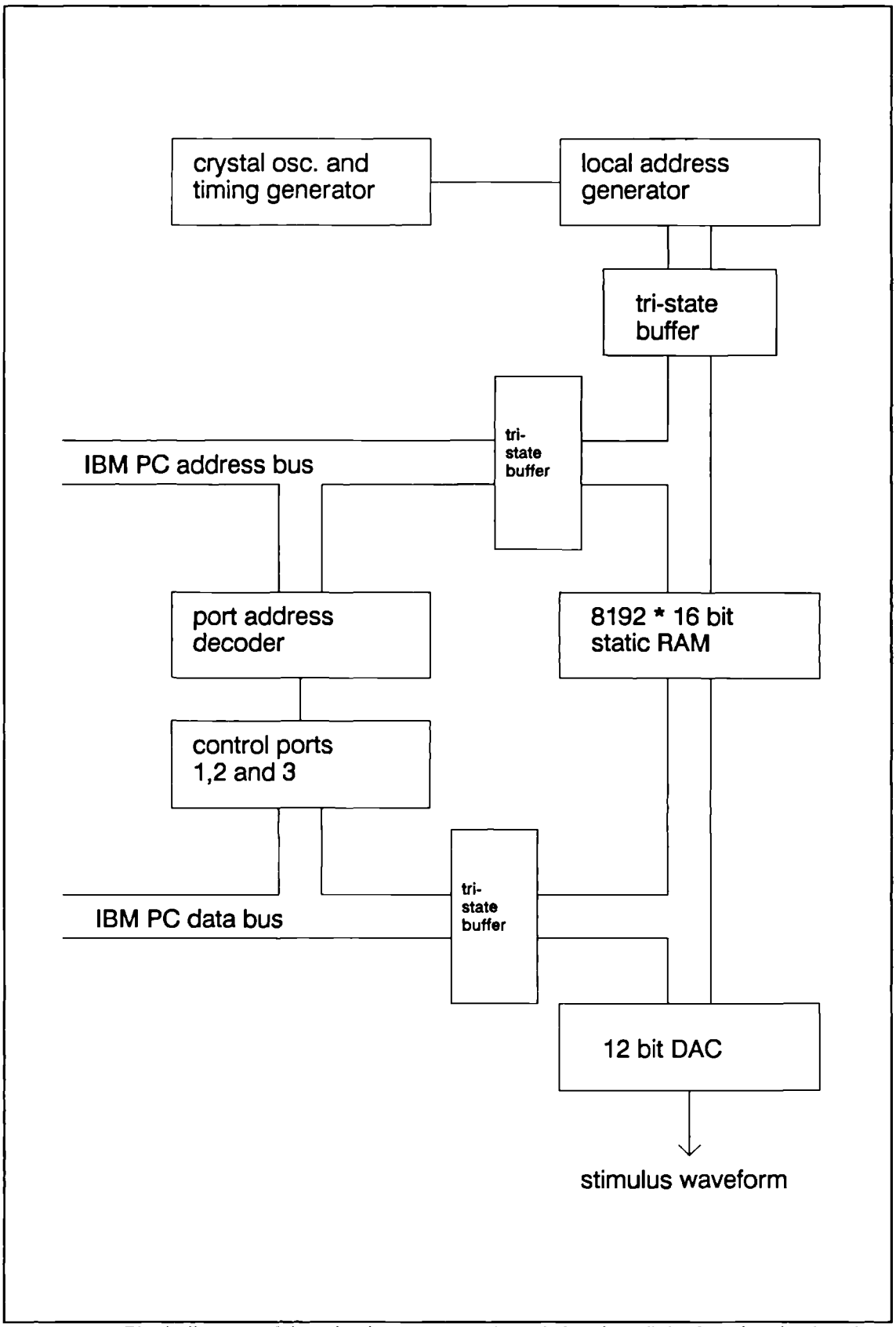

figure 4.4 Block diagram of the stimulus generator board showing all the functional sub-units.

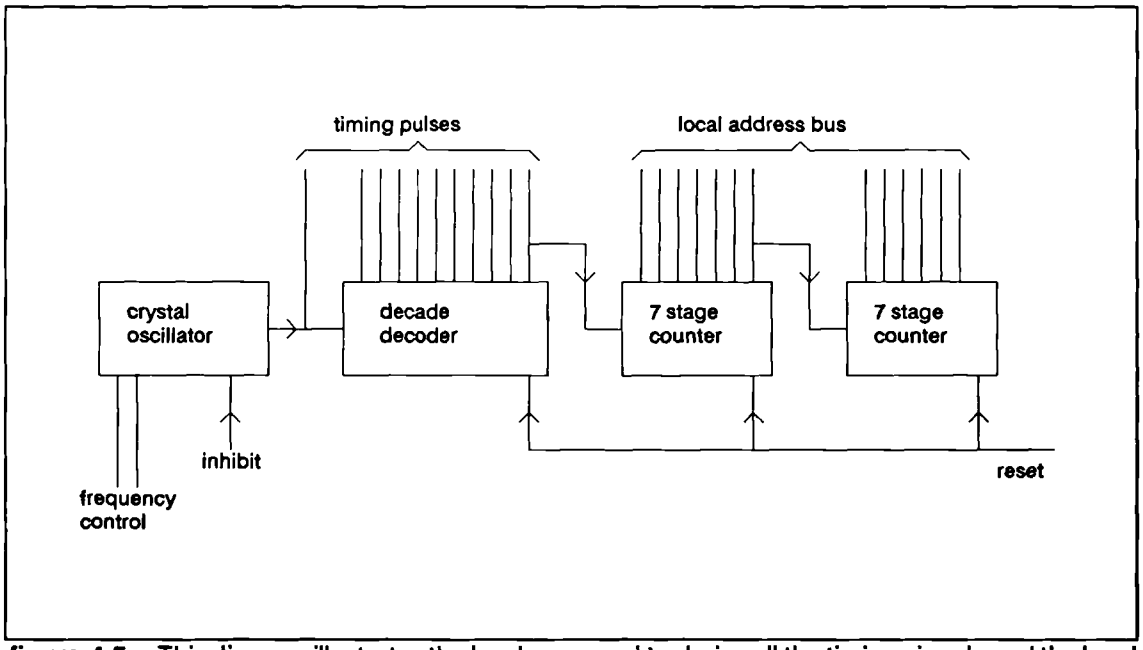

figure 4.5 This diagram illustrates the hardware used to derive all the timing signals and the local address bus which control the board function when it is operating independently.

binary dividers (see fig.4.5). The address counts to a preset value and stops. Therefore the entire waveform is output once, and then halted. This cycle can be initiated by a single command from the host computer to the board. This on-board memory address bus is termed the **'Local Address Bus'**.

One of the key features of the instrument is the synchronous operation of the stimulus generation and response processing boards. This is achieved by running the two boards from the same clock signal. To avoid unnecessary duplication, the local address bus, which is derived on the stimulus generator card, is connected to the response processor card, along with all the timing pulses via a ribbon cable. This ensures absolute synchrony of the two boards.

The address bus of the host computer is also connected to the on-board memory, via tri-state buffers. Only the lower 13 lines of the address bus are required to address the 4096 words of memory. The remaining 7 address lines are also brought onto the board so as to provide the necessary address decoding. The method of decoding used is an 8 bit comparator. One set of inputs is connected to the upper address bits, and

the other input is connected to a miniature 8 way switch. The position of the dual port memory in the memory map of the host computer can be altered by different settings of the switch. This feature allows increased compatibility between computers (in case there are differences in memory map usage between the computers).

Both the local and host address buses are connected to the on-board memory via tri-state buffers. Control of the tri-state buffers is achieved by one of the control bits from the on-board control port. As a result, depending upon whether the control bit is high or low, either the local or host address bus is connected through to the memory. This allows the memory to be loaded from the host computer and then isolated from the computer so that the board is 'unaware' of the host computer's activities.

The stimulus generator board can also 'communicate' with the host computer regarding the current operational status. This is important as it minimises the 'lost time' during data collection. The information is passed to the computer via the third port address. The port is a 'read only' port. When the board is running (i.e. outputting a stimulus), a different number is read from the port than when it has finished the task. Therefore, in order to achieve the most efficient use of the subject's time, as the end of the stimulus waveform approaches, the host computer can 'poll' (repeatedly read) the port to establish the exact finishing time of the cycle. The data from the response processor board is then quickly read, and the cycle is re-initiated.

This method, of allowing the stimulus generation and signal capture processes to run independently of the host computer has many advantages.

- It frees the host computer from the time consuming tasks of continually loading the DAC and reading the ADC.
- It allows extremely accurate data point intervals to be achieved, as the DAC and ADC conversion cycles do not have to be interwoven with the instruction cycle of the host computer.

- The host computer can be engaged in further processing of the collected data from the previous cycle, such as data quality assessment and averaging, as well as data display. This parallel approach permits a far greater number of computing processes to be achieved in 'real time'.
- The technique allows for 'full speed' running on a greater variety of speeds of host computer. Software can be written with the various data processing subroutines arranged in order of priority. The status of the data cycle is checked at the start of each subroutine, and if the cycle is complete the subroutine is 'skipped'. Therefore on a slower machine, only the most important data processes are performed before the cycle is finished. However on a more powerful computer, there is time even for the more 'cosmetic' subroutines to be performed.

Stimulus generator board - a detailed examination of the timing cycle.

The stimulus generator board, when running independently of the host computer, executes a 'one shot' cycle of the on-board memory. The control logic for this cycle is derived entirely from the crystal oscillator, via a series of counters and dividers.

Fig.4.6 shows the clock signal, and all the pulses derived from it. These derived pulses cause the action shown in the diagram. At the end of this cycle, a seven stage counter is advanced. The last output of the counter is cascaded to another seven stage counter. Thirteen of the possible fourteen outputs of the counter are used to form the local address bus. Therefore, at the end of each cycle shown in the figure, the local address bus increments to the next address, ready to repeat the process.

When the last address is selected, the clock is inhibited. In addition, the byte that is present at the status port is altered to indicate that the complete cycle is finished. There is a choice of end addresses to the cycle, the last address being determined by a two pole switch which selects either 2048 or 4096 words of data. Once the host

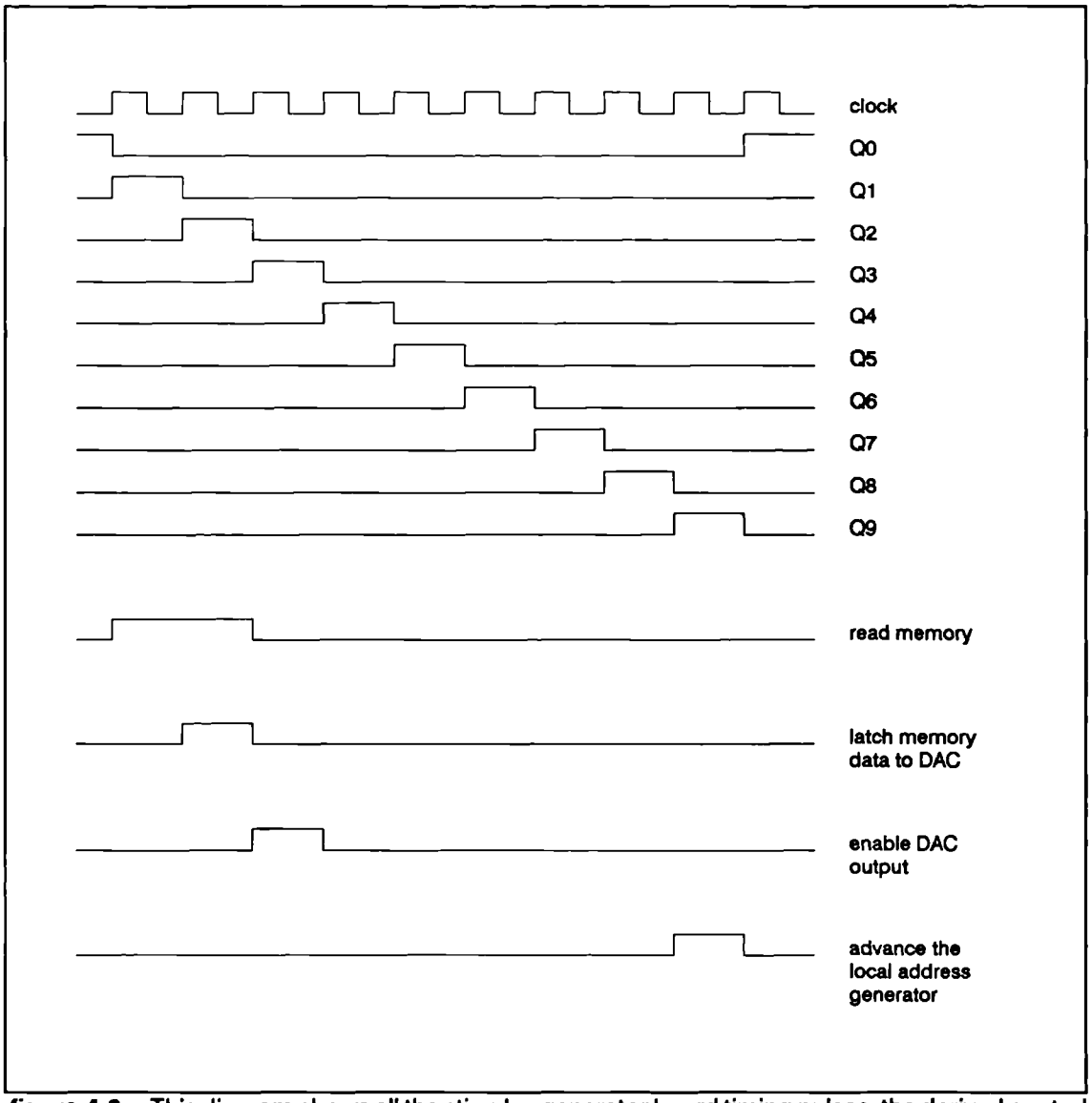

figure 4.6 This diagram shows all the stimulus generator board timing pulses, the derived control pulses, and their functions.

computer has observed that the cycle is complete, by reading the port, the independent mode is turned off. This is achieved by the host computer writing to the control port. Once this has been carried out, the host computer can again communicate with the on-board memory.

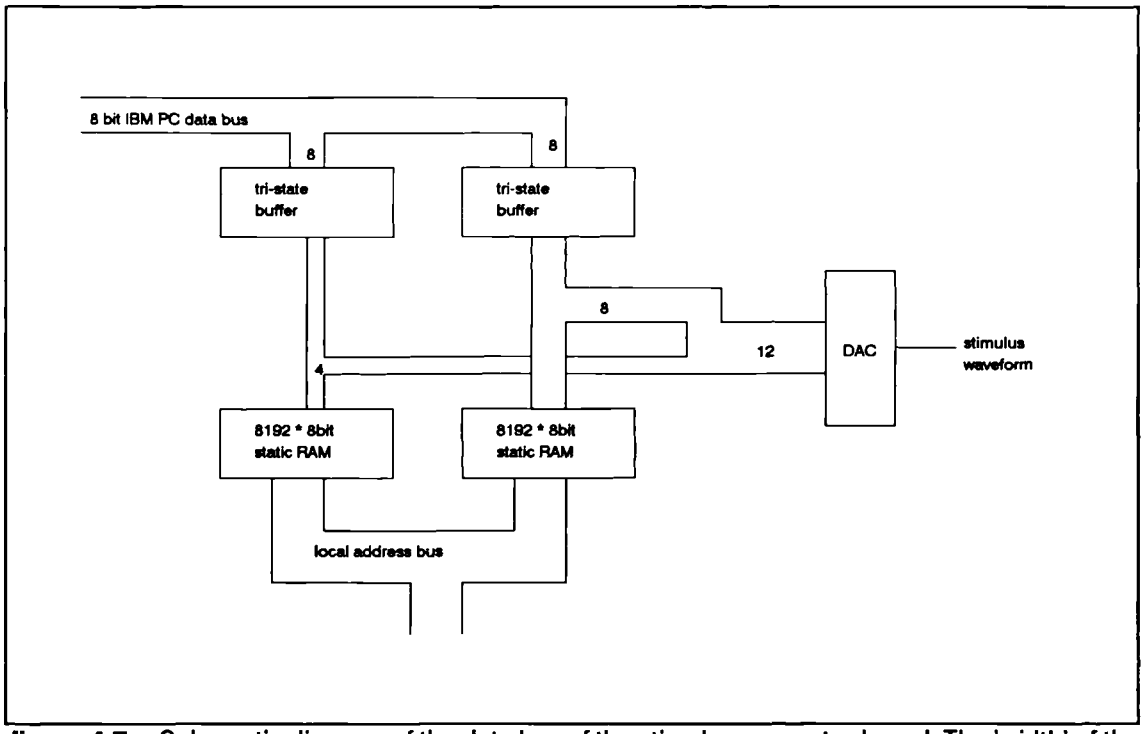

figure 4.7 Schematic diagram of the data bus of the stimulus generator board. The 'width' of the bus is shown either numerically or by the diagrammatic width.

Stimulus generator board - data bus details.

There were several considerations when designing the 'width' of the data bus for this instrument. The IBM AT computer has a 16 bit data bus,[1] whereas the IBM PC and XT have only 8 bit buses. However, a 12 bit DAC was selected to perform the stimulus conversion (a 16 bit DAC is unnecessarily precise and expensive, and an 8 bit DAC has insufficient dynamic range for accurate stimulus waveform conversion). In order to maintain compatibility with the PC and XT models of computer, an 8 bit data bus was used. Therefore, the 12 bit data required by the DAC has to be loaded as two bytes. This poses little difficulty from the hardware point of view, but results in an increase in the minimum possible data transfer time to the on-board memory

1 The expansion slot in the IBM AT has additional connections for the upper byte of the data bus as well as extra address lines and control lines. This is arranged so that expansion cards for the PC and XT can fit into the AT but they do not take advantage of the extended facilities.

on the AT model. The data bus on the board itself is 12 bits wide. This is so that the 12 bit DAC can be parallel loaded with the waveform data.

In the same way as the address bus, tri-state buffers are used to isolate the data bus from the host computer. When the boards are under control of the host computer, the data bus exists as an 8 bit bus (so that each 8 bit memory can be loaded with the high and low byte of the data word). However, when the boards are running under independent control, the data buses from the two 8 bit memories operate separately, and feed data to the DAC in parallel. This is detailed in the schematic diagram, fig.4.7.

Stimulus generator board- constructional details.

A circuit diagram of the entire instrument is included in the appendix. The first prototype instrument was constructed on an IBM PC prototyping interface board (supplied by BICC VERO). The board was designed to be used with pins and a wire wrapping tool. It was decided not to use the pins and to solder the wires, as this resulted in a board of less width.

By minimising the power consumption of the interface boards, it is possible to fit the system into a battery powered portable IBM PC compatible. This allows the entire instrument to be carried in a small suitcase, thus facilitating field trials. The low power consumption of the board was achieved by using 74HC series logic where possible (a TTL compatible CMOS chip). The host computer relies on interfacing to an impedance which is low enough to sink or source sufficient current to permit the bus voltage transitions to occur quickly. For this reason, 74HCT series logic (a TTL interfaceable version of the 74HC series) was used for any connections from the host computer to the board, and 74LS series (TTL) was used for signals that go from the board to the host.

In order to reduce circuit duplication, and to assure synchrony of the stimulus generation and data collection, many of the signals derived on the stimulus generator

board are carried over to the response processor board. These signals include the local address bus, the clock and timing cycle pulses, as well as the bits from the control port. In total, the number of signals that are connected between the two boards are 32. A 34 ribbon cable, terminated with IDC connectors provides the link.

Stimulus generator board - testing and calibration.

A Pascal programme was written to carry out testing and calibration of many of the individual 'chips'. For example, the address decoder section is tested by writing a byte to an address in the correct area of the memory map. The presence and duration of the decode pulse from the circuitry is then checked with the logic analyser. Similarly, the memory access timing (which involves the correct timing of four different signals) can be checked by writing to the memory and observing the different timing signals at the memory chip.

The DAC operates in a bipolar mode, with a full range of ±5 volts. There are two adjustments that can be made to the DAC, namely, the offset (i.e. the lower point), and the gain (i.e. the upper point). The Pascal test programme was again utilised. Data is written to the on-board memory, such that when a one shot cycle of the memory is initiated, the last value that the DAC receives from the memory is the value for calibration purposes. The DAC holds the output at the last value, and is not reset, allowing the calibration adjustments to be made using a digital voltage meter (DVM).

Fig.4.8 is a photograph of the stimulus generator board. The photograph shows the printed circuit board version, which was produced about 6 months after the initial prototype.

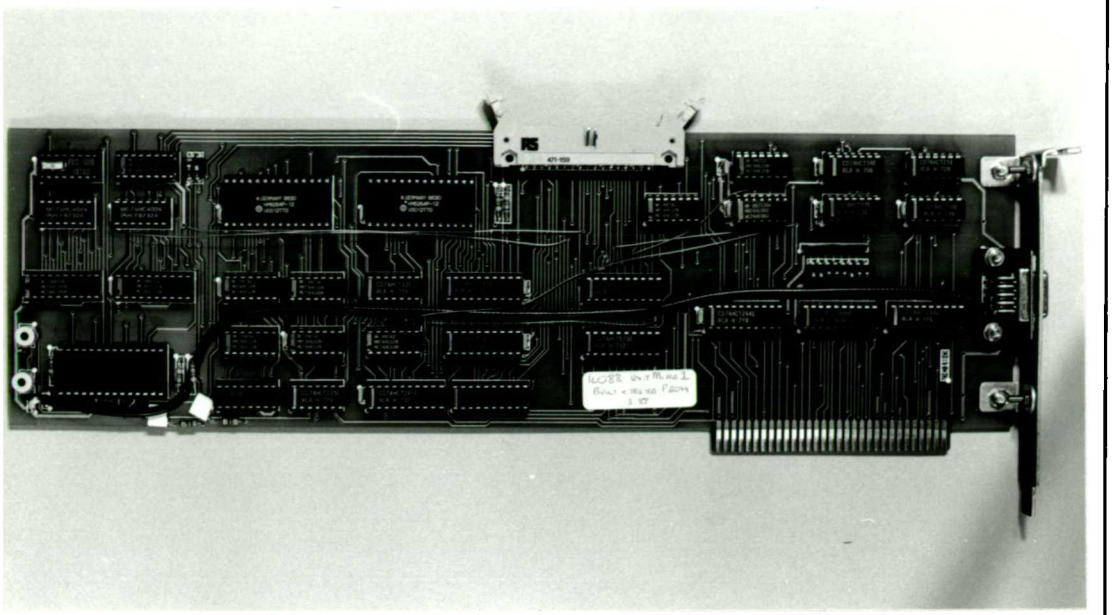

figure 4.8 Photograph of the completed stimulus generator board. The photograph shows the pcb version of the board.

4.2.2 Response processor board - functional description.

The response processor board digitises the amplified response from the probe microphone. In addition, the response is arithmetically processed and stored in the on-board memory. At the completion of the one shot cycle of the stimulus, the data stored in the response processor on-board memory is read into the host computer, and the cycle then repeated.

The design employs two ADCs. One ADC digitises the highly amplified microphone output, and the other digitises a lesser amplified version of the same signal. The high gain channel is for measuring the OAE, whereas the low gain channel is for monitoring the initial transient response of the ear canal to the stimulus. It is possible to measure both parts of the response with one high precision ADC. However an ADC of at least 16 bits of precision would be required. The higher the precision of an ADC the slower the conversion time. The 12 bit device selected to measure the OAE completes the conversion in 25 microseconds, which is only just fast enough to allow the specified data point interval of 40 microseconds. For monitoring the initial transient an 8 bit ADC was selected.

The 8 bit ADC writes the digitised data directly into one of the memory chips. This can then be read by the host computer upon completion of the cycle, enabling analysis of the initial transient response.

The key feature of the response processor board is the use of dedicated signal averaging on the board. This takes the form of sub-averaging the individual responses to each stimulus presented in the 'stimulus package' from the stimulus generator board. The response processor board implements the 'nonlinear derived response technique', described in chapter 2, within the hardware of the design.

Response processor board- processing of the OAE signal.

The OAE measurement instrument has been designed to perform the following signal processing functions.

- Record both the initial transient response of the ear canal, and the much smaller delayed cochlear response.
- Perform a subaverage to a set of four stimuli. The stimuli are arranged so that they present a linearly balanced set of 3 stimuli of one size, and 1 of 3 times the size.
- Assess the quality of the subaveraged response data with regard to contamination by noise.
- Average the subaveraged responses, of sufficient quality, into alternate data pools.
- Provide some degree of operator feedback as to the quality of the data, and the stability of the initial transient (i.e. to indicate that the original probe fit in the ear canal has been maintained).
- Repeatedly calculate the correlation between the averaged responses present in each data pool, thereby indicating the certainty of a successful OAE response measurement.

The implementation of this design is such that these functions can all be achieved whilst still collecting data from the subject for over 95% of the time. This is true for even the relatively slow IBM PC computer (slow relative to the XT and AT models). This is achieved by 'off loading' the subaveraging process onto the response processor board, thereby reducing the computational load on the host computer's CPU.

There are only three arithmetic functions required by the response processor board, namely adding data to memory, subtracting data from memory, and overwriting the data in memory (in addition, a 'no operation' function is useful). These arithmetic

processes can easily be achieved using an 74 series logic device called the arithmetic logic unit (ALU). This device is programmable and can perform all the required functions on two sets of 4 bit inputs.

The use of a separate processor, dedicated to signal processing and situated on the board, was also considered. However, the use of the ALU approach has several advantages. For example, the small number of arithmetic operations required can easily be performed by the ALU (each function is programmed by the logic levels on six control lines). To perform 16 bit arithmetic requires a total of 6 chips (including the operation controller), and the addition can be executed in only 60 nanoseconds[2]. Finally, the biggest disadvantage of using a separate processor is the increased complexity of the circuit which is required to interface the on-board CPU to the host computer.

Fig.4.9 shows a schematic diagram of the 16 bit ALU used in the design. Each ALU chip has two sets of four inputs, four outputs, a 'carry' output, and 'borrow' input, in addition to the four controls lines and mode control line. The devices can operate in parallel with the addition of a 'look ahead carry' device. This latter device is connected to all the carry and borrow connections to allow parallel rather than serial (ripple through) operation.

The two sets of data input to the ALU are from the 12 bit ADC and the data bus of the on-board memory. For the first stimulus of each cycle of the 'stimulus package' it is necessary to overwrite the contents of the current memory address, so the ALU has a 'straight through' function which allows the ADC data to overwrite the memory. For the second section of the stimulus, the response from the ADC needs to be added to the memory. Thus the two inputs to the ALU are the ADC and the current memory

2 Typically, a double precision addition subroutine on an 8 bit processor requires about 16 instructions. On a typical CPU running at 4MHz this would take in excess of 20 microseconds to complete.

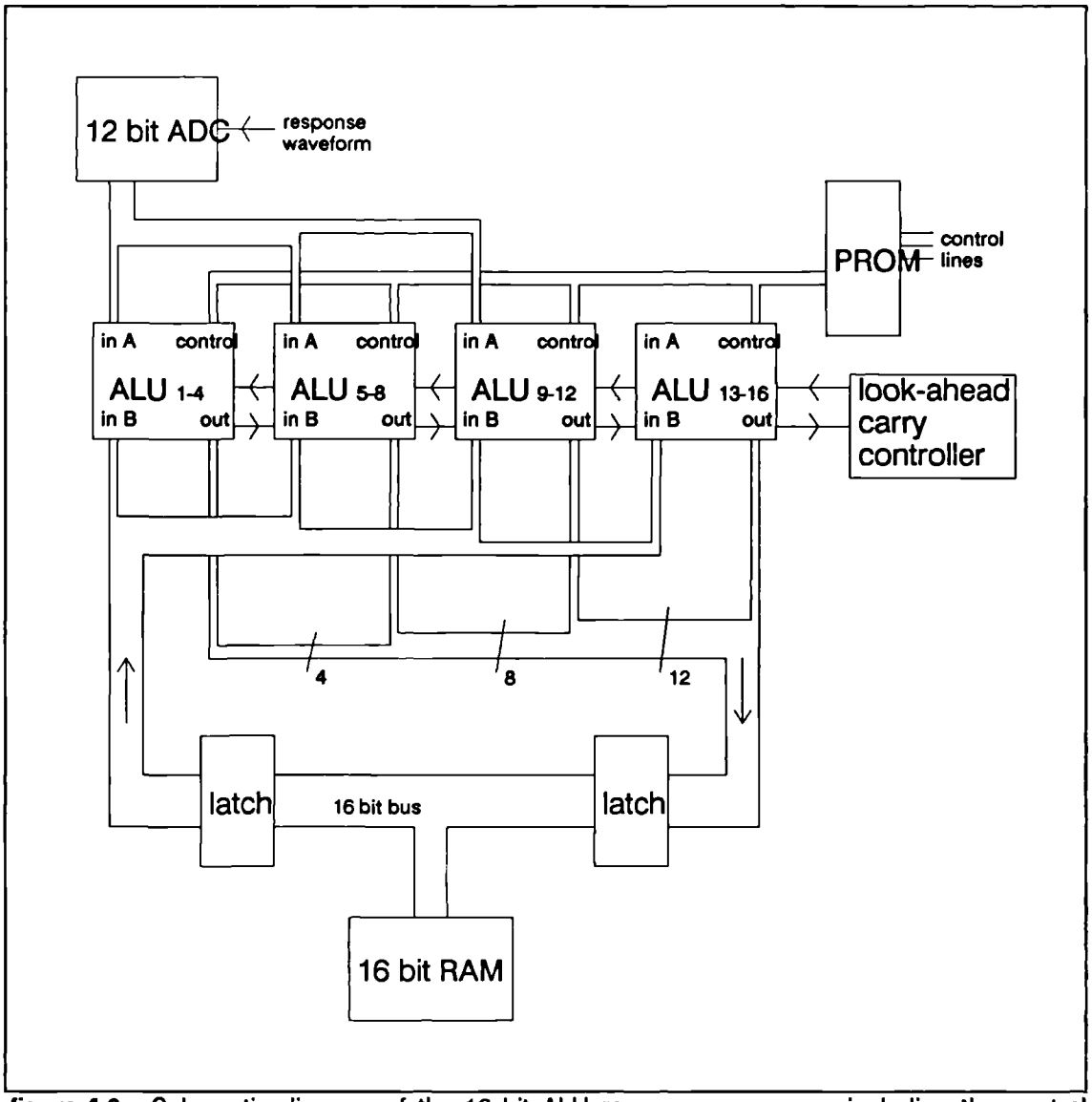

figure 4.9 Schematic diagram of the 16 bit ALU response processor, including the control components, the ADC and on-board memory. The diagrammatic bus width is representative of the 'bit width' of the bus.

contents. The result of the addition is then written to the current memory address, therefore overwriting the previous value.

The operation of the entire ALU is controlled by a 'programmable read only memory' (PROM). This PROM provides a means of decoding three lines from the local address bus and providing six lines of output to control the ALU. As the functions of the ALU need to change as each section of the 'stimulus package' is output from the stimulus generator board, the upper address lines of the local address bus provide the necessary information as to when to alter the arithmetic function.

Although the primary aim of the design was to perform subaveraging of the response data before being read by the host, the facility was also provided to allow access to the unprocessed data. This was achieved by using one of the bits from the control port to override the subaveraging process, and allow access to more of the on-board memory. The response data can then be written directly to the memory without modification. This facility was provided in order to allow possible further investigation of more complex data processes on the raw data.

Response processor board- data bus details.

Similarly to the stimulus generator board, the interfacing of the 8 bit computer bus to the 16 bit on-board memory required careful consideration. Octal tri-state buffers were used to isolate the individual memory data buses. The control of these buffers

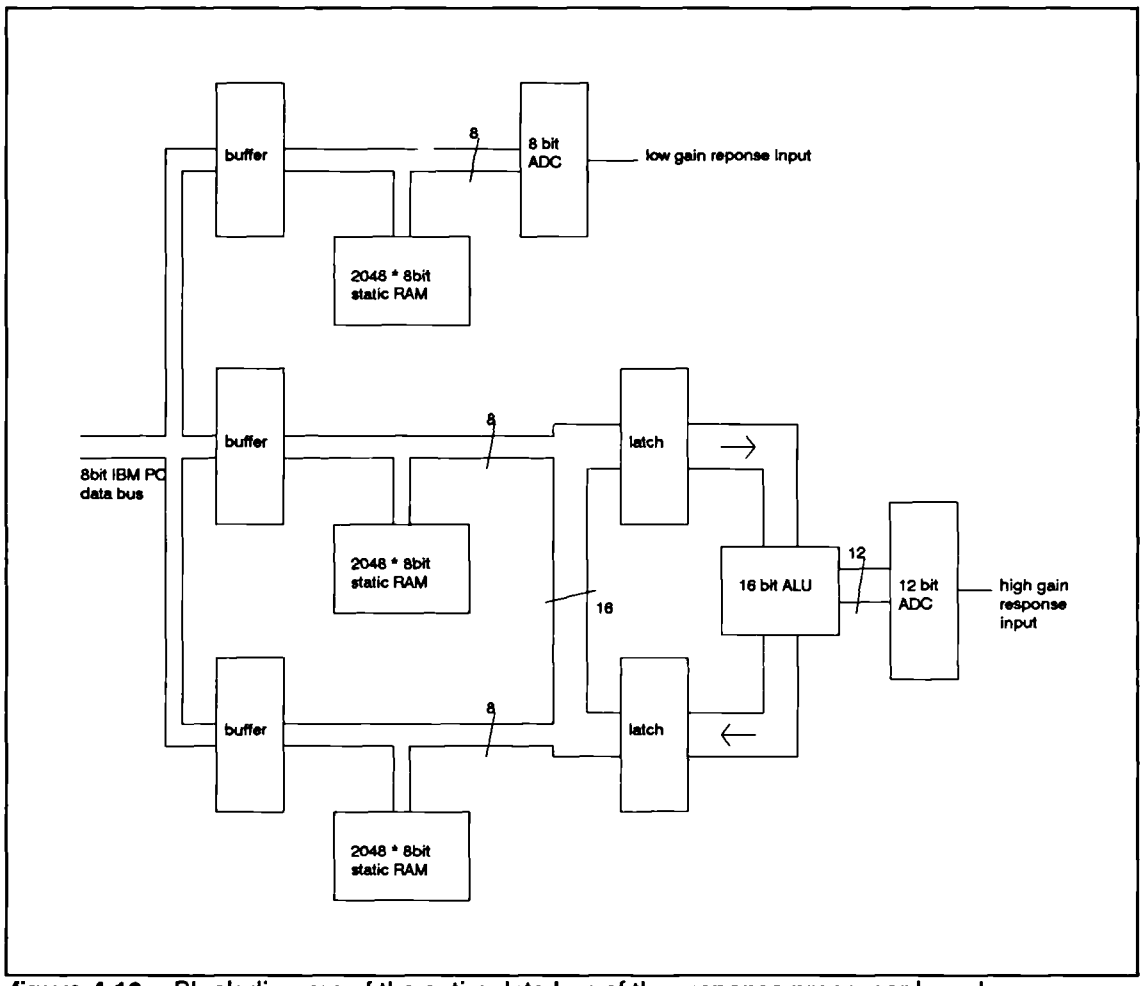

figure 4.10 Block diagram of the entire data bus of the response processor board.

required a considerable number of logic gates. It is important that at no time are two buffers attempting to assert data onto the computer bus and, more importantly, the buffers must only assert data onto the computer bus when the host computer requests it.

Fig.4.10 shows the details of the data bus from the 12 bit ADC to the ALU, and the interfacing of the memory data bus. Octal latches, with tri-state outputs are used to buffer and hold data from the memory to the ALU.

Response processor board- timing details.

Details of the timings of the various activities of the response processor board during a single data point cycle are given (see fig.4.11). All these processes are derived from the crystal clock and decade decoder sited on the stimulus generator board. The originating timing signals are connected via a 34 way IDC connector and ribbon cable and any further logic functions are performed on the response processor board.

The 12 bit ADC has a conversion time of approximately 25 microseconds. After the conversion period, the data is automatically placed on the ADC data bus to the ALU. During the conversion period, data from the current memory address is read and stored in the data latches that are connected to the ALU. Therefore, 60 nanoseconds after the ADC has completed the conversion, the output of the ALU holds the processed data, which is then written to the same memory address.

The 8 bit ADC has a much faster conversion time (about 10 microseconds). After conversion, the data is placed on the ADC data bus. The 8 bit ADC is connected directly to the on-board memory. At the end of the data point cycle, the data is written to the memory, utilising the same memory timing control signals as those used to write the ALU output data.

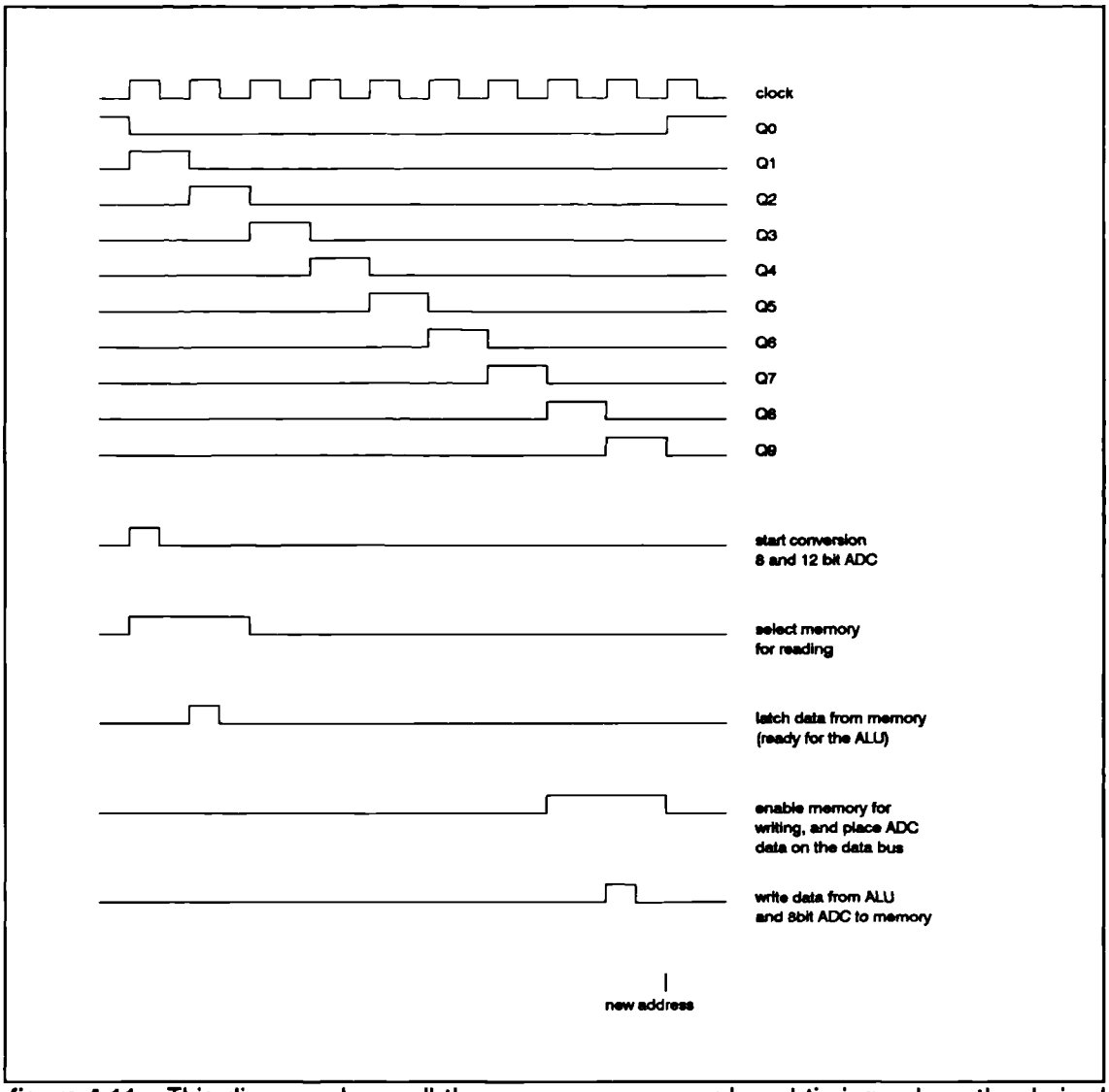

figure 4.11 This diagram shows all the response processor board timing pulses, the derived control pulses, and their functions.

The instrument was designed to collect and process data at a maximum rate of 40 microseconds per point. The length of a single response is 512 words, therefore the response time is 20.48 milliseconds. However, as the crystal clock can run at four different frequencies under the control of two of the control port bits, additional sample rates of 50, 60 and 120 microseconds per point are possible.

Response processor board - construction details.

The response processor board was also constructed on 'BICC VERO' IBM PC prototyping board. Because the board mixes low level analogue and digital signals, great care was taken during the routing of various signals. In addition, the earth reference point of the analogue signal was chosen with caution. In this design the primary function of the instrument is to measure the OAE, which is digitised by the 12 bit ADC. The 8 bit ADC serves more as a monitor, and therefore does not need to

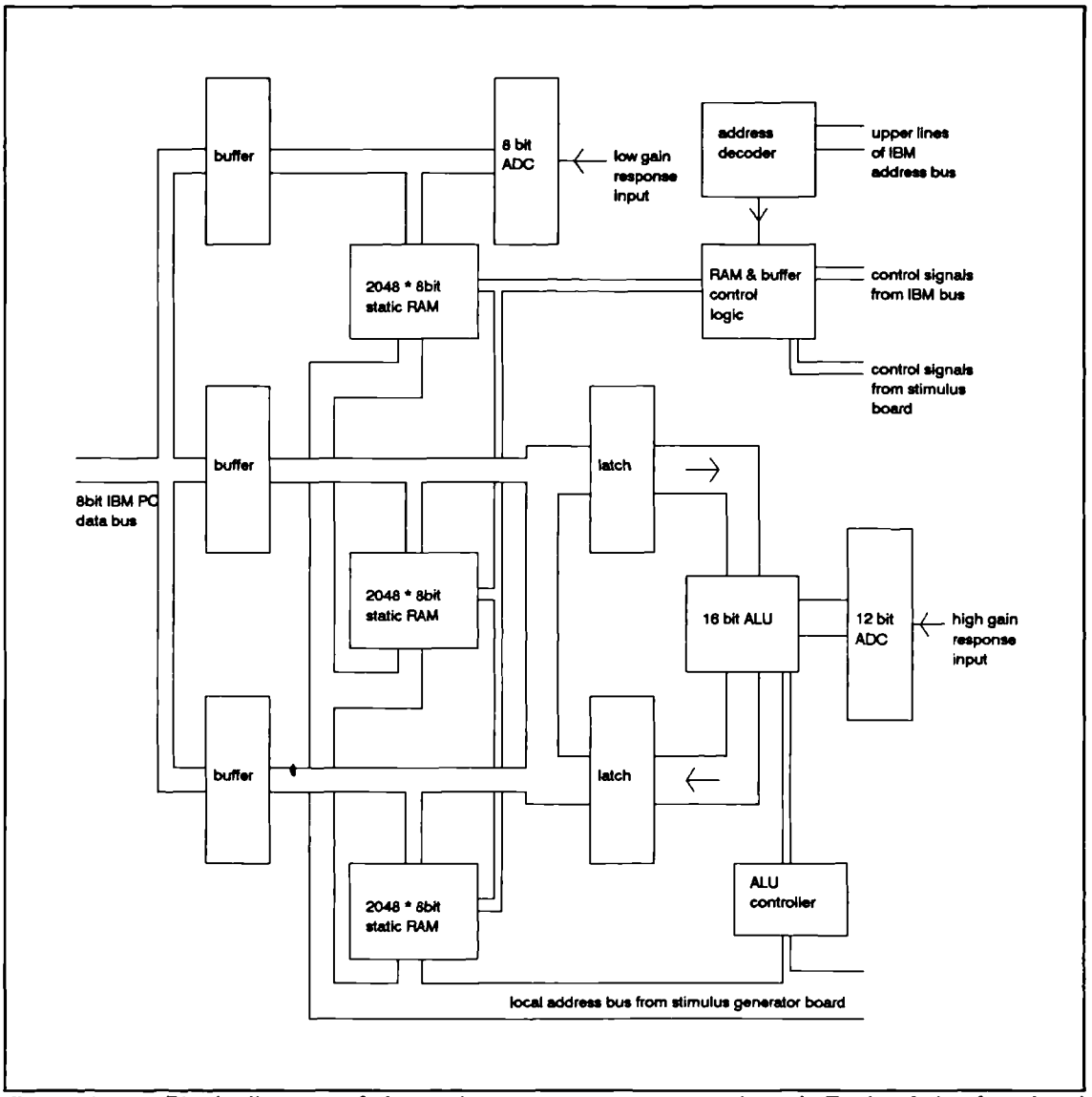

figure 4.12 Block diagram of the entire response processor board. Each of the functional sub-units, and the data and address bus are shown.

be as accurate. As a result, the 'central' analogue earth reference for the entire instrument is the earth pin of the 12 bit ADC.

A block diagram of the entire response processor board is shown in fig.4.12. A complete circuit diagram of the response processor board is given in the appendix. In total, both the stimulus and response boards consist of approximately 40 chips, which includes several 28 pin devices. This led to a reasonably high chip density, and complex wiring network.

Both ADCs are configured in bipolar modes, with a range of ±5 volts. Each ADC has an offset and gain adjustment. Once the board was completed and the individual chip functions tested using the Pascal test programme, the ADCs were calibrated using a voltage reference source. The test programme cyclically read the response data from both ADCs and displayed the digitised data. The offset and gain controls were then adjusted according to the manufacturer's specifications.

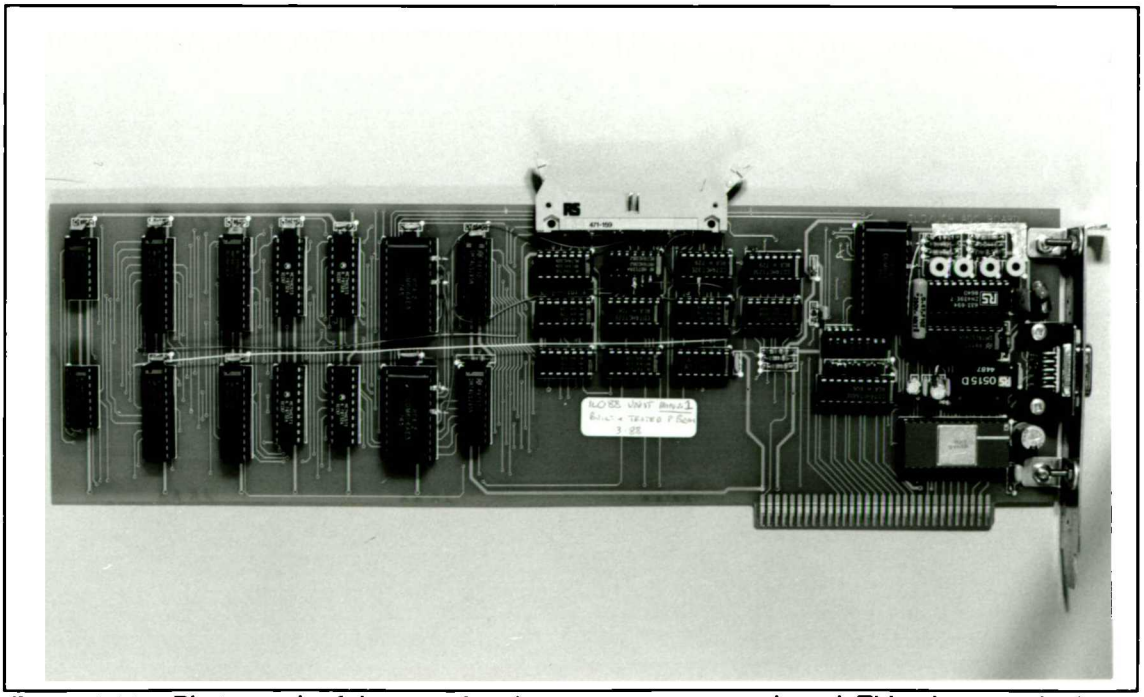

figure 4.13 Photograph of the completed response processor board. This photograph shows the pcb version of the board.

Fig.4.13 shows a photograph of the completed response processor board. Again, the photograph shows the printed circuit board version.

Once both the stimulus generator and response processor board were completed and calibrated, various tests of function were performed. By connecting the output of the stimulus board to the two inputs of the response board, various waveforms could be 'sent' to the response processor board, enabling more detailed assessment of the board function.

4.2.3 Analogue signal conditioning of the stimulus and response.

The stimulus waveform, generated by the DAC, needs to be buffered and filtered before arriving at the probe loudspeaker. In addition, the microphone output needs to be amplified and filtered at two different levels of gain before being digitised by the two ADCs. All these functions take place in a separate box, which is connected to the two interface boards via a series of wires. The box contains amplifiers, filters and an attenuator and is powered by its own mains derived power supply.

The stimulus signal from the DAC requires filtering to remove the high frequency components of the waveform, introduced by the 'digital steps' in the analogue waveform from the DAC. In addition to the control of the stimulus size that is possible by using different waveform data in the on-board memory, an attenuator is also used to control the output signal to the probe loudspeaker. This attenuator is digitally controlled by six of the eight lines of one of the control ports on the stimulus generator board. The attenuator has a 96dB range in 1.5dB steps. The block diagram of the various stages of stimulus signal treatment is shown in fig.4.14.

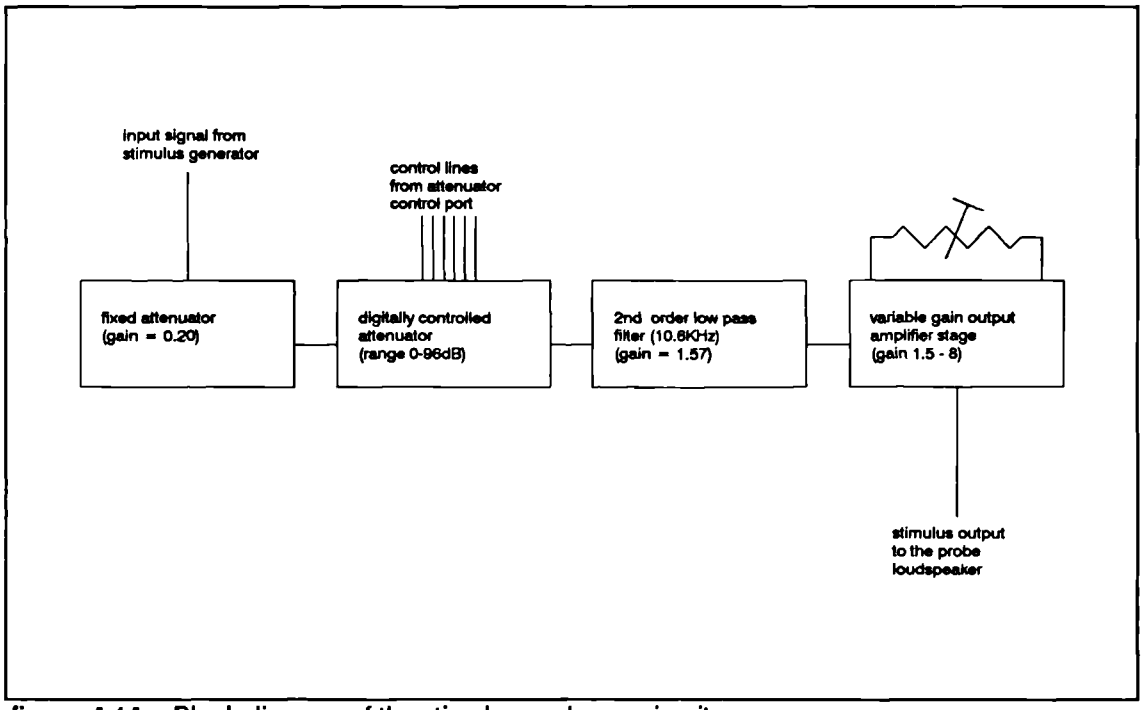

figure 4.14 Block diagram of the stimulus analogue circuits.

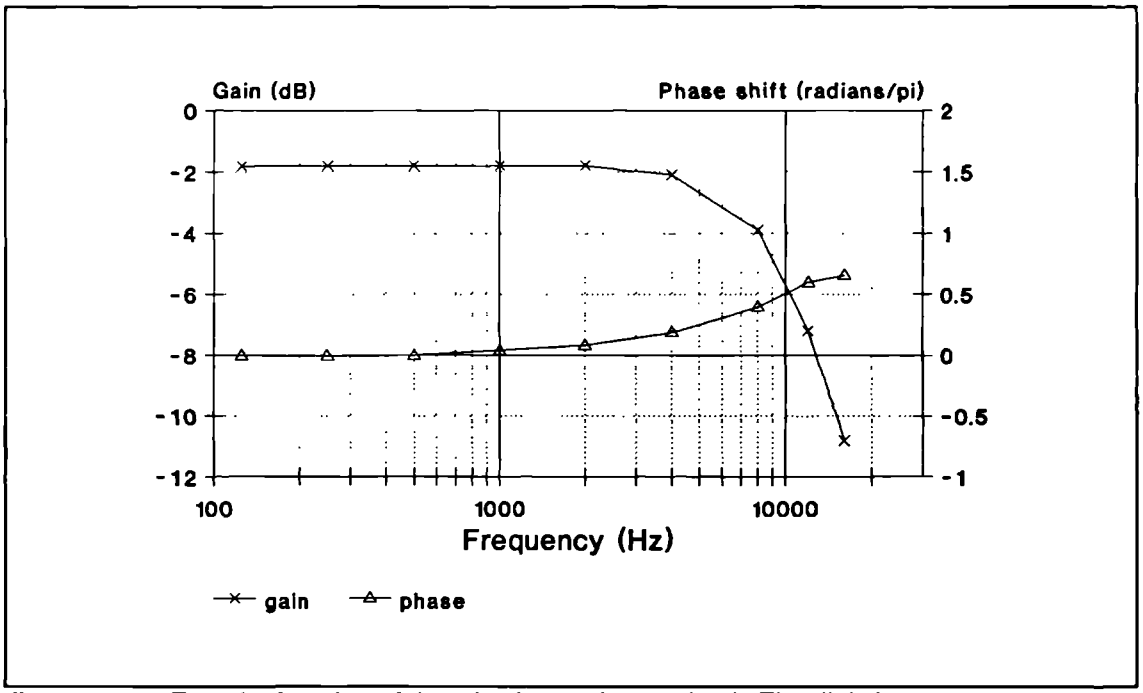

figure 4.15 Transfer function of the stimulus analogue circuit. The digital attenuator was set to 0dB attenuation for this measurement.

Fig.4.15 shows the transfer function of the analogue circuit for the stimulus signal (with the attenuator set to 0dB attenuation). The digital attenuator control and analogue connections for both the stimulus and response are conveyed in a high quality cable consisting of 7 pairs of double screened conductors.

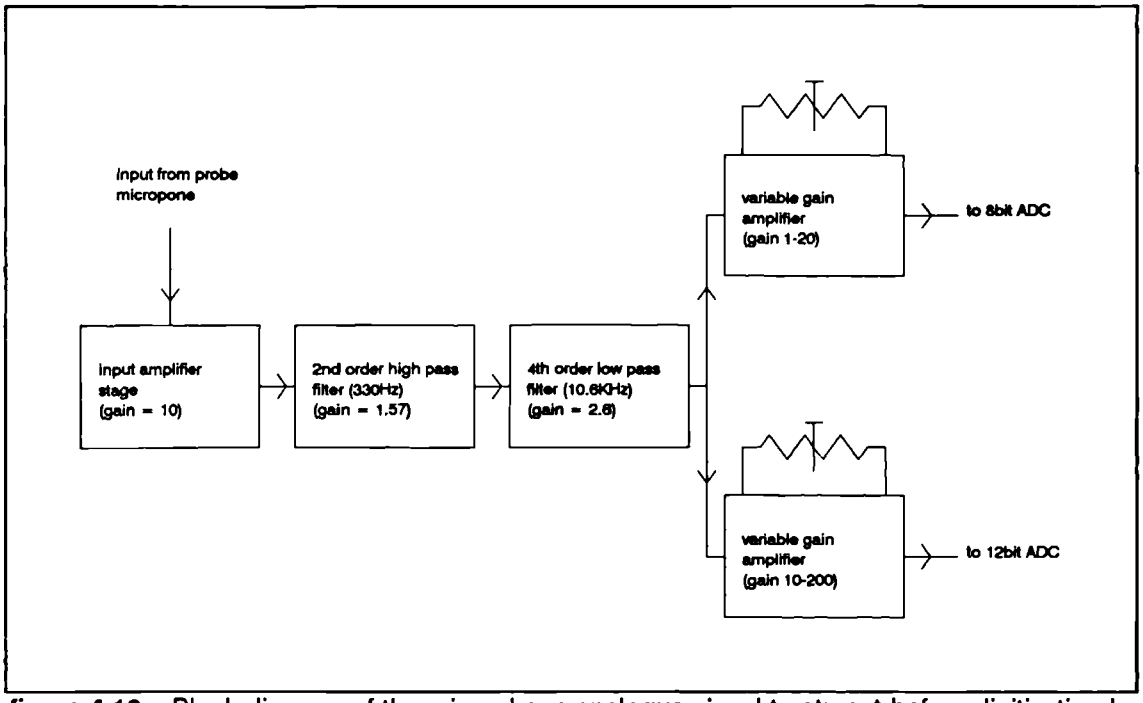

figure 4.16 Block diagram of the microphone analogue signal treatment before digitisation by the two ADCs on the response processor board.

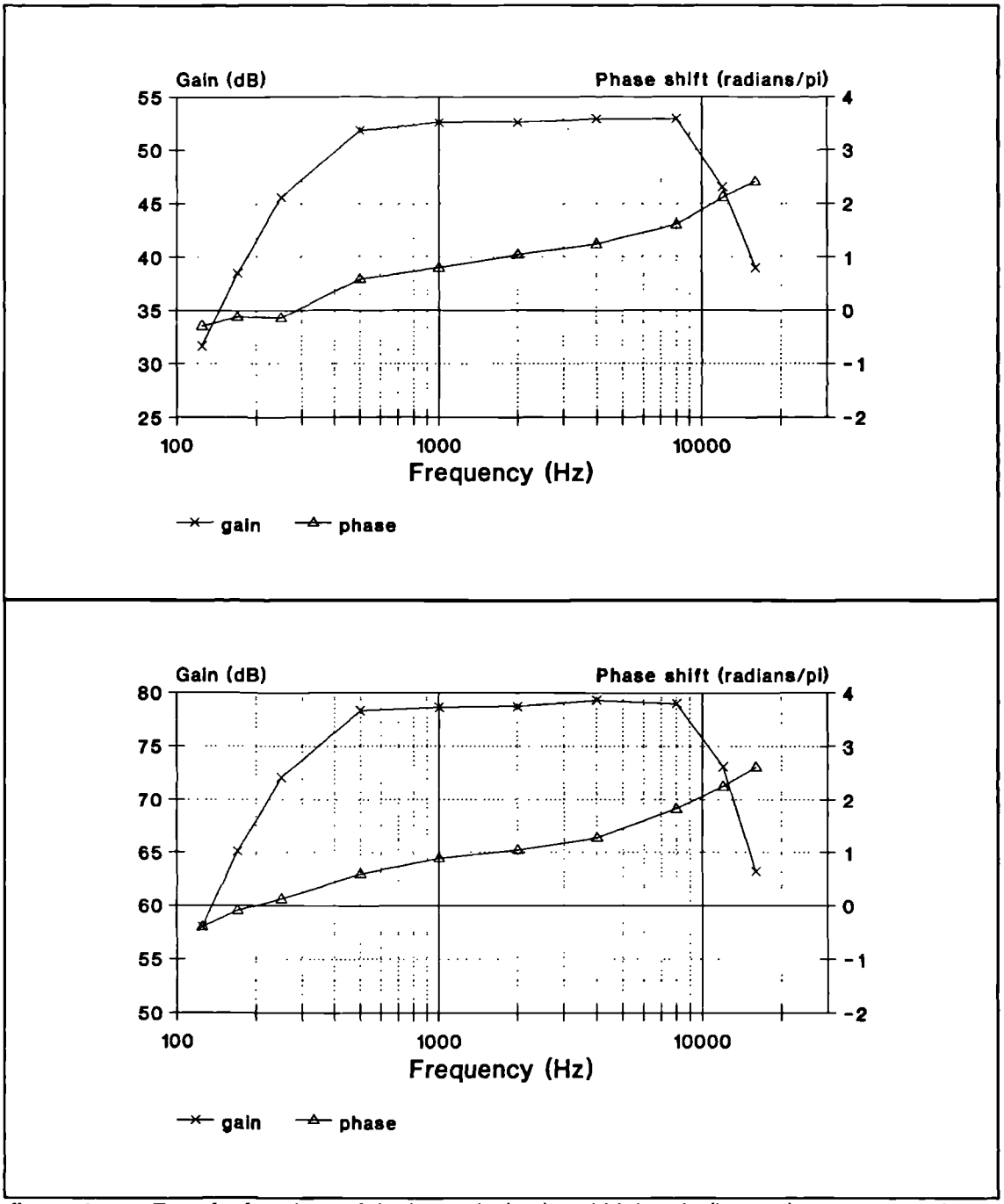

figure 4.17 Transfer functions of the low gain (top) and high gain (bottom) response analogue circuits.

Before arriving at the 12 bit ADC, the signal from the probe microphone undergoes an amplification of 8500. This high amplification of a very small signal requires that great care be taken in the design of the circuit and the routing of signal cables. The amplification of the response signal which is digitised by the 8 bit ADC is only 400.

Before any analogue voltage is digitised, the signal must be low pass filtered to remove any frequency components in the waveform which are higher than half the sampling frequency. Any frequencies higher than half the sampling frequency are 'aliased' down in frequency, and appear in the digitised data as artifact waveforms. Fig.4.16 shows the block diagram of the various stages of amplification and filtering that the response signal undergoes for each of the high and low gain channels. Fig.4.17 illustrates the transfer function of the high and low gain channels, and serves to illustrate the filtering applied to the signal to ensure that no erroneous aliased signals are present in the digitised data. In this particular implementation the probe microphone has a limited high frequency (above 5KHz) output (see fig.2.5b) and therefore the problem of aliasing is not serious.

The probe microphone requires a D.C. voltage to supply the microphone's internal FET amplifier. This is derived from the power supply of the analogue circuits. A five pin DIN connector was used to connect the probe to the box containing the analogue circuitry.

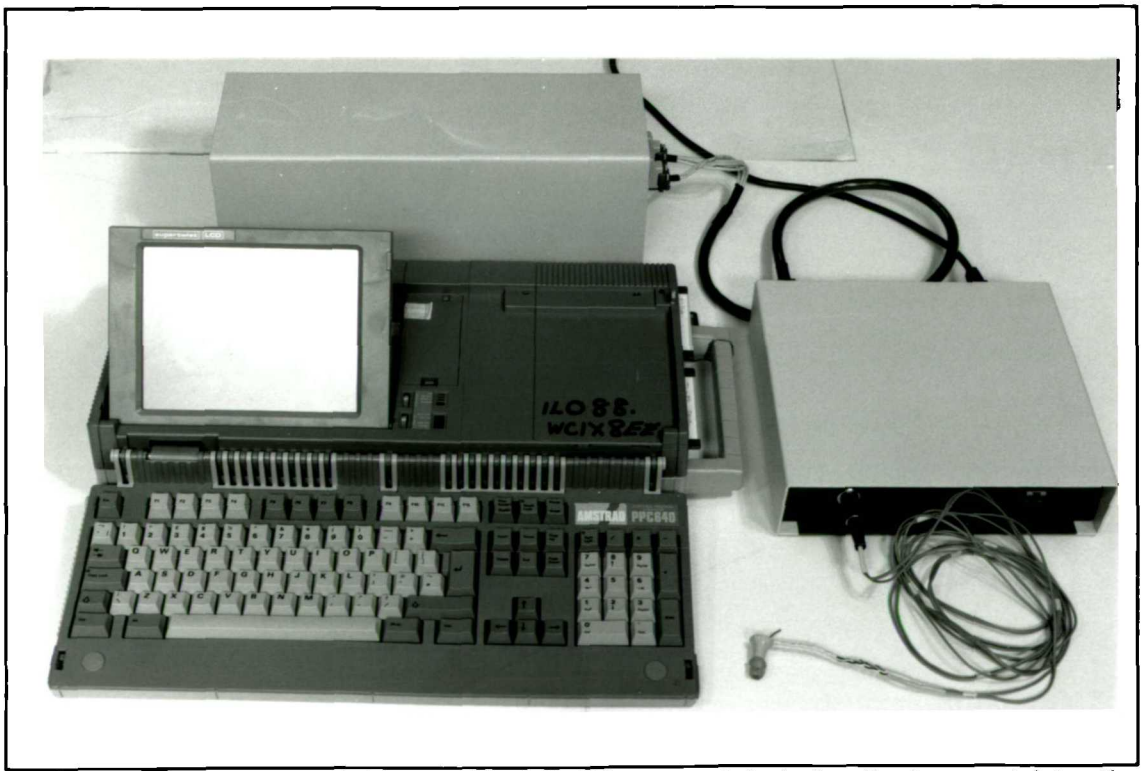

figure 4.18 Photograph of the completed OAE instrument, including the box containing the analogue circuits. The host computer in this photograph is an AMSTRAD PPC portable computer.

Fig.4.18 is a photograph of the completed instrument. The 'host' computer in this photograph is in fact a portable AMSTRAD PPC computer. The interface boards are housed in a separate metal box at the back of the computer.

Electrical standards for patient safety.

The analogue circuit design predominantly uses low noise BIFET operational amplifiers, although a bipolar device was used as a final buffer of the stimulus signal. The unit was housed in a steel box (approximate dimensions- 240*240*60mm). Great care was taken in the design of the power supply and other matters of patient safety. The unit conforms to the recommended British standard for medical equipment safety (B.S.3754). For example, the design uses double fusing of the mains wires, a mains isolation transformer, neon indicators and double insulation.

4.2.4 Software control of the OAE instrument hardware.

The instrument hardware was designed to be controlled by a minimum of software instructions. The functions of both interface boards are controlled by a single output port. The attenuator is controlled by a second port, and the status of the data cycle is determined from a third port. Writing and reading the stimulus and response waveforms is the same as writing to, and reading from, the memory of the host computer, once the interface boards are set to the appropriate mode.

The necessary input/output (IO) and memory data transfer functions are available in most languages. The languages which have been used for the OAE instrument hardware control are BASICA, Turbo PASCAL and Microsoft Assembler.

The main clinical/laboratory OAE instrument control programme is written predominantly in Turbo Pascal. However a 'library' of very fast, instrument specific subroutines was written in assembly language. These subroutines are called from the Pascal programme, simplifying and increasing the speed of the main programme.[3]

A significant advantage of this instrument over the previous system used for OAE measurement, is that the interface boards require a minimum of the host computer's CPU time during data collection. This is due to the dual-ported memory and dedicated signal processing functions of the boards.

Typical data collection cycle: Once the stimulus generator board has been loaded with the stimulus waveform, the attenuator is set to the correct level and the boards are triggered via the software. The host computer then has 80ms of processing time before the hardware completes the data collection and processing. The processed response is read from the hardware and the boards are retriggered as necessary.

3 These instrument specific subroutines were assembled into a library so as to enable programmers who are less familiar with the specific hardware details of the system to write efficient software for the instrument.

4.3 Software requirements of the OAE instrument.

Introduction.

The basic function of the OAE instrument is to present a click stimulus to the ear canal, measure the response, compute the nonlinear component of the response, average the responses to many stimuli and present the averaged response to the user.

The main clinical/laboratory OAE instrument software was written predominantly in Turbo Pascal. Linked into the main programme was the OAE instrument 'hardware driver' software library, a graphics driver library and a library of signal processing subroutines.

The programme allows the operator to perform a 'routine' emission measurement consisting of probe fitting, data collection and analysis, and the production of a detailed measurement report.

The programme displays several 'windows' on the VDU which show response waveforms and operational feedback. The control of the programme is achieved via a series of operator selections from 'pop-up' menus. In addition to the basic measurement functions, there are also a large number of facilities offered to the operator such as to 'save' and 'recall' data from disk, as well as access to many of the operational control parameters (for example, the stimulus level).

Fig.4.19 summarises the central sequence of events during OAE data collection, and includes special features which were required to meet the instrument specification (i.e. inter-waveform correlation).

The 'end product' of this sequence of events is two nonlinear response waveforms. The waveforms are normalised (scaled to represent 256 subaverages) bandpass filtered (400Hz to 6.4KHz) and gated to remove the ADC overload artefact present in the first 1 to 2ms. The waveforms are then displayed on the VDU, superimposed

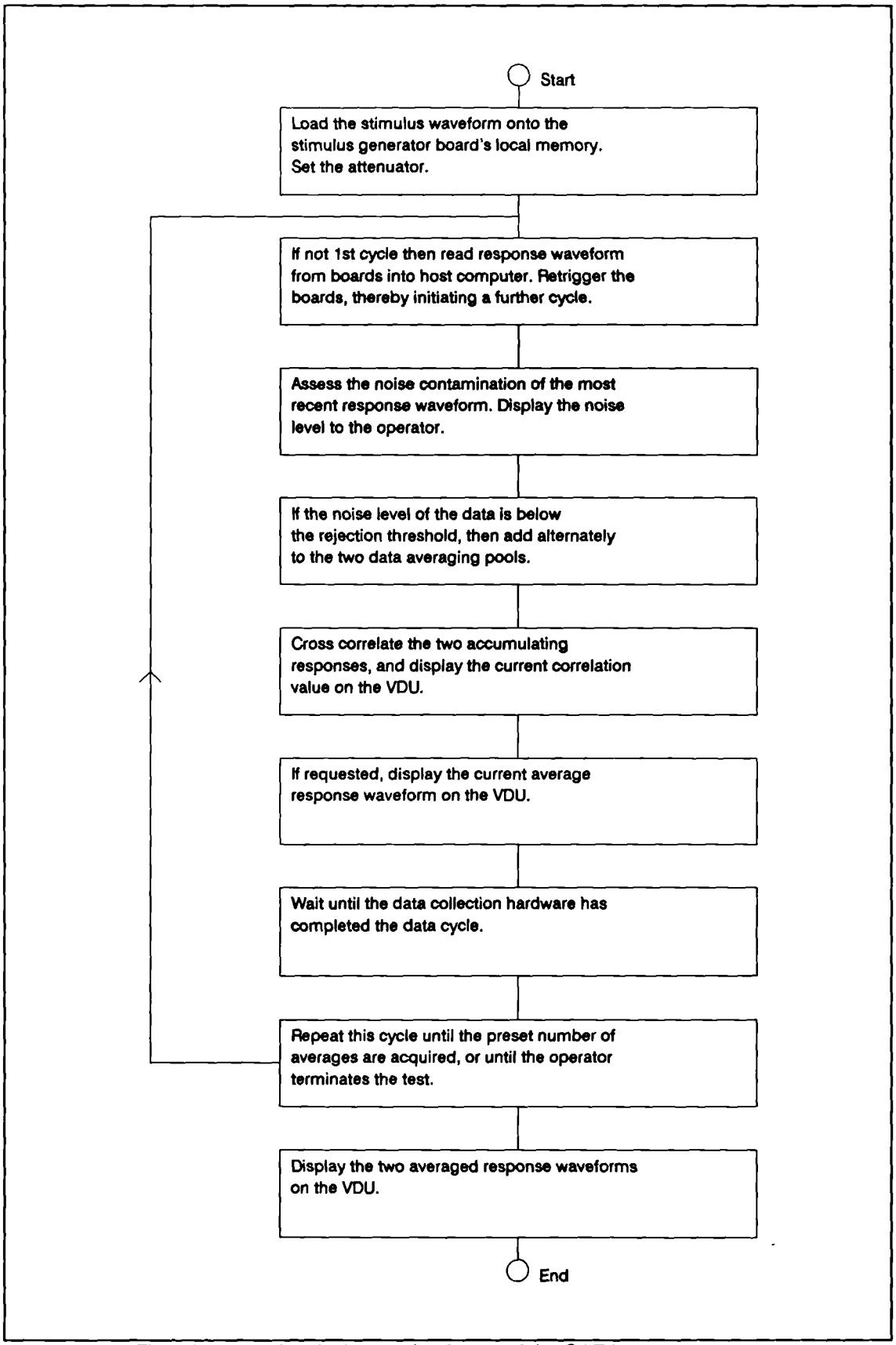

figure 4.19 Flow diagram of typical control software of the OAE instrument.

so that the operator can visually guage the 'quality' of the response measurement and the presence or absence of an OAE.

Assessing the noise contamination of the response data.

During this data collection cycle the level of noise contamination of the response data is assessed. Effective assessment of the noise contamination of the response data leading to the acceptance/rejection of the data minimises the test time required to obtain the necessary signal to noise ratio of the averaged response data.

The OAE measurement instrument assesses the response data quality **after** the subaveraging of the four responses to the 'stimulus package'. This was determined on the experimental minicomputer system as being advantageous over the alternative technique of assessing the raw unaveraged data, due to the extent of contamination of the cochlear component of the response by the middle ear response.

The noise level in the response measurement is gauged by measuring the peak amplitude of the emission response waveform. To achieve the maximum averaged response data quality in a limited amount of time, it is necessary to reject response data samples with noise levels which are comparable to the emission amplitude. Because the initial transient stimulus is much larger than the small emission response, accurate noise detection, close to the emission amplitude is impossible until the initial transient has decayed below the level of the response. The alternatives are to either raise the threshold of noise rejection, or delay the onset of noise detection until later in the sample (i.e. when the middle ear response has decayed). Neither of these solutions allow accurate noise detection.

By performing a subaverage of the emission responses to the linearly balanced stimulus set, the large initial transient is completely eliminated. This allows accurate noise measurement along the whole response length. This technique is detailed in a paper by the author[5], and is patented[6].

Post OAE measurement - options available.

After completion of the OAE response data collection process (fig.4.19), the two response measurements are displayed on the VDU. The cross power spectrum of the two response waveforms is calculated along with the spectrum of the noise in the emission measurement. These spectra are then displayed in a 'window' on the VDU. The cross power spectrum is displayed in one colour, and the noise spectrum is superimposed in another colour. Various numerical data pertaining to the test conditions and OAE measurement parameters are derived and displayed in another window of the VDU (see chapter 5).

Three 'pop-up' menus can be summoned via the [esc] key. These menus provide over 20 options to the operator. These include saving and reviewing OAE response files from disk, initiating further OAE measurements, and more detailed analyses of the current OAE data. Fig.4.20 summarises the operations available upon completion of the OAE measurement phase.

Alternative modes of instrument operation.

Although the instrument was designed to implement the derived nonlinear response data collection technique, other options are available.

The 'nonlinear' mode is achieved by using 3 stimuli of one size, and 1 stimulus of 3 times the size. By arranging the large stimulus in opposite polarity to the three smaller ones, the subaveraging process of the four stimuli can be performed using only addition.

By using a 'stimulus package' which has only one size and polarity of stimulus, the instrument performs as a normal averager, and the emission response to 'normal', single level excitation can be measured (although subaverages to groups of four stimuli are stilled performed). This arrangement allows considerable flexibility. For example, the stimulus package can include two pairs of equal and inverted stimuli

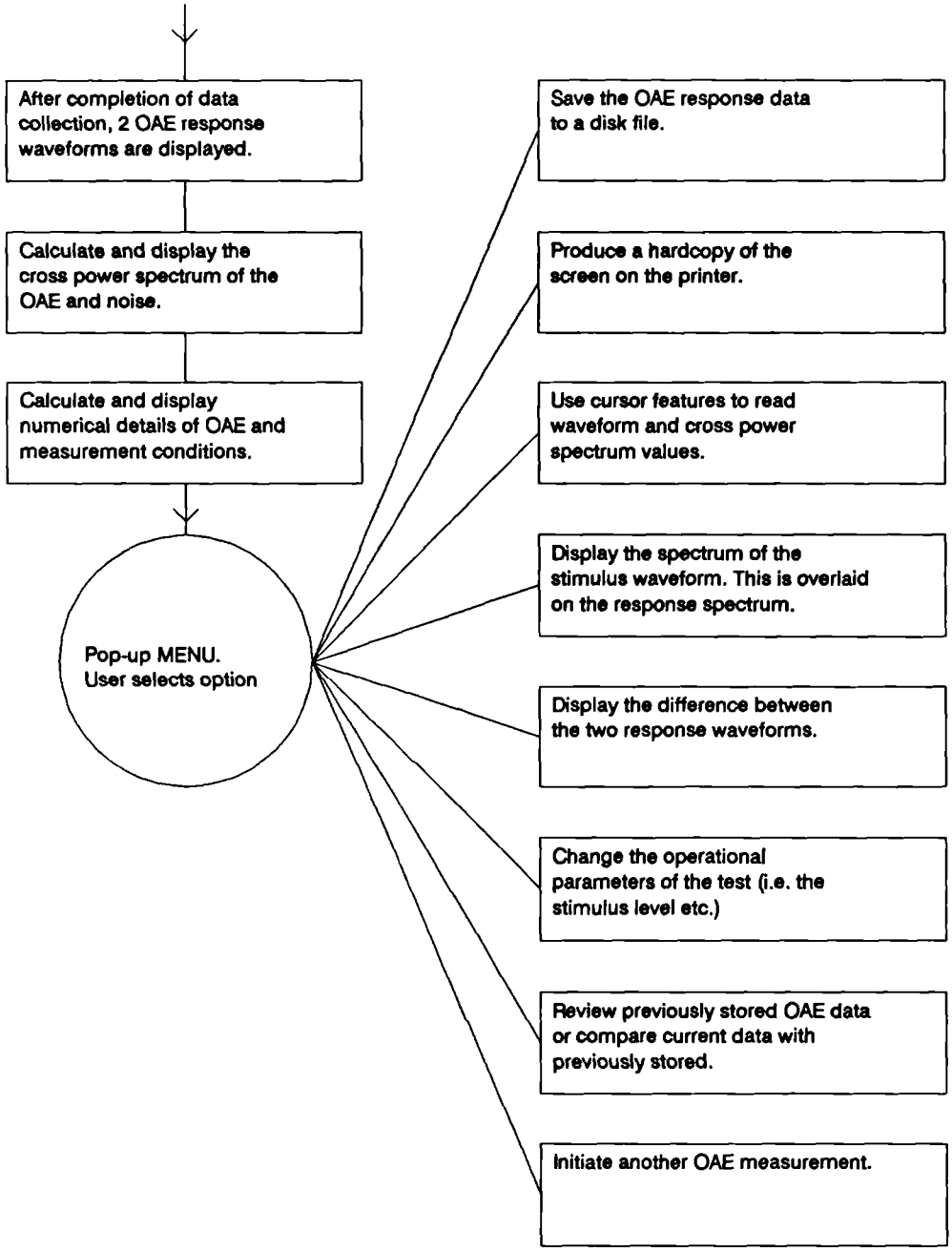

figure 4.20 Summary of the OAE response processing after completion of data collection and the various operations available to the user.

which completely cancel in the subaveraging process. This is useful in experiments to investigate the 'masking' effect of various stimuli.

To enable still further flexibility, the instrument has a 'subaveraging override' facility. By setting one of the bits of the control port, the response processor board no longer subaverages the data, but instead writes the data straight from the 12 bit ADC into 2048 words of memory. This allows access to the whole response to each section of the stimuli. This facility can be used to implement more complex data processing of the raw data.

Other programmes were written using these 'extended' functions. For example, by setting the stimulus waveform to zero, and setting the response processor board to write the response data directly to memory, the instrument could perform as a spectrum analyser. This was useful during various calibration procedures.

4.4 Calibration of the complete OAE instrument.

In the appropriate sections, consideration has been given to the calibration and response of each individual component of the instrument (i.e. the probe was discussed in chapter 2). It remains to consider the calibration of the instrument as a whole.

By using fixed gain input and output amplifiers (trimmable gains only), the process of calibration is simplified. For example, when the host computer reads data from the response processor board, the size of the array data values correspond exactly to a sound pressure level in the ear canal. Therefore the entire system can be calibrated by placing the probe microphone in a known sound field and monitoring the response array data size.

Fig.4.21 shows a summary of the transfer functions of each of the components in the stimulus and response chain. These values are measured at 1KHz (the complete

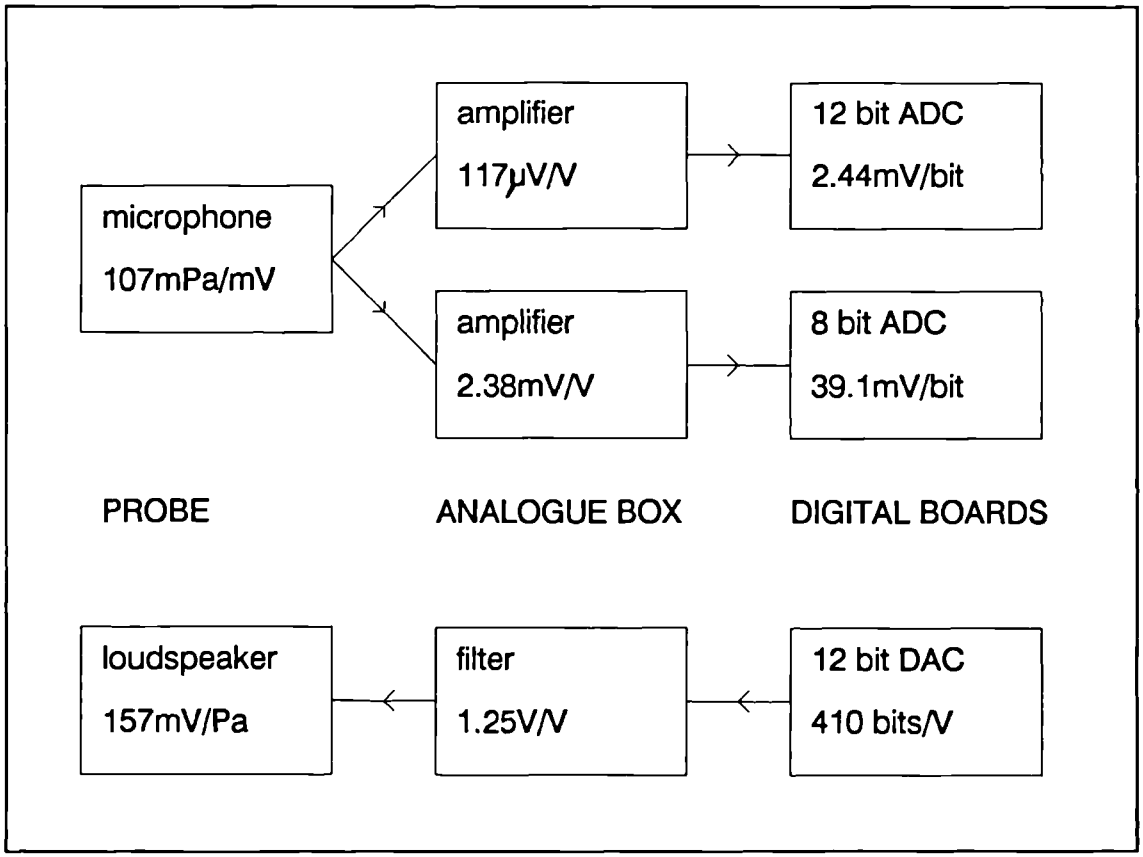

figure 4.21 This diagram shows the gains of each of the different stages of the response and stimulus signal treatment (digital and analogue).

transfer functions are shown in chapter 2 for the probe transducers, and in this chapter for the analogue circuits).

Free field sound measurements using the instrument probe were performed. The sound level was monitored through the low gain (8 bit ADC) and high gain (12 bit ADC) channels. A free field audiometer was used to provide the sound source, and a B&K sound level meter was used to check the sound field at the probe tip. A totally independent second measurement was performed to check for errors in the calibration. The probe loudspeaker was used as the sound source and a B&K measuring amplifier connected to a 1/4 inch microphone was used to measure the sound level developed in a $1cm^3$ test cavity (see chapter 2).

The Pascal test programme was elaborated to include provision for the above mentioned methods of calibration. This takes the form of a constantly updated 'window' of the screen which displays either the 8 bit or 12 bit response waveforms (i.e. a 'digital oscilloscope'). An rms calculation of the response waveform is performed, and the value is converted to dB spl according to the conversion factors shown in fig.4.21 (i.e. 30μPa/bit for the 12 bit ADC, and 9.9mPa/bit for the 8 bit ADC). If the calibration measurements are correct, this then corresponds to the reading on the sound level meter, or the measuring amplifier.

The subaveraging process introduces a further calibration factor which varies depending upon the nature of the signal which is being measured. Three types of signal are considered:-

- Signals which grow linearly in response to increased excitation levels.
- Signals which are evoked, but which behave in a saturated manner to increasing excitation level.
- Random noise which is independent of excitation.

Because the 12 bit ADC response data is subaveraged on the board, and each signal type behaves differently to averaging, for calibration purposes, each of these signals must be considered individually. After subaveraging, the bit level of the response data corresponds to a different sound pressure level at the microphone input for each type of signal.

Linearly evoked responses, after 4 subaverages, have a sensitivity of 7.5μPa/bit (i.e. 30/4μPa/bit) in the response array. If, however, a linearly balanced set of four stimuli are used (i.e. 3 stimuli of one size, and one stimulus of three times the size and inverted), then the sensitivity is zero (as previously explained, any linear signal will completely cancel in the subaveraging process).

In the case of the nonlinear (saturated) response, the sensitivity depends upon the specific details of the linearly balanced stimuli set. However, for the normal stimulus package of 3 of one level and one of three times the size, the sensitivity of the subaveraged response array is 15μPa/bit. This is because for a completely saturated response, after a subaverage of the four stimuli, the response is twice the size of the single saturated response (i.e. the inverted response to the large inverted stimulus exactly cancels the response to one of the other three stimuli).

The magnitude of an array of averaged random noise is equal to the magnitude of a single array of noise, multiplied by the square of the number of averages. Therefore, after 4 subaverages the sensitivity of the subaveraged response array is 15μPa/bit.

The above listed sensitivities all relate to the response data which is read from the response processor board. However, there are further matters of calibration to be considered. During the measurement of an OAE the many subaveraged responses are averaged. Again the treatment of each signal type is different, as the signals average differently.

The fixed gain concept of the instrument is implemented not only in the hardware but also in the software. The OAE software collects a number of averages. This is normally 256 subaverages in each of the two averaging pools. However, the total number varies considerably (depending upon the noise conditions during testing etc.). Upon completion of data collection the programme always normalises the averaged data to be equivalent to 256 samples (i.e. the averaged data is multiplied by 256/n, where n is the actual number of averages). This means that, at the end of the test, the size of the response array data corresponds to a sound pressure level in the ear canal.

The only other factor affecting the calibration is the display scaling of the data responses on the screen. The display windows of the OAE software show the response data, and a scaling factor is used on the data so that the response fits within the window. In the case of the main emission response window of the OAE software the response is scaled by 256. Therefore, after the test is completed and the response has been normalised and displayed, the sensitivity of the displayed response on the screen is 15μPa/bit.

4.5 Summary.

An instrument was designed and built to the specification discussed at the beginning of this chapter. This entailed careful consideration of the biophysical properties of the transient evoked acoustic response and the additional requirements necessary when designing an instrument for clinical use. These considerations resulted in a series of specifications for the hardware, signal processing and the operator interface software.

An instrument was designed and constructed which meets almost all the criteria (real time display of the accumulating response waveforms was compromised, to allow the CPU more time for data processing). The instrument is based on an IBM PC, and consists of two additional interface boards and an analogue signal conditioning unit.

A detailed investigation of the instrument performance is necessary in order to test to what extent the instrument, and therefore the original specifications, satisfy the fundamental design aims of the instrument. Such an investigation requires placing the instrument in the clinical environment (preferably several differing environments) and monitoring the performance.

The performance of the instrument is measured in many ways.

- How quickly is the test performed?
- Does it produce a result which is consistent with known diagnosis?
- How easy is the instrument to use?

In practice, this process of assessment, re-specification and re-design commences before the instrument is 'completed'. In addition, the process is repeated several times. With each refinement of the instrument, hopefully, achieving a result which brings the instrument closer to the 'ideal'.

The hardware specifications, such as the data sampling rate and the response length, were formulated as a result of several years of experimental OAE measurement experience. Whereas the software specifications, such as the screen display layout which provides the right information for the operator in a clinical environment, could only be achieved through speculation (as experience in the clinical environment could only be achieved through the use of the new instrument). As a result, much of the re-specification and re-design of the instrument was specific to the software.

Evaluation of the OAE instrument.

The OAE measurement instrument was developed (see chapter 4) to fulfil the task of recording OAEs in the demanding conditions of clinical testing as well as for experimental use in the laboratory. Software for the instrument was developed to enable a simple 'screening' type test of cochlear activity. In addition, further software facilities were made available to the operator to enable more complex analysis of the OAE data.

The aim of this chapter is to report on an evaluation of the instrument and the results obtained, based on practical use of the OAE instrument. As part of this evaluation OAE instruments were placed in four different auditory test centres. These were the Nuffield Hearing and Speech Centre (part of the Royal National Throat Nose and Ear Hospital, Gray's Inn Road), the Institute of Hearing Research (Southampton), Royal Hallamshire Hospital (Sheffield), and the Hôpital St. Charles (Montpellier, France). These instruments have been used to test children and babies as well as adults.

There are currently over 20 staff with experience of operating the OAE instrument at the Nuffield. All clinical OAE data shown in this chapter was recorded using the the Nuffield Centre OAE instrument.

Evaluation of the instrument is subdivided into four sections:-

- **Practical use.** If the instrument is not easy to use then reliable data is less likely to be obtained. This section reports on the procedures involved in preparing to measure an OAE in the clinical situation. In addition, summaries are given of the experiences of the various operators (persons not

associated with the design and construction of the instrument) in the execution of these procedures.

- **Interpretation of test conditions.** During the emission measurement it is important that the operator receive adequate information pertaining to the test conditions (e.g. the stability of the probe fit, and quality of the data collected to date). This section discusses the appropriateness, or otherwise, of the selected information on display to the operator.

- **Interpretation of processed emission data.** Upon termination of the test, the emission data is processed and displayed on the VDU. This section reports the relevance, or otherwise, of the various items of information displayed in forming a conclusion of the cochlear status of the subject.

- **Evaluation of emission data obtained in relation to clinical data.** The results of emission measurements from subjects with different auditory pathological conditions are shown and discussed. The success of the OAE instrument as a predictor of auditory function is also discussed.

The aim of this evaluation is to assess the degree of success of the instrument design and implementation, leading to conclusions as to any necessary further developments to the design.

Much of the evaluation involves the instrument software, as it is this which primarily determines the function and 'user friendliness' of the instrument. The instrument screen is divided into 5 panels which are 'active' at various stages of the measurement proceedings. Instructions are relayed to the operator via a menu/information panel which is overlaid on the screen. Figures 5.1 and 5.2 show the screen during, and immediately after, an emission measurement. The figure captions describe the various screen panels and the numerical data. These figures serve as a reference for the remainder of the chapter.

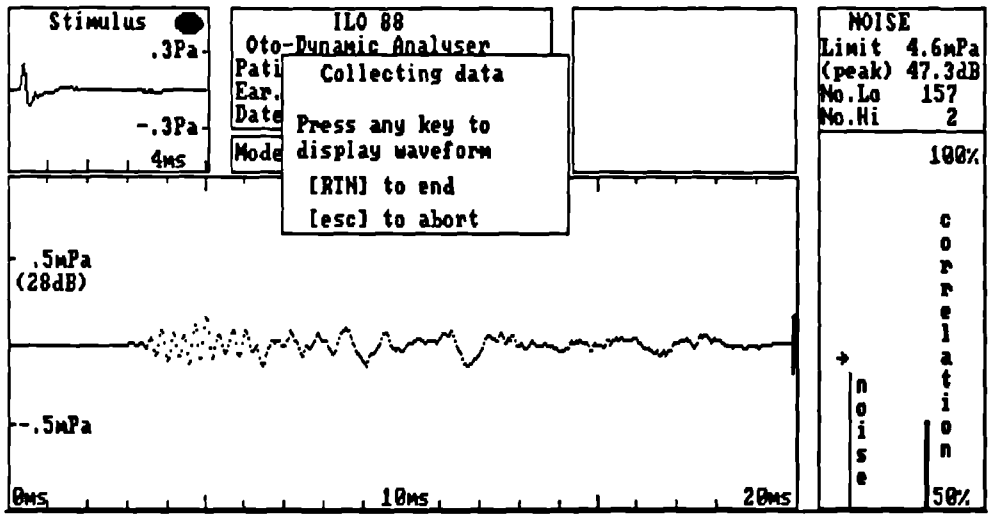

figure 5.1
OAE instrument screen approximately 20 seconds after commencing an emission measurement. Below is a brief summary of the contents of each of the panels on the screen.

'Stimulus' panel (top left). Shows the transient response of the ear canal at the start of the recording period. The 'spot' in the upper right hand corner changes colour, representing the stability of the probe fit (see text).

'Patient' panel (top centre). Indicates the patients name, ear etc. 'Mode' relates to the stimulus mode (linear or nonlinear), and 'Op gain' is the stimulus channel gain setting.

'Cochlear response' panel (main panel). Displays a sketch of the averaging response data upon operator request (key press). Two narrow bars at the right hand side indicate the amplitude of the response data in each buffer.

'Numerical' panel (right hand side). The upper part of this panel shows the number of accepted/rejected subaveraged response data samples, and the current noise rejection level. The lower part of the panel has two bar graphs. The left hand bar indicates the noise level in the most recent subaveraged data sample. This is updated for every data sample, and therefore provides 'realtime' feedback as to the current ear canal noise level. The right hand bar is the inter-waveform correlation of the two data averaging buffers. This serves to indicate the 'quality' of the data collected up to that point.

'Overlaid Menu'. At various stages of the instrument function, menus are overlaid on the screen to inform the operator of the current operation, and any key presses which may be required.

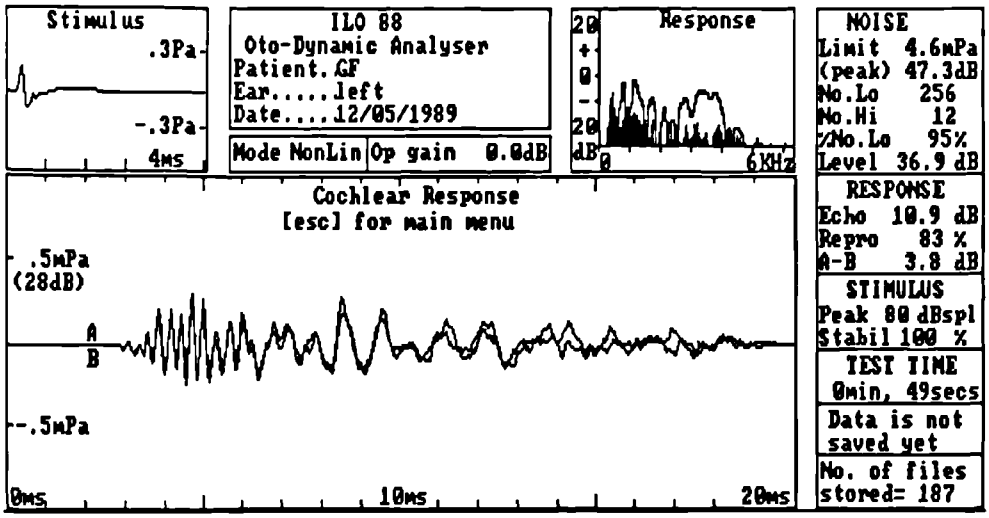

figure 5.2
The OAE instrument screen upon completion of the OAE measurement. The stimulus panel shows the transient response at the end of the test. The patient panel displays the same information as fig.5.1. The cochlear response panel shows the two response waveforms, after processing, superimposed.

'Response spectrum' panel (top right). The cross power frequency spectrum of the two response waveforms is calculated and displayed. The frequency spectrum of the difference between the two waveforms (i.e. an estimate of the noise in the measurement) is superimposed (shaded).

'Numerical' panel. The far right hand panel contains the numerical data pertaining to the emission measurement. The following list gives a brief description of the derivation of each of the figures.

NOISE:- **Limit:** The rejection threshold of peaks in the response data expressed in both mPa and dBspl. **No.Lo:** The total number of subaverages which were below the rejection threshold, and therefore added to the averaged response data. **No.Hi:** The total number of subaverages which were above the rejection threshold and were therefore rejected during the recording period. **%No.Lo:** The total number of accepted subaverages expressed as a percentage of the total number during the recording period. **Level:** The actual noise level which was present in the ear canal during the recording of accepted subaverages. This is derived from the noise level in the averaged response, and multiplied by a factor calculated from the number of accepted subaverages (i.e. No.Lo.).

RESPONSE:- **Echo:** The calculated power of the emission waveform expressed in dBspl. **Repro:** The inter-waveform correlation of the two response waveforms, expressed as a percentage. **A-B:** The calculated power of the difference of the two response waveforms, expressed in dB spl. This figure is used as the basis of the 'NOISE Level' parameter, above.

STIMULUS:- **Peak:** The intensity of the maximum pressure excursion of the stimulus waveform, expressed in dBspl. **Stabil:** The waveform cross correlation of the initial and final stimulus waveforms. This is an indicator of the stability of the probe fit in the ear canal.

TEST TIME:- The total time of the recording period.

FILE NUMBER:- This panel indicates the file number of the data shown on the screen. If the data is not saved, this is reported on the screen.

NO. OF FILES:- Indicates the total number of data files stored in the current data directory.

After preliminary trials of the instrument a number of programme modifications were suggested. Many of these related to the ergonomics of programme control, such as, the use of 'function keys' to allow the operator to quickly select commonly used menu options. However, there were other suggestions which related specifically to data collection and operator feedback. These were:

- The original software used a bar graph to indicate the cross correlation between the stimulus waveform at the start of the test and the stimulus waveform during the data collection (i.e. for monitoring the stability of the probe fit in the ear canal). This was found to provide too much detail, and was replaced with a three level 'traffic light' system. Green for stable fit, amber for slight instability, and red for severe probe instability.

- A small artefactual emission type waveform was found to be present when an emission measurement was performed on a 1cc test cavity. This was found to be caused by electrical interference which was 'phase locked' to the averaging data (and therefore remained after aver .ging), and was present to a higher degree in the Amstrad PC1640 than the Ferranti AT which was used for the instrument development. This problem was alleviated by inverting the stimulus polarity every 5 epochs, and subtracting rather than adding the data to the averaging data pool. This resulted in a cancellation of the interference, and a flat response from the test cavity.

5.1 Practical use.

Preparation of the instrument.

From the DOS prompt, the instrument software was invoked via a batch file titled 'ILO88'. This loaded the necessary 'screen dump' and graphics drivers before loading the main programme.

Two OAE probes (adult and infant) were used with each instrument, and a selection of different sized soft rubber tympanometry tips were kept clean and sterilized ready for use.

Upon entering the test room, the patient was seated comfortably, and the patient details (i.e. name and ear) were entered on the keyboard at the appropriate prompt.

Procedure for fitting the OAE probe in the ear canal.

A visual inspection of the ear canal was carried out in order to reveal the presence of any ear wax, and to enable the correct size of probe tip to be selected. The tip was then pushed onto the end of the probe so that the tip was flush, or protruding no more than 1mm beyond the end of the probe. The probe was then carefully inserted into the ear canal (gently pulling the pinna if necessary to straighten the ear canal). The correct probe fit was determined by observing the stimulus waveform relayed to the operator via the stimulus panel (which acts as an oscilloscope during the 'check fit' phase of the programme). A well fitted probe resulted in a sharp transient waveform with the minimum of oscillatory 'ringing'. Upon achieving a satisfactory probe fit, the operator terminates the 'check fit' phase. The frequency spectrum of the stimulus waveform was then calculated and displayed. Based on the 'flatness' of this spectrum the operator decided whether the probe was to be refitted or to continue to the 'emission measurement' phase of the programme.

Observations: *Blockage of the probe by ear wax was immediately apparent if the microphone or loudspeaker holes were blocked (no stimulus was shown in*

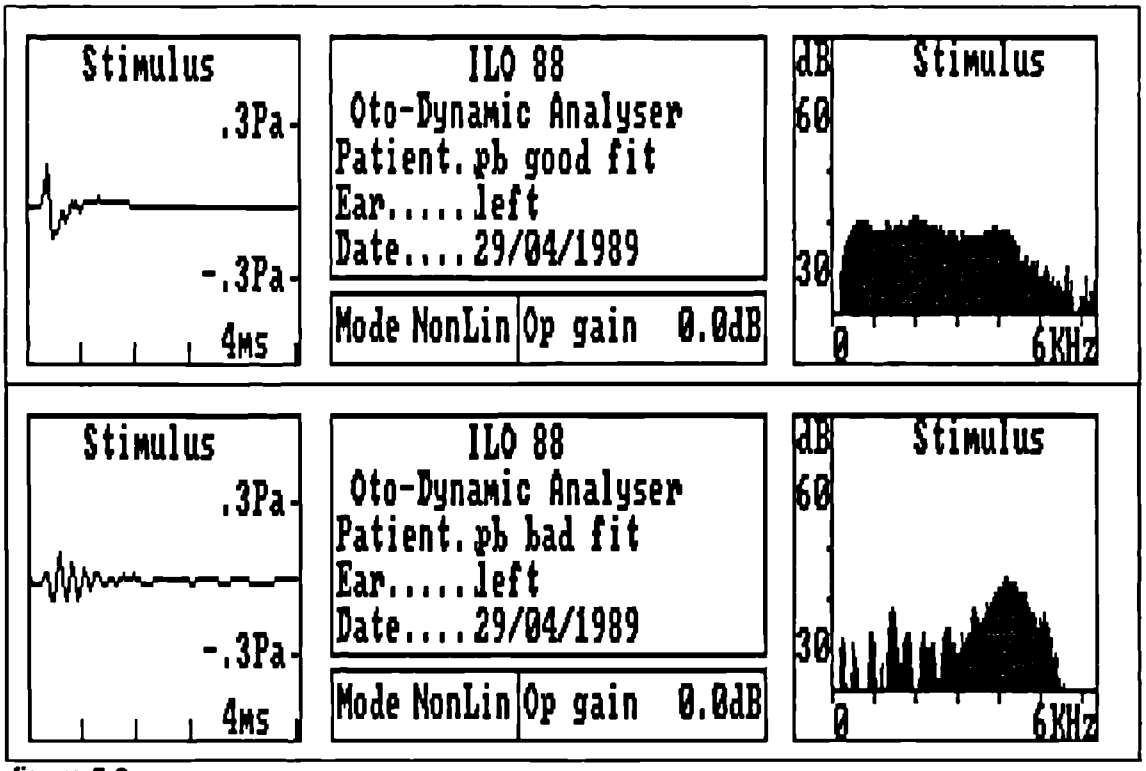

figure 5.3
A comparison of a good (upper) and poor (lower) probe fit in the ear canal. Note the flatter frequency response of the well fitted probe.

the stimulus panel on the screen). However, if the pressure equalisation hole was blocked this was not apparent during the OAE test, but the possible pressure offset in the ear canal affected the middle ear impedance, and therefore the OAE. It was noted that if the probe tip was pushed onto the probe and left 1mm proud of the end of the probe, this reduced the likelihood of blockage of the small probe ports. In the event of one or more of the probe ports becoming blocked with wax, the wax was carefully removed using a pin.

Two conditions were noted which resulted in oscillatory stimulus waveforms. When the probe was inserted but failed to obtain a seal in the ear canal, the resulting 'leak' past the tip of the probe and the ear canal cavity formed a Helmholtz resonator. This was remedied by refitting the probe or if necessary using a different probe tip size. Secondly, on occasions, despite an apparent 'good fit' of the probe, the stimulus panel still indicated a very oscillatory stimulus. On

removal of the probe from the ear canal, the cause of this was often found to be due to the probe tip 'overhanging' the end of the probe by more than 1-2mm (this affects the transient response and increases the resonance). Fig.5.3 shows the transient response waveforms and frequency spectra of a correctly and incorrectly fitted probe.

Procedure for controlling the noise in the ear canal.

During the 'check fit' (and 'emission measurement') phase of the programme a realtime measure of the ear canal noise is relayed to the operator via the 'noise bar graph' (see fig.5.1). Once the probe was fitted and the patient was quiet, the noise rejection threshold was adjusted (using the 'up' and 'down' cursor keys) to just above the noise level indicated by the bar graph.

Observations: *The noise in the ear canal emanates from both the patient and the environment. Patient generated noise consists of breathing and other physiological sources. In addition, it was noted that acoustic noise caused by movement of the probe connecting wire resulted in significant noise measured in the ear canal. Computer fans and disk drives contributed to the ear canal noise resulting from the environment.*

During the fitting of the probe it was often noted that the noise was reduced as the probe was inserted. This was due to the probe achieving a seal in the ear canal and therefore reducing the contribution to the ear canal noise from the environment. This functioned as a useful indicator of the 'quality' of probe fit, supplementing the stimulus waveform display. Testing the patient in a sound treated room with any noisy equipment in a separate room obviously would reduce the environmental contribution to the ear canal noise still further but was found to be unnecessary.

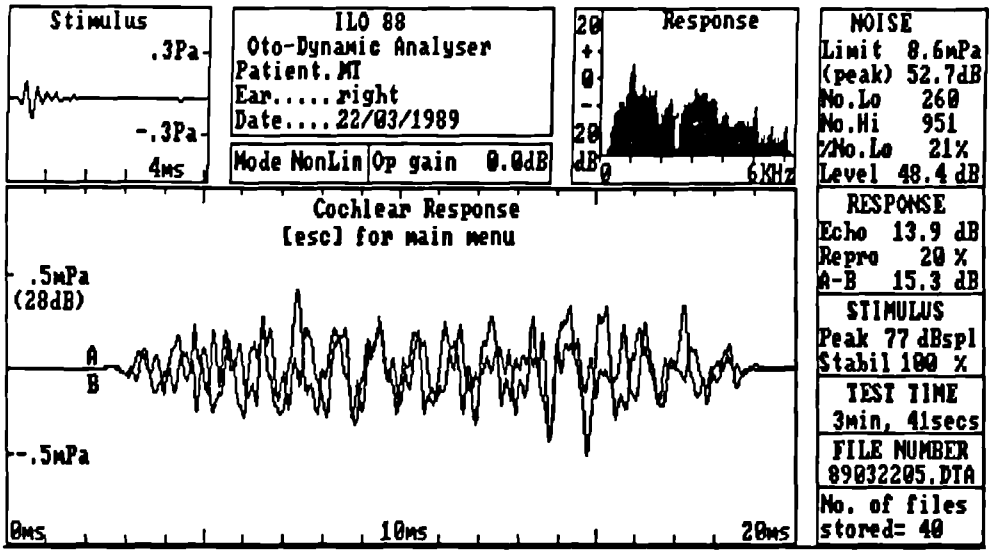

figure 5.4
An OAE measurement from a young child, showing a high degree of noise contamination in the final response. The frequency spectrum shows that no correlation exists at any frequency.

On occasions it was necessary to wait for the patient to quieten before proceeding with the emission measurement. In the case of a particularly noisy infant, this sometimes involved waiting for the child to fall asleep. It was found that many children enjoyed attempting to keep the noise bar graph at a low level once they realised that they were able to control the height of the bar.

A few cases were noted where the noise bar never fell below the default noise rejection threshold. Therefore, in order for data to be collected during the emission measurement period, the rejection level was raised. This high noise level was due either to a badly fitted probe, allowing environmental noise into the ear canal, or a high level of patient generated noise. Upon completion of the emission measurement, when the emission was of large amplitude, it was often identifiable above the noise level in the processed emission data. However, it was often not possible to confirm the presence of the emission when it was small. Fig.5.4 shows an example of this type of emission data. The noise rejection level was raised by

5dB so that sufficient data fell below the rejection threshold. However, as can be seen from the figure, the noise in the final result is such that it is not possible to determine whether an emission is present.

5.2 Interpretation of test conditions.

Once the operator was satisfied that the probe was fitted correctly, and the noise rejection threshold adjusted as necessary, the emission measurement phase was invoked. During the emission measurement phase the following information was displayed to the operator via the instrument screen:-

- An indicator of the maintenance, or otherwise, of the initial probe fit in the ear canal was displayed approximately every 1 second.
- A realtime display of the ear canal noise level.
- A realtime update of the number of accepted and rejected OAE data samples.
- A regular update of the cross correlation of the data accumulating in the two response data buffers was displayed as a 'correlation bar'.
- A 'sketch' of the accumulating response data could be requested by the operator with a single key press.
- Regular update of the amplitude of the accumulating data in each of the buffers was displayed.

The programme was set to collect a default number (256 subaverages in each of the two averaging pools) of OAE data samples. The time taken to collect this quantity depended upon the number of samples which were rejected because of noise contamination. If no data samples were rejected, the time taken was approximately 40 seconds.

Observations: *It was found that the revised probe stability indicator provided useful feedback as to the probe stability. It was found that if the probe fit was altered significantly (i.e. it falls out of the ear canal- a red light) it could be refitted*

without terminating the test. The attainment of the original probe fit was indicated by the green light reappearing on the screen.

The noise bar provided an immediate assessment of the 'incoming' data quality. With very cooperative patients it was found that the realtime noise bar display could be used for positive feedback to enable them to remain quiet.

The correlation bar graph only displayed correlation value between 50% and 100%. This was found to reduce the confusion which arose from the highly fluctuating, and insignificant correlation values occurring during the early part of the emission measurement period.

It was found that if the patient was quiet, and the emission was large, the cross correlation reached high values during the early part of the emission measurement period. Under these conditions the operator often elected to prematurely terminate the test (by pressing the [rtn] key), whilst still achieving a satisfactory emission measurement. Fig.5.5 shows an example of an emission measurement which was prematurely terminated because of the high correlation value. In this example, only 39 pairs of subaveraged data were required to achieve a correlation of 86%. The time taken to perform this measurement was 7 seconds.

At any stage during the emission data collection phase the current averaged waveform could be viewed on the screen (by pressing the 'space bar' on the keyboard). This was found useful for observing features of the data which 'grew' during averaging, indicating the presence of an emission.

The amplitudes of the each of the averaging responses were displayed at regular intervals as a single bars at the right hand end of the response display window (see fig.5.1). This was found useful for indicating the steady growth, or

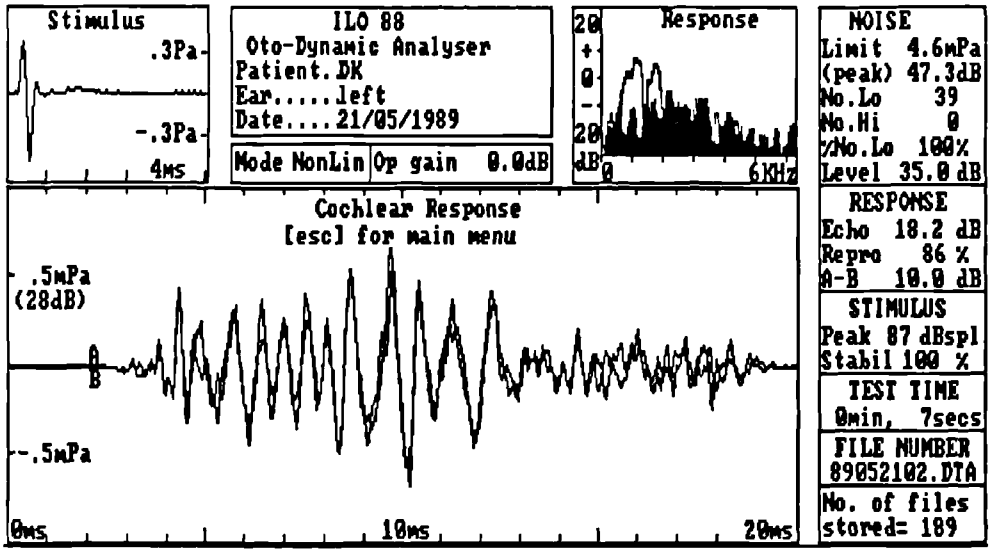

figure 5.5
An OAE measurement from a normal adult ear. This measurement was prematurely terminated because of a high inter-waveform correlation (the total test time was only 7secs).

otherwise, of the accumulating response data without constantly refreshing the waveform display (with the associated time penalty).

The emission measurement period was terminated either automatically once the preset number of data samples had been collected, or prematurely by the operator. The software then processed the emission data. The final data was then displayed on the screen for evaluation by the operator (the screen at the end of the measurement is shown in fig.5.2). If no further emission measurements were required from that ear then the probe was carefully removed from the ear canal, and the probe tip was removed and placed in sterilising fluid.

5.3 Interpretation of processed emission data.

Ideally, all emission measurements should be categorised as definitely present or absent. Unfortunately a third category exists when the measurement has failed to provide conclusive results. Interpretation of these three categories of emission data are described below.

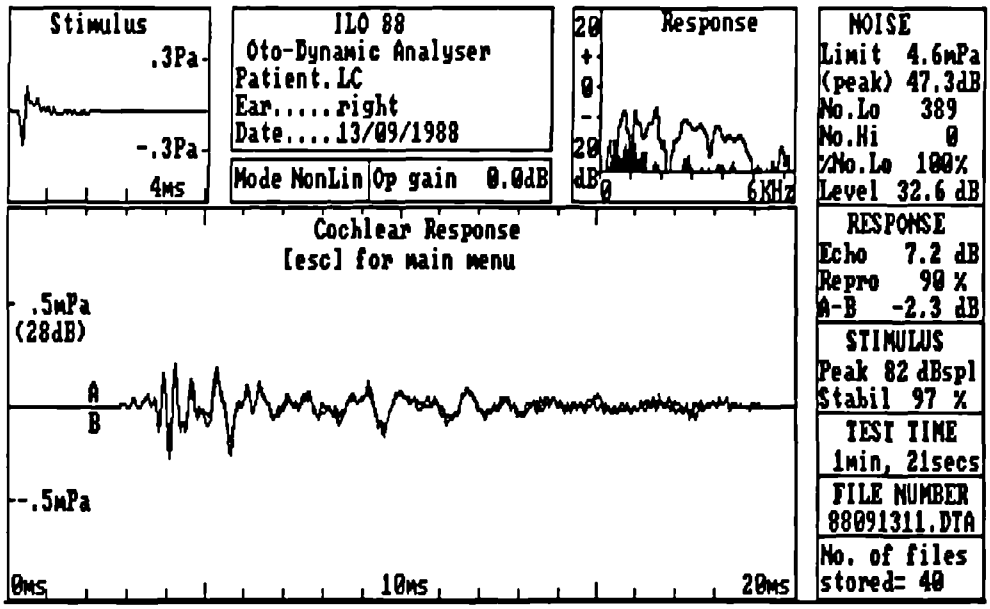

figure 5.6
An OAE measurement from a normal adult ear.

Normal cochlear function - emission present.

Patients having normal hearing almost always showed a positive OAE response. This was confirmed by the following means:-

- The response waveform panel showed two similar waveforms superimposed. If the noise level in the final processed emission waveform was low, then many of the features of the two waveforms corresponded exactly.
- The response spectrum panel showed the cross power frequency spectrum above the noise spectrum at most frequencies.
- The figures in the numerical panel indicated that the 'Echo' power is far greater than the 'A-B' (i.e. noise) power, and the 'Repro' (i.e. inter-waveform correlation) figure was high (e.g. greater than 50%).

Fig.5.6 shows the instrument screen after recording an emission from an ear possessing normal cochlear function. All of the features described above are present in this example.

Emission not present.

The true absence of an emission was determined by the presence of all of the following features:-

- The two response waveforms showed no common features, and contained a low level of noise contamination.
- The stimulus panel showed a normal stimulus waveform.
- The response spectrum panel indicated that the noise was low, and completely obscured the emission cross power spectrum.
- The numerical panel figures showed that the noise (A-B), emission (Echo) and inter-waveform correlation (Repro) were all low.

An example of an emission measurement which shows all of these features is given in the next section (see fig.5.7).

Indeterminate test outcome.

In the case when **any** of the below listed conditions were encountered, the test outcome was deemed as indeterminate. In this case the test was repeated in an attempt to obtain a test outcome which was either 'emission present' or 'absent'.

- The stimulus panel indicated a highly abnormal or absent stimulus waveform.
- The noise level in the response waveforms was sufficiently high ('A-B' › 0dB) so as to obscure the presence of a small emission waveform.

- The noise spectrum obscured the emission cross power spectrum at all frequencies, but was unusually high (i.e. above -20dBspl/√Hz).

Observations: *The most common cause of a highly abnormal or absent stimulus waveform was found, upon removal of the probe from the ear canal, to be due to the presence of ear wax in the microphone or loudspeaker port. This was remedied by careful removal of the wax from the port with a pin.*

A high noise level in the processed emission waveforms was found to result from either raising the rejection threshold or collecting insufficient data to overcome the intrinsic signal to noise ratio of the emission data. Both of these conditions were combated by recording the emission data for a greater length of time. In the case of one particular patient (see fig.5.4), despite a long emission measurement period (over 3.7 minutes), the resulting emission response still contained too much noise to enable the outcome of the test to be judged.

5.4 Evaluation of OAE data obtained in relation to clinical data.

Examples of OAE measurements from patients with hearing pathologies.

Five examples of OAE recordings from ears with different hearing pathologies are given. In each case the full instrument screen is shown, with an explanation of various features observable in the emission measurement, along with any supporting audiometric data.

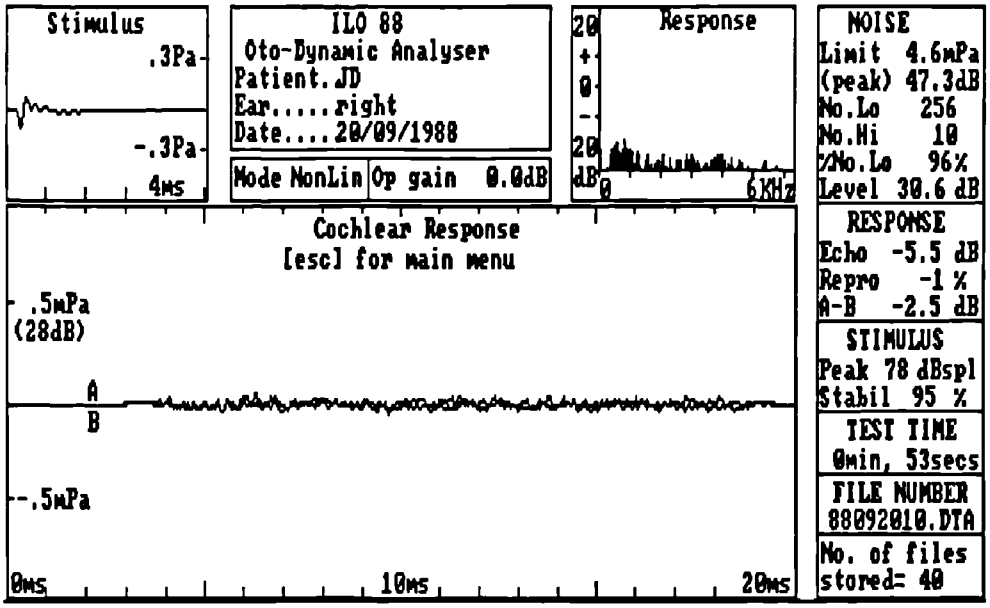

figure 5.7

In this example the patient had pure tone audiometric thresholds in excess of 40dBHL at all frequencies in the range 250Hz to 8000Hz. The hearing loss had been diagnosed as having cochlear origin. The patient was aged 46 at the time of the OAE test, and he remained quiet and cooperative during the test.

All of the information present in the figure above indicates that no emission was detected from this ear. The 'cochlear response' panel shows two waveforms which are almost 'straight lines'. This shows that not only was no emission present, but that the patient was extremely quiet during the test. The same conclusions can be drawn from the response spectrum panel. This indicates that at no frequency is the cross power spectrum of the two emission measurements greater than the noise spectrum. In addition, the noise spectrum indicates a low level of noise at all frequencies.

A similar emission reponse can be attained if either the microphone or the loudspeaker ports at the probe tip become occluded with ear wax. This however results in a flat waveform observable in the stimulus panel. In this example a normal transient stimulus waveform is present (which has a peak sound level of 78dBspl).

Other notable features of the above figure are that the probe remained correctly fitted in the ear canal during the recording (i.e. stabil = 95%), the total test time was 53 seconds, and that the patient remained quiet during the test (i.e. 96% of the subaverages were accepted for averaging).

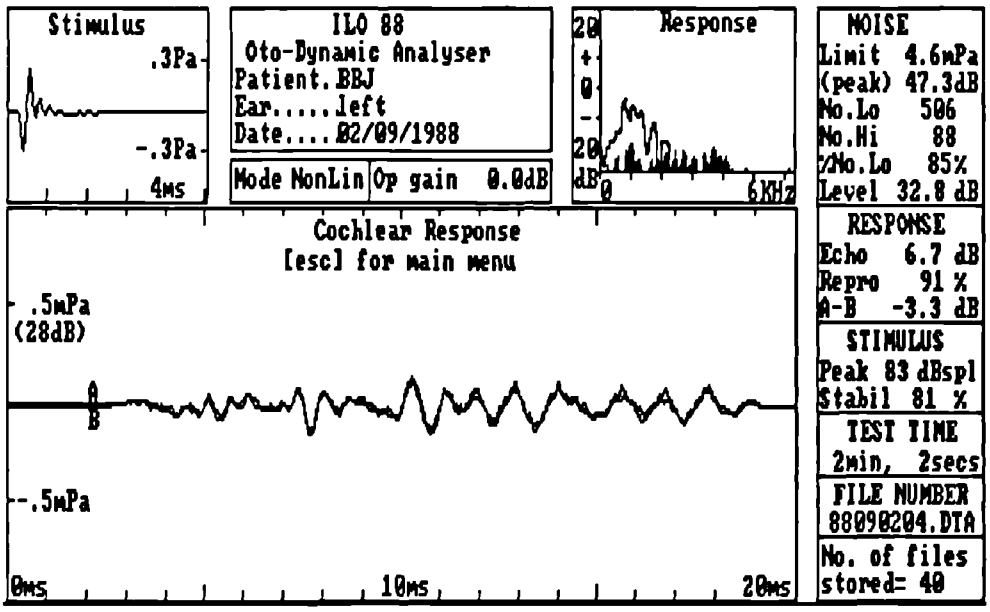

figure 5.8
In this example the patient possessed a high tone loss in the left ear. The pure tone audiometric thresholds are shown on the audiogram below. The patient was aged mid-forties and was quiet and cooperative during the test.

The 'cochlear response' panel shows two superimposed similar waveforms which have a high inter-waveform correlation (Repro = 91%). Although the emission waveform appears normal, the response cross power spectrum reveals that the frequency content of the emission is limited to 500Hz to 2KHz. This corresponds to frequencies where the audiometric thresholds are better than 20dBHL (i.e. below 2KHz).

All other features of the emission measurement are normal. The transient stimulus indicates the probe was well fitted in the ear canal, and that the probe fit remained reasonably stable. The patient noise level was average, with 85% of the subaverages falling within the acceptance criteria.

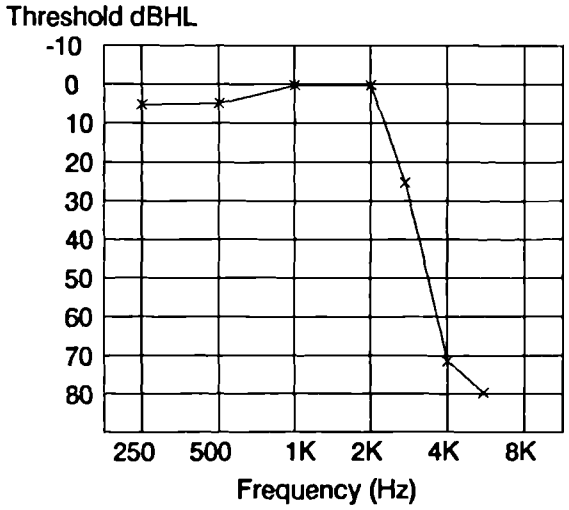

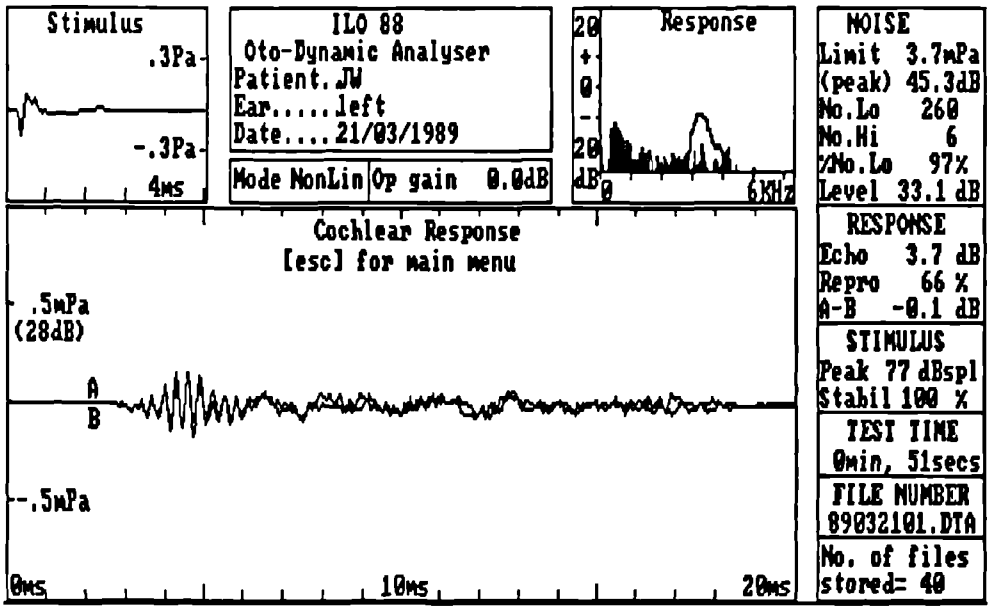

figure 5.9

In this example the patient was suffering from Menières disease. This disorder affects the cochlea and vestibular system often causing a fluctuating low frequency loss and dizziness. The Békésy audiogram taken immediately prior to the emission measurement is summarised by the audiogram below.

The patient remained very quiet during the test. As the 'Limit' figure shows, the rejection threshold was lowered by 2dB and still 97% of the subaveraged data samples were accepted.

An emission waveform is evident in the cochlear response panel, with an inter-waveform correlation of 66%. As with the previous example, an inspection of the response cross power spectrum reveals that the emission does not contain the normal frequency range. The emission cross power spectrum is only above the noise spectrum in the range 3-4KHz. This corresponds with the audiometric thresholds measured prior to the test.

A normal transient waveform is observed in the stimulus panel (77dBspl peak) and the transient waveform at the beginning and end of the test were 100% correlated.

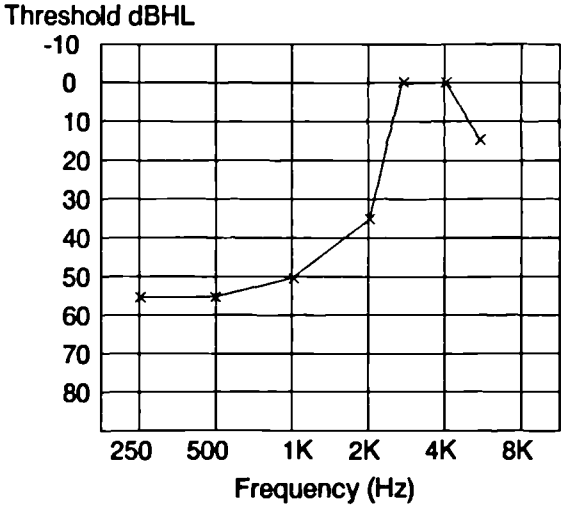

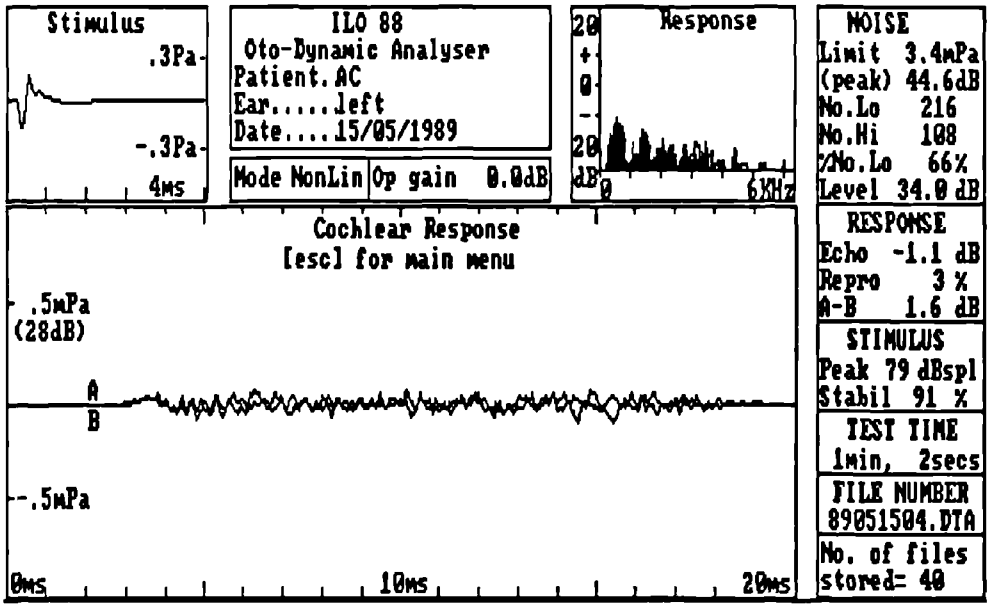

figure 5.10

In this example the patient (aged 3 years) was diagnosed as having the condition of 'Glue ear'. This occurs following middle ear infection and causes a conductive loss of the sound transmission through the middle ear. The 220Hz tympanogram showed a flat trace which is consistent with this pathological condition.

This case is a typical example of several emission measurements where normal cochlear function was suspected, but no emission was obtained due to middle ear abnormality.

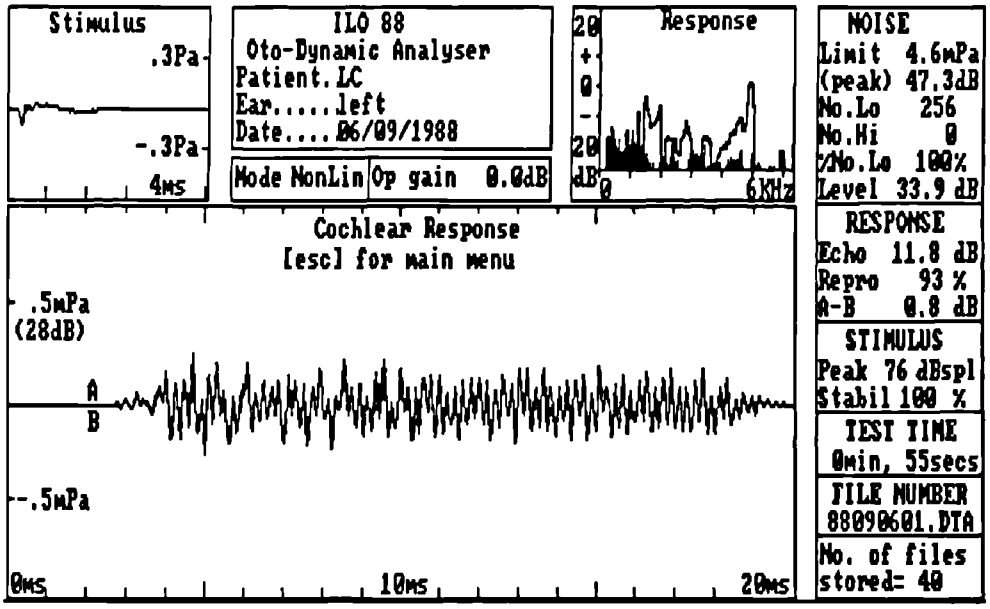

figure 5.11

This is an emission measurement from an audiometrically normal ear belonging to a patient aged 20 years. Although an emission is identifiable by the normal criteria, it clearly shows abnormal features. The emission waveform is dominated by a single tone which persists for the entire duration of the waveform display. This is reflected in the response spectrum as a peak at 4.9KHz. The figure below (a spectrograph similar to those shown in chapter 3) illustrates this unusual distribution of frequency components within the emission waveform. Chapter 3 shows the average pattern of frequency dispersion found in the normal emission waveform. This phenomenon is probably due to an area of overactivity in the cochlear partition. However, no subjective 'tinnitus' tones were perceived by the patient, suggesting that the overactivity was 'evoked' by the click stimulus. Emissions of this type were found to occur in approximately 1 in every 30 tested.

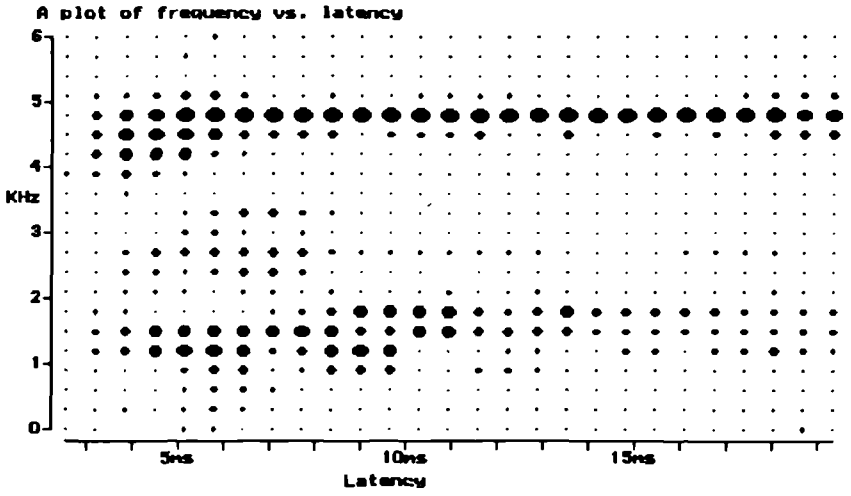

Summary of a clinical trial of the OAE instrument performed on 75 children.

The use of the OAE instrument for the identification of hearing pathology was investigated on an unselected sample of 75 children attending the Nuffield centre (age range 10 months to 10 years). This trial was performed by Siobhan Ryan as part of the OAE instrument evaluation programme. The total number of ears tested was 139. Of these, 74 had abnormal hearing (worst pure tone threshold greater than 20dBHL in the range 500Hz to 4KHz), 33 had normal hearing but some degree of middle ear abnormality, and the remaining 32 had normal hearing and a normal middle ear. The results of this trial are summarised below.

In 70 of the 74 ears with abnormal hearing no emission was present. Of the remaining 4/74, an emission was present. Further investigation of the pure tone audiograms of these 4 ears revealed that although the worst threshold was greater than 20dBHL, in all cases there were frequencies in the emission bandwidth at which the thresholds were better than 20dBHL.

An emission was present in 30 out of the 32 normal ears. From the other 2 ears no emission was detected. Further investigation of the known audiometric data on these ears revealed no explanation for the absence of an emission.

Of the 33 ears with normal hearing and abnormality of the middle ear, 25 were found to produce emissions. In 6 ears no emission was recorded and in 2 cases the test outcome was indeterminate. In this group the average emission size was found to be 4.0dB less than the normally hearing/normal middle ear group.

Application of OAE instrument to the screening of auditory function in neonates.

A trial was undertaken at the Hillingdon hospital neonatal unit to test a group of 92 newborns with the OAE test. This trial was performed by Siobhan Ryan using the OAE instrument loaned from the Nuffield centre. The purpose of this trial was to

evaluate the OAE test instrument for the purpose of neonatal hearing screening. Although a full analysis of this trial is not presented, several points pertaining to the instrument function are discussed.

Physical dimensions of the infant OAE probe.

The infant OAE probe was constructed following the experience of testing many infants at the Nuffield centre. The youngest of these was 4 weeks old. The smaller size of the ear canal of newborns resulted in difficulties during probe insertion. As a result, the plastic body of the speculum tip was removed for 5mm at the tip of the speculum. The epoxy resin which secures the internal components of the probe became the probe tip. For small ear canals a short length of rubber tubing was used, instead of a tympanometry tip, to obtain the seal in the ear canal. With rubber tubing on the narrowed probe tip, the external diameter of the probe tip was reduced to 3.5mm.

Difficulties of obtaining a seal in the infant ear canal.

Even after the modification described above there were difficulties encountered in obtaining a seal in the ear canal. Often the infants were asleep when they were presented for OAE testing. By fitting the probe with the minimum disturbance, the infant often remained asleep. This gave the advantage of keeping the patient generated noise level at a lower level during the OAE test. However, as a result of this care not to disturb the infant, and the short length of the ear canal over which to obtain a seal with the probe, a good seal was often not achieved. A combination of this and the high background noise level of the particular test room (a non sound treated room close to the ward) resulted in a high noise level in the ear canal. An acoustic attenuating cup was developed which was placed over the infant's ear once the probe was inserted. Although this reduced the noise sufficiently to enable emission measurements to be performed, it is recommended that a room with low ambient noise be used in which to perform OAE tests on neonates.

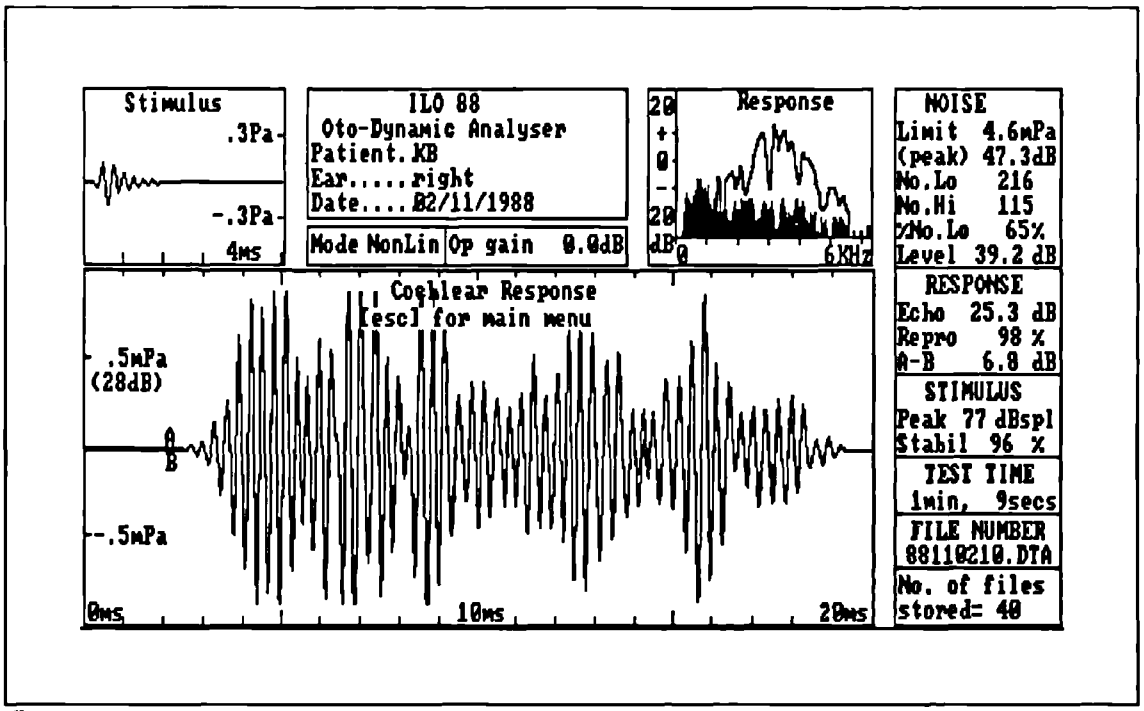

figure 5.12
The OAE measurement from a normal 4 week old baby.

The small enclosed volume of a sealed infant ear canal.

When the probe was correctly inserted into the infant ear canal the enclosed volume was approximately one tenth that of an adult ear canal. For this reason a 20dB attenuator was fitted to the infant probe loudspeaker wire. In most cases this resulted in the peak transient level of the stimulus being approximately the same as for an adult.

The emission produces a higher sound pressure level in the smaller ear canal volume of the infant. As a result the cochlear emission for a normal infant appears considerably larger than that for an adult.

Fig.5.12 shows the emission for a baby of 4 weeks of age. As the figure shows, the emission waveform is considerably larger than the previous examples of normal emissions from adults.

The stimulus waveform is rather oscillatory, despite an apparent good fit of the probe in the ear canal. This illustrates the difficulties often encountered in obtaining a probe fit in infant ear canals of a similar quality to that in ear canals of adults.

Summary.

The instrument was used and evaluated on several different clinical populations. The instrument was found to be useful in determining cochlear function. The instrument continues to be used in all the test centres to which it was supplied for evaluation. The instrument has since been commercially manufactured and sold through major audiological instrument suppliers to European countries, the USA and Japan.

Two areas requiring further investigation were highlighted, namely the influence of the middle ear upon the emission and the possibility of further reducing noise contamination of the final processed emission data.

Additional techniques to assist the interpretation of OAE data.

Introduction.

An OAE measurement instrument was developed following basic research into the physical properties of the OAE emission as detailed in chapters 2 and 3. The instrument was specified and built (chapter 4) and was applied to several different clinical population groups so that its performance could be evaluated (chapter 5).

Although a high degree of success was achieved in measuring OAEs in the clinical environment, in chapter 5 two conditions were noted under which interpretation of OAE data proved essentially difficult. These were:-

- When, despite substantial averaging, the noise level in the measurement obscured the emission waveform (if it was present) (see fig.5.4).
- When the transfer function of the middle ear was modified by a pathological pressure differential across the tympanic membrane. This causes attenuation at frequencies in the emission bandwidth causing the emission at these frequencies to be rendered below the noise floor of the measurement (see fig.5.10).

In this chapter techniques are discussed to aid the interpretation of the emission data under these two adverse conditions.

6.1 Techniques to aid interpretation of OAE data under conditions of high noise contamination of the measurement.

Using the OAE test instrument, the presence of cochlear activity is determined by identification of a cochlear emission. To achieve this, the emission must be greater than the level of noise contamination in the final processed measurement data. As

shown in chapter 5, this is achieved by several methods in the time and frequency domain. Two independent response measurements are obtained by alternately averaging the emission data into two accumulators. A cross correlation of the two averaged waveforms is calculated, yielding a figure which is representative of the overall signal to noise ratio. In addition, the cross power frequency spectrum is calculated and displayed and superimposed with the frequency spectrum of the noise[1]. This allows frequency domain analysis of the signal to noise ratio. This is particularly advantageous in the case where a large noise at one frequency spoils the overall waveform correlation. Using the frequency domain analysis, it is still possible under this condition to observe the presence of an emission at frequencies other than the high noise band. Finally, rms calculations are performed on the averaged emission waveform and the derived noise waveform.

A reduction in the incidence of indeterminate test outcomes would be achieved by an improvement of the signal to noise ratio of the processed emission data. During the specification and development of the OAE test instrument much consideration was given to obtaining a high signal to noise ratio. The current implementation has been shown to be adequate in most circumstances (see chapter 5) for determining the presence of an emission. However, the rigorous demands of using the instrument for a clinical screening test for infants have highlighted the need for further consideration (see fig.5.4) to be given to increasing the signal to noise ratio of the emission data.

In a clinical screening test set-up, both the indeterminate test outcomes and those which indicate that no emission is present require that a follow-up test be performed. Using the data from Stevens & Ip[41] (400 infants), 21% of the sample failed the OAE test in one or both ears (of which approximately a quarter had cochlear deafness later confirmed). Therefore 83% of those with normal cochlear function passed the test. If

1 An approximation of the noise is determined by calculating the difference between the two response waveforms.

the number of positive test outcomes could be increased from 83% to say 86%, then this would result in a 20% reduction in the number of normal patients referred for a follow-up test. This advantage is further accentuated by the fact that the average time taken to perform a follow-up test is far greater than the screening test time. It is therefore clear that for even a small increase in the number of positively identified emissions, this will result in a significant decrease in the resources required by the follow-up centre.

A study was performed to establish the increase in the signal to noise ratio necessary to achieve this degree of reduction in the number of patients referred for a follow-up test. Fig.6.1 shows the distribution of OAE waveform rms values for 47 normal ears. This distribution is assumed to approach a 'normal' distribution for a higher number of subjects. The mean and standard deviation of this population are 7.75dB and 3.96dB respectively.

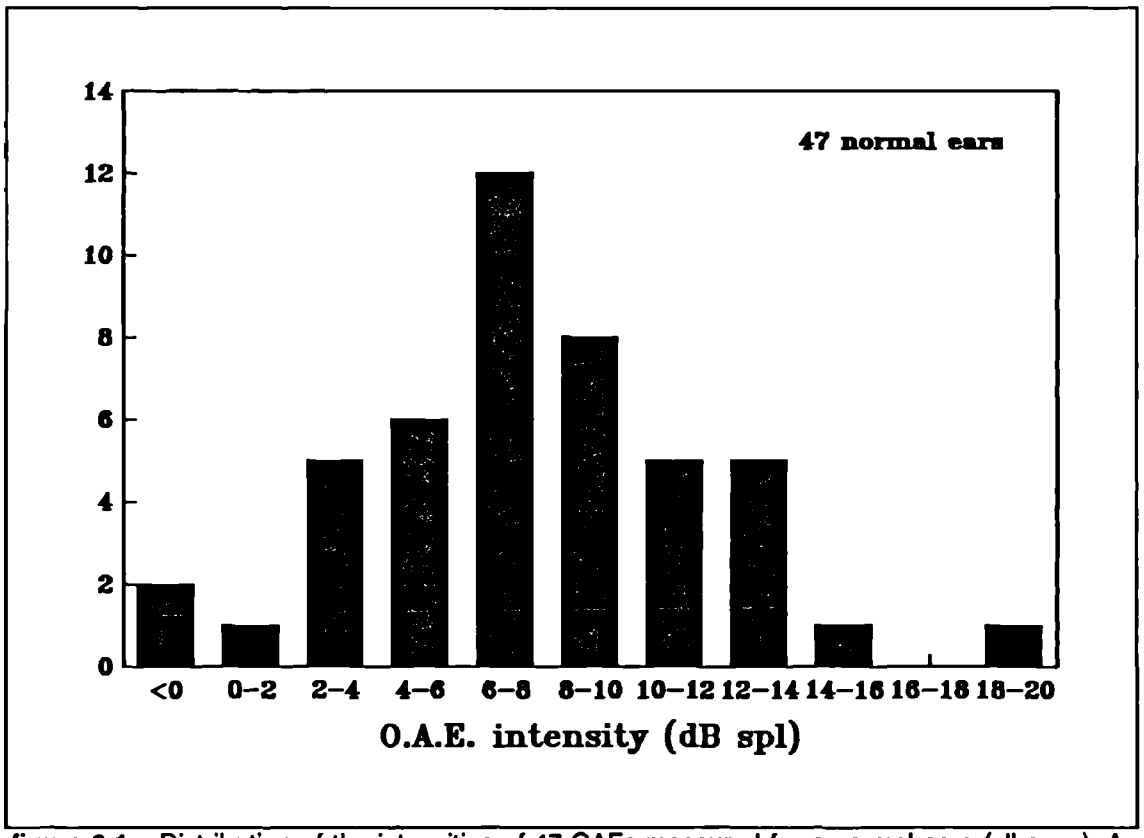

figure 6.1 Distribution of the intensities of 47 OAEs measured from normal ears (all ages). An rms of each emission waveform is calculated, and expressed in dBspl.

Using statistical tables of the normal distribution it is apparent that 83% (from the Stevens & Ip data discussed above) of the distribution occurs above 0.95 standard deviations below the mean. To increase the 'pass' percentage from 83% to 86% requires an increase in the signal to noise ratio of just 0.14 standard deviations. From the data shown in fig.6.1 this amounts to an increase of just 0.6dB in the signal to noise ratio.

The aim of this study is to investigate techniques to increase the signal to noise ratio of the processed data and thereby ease the task of emission assessment and reducing the number of indeterminate emission test results. It is clear from the above study that even a small increase in the signal to noise is of significance in the clinical screening environment.

A reduction in the number of indeterminate test outcomes is achieved by increasing the signal to noise ratio of the processed emission data. A reduction of the noise contamination in the final processed emission data can result from either:-

- a reduction of the noise at source (i.e. by reducing the noise in the ear canal),
- a reduction of the noise in the averaged data by either longer averaging, or by a more rigorous data sample selection/rejection criteria, or
- a reduction of the noise contamination in the final processed data by enhancing features which are specific to the emission.

Chapter 5 contains discussion of the techniques employed to reduce the noise in the ear canal during testing (e.g. obtaining a sealed fit of the probe in the ear canal). In chapter 4 the details of the 'post subaveraging noise rejection technique' are described. This technique provides a more efficient means of assessing the level of noise contamination in each data sample than normal noise level detection. This ensures that the level of noise contamination of each data sample can be correctly monitored, leading to the decision of whether to add the data to the averaging pool.

This chapter details investigations of the effect that the choice of rejection threshold level has upon the processed response data quality.

In addition, this chapter describes a method of emission enhancement of the averaged data. This method uses a special filtering technique which enhances features of the averaged data which are specific to the OAE response. Both of these methods increase the signal to noise ratio of the final processed data and therefore facilitate data assessment.

Investigations of the effect of the rejection threshold on the quality of the averaged response data.

Whatever techniques of signal enhancement are employed for a fixed data capture protocol, there will always be a limit to the noise conditions under which emission measurements can be made and assessed. This limit is obviously dependent upon the size of the emission and therefore varies for different subjects. When testing patients in a routine clinical environment, the total test time dictates the number of patients tested, and therefore must be kept short. Therefore, averaging for great lengths of time in order to overcome the high noise contamination, is not an attractive solution. It was for this reason that the noise rejection scheme was implemented (chapter 4) in the instrument. This noise rejection scheme assesses the noise contamination in each of the subaveraged (3 + 1) responses. If the noise in the response is above a certain threshold, then the 'contaminated' response is not added to the averaging data pool.

The selection of this threshold for rejection requires careful consideration. If the threshold is relatively low, many of the responses will register as contaminated. This ensures that only very 'clean' data is added to the pool. However, because so many responses are rejected, a greater time is required to obtain a sufficient number of low noise responses to observe the response above the intrinsic low level noise (i.e. noise comparable in size to the response). Conversely, if the rejection threshold is set relatively high, then responses with a high degree of contamination are added to the

averaging pool. This results in a greater averaging time to obtain a sufficiently high signal to noise ratio in the averaged response.

Two studies were performed on the effect of varying the rejection threshold. The first of these involved recording a fixed number of raw OAE responses onto a high capacity winchester disk in real time. This permitted 'off-line' processing of the same 'raw' data many times at varying rejection thresholds, thus allowing a study of the effect of rejection threshold on the 'quality' of the final processed emission data. The data was reprocessed at approximately 20 different rejection threshold levels. The waveform cross correlation was used as a measure of the final data contamination. The data was collected for exactly 1 minute (approximately 800 sets of the 3 + 1 stimulus group). The data was collected from an adult subject who has a normal cochlear emission. Three sets of data were collected. For the first set (A), the subject remained as absolutely quiet as possible during the measurement. For the second and third tests the subject partook in noisy breathing (B), and noisy breathing with considerable body movement (C), since these are often the conditions encountered when testing young children. Fig.6.2 shows the result of this experiment. The three curves show the waveform cross correlation as a function of the rejection threshold level. The figures on the graph by the curves indicate the percentage of data accepted from the complete pool of raw data after processing at that particular rejection threshold.

From result (A) it can be seen that 65% of the raw data have a spl level which falls between 32.5 and 35dBspl. This shows that the noise level was both low and consistent during this measurement. It can be assumed that such a consistent level of noise is not characteristic of subject generated noise (such as breathing), and therefore the noise is predominantly from the instrument and environment (i.e. electrical noise in the microphone and amplifiers, and noise from the air conditioning in the room).

The results of the measurements under the other two noise conditions (B and C) show that a maximum signal to noise ratio is achieved at a particular level of rejection

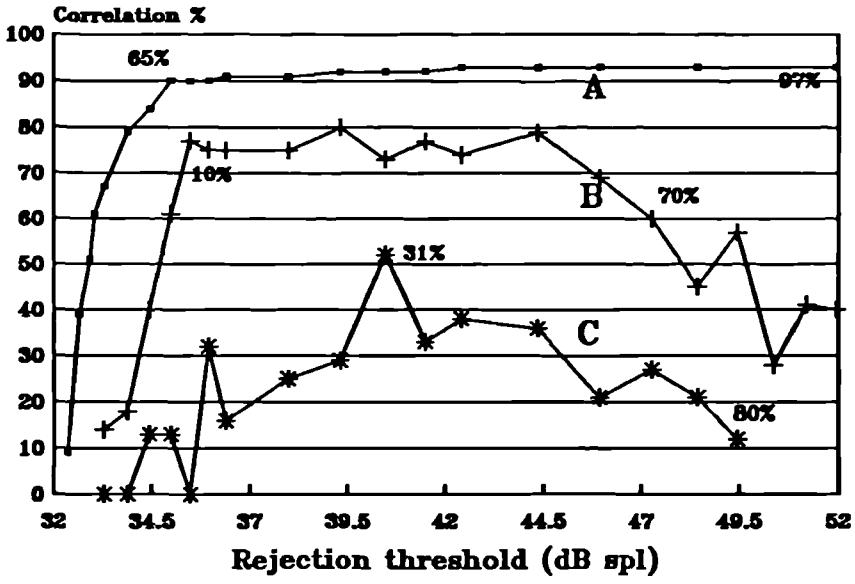

figure 6.2 Th effect of altering the rejection threshold on three degrees (see text) of noisy OAE data from a normal ear. The inter-waveform correlation is taken as the measure of quality.

threshold. For the curve (B), this optimum rejection threshold is between 35 and 44dBspl. However, for curve (C), there was only one rejection level (40dBspl) at which the cross correlation value exceeded 50%. The shape of these curves is dependent upon the statistical properties of the noise contamination.

The second study further illustrates the importance of the rejection threshold on the quality of the final processed data. The distribution of the level of noise in ear canal acoustic measurement samples was investigated under different subject conditions. For each of these measurements a theoretical examination of the optimum rejection threshold was undertaken (the level which resulted in the lowest level of noise in the final averaged response).

The distribution of the level of noise in the ear canal was investigated in the following way. Using a specially written Pascal programme, and the OAE test instrument hardware, 20 millisecond samples of the ear canal noise were measured using the normal OAE probe microphone. Each sample was then processed so as to

ascertain the level of noise (expressed as an rms level in milli Pascals). The noise level from each sample was displayed as a frequency histogram. This procedure was repeated for the same three conditions of subject noise used in the previous experiment (i.e. (A) = quiet, (B) = noisy breathing and (C) = noisy breathing and body movement).

Once the data had been collected, an analysis of the calculated noise levels in the averaged response data as a function of rejection threshold was undertaken. This was expressed graphically as the signal to noise ratio relative to the maximum attainable. This curve is not only dependent upon the shape of the noise distribution, but also the total number of data samples collected. For this reason, the noise distribution is always normalised to the same number of data samples in this case, equivalent to 256 pairs of samples of the 3 + 1 nonlinear stimulus group, which is the default number of averages used in the OAE test instrument. In addition, the minimum noise contamination of the averaged response data is calculated (i.e. at the maximum signal to noise ratio) and displayed along with the rejection threshold at which this minimum noise contamination occurs.

Fig.6.3 shows the result from the quiet subject noise condition (A). The lower panel shows the noise level distribution. As inferred in the previous experiment, the majority of the samples have a noise level which falls in a very narrow band of low level noise (between 0.4 and 0.7mPa rms). In addition there are no samples which have a noise level higher than 1mPa rms. The upper panel shows the calculated signal to noise ratio (relative to the maximum signal to noise ratio) as a function of rejection threshold. The graph shows that the signal to noise ratio rises sharply to a maximum just above the level of noise of the samples, and remains at this level for all rejection thresholds above this value. This illustrates that under these noise conditions the rejection threshold is not critical, as the signal to noise ratio is high for all values of the rejection threshold above approximately 1mPa. This shows, as expected, that if the patient is very quiet there is little need for noise rejection.

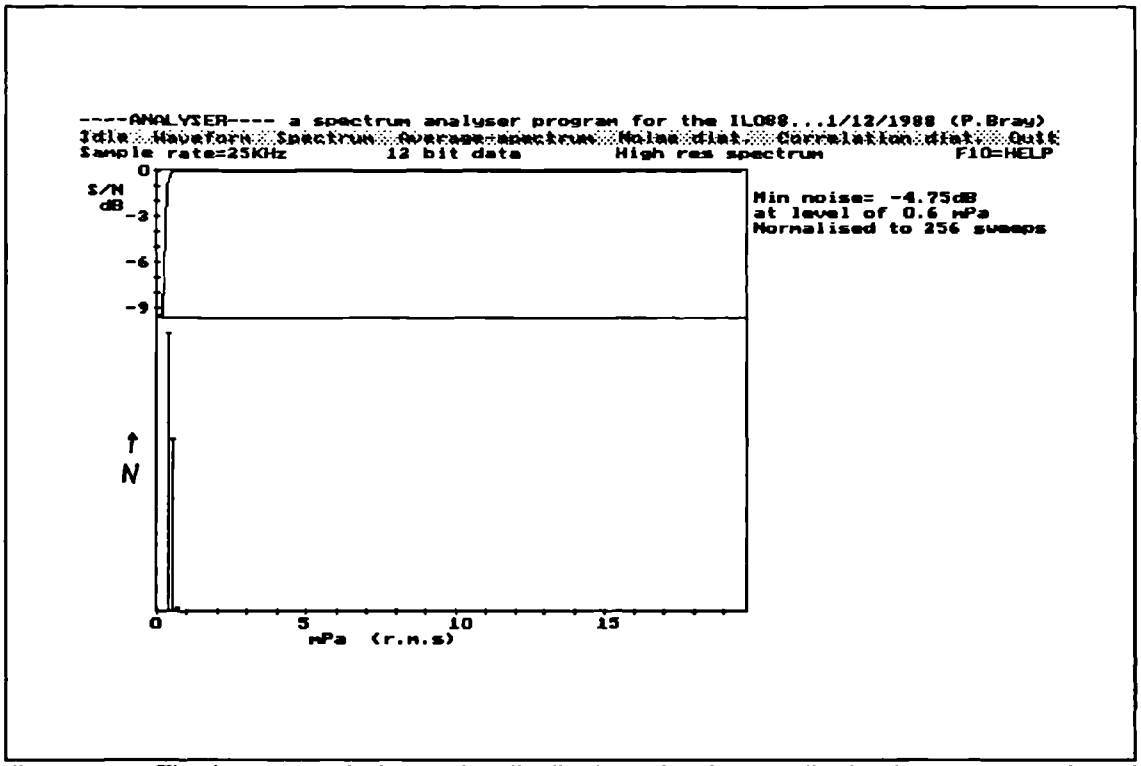

figure 6.3 The lower panel shows the distribution of noise amplitudes in 20ms samples of acoustic data recorded from the ear canal. The upper panel shows the calculated signal to noise ratio of the averaged data as a function of rejection threshold (relative to the maximum S/N ratio). The two panels share the same x-axis. As a way of standardisation, the noise distribution is normalised to a fixed number of samples (256). The figures at the top right show the calculated minimum noise (dBspl) in the averaged waveform if the optimum rejection threshold level is chosen. In this example, the subject was absolutely quiet.

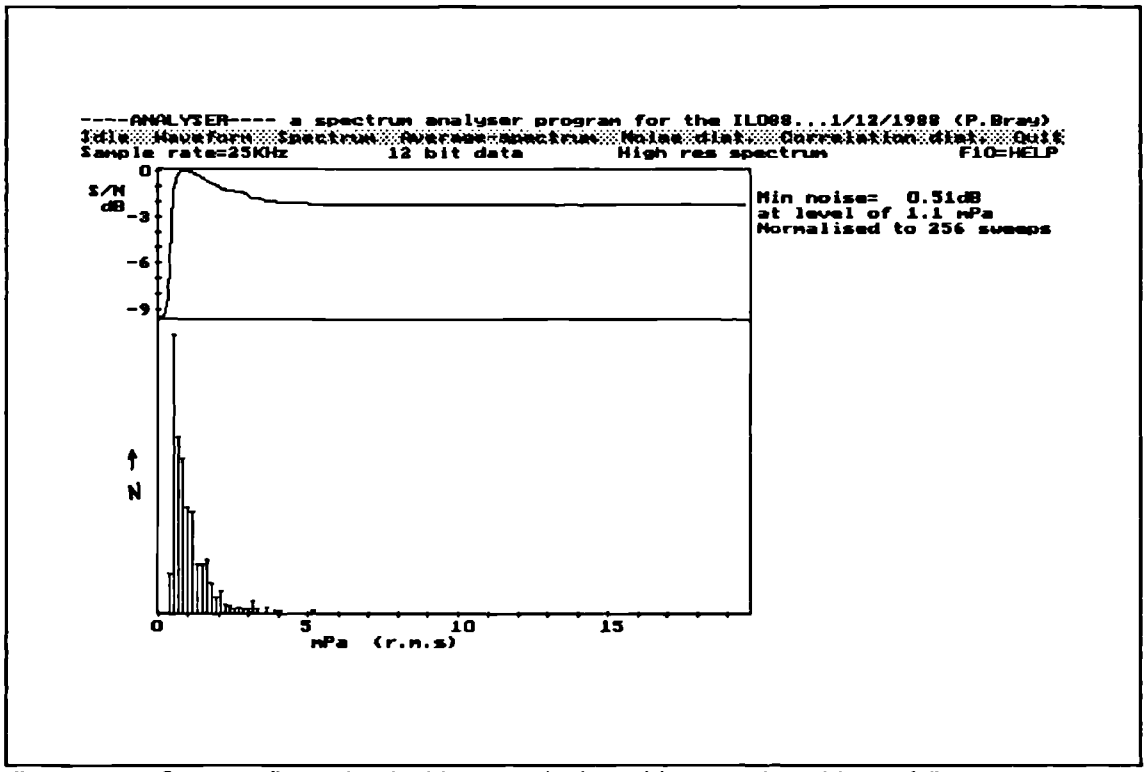

figure 6.4 Same as fig.6.3 but in this example the subject was breathing noisily.

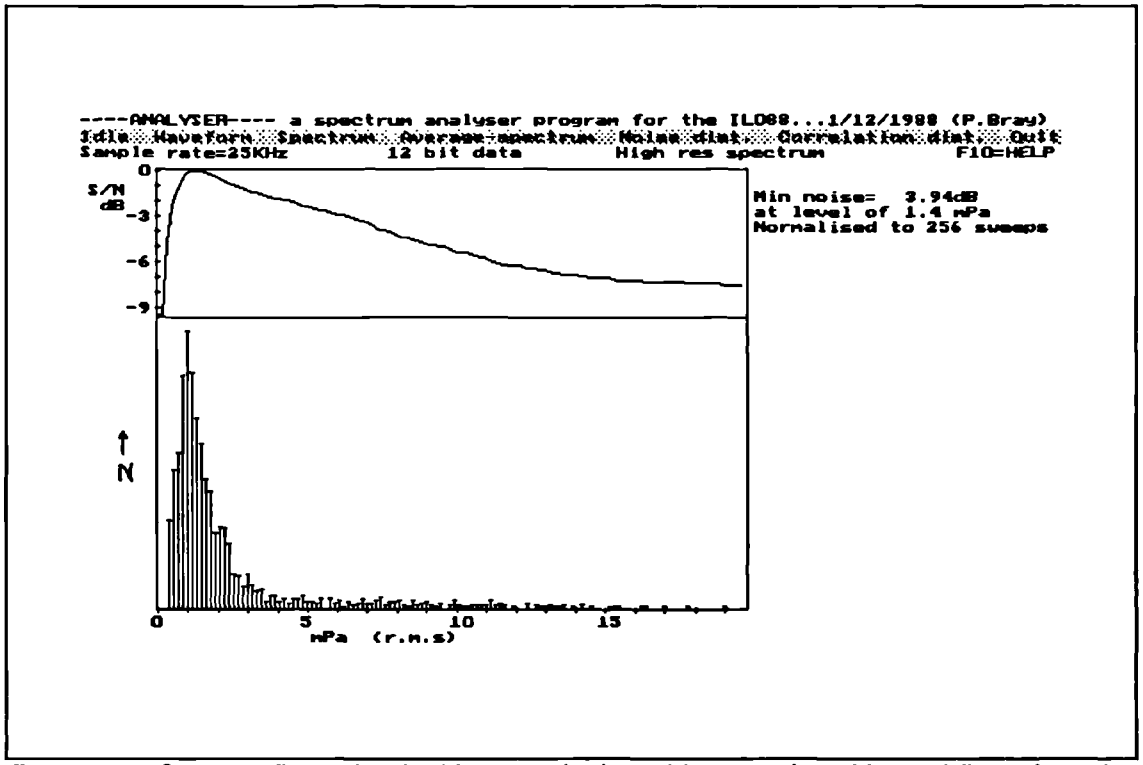

figure 6.5 Same as fig.6.3 but in this example the subject was breathing noisily and moving occasionally.

Fig.6.4 and fig.6.5 show the results of the same analyses for the other two subject noise conditions (B) and (C). In all three cases the same lower limit exists for the noise contamination (approximately 0.3 mPa rms). This is the 'noise floor' of the instrument and environment noise combined. This indicates that even when the subject was noisy, there were quiet intervals during which the subject was as quiet as during measurement condition (A). Fig.6.4 and fig.6.5 differ from fig.6.3 in that, as expected, there is a spread of the noise distribution which encompasses higher noise levels. Noise condition (B) (fig.6.4) has a large number of samples with noise contamination below 1mPa rms but some of the 20ms samples have noise levels up to 5mPa rms. In fig.6.5 (noise condition(C)) the spread of the quieter samples is greater than in the other two cases, and in addition there are samples with noise contamination as high as 20mPa rms. These louder noises in the ear canal are due to the body movements and swallowing.

The upper panels of fig.6.4 and fig.6.5 show the effect of increasing the rejection threshold upon the signal to noise ratio. In both cases there is a maximum of the signal

to noise ratio at a particular rejection threshold. The nature of these maxima is slightly different in the two examples. In fig.6.4 the signal to noise ratio rises sharply above 0.6mPa rms reaching a maximum at 1.1mPa rms. The signal to noise ratio then falls 3dB progressively as the rejection threshold is increased to 5mPa rms. Above this the signal to noise ratio is constant (indicating that there are no highly contaminated samples to 'spoil' the averaged data). In fig.6.5 the signal to noise ratio rises less quickly, reaching the maximum value at 1.4mPa rms. Above this rejection threshold, the signal to noise ratio falls steadily up to values of 20mPa rms. This continuing decline is due to the few highly contaminated samples.

The calculated minimum noise contamination values of the averaged data (on the right hand side of the figure) show that the minimum noise in (A) is only -4.75dB, whereas in the case of (C), the minimum noise is 3.94dB.

In conclusion, it is apparent that under the more noisy test conditions the level of the noise rejection is far more critical in order to obtain the optimum signal to noise ratio. This analysis has shown that under noisy test conditions some form of rejection threshold optimisation is beneficial in obtaining an increased signal to noise ratio of the final processed emission data. This rejection threshold optimisation could be integrated into the OAE measurement software. For example, after using a default rejection threshold for the early part of the measurement, a new calculated rejection threshold could be utilised for the latter part of the test, based on an analysis of the noise during the earlier part of the measurement. This process of rejection threshold optimisation could be repeated several times throughout the duration of the OAE measurement.

Investigation of a feature specific emission enhancement technique.

The above investigation into maximising the averaged data quality by optimisation of the rejection threshold leads to a technique whereby the highest quality response data can be attained in a given time. In circumstances where the noise conditions are such that, despite the application of all the techniques of signal processing implemented in the instrument, the data still remains difficult to interpret, further techniques need to be considered.

Three investigations into the frequency characteristics of the emission waveform as a function of post stimulus time were presented in chapter 3. The conclusion of these studies was that a characteristic pattern existed for the frequency content of the emission waveform in relation to post stimulus time. The early part of the response (approximately 5ms pst) contained predominantly high frequencies (4KHz), whereas at greater pst lower frequencies were present. As a result of this investigation it is proposed that a bandpass filter can be implemented which varies the pass band as a function of pst. This filter will remove proportionally more low frequencies at the early part of the response waveform and high frequencies at the later portion of the response. By filtering frequencies 'outside' the expected emission range at a particular pst, the overall noise contamination of the response is reduced. This therefore increases the signal to noise ratio of the resulting response data.

After averaging, the response data is normally bandpass filtered from 400Hz to 6.4KHz. This increases the signal to noise ratio of the final data by reducing frequency components which fall outside the expected bandwidth of the emission signal. The variable bandpass filter, described above, extends this principle by adjusting the pass band of the filter to the specific 'frequency dispersion' pattern of the emission. In an ideal situation this would leave only noise which was of the expected emission frequency at any particular pst.

The 400Hz to 6.4KHz bandpass filter is a digital implementation of the simple RC high and lowpass filters. The values of the Rs and Cs translate directly to the software and determine the filter frequencies. The filter subroutine is written in assembly language, for the sake of speed, and is 'called' from the main programme. The bandpass filter passes once 'down' the response waveform, and then in reverse from the end to the beginning of the waveform. This causes the data to be filtered twice (i.e. 12dB/octave cut-off). The reason for this second, reverse pass is to negate the phase delay introduced by the first forward pass. The pass band of the filter can be altered by changing the 'R' and 'C' values of the subroutine as it 'progresses through' the response waveform.

A Pascal programme was written to study the effect of altering the 'filter constants' (i.e. the R and C values) as a function of pst. The programme displays the cut-off frequencies as a function of pst, and allows various incremental factors of the filter constants. The 'area' of the pass band was then adjusted to suit the characteristic frequency dispersion pattern of the emission (see fig.3.12). Fig.6.6 shows the pass band area which was best suited to the experimental data from chapter 3. The initial and incremental values of the 'filter constants' for these curves were then used for the assembly language bandpass filter.

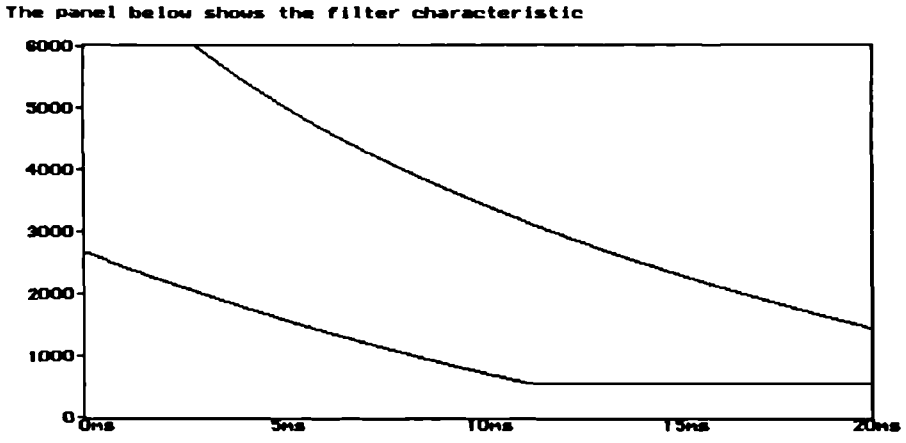

figure 6.6 This figure shows the calculated 6dB points of the template bandpass filter as a function of post stimulus time.

Fig.6.7 shows the effect of the 'templated filter' upon a test waveform consisting of three pulses at different temporal positions. This illustrates the variation of the pass band of the filter as a function of waveform position.

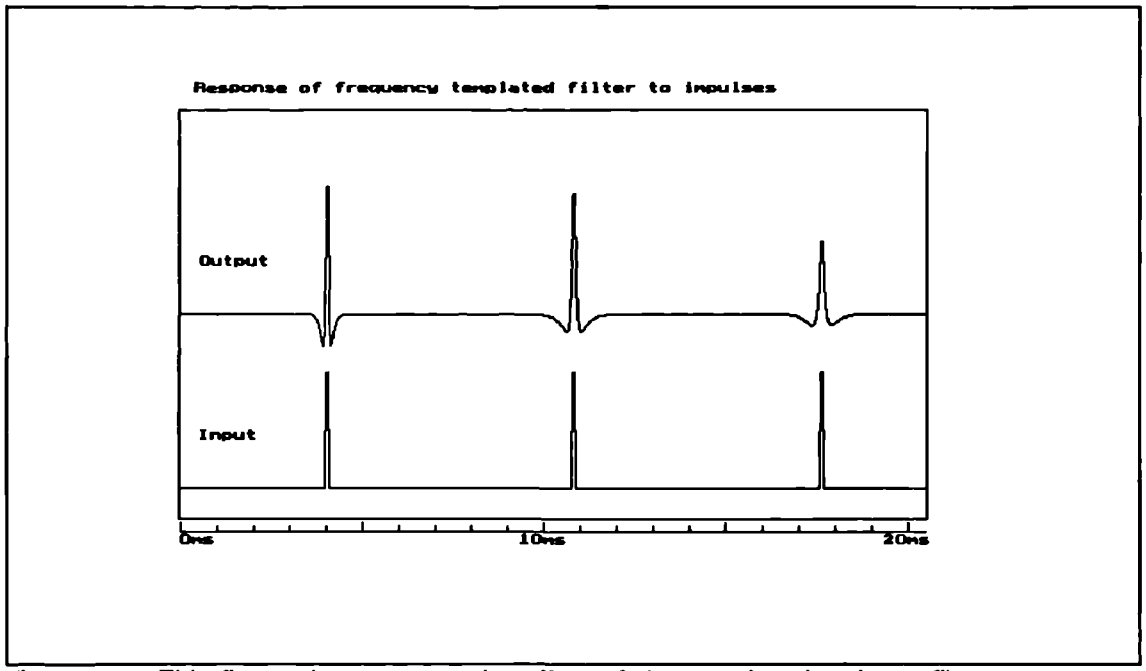

figure 6.7 This figure demonstrates the effect of the template bandpass filter upon a test waveform consisting of three impulses at different pst (lower trace). The upper trace shows the result of filtering the test waveform with the template filter.

Investigation of the effect of the templated filter upon the distribution of cross correlations of samples of random noise.

Before using the filter on emission waveforms, it is important to test the effect of the filter upon the cross correlation of two samples of random noise. By limiting the bandwidth of the noise, the spread of the cross correlation values increases. As a result, the chance of achieving a false positive emission result is increased. The effect of the template filter upon the distribution of cross correlations for random noise must be ascertained.

Using a Pascal test programme, 20ms samples of broad band noise were recorded using the OAE measurement instrument hardware. Pairs of 20ms samples were then cross correlated and a frequency histogram plotted of the correlation values. Each

pair of the 20ms samples were duplicated and filtered in three different ways. The standard fixed bandpass filter was applied to one set. The template filter was applied to another, and the third set received two applications of the template filter. The frequency histograms of the three sets of cross correlation data were plotted together to enable comparison. Fig.6.8 shows the three frequency histograms. As the same noise samples are used for each histogram, the number of samples in each is the same. The total number of cross correlation calculations for each histogram is 418.

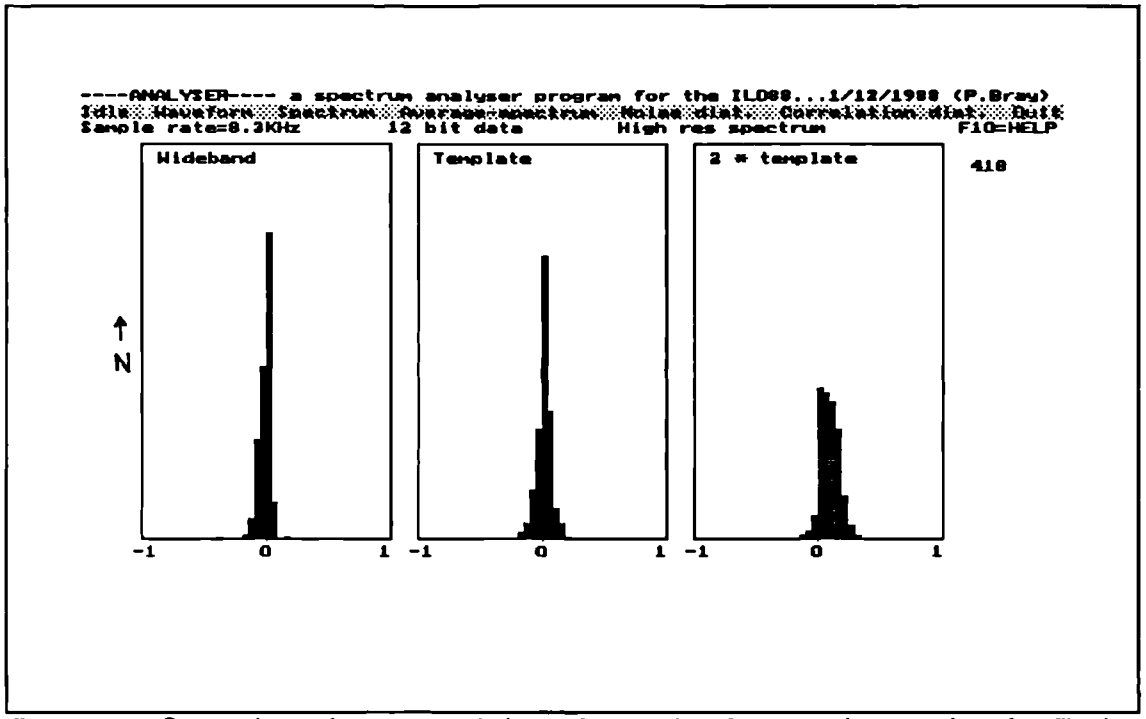

figure 6.8 Comparison of cross correlations of 418 pairs of 20ms noise samples after filtering with the normal wideband filter (left), the template filter (centre), and two applications of the template filter (right).

The left hand panel of fig.6.8 shows the cross correlation of the noise after the normal 400Hz to 6.4KHz bandpass filter. The distribution is narrow, and centred at zero. The distribution has no cross correlations which fall outside of the range -0.2 to 0.2. The centre panel shows the distribution of cross correlation after the application of the template filter upon the noise data. In this case, the distribution is also centred at zero. Similar to the left hand panel, no correlation values fall outside the range of -0.2 to 0.2, although the distribution is slightly broader (i.e. the variance of the distribution is greater, even though the range is not). The right hand panel of fig.6.8

shows the distribution after the noise samples were filtered twice with the template filter. In this case, the mean of the distribution is at 0.1, and the range is from -0.15 to 0.3. The variance of the distribution is greater than in the other two cases (as would be expected when limiting the bandwidth of the noise data).

In summary, the effect of using the template filter upon random noise, with a view to investigating any possible increase in false positive emission identification was undertaken. It was found that after one application of the filter the effect upon the cross correlation of random noise is of no significance.

Evaluation of the templated filter upon OAE data.

The OAE measurement software was modified to enable the averaged emission data to be 'saved to disk' before the application of any filter subroutine. This permitted an investigation of the effect of the templated filter versus the fixed bandpass filter.

Figures 6.9, 6.10 and 6.11 show an OAE from a normal ear with no (digital) filtering, fixed bandpass filtering (400Hz to 6.4KHz), and filtered using the template filter, respectively. The overall waveform correlation (Correl), the cross power and noise spectrum, and the figures for the echo intensity (Echo E) and waveform contamination (Contam), all serve to illustrate the effect of the various processes upon the signal to noise ratio of the emission response. In this example, the signal to noise ratio is improved by 2.5dB by using the fixed bandpass filter, and is improved a further 1.1dB by using the templated filter.

The degree of improvement is dependent upon how precisely the frequency dispersion of the particular emission waveform fits the template to which the filter operates. A study was undertaken to gauge the degree of improvement in the signal to noise ratio of the emission response data for a larger population. As above, the OAE data was saved in an unfiltered form, and the signal to noise ratio of the emission response was compared under the same three conditions (i.e. unfiltered, bandpass

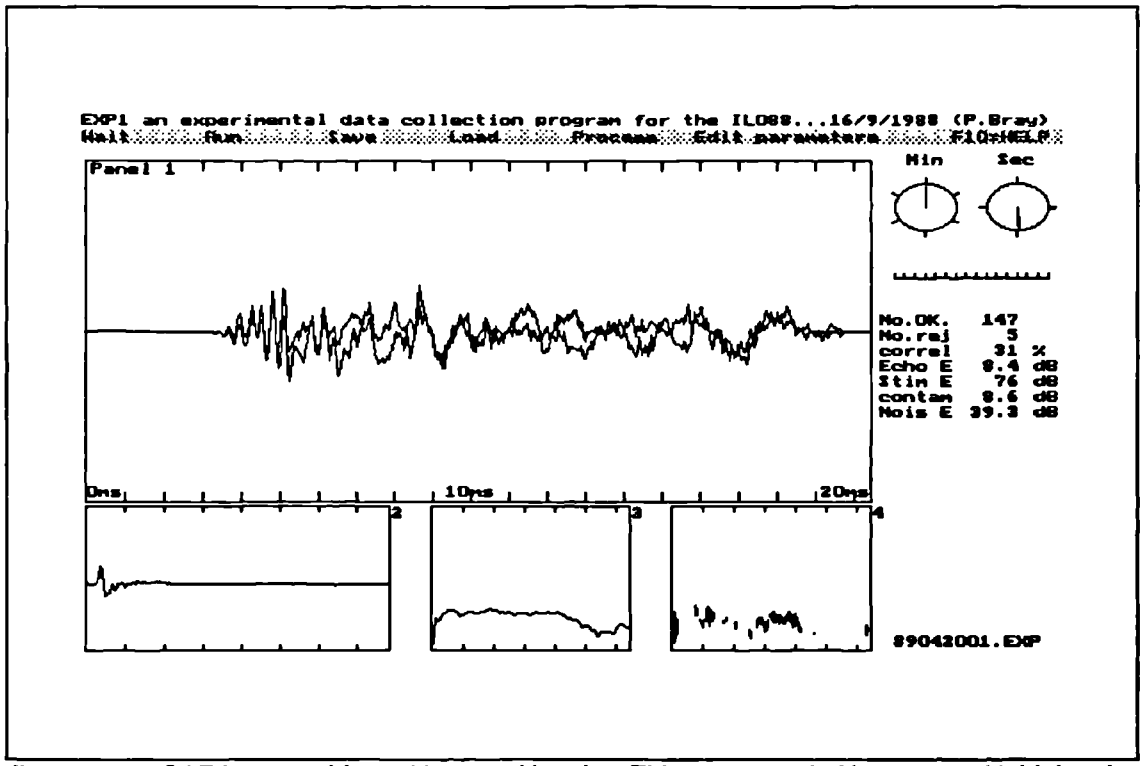

figure 6.9 OAE from a subject with normal hearing. This was recorded in a room with high noise level (i.e. computer fans etc). The OAE has not been filtered (except by the analogue filters, see chapter 4). Panel 1 shows the two OAE response waveforms. Panel 2 shows the initial transient stimulus. Panel 3 shows the frequency spectrum of the stimulus, and panel 4 shows the cross power spectrum of the OAE responses and the spectrum of the noise (unshaded).

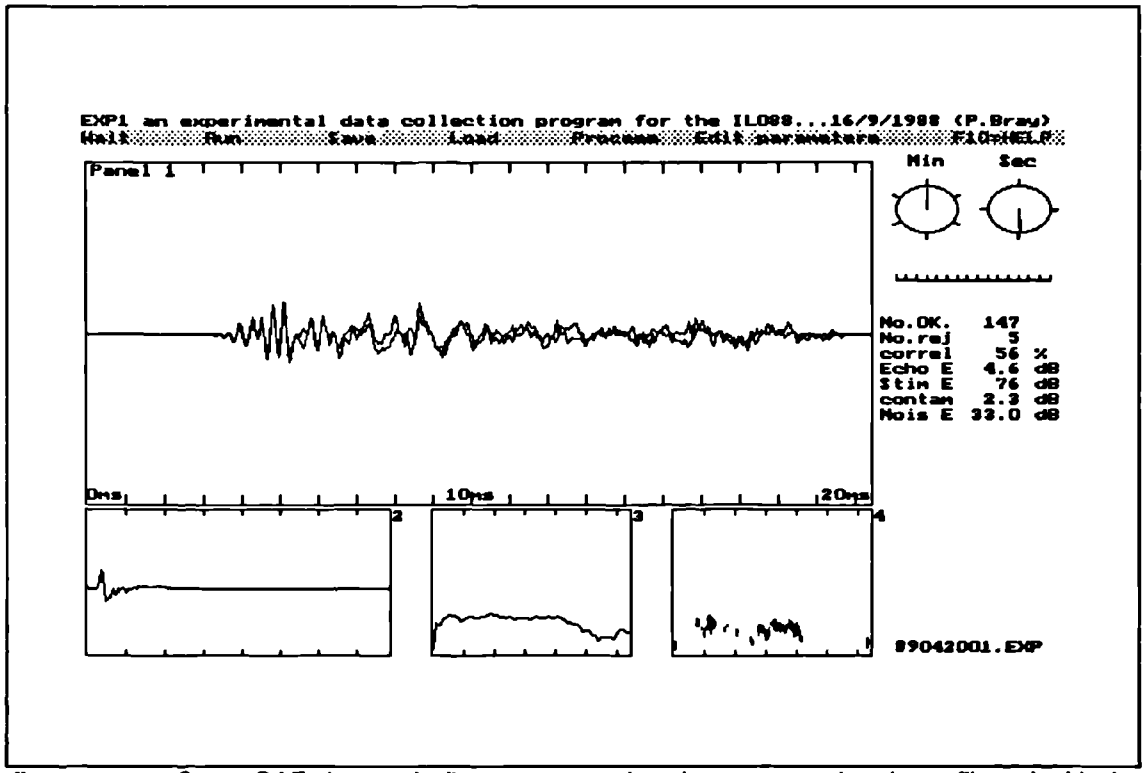

figure 6.10 Same OAE data as in fig.6.9, except that the response has been filtered with the standard 400Hz-6.4KHz bandpass filter.

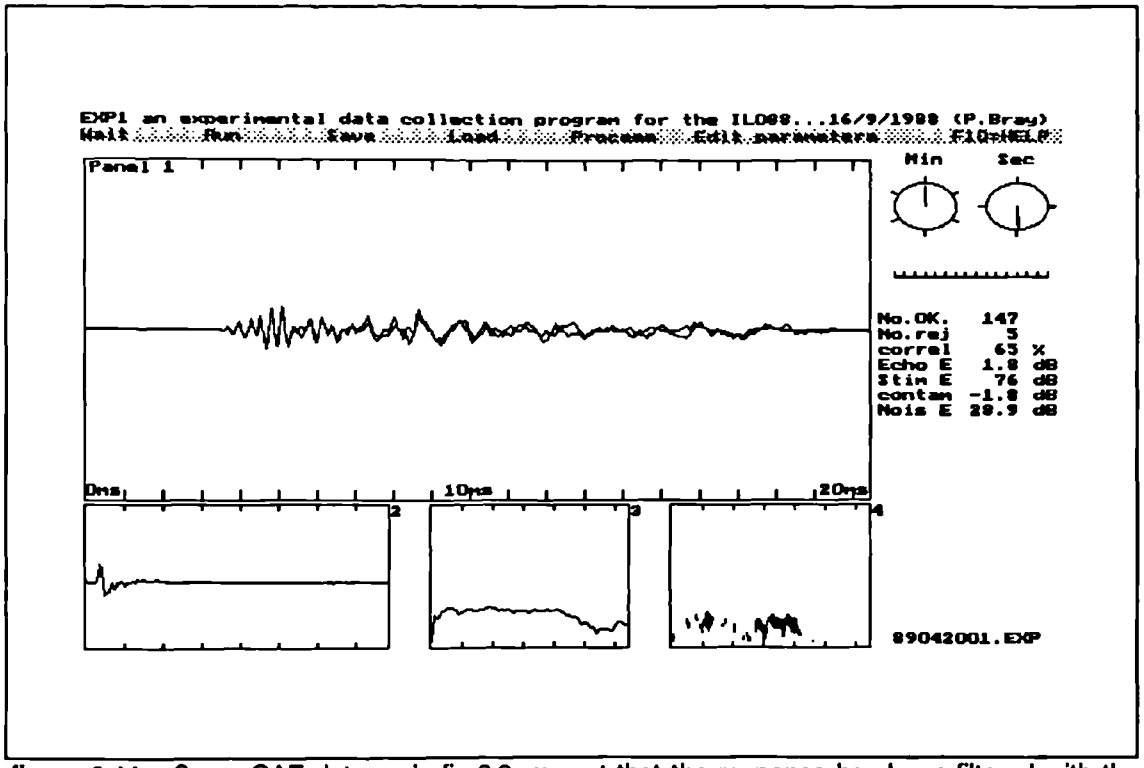

figure 6.11 Same OAE data as in fig.6.9, except that the response has been filtered with the templated bandpass filter.

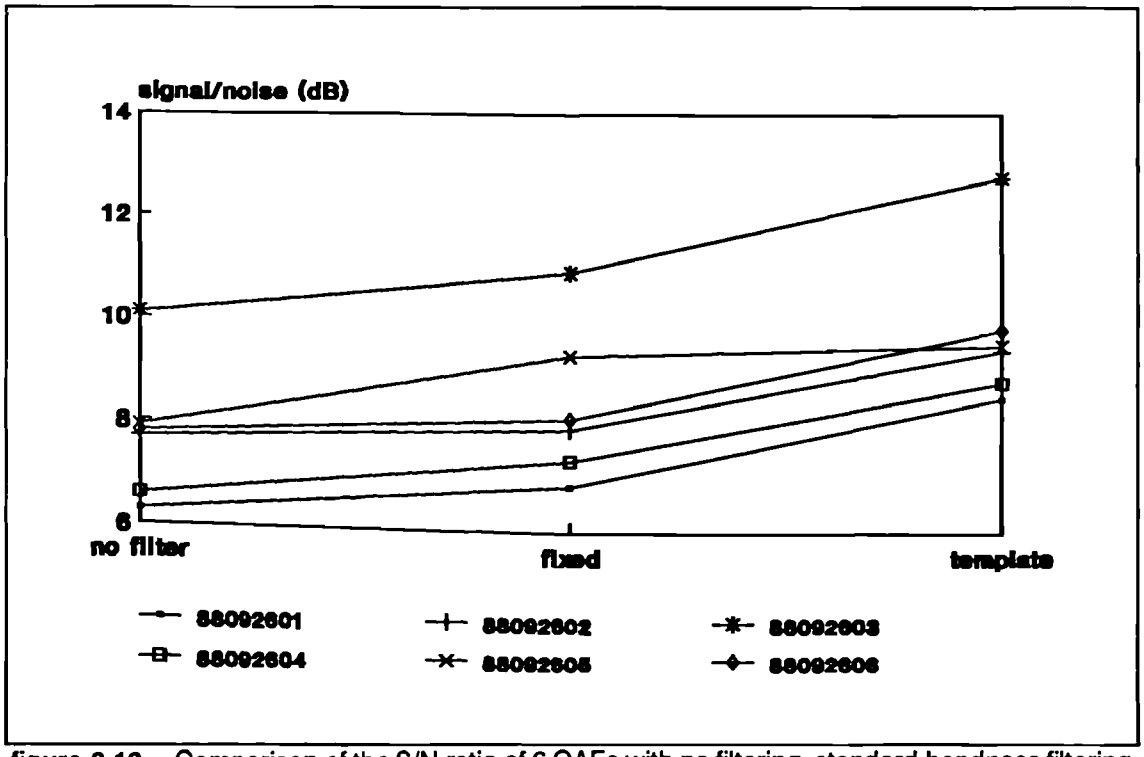

figure 6.12 Comparison of the S/N ratio of 6 OAEs with no filtering, standard bandpass filtering, and template bandpass filtering.

filtered and template filtered). Fig.6.12 summarises the results of this study. Each of the 6 lines 'maps' the signal to noise ratio under the three processing conditions. In each case, the application of the fixed bandpass filter improves the signal to noise ratio of the unfiltered response data. However, in each case, the application of the templated filter improves the signal to noise ratio of the data to a greater extent than the fixed bandpass filter. The average improvement in the signal to noise ratio of the templated filter over the fixed bandpass filter is 1.3dB (total of 11 ears tested).

Summary.

A new filter was devised which was tailored to the specific frequency dispersion characteristics of the OAE. This filter is a bandpass filter which varies the pass band as a function of post stimulus time. Any increase in the probability of false positive emission identification was investigated by cross correlating samples of random noise before and after the application of the templated filter. This investigation indicated that after one application of the templated filter, no such increase was likely. The templated filter was applied to a small population of normal OAEs, and the average improvement in the signal to noise ratio was 1.3dB. From the statistical investigation detailed earlier in this chapter, this increase in signal to noise ratio would be expected to decrease the percentage of indeterminate emission measurements from 21% to 15%. In a screening application this reduces the number of cases where a follow-up test is required by nearly 30%.

6.2 Interpretation of OAE data under conditions of middle ear abnormality.

In chapter 2 a technique was described (derived nonlinear technique) which overcame the difficulties of differentiating the middle ear and cochlear responses to transient acoustic excitation. This technique has proved useful in using OAEs to measure cochlear function. Although the acoustic response of the middle ear is eliminated from the recorded data by the derived nonlinear technique, the stimulus and cochlear response are nevertheless influenced by the forward and reverse transfer functions of the middle ear, respectively.

The cochlear emission has a 'two fold' dependence upon the transmission characteristics of the middle ear. The stimulus signal received by the cochlea is dependent upon the stimulus signal in the ear canal being conveyed by the middle ear. Similarly, the cochlear response measured in the ear canal depends upon reverse transmission through the middle ear. In the case of middle ear abnormalities (e.g. fluid in the middle ear, pneumatic pressure in the middle ear cavity, or reduced articulation of the ossicular joints) any change in the transfer function of the middle ear would be expected to have a large influence on the cochlear emission measured in the ear canal.

When testing young children, a disturbance of the transmission characteristics of the middle ear, due to middle ear pathology, is sufficiently commonplace to pose a problem for screening of cochlear function using the OAE test. Therefore it is important that the condition of the middle ear is known, particularly if the emission is absent.

The current clinical practice for ascertaining the impedance of the middle ear is to use tympanometry. This technique employs an acoustic probe containing a microphone, a loudspeaker and a pressure feed pipe. Typically, a 220Hz sine wave is applied to the loudspeaker and the microphone measures the sound pressure level in the ear canal under a range of pneumatic pressures applied to the ear canal. The technique

of tympanometry gives a 'limited picture' of the middle ear impedance 'seen' through the ear drum. As a result, the measured impedance is determined largely by the impedance of the ear drum, and the 'malleus end' of the ossicular chain.

The tympanogram shows the middle ear compliance as a function of ear canal pressure. This is achieved by measuring the acoustic compliance of the ear canal under a range of pneumatic pressures. If the maximum compliance does not occur at ambient pressure, then this indicates that a pressure differential exists across the tympanic membrane. This pressure differential results in a displacement on the stapes (as well as the tympanum), and increases the tension (and therefore stiffness) in the membrane at the oval window and the tympanum. In addition, at larger pressure differentials, the stapes displacement becomes restricted by a ligament. All of these changes, brought about by a pressure differential, lead to a modification of the forward and reverse transfer functions of the middle ear.

Although the 220Hz impedance measurement can show that a pressure differential exists, it cannot quantify the extent of the modification of the transfer function at the OAE frequencies (i.e. >1KHz). There are therefore likely to be large variances in the OAE measurements of middle ear origin which remain 'unexplained' by conventional tympanometry. It has been observed that a pathological disturbance of the middle ear transfer function can severely affect the OAE measurement (see fig.5.10). Because of the two-fold dependence of the OAE upon the middle ear, even a minor deterioration of the transfer function causes a significant reduction in the OAE. In the clinical environment, where a combination of noise and limited test time often results in the signal to noise ratio of the emission data being only 6dB, even a small reduction of the transfer function can render the OAE measurement as indeterminate.

From the above, it is therefore appropriate to investigate the effect of middle ear abnormality upon the OAE.

The common middle ear pathological condition is a relative negative pressure in the middle ear. This is caused when the middle ear cavity can no longer equalise with ambient pressure. Normally, the eustachian tube allows this pressure equalisation. However, during a head cold, the increased mucus secretion often blocks the eustachian tube. Tissue absorption of the gases which are then sealed in the middle ear causes a reduction in the pressure. This pressure differential causes the tympanic membrane to be drawn inwards.

At the ear drum this inward tympanic membrane displacement (and resulting increase in stiffness) can be simulated by a positive pneumatic pressure applied to the ear canal. This provides an experimental possibility to examine the influence of trans-tympanic pressure differential upon the OAE. For the purpose of this qualitative study, it is considered to be an appropriate approximation to the pathological condition. However, in the condition of negative pressure in the middle ear, the stapes footplate is displaced outwards from the cochlea, whereas in the case of a positive pressure applied to the ear canal the opposite is true. It is therefore not possible to exactly reproduce the effect of a middle ear pressure offset by using pressure in the ear canal.

Another pathological condition is the presence of fluid in the middle ear. This fluid increases the inertia of the sound conducting elements of the middle ear. This condition can be modelled simply by the presence of a water coating on the exterior face of the tympanic membrane.

A study of the effect of fluid loading upon the tympanic membrane.

The subject for this experiment was lying horizontal with the left ear canal facing upwards. After an initial 'normal' emission measurement, three further emission measurements were performed with increasing quantities of water introduced into the ear canal. A glass pipette was used to carefully place drops of water into the centre of the ear canal, ensuring that the droplet fell to the tympanic membrane, without

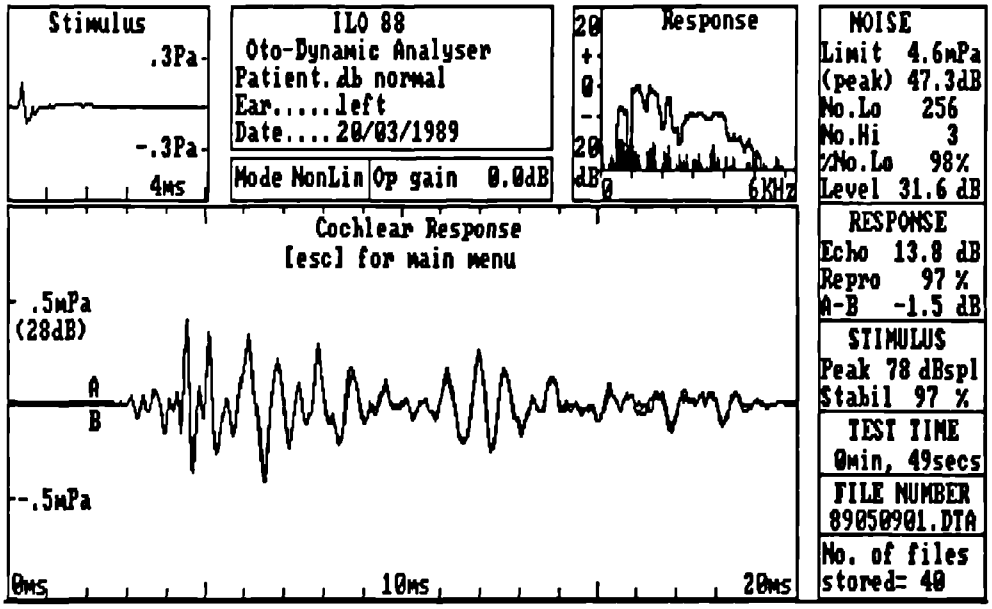

figure 6.13 Emission from normal subject, prior to introduction of water droplets. Note the wide frequency range of the emission.

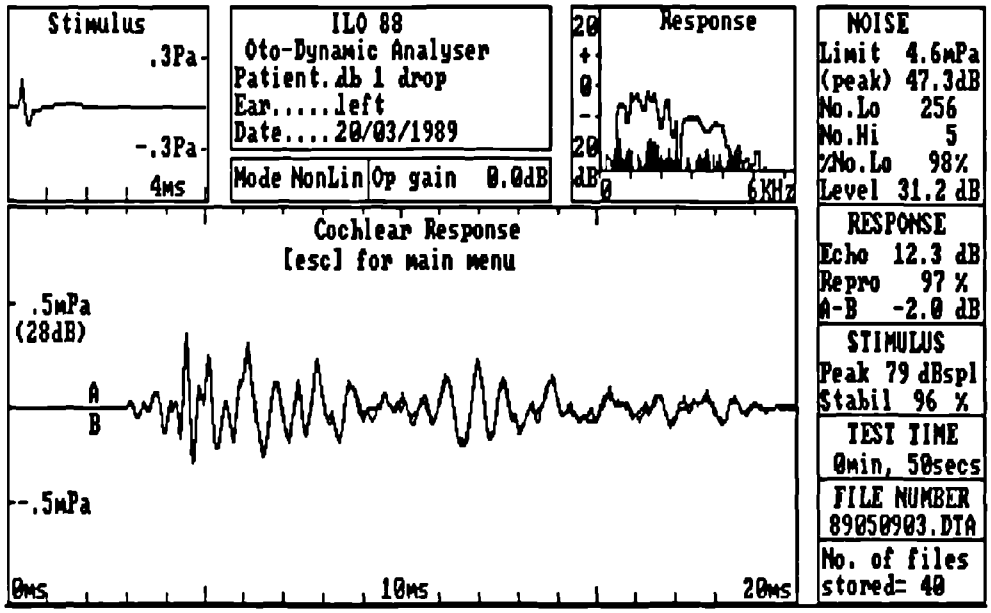

figure 6.14 Emission after introduction of 1 droplet of water (approx. 2mm diameter) into the ear canal.

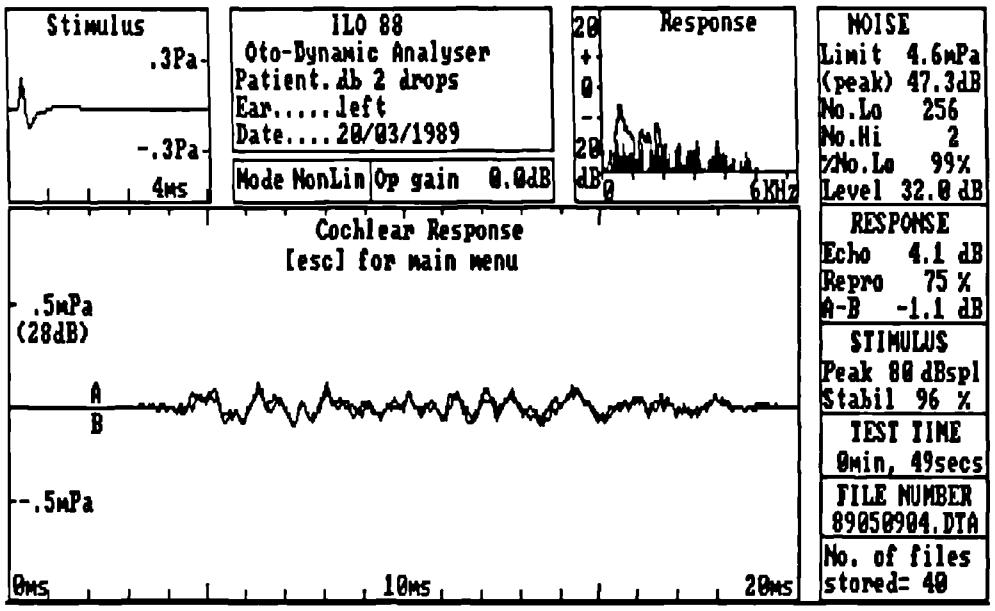

figure 6.15 Emission after introduction of 2 droplets of water into the ear canal.

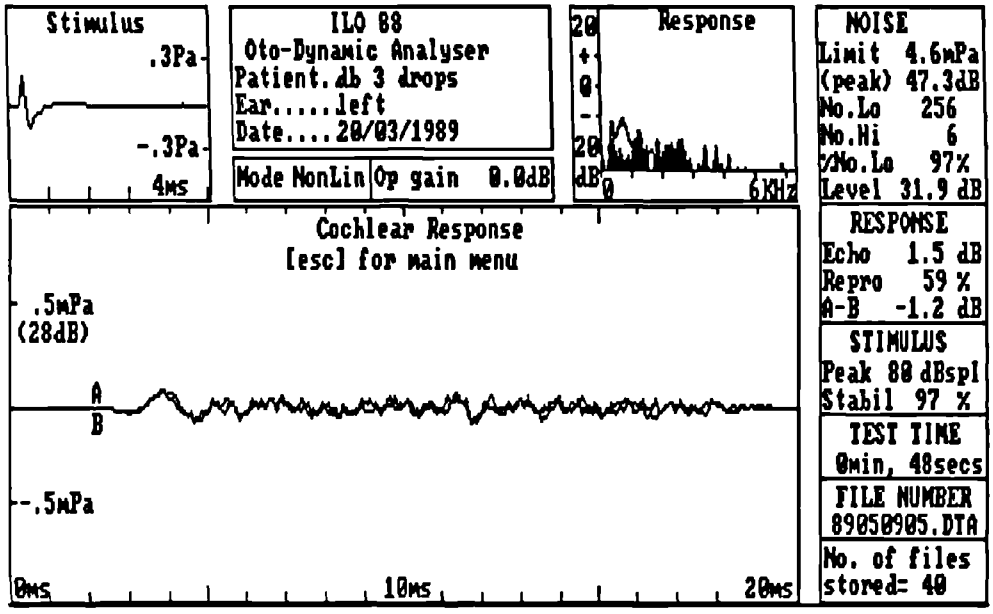

figure 6.16 Emission after introduction of 3 droplets of water into the ear canal.

touching the ear canal. Between each emission measurement a further droplet was added. Each droplet was approximately 2mm in diameter. Figures 6.13 to 6.16 show the four emission measurements.

The normal emission from this subject contains a broad frequency range from 500Hz to 5KHz (fig.6.13). One drop of water decreased the overall size of the emission by approximately 1.5dB (fig.6.14). The second drop produced a large effect (fig.6.15), reducing the emission by 8dB. Furthermore, frequencies above 2KHz were reduced disproportionately and were 'lost' below the noise floor of the measurement. After the introduction of the third droplet (fig.6.16), the emission was reduced still further. Remnants of the emission are just visible at 12ms. An artefact between 3-5ms was present in this measurement, which manifests in the frequency spectrum as an emission at 500Hz.

In conclusion, the presence of fluid on the tympanic membrane increases the inertance of the membrane and therefore constitutes a conductive loss, particularly at the higher frequencies. Little effect in the emission was noted after the introduction of just one droplet of water. This is most likely due to either failings of the experimental method to reliably place the water on the membrane, or the water droplet covering only a small area of the membrane and therefore causing little effect on the overall membrane inertance. However, after the introduction of three droplets the emission was almost completely absent.

A study of the influence of trans-tympanic pneumatic pressure differentials upon the OAE.

To aid the interpretation of OAE data under the clinically encountered condition of trans-tympanic pneumatic pressure differential, a study was undertaken to measure the effect of a pneumatic pressure displacement of the ear drum upon the waveform and spectral content of the OAE data from a normal ear.

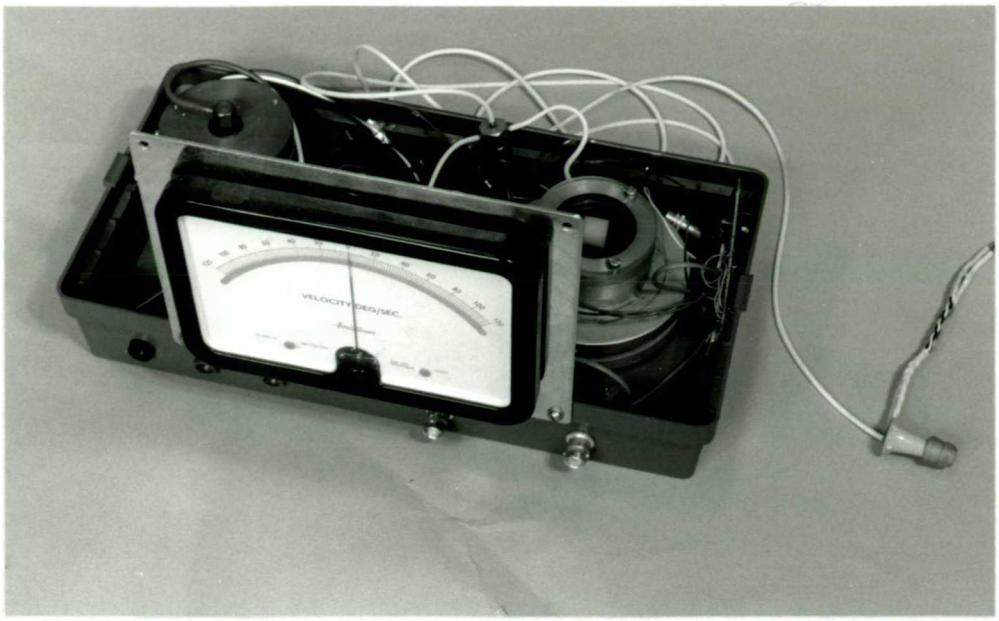

figure 6.17 Photograph of the additional hardware required to produce and monitor external ear canal pressures in the range -300 to 300mmH2O.

The pneumatic pressure for this experiment ranged from -300 to 200mmH2O. This is the range which is commonly used in clinical tympanometry (and is therefore considered safe). This pressure was produced by a purpose built addition to the OAE test instrument. The device consists of a pump and pressure sensor (kindly supplied free of charge by Meditech UK Ltd) and interface circuitry. Fig.6.17 shows a photograph of the completed hardware. A large panel meter was added to enable a visual check of the pressure, and was calibrated from -300 to 300mmH2O.

The probe which was designed for OAE measurements (chapter 2) has a microphone, a loudspeaker and a pressure venting tube. This probe was easily adapted for use in this experiment by joining a length of pipe from the venting tube to the pneumatic pump. To achieve an airtight seal in the ear canal selection of the correct size of probe tip was necessary. During the fitting of the probe in the ear canal, the seal was checked by observing (on the panel meter) the maintenance of a pressure offset in the ear canal.

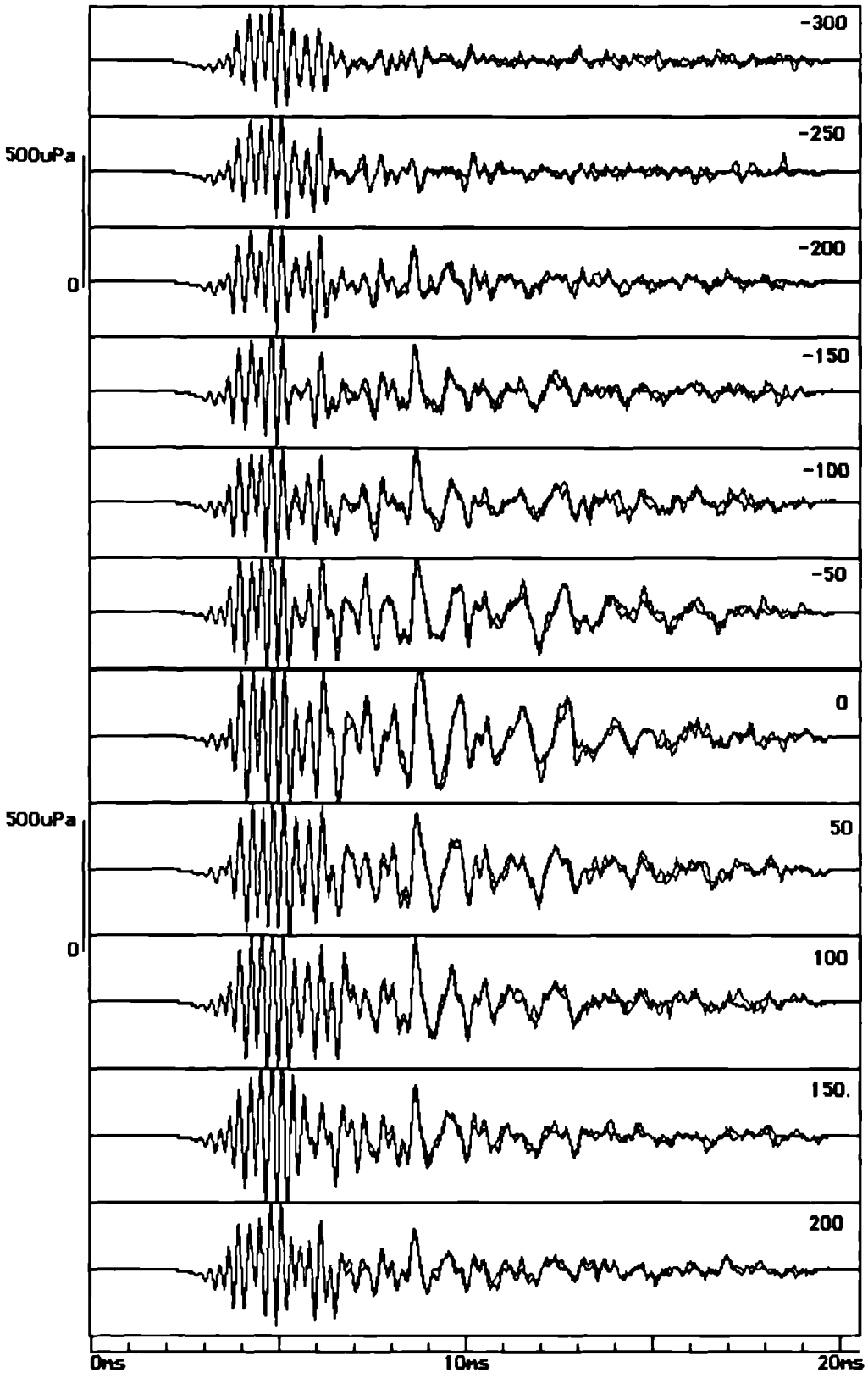

figure 6.18 11 OAE waveforms from the same ear taken with ear canal excess pressure ranging from -300 to 200mmH2O, in steps of 50mmH2O. The uppermost emission was measured at -300mmH2O and the lowermost at 200mmH2O.

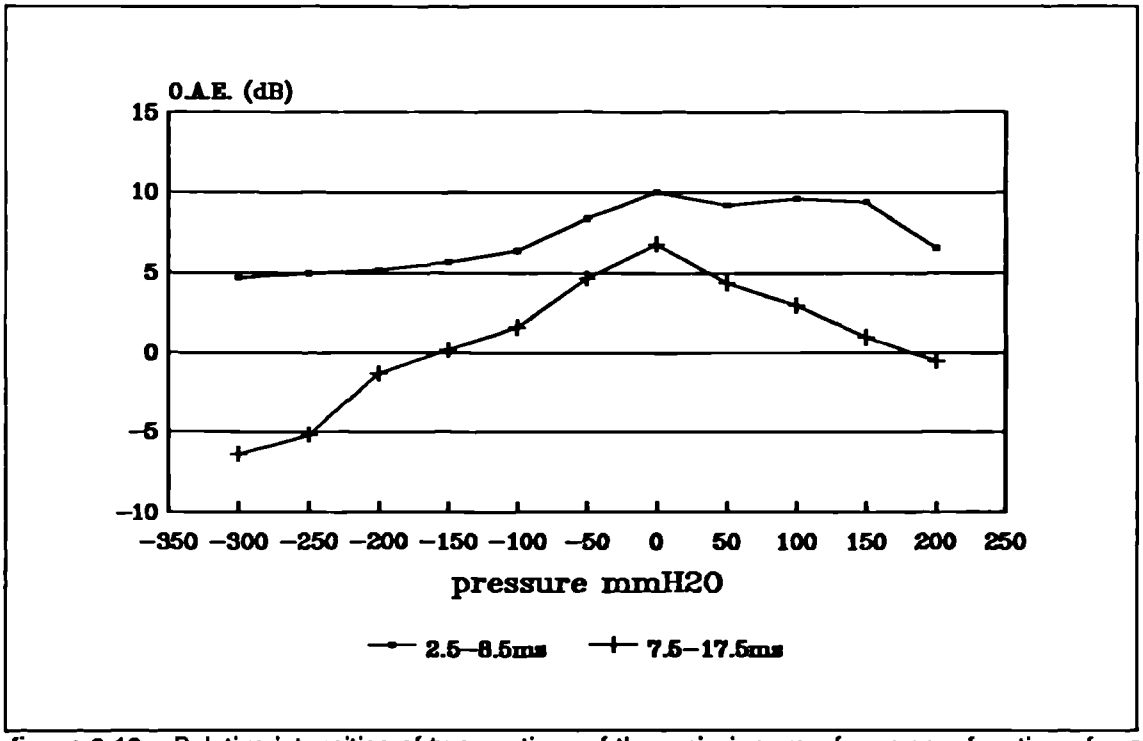

figure 6.19 Relative intensities of two sections of the emission waveforms as a function of ear canal pressure.

A series of OAE measurements were made from an adult ear. The OAE from this ear under normal conditions contains frequencies from 600Hz to 4.5KHz. Eleven OAE measurements were performed in total, with the ear canal pressure ranging from -300 to 200mmH2O in steps of 50mmH2O. The subject had to remain extremely still during these measurements, as any movements caused a considerable amount of extra noise in the ear canal, introduced by the pressure connecting pipe. The total test time for these 11 measurements was 16 minutes.

Fig.6.18 shows the 11 OAE response waveforms at the different pressures. This particular OAE waveform is normally dominated by two 'packets' of energy. One of these is centred at 5ms and has a frequency of approximately 4KHz, the other is centred at 10ms and has a frequency of approximately 1KHz. From the figure, it is clear that these two 'packets' are affected differently by the application of a pneumatic pressure. The high frequency part of the waveform remains relatively unaffected by the pressure differential, whereas the low frequency section of the waveform varies

considerably. At -300mmH_2O the emission waveform beyond 7ms is almost absent. At ambient pressure the waveform is at a maximum amplitude. As the pressure is increased towards 200 mmH_2O the latter part of the waveform decreases in amplitude. Fig.6.19 illustrates the relative intensities of the early and latter sections of the 11 OAE waveforms.

The effect of the trans-tympanic pressure differential upon the different OAE frequencies was studied using a purpose written (Pascal) analysis programme. The programme displays the frequency spectra of the 11 OAE measurements as a 3D (waterfall) plot. A cross section of this plot (i.e. a section parallel with the pressure axis) displays the variation of the OAE at a particular frequency as a function of pressure. The programme is operated by the keyboard cursor keys, enabling the cross-section at any frequency to be viewed.

Fig.6.20 shows the frequency spectra of the 11 OAE response waveforms shown in fig.6.18. Two different cross-sections are shown, one at 1KHz, the other at 3.9KHz. These frequencies are both peaks in the frequency spectrum of the OAE of this ear taken under normal conditions. At 1KHz the emission intensity shows a clear peak at 0mmH_2O. The intensity falls by 10dB at pressures of ±200mmH_2O, and by 20dB at -300mmH_2O. In contrast, at 3.9KHz, the emission intensity remains relatively constant as a function of pressure. The total variation in intensity at 3.9KHz over the whole pressure range is only 4dB.

Further acoustic measurements of the same ear were undertaken to aid interpretation of the above result. The ear canal impedance was measured at 220Hz and 660Hz using the OAE probe, a signal generator, an oscilloscope and the pressure pump. This enabled the compliance as a function of pressure to be established at the 'normal' tympanometric frequencies (compliance = 1/impedance). Fig.6.21 shows the compliance at 220Hz and 660Hz for this ear. The curves are shown as percentage increases in the compliance relative to the minimum compliance (at -300mmH_2O the ear drum

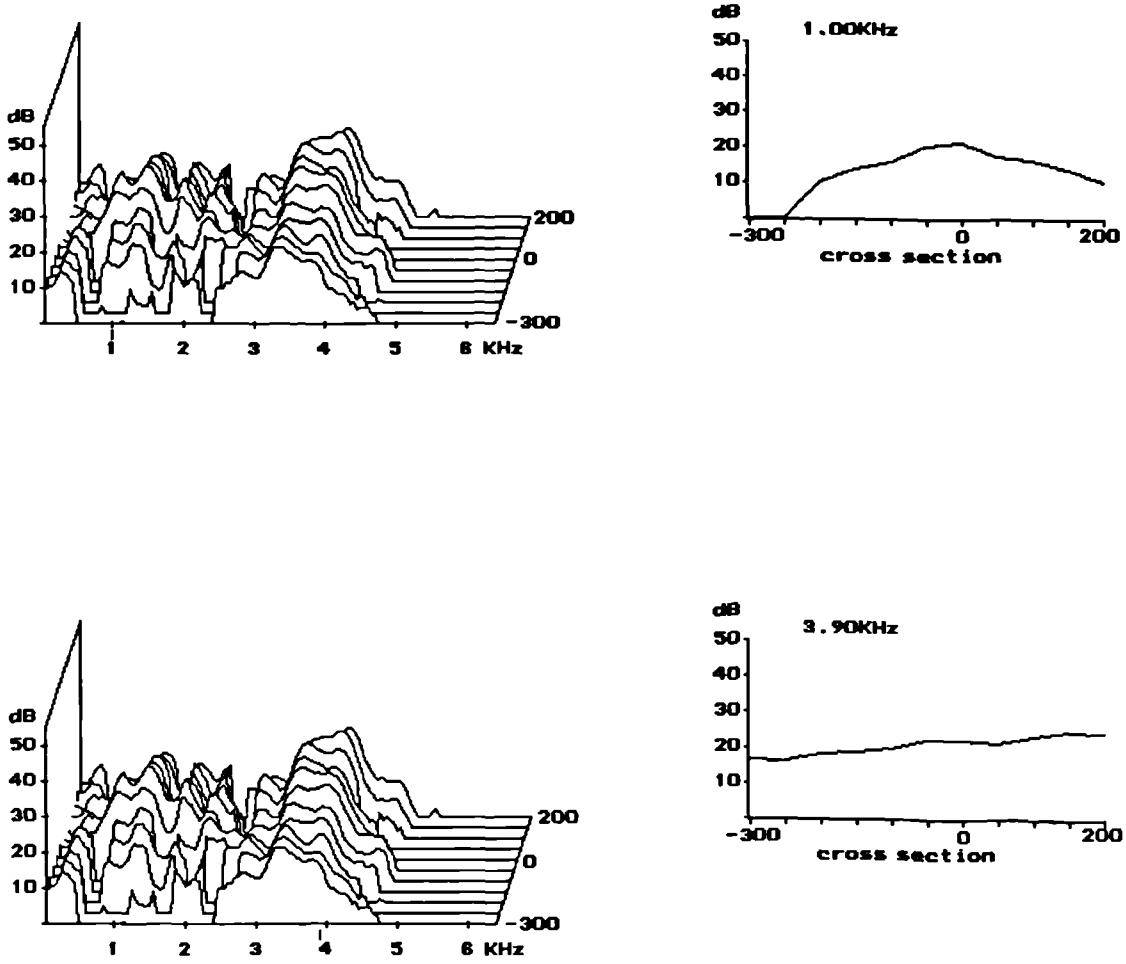

figure 6.20 Frequency spectra of the 11 OAE measurements shown in fig.6.14. The spectra are displayed in a 'waterfall' plot, with the measurement at -300mmH2O nearest, and the 200mmH2O furthest away. The right hand panels show the cross-section of the 11 spectra at the frequencies indicated.

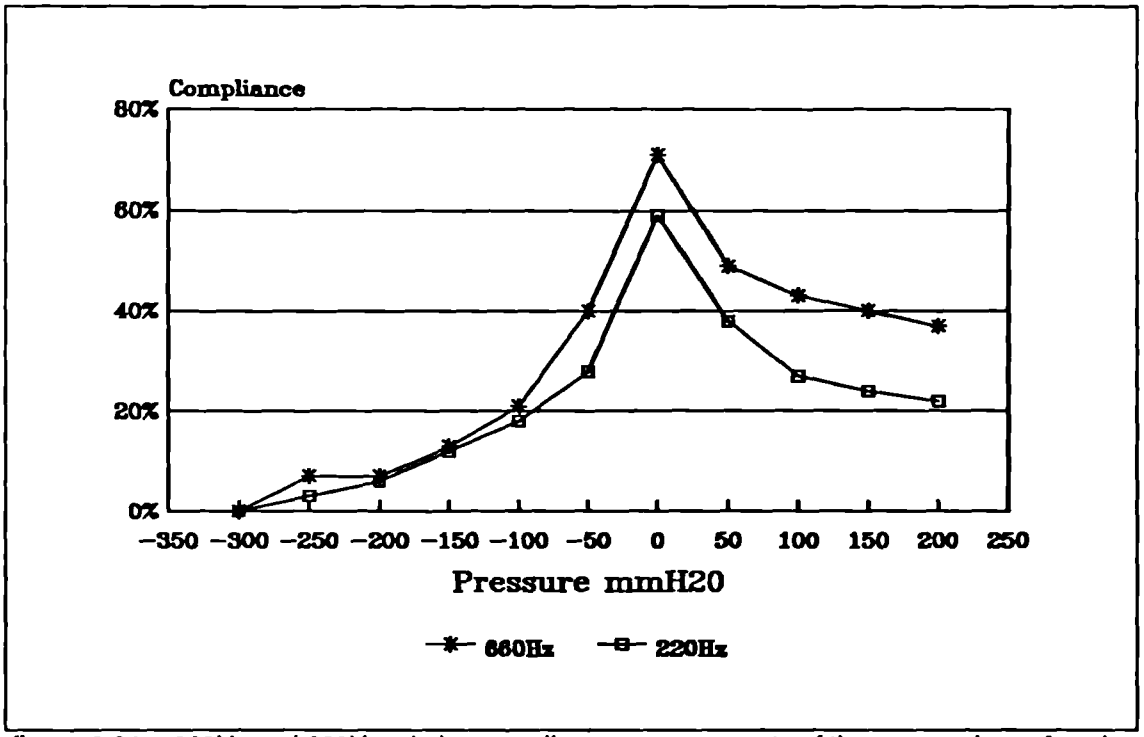

figure 6.21 220Hz and 660Hz relative compliance measurements of the ear canal as a function of ear canal pressure.

is assumed to be approximately immobile to 220 and 660Hz tones, and therefore the ear canal is a rigid cavity). This figure shows the typical compliance curves of a normally functioning middle ear. The compliance attains a maximum at ambient pressure. The compliance at maximum is 70% greater than the compliance of just the ear canal, indicating that the middle ear has a compliance of 70% of the ear canal.

The measurement of the initial transient response of the ear canal during each of the 11 measurements at different pressures provides a record of the relative ear canal impedance at frequencies from 600Hz up to 4.5KHz. The frequency spectra of the initial transient response of the ear canal were also analysed by the same method as the spectra of the OAE. Fig.6.22 shows the 11 frequency spectra of the initial transient response of the ear canal. The same two cross-section frequencies are shown as for fig.6.20 (i.e. 1KHz and 3.9KHz). At 1KHz the maximum impedance (i.e. minimum compliance) occurs at -300mmH2O. This indicates that at this pressure the middle ear and cochlea receive relatively less sound at 1KHz for a given stimulus level than

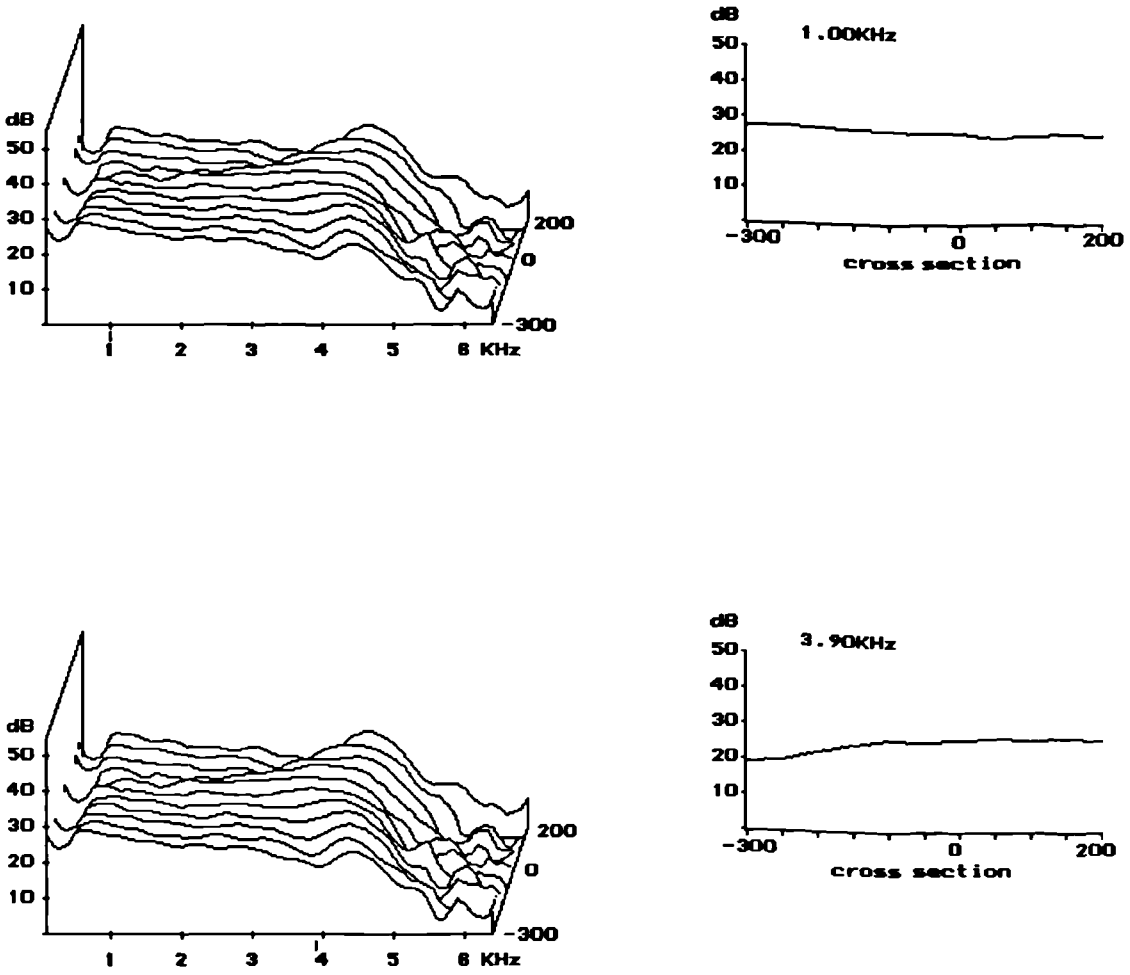

figure 6.22 Frequency spectra of the 11 measurements of the initial transient response of the ear canal (i.e. the stimuli used to elicit the responses shown in fig.6.14). The spectra are displayed in a 'waterfall' plot, with the measurement at -300mmH_2O nearest, and the 200mmH_2O furthest away. The right hand panels show the cross-section of the 11 spectra at the frequencies indicated.

at ambient pressure. This suggests a possible explanation of the reduction in the 1KHz component of the OAE at -300mmH2O. However, the total change in impedance between -300mmH2O and ambient pressure is only 2dB, which equates to a 26% change in compliance. The emission intensity between the same two pressures changes by over 20dB. Therefore the impedance measured in the ear canal does not fully reflect the transmission of sound through the middle ear.

The OAE is dependent upon transmission through all of the components of the middle ear twice over. The ear canal compliance measurements are dominated by the behaviour of the ear drum. The poor correlation between the OAE as a function of pressure variation and the ear canal compliance suggests that the ear canal pressure is affecting the sound propagation through the whole of the middle ear components rather than just the ear drum. It was decided to study the effect of the sound propagation through the entire middle ear, to the cochlea, by measuring the subjective auditory threshold at 1KHz and 3.9KHz as a function of ear canal pressure.

The loudspeaker of the OAE probe was connected to a signal generator, and the probe was then carefully inserted and sealed into the ear canal. The same pressure range was used, and the threshold was determined at each pressure for the two frequencies. Fig.6.23 shows the two thresholds as a function of pressure. The thresholds are plotted relative to the best threshold. These curves represent the attenuation of the middle ear (relative to minimum attenuation) as a function of ear canal pressure. At 1KHz a distinct minimum threshold exists at ambient pressure. Either side of ambient pressure the threshold curve is symmetrical for ±200mmH2O, reaching 4dB at these pressures. By -300mmH2O the threshold is raised by 12.5dB. The 3.9KHz threshold behaves very differently. The total threshold variation over the whole range of pressures is only 1.8dB. The threshold only increases by more than 1dB for pressures less than -200mmH2O.

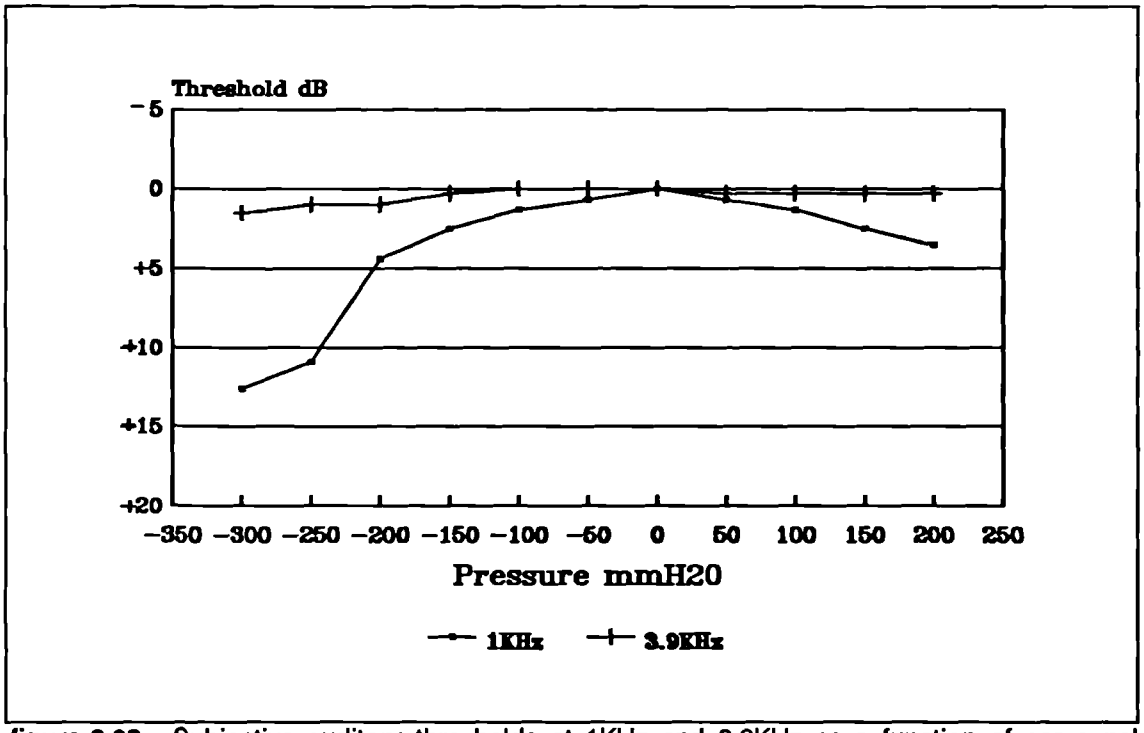

figure 6.23 Subjective auditory thresholds at 1KHz and 3.9KHz as a function of ear canal pneumatic pressure.

The auditory threshold curves indicate the attenuation 'through' the middle ear in the forward direction. If it assumed that this attenuation is the same for the reverse propagation of sound through the middle ear, then the threshold curves of fig.6.23 and the emission intensity curves of fig.6.20 correspond to a very high degree. This is true for both the 1KHz and 3.9KHz curves.

Conclusions of the trans-tympanic pressure differential experiment.

An investigation of the effect of trans-tympanic pressure differential upon the intensity of the OAE at different frequencies was performed. From this investigation it was possible to conclude that:-

- At the lower OAE frequencies (i.e. 700Hz to 1.5KHz) the intensity of the emission in the normal ear is maximum at ambient pressure. In the example given, the emission intensity was 10dB less at ±200mmH2O, and 20dB less at -300mmH2O. Similar effects were noted in other ears tested.

- At the higher OAE frequencies (i.e. 3KHz to 4KHz) the intensity of the emission was relatively independent of pressure (in the range -300 to 200mmH2O).
- Over the whole range of OAE frequencies, the emission intensity variation as a function of trans-tympanic pressure corresponds to the variation of subjective auditory threshold at these frequencies (i.e. the reduction of emission intensity is attributable to a conductive loss in the middle ear).
- The loss of emission intensity as a function of pressure was approximately twice the subjective auditory threshold shift. This indicates that the forward and reverse transmission of the middle ear were affected by trans-tympanic pressure to a similar degree.
- The study of emission intensity as a function of trans-tympanic pressure reveals a far greater variance than the impedance measured in the ear canal at OAE frequencies. This suggests that the emission intensity is largely affected by elements of the middle ear which have little influence upon the ear canal impedance.

This investigation has shown that for trans-tympanic pressures in the range -300 to 200mmH2O it would be expected to be able to measure an emission at 3-4KHz. With this knowledge, and the fact that young children have a relatively high prevalence of middle ear abnormality, and tend to generate more noise during testing, it is suggested that the use of a narrow band filter at 2-4KHz would yield a higher pass percentage for OAE screening. This filter could be inserted in the analogue circuit, and would reduce patient generated noise (which tends to be at frequencies lower than 2KHz). This filter could be implemented if the outcome of the first OAE test was indeterminate.

Testing neonates soon after birth reduces the chance of middle ear pathology having developed, which suggests that there is a considerable advantage to be gained

by OAE screening at the earliest possible age. Furthermore, the cochlear emissions of neonates are much larger in amplitude than older children and adults due to the small ear canal volume (see chapter 5) and are therefore easier to measure. This is contrary to the case for BSER where the signal is sometimes difficult to interpret in neonates because of a variation of the signal characteristics due to maturation within the first few weeks of age[17].

Conclusions.

Summary of thesis.

The field of otoacoustic emissions (OAE) was introduced and reviewed, with particular reference to the development of the clinical application of OAEs. A re-examination of the acoustic properties of the ear canal with regard to transient acoustic excitation led to a rigorous technique for OAE signal extraction. A clinically useful **derived nonlinear** OAE signal component was defined and its physical properties investigated.

An OAE measurement instrument was specified, designed and constructed. The derived nonlinear OAE technique was implemented to aid reliable OAE measurement in the clinical test situation. The instrument also incorporated special analyses and VDU displays to aid the operator during interpretation of the OAE test conditions and outcome.

To evaluate the OAE clinical test system, it was installed at four test sites. Operational aspects of the instrument proved to be satisfactory. Good agreement was achieved between the OAE test result and the known auditory pathology. The OAE instrument/technique was found to be limited in a minority of cases by uncertainty about the influence of the middle ear and by OAE recognition in low signal to noise conditions. New experiments were conducted in order to evolve practical solutions and thereby increase OAE measurement reliability.

Outcomes.

It was found possible to separate the ear canal transient response and the nonlinear OAE, based on the growth of each signal to increasing excitation levels.

The study of noise in relation to the nonlinear signal component led to the observation that the maximum signal to noise ratio in the derived nonlinear emission response was obtained when the ratio of the number of measurements at each of the two excitation levels was inversely proportional to the ratio of the two excitation levels.

The system for OAE measurement, implemented on an IBM PC, proved to be an efficient, portable, reliable and user friendly OAE instrument suitable for clinical usage. It was effective at obtaining an OAE measurement from a normal ear in less than 1 minute.

The system was found suitable for screening the cochlear function of neonates. Trials revealed the need for special attention in the area of probe design, and a test room with a lower ambient level of noise was required. Due to the small ear canal volume of an infant, the emission amplitude was greater than that of an older child or adult.

Middle ear abnormalities were found to influence the OAE measurement, and further research revealed the extent of this influence. It was found that for middle ear excess pressure in the range -300 to 200mmH_2O the emission, although altered, was not absent.

Further improvements in OAE recognition in conditions of high noise contamination were achieved following the design and implementation of an OAE specific 'templated' filter.

The OAE instrument has been commercially manufactured and introduced to more than 40 hospitals and universities in Europe, U.S.A. and Japan.

Discussion of possible future developments.

It is currently known that OAEs are present only when the subjective auditory threshold is better than 20dBHL (within the emission bandwidth) and absent when

the threshold is worse than 20dBHL. Following the new technical developments, detailed in this thesis, the OAE test could be adopted as a routine practical test of cochlear function in audiological investigation centres. However, the full significance of the OAE in relation to pathology has yet to be fully explored. Greater understanding of the cochlear origin and basis of OAEs is therefore needed. This is the subject of much current research.

One area where improvement of the instrument performance is required is in the control of the variance of OAE intensities. In this thesis it is shown that the middle ear has a great influence upon the OAE. Variability of the middle ear function could well account to a large degree for the observed variance of emission intensity in the normal population. Ideally, tympanometry should be performed as a precursor to OAE measurement as a means of verification of middle ear normality. As many of the components essential to both OAE measurement and typmanometry are the same, integration of the tympanometry test into the OAE instrument would be a relatively simple and worthwhile improvement. However, to achieve greater understanding of the influence of the middle ear upon the OAE, more comprehensive investigation of middle ear function is necessary over a wider range of frequencies.

Although the general OAE instrument concept has been developed and proved effective, it could be further developed to form the basis of a second generation OAE instrument. The current implementation on an IBM PC could develop into a more portable version on a battery powered portable computer. Alternatively, the instrument may develop to satisfy more specific roles such as a dedicated screening instrument or a comprehensive clinical instrument.

Further study of the properties of OAEs and the experiences of OAE measurements in the clinical situation should lead to further improvements in the signal processing of emission data. This will lead to a shorter emission test time and a reduction in the number of indeterminate emission test outcomes.

It is clear that we look forward to further improvements in the OAE technique. It is hoped that the OAE test will become a useful addition to the auditory 'test battery', particularly in the early detection of hearing impairment in infants.

References.

1. Allen, J.B.(1985). Measurement of eardrum impedance, in Peripheral Auditory Mechanisms: ed S.Levin, Boston.

2. Anderson, S.D and Kemp, D.T. (1979). The evoked cochlear mechanical response in laboratory primates. Arch. Otorhinolaryngol. 224, 47-54.

3. Békésy, G.von.(1960). Experiments in hearing, McGraw-Hill, New York.

4. Bonfils, P., Bertrand, Y. and Uziel, A. (1988). Evoked otoacoustic emissions: Normative data and presbycusis. Audiology 27, 27-35.

5. Bray, P.J. and Kemp, D.T. (1987). An advanced cochlear echo technique suitable for infant screening. B.J.A. 21, 191-204.

6. British Patent No.8713116, (1987).

7. Brownell, W.E., Bader, C.R., Bertrand, D. and de Ribaupierre, Y. (1985). Evoked mechanical responses of isolated cochlear outer hair cells. Science 227, 194-196.

8.Dijk, P.van, and Wit, H.P. (1987). The occurrence of click-evoked otoacoustic emissions ("Kemp echoes") in normal-hearing ears. Scand. Audiol. 16, 62-64.

9. Elberling, C., Parbo, J., Johnsen, N.J., and Bagi, P. (1985). Evoked acoustic emission: Clinical application. Acta. Otolaryngol (Stockh), suppl. 421, 77-85.

10. Elliot, E. (1958). A ripple effect in the audiogram. Nature 181, 1076.

11. Evans, E.F. & Wilson, J.P. (1973). The frequency selectivity of the cochlea. Basic mechanisms in hearing. Ed. Møller. 519-551.

12. Flock, A. and Cheung, H. (1977). Actin filaments in sensory hairs of inner ear receptor cells. J. Cell. Biol. 75, 339-343.

13. Foulkes, A. (1989). Hearing screening in special schools. B.S.A. Newsletter Feb.

14. Gold, T. (1948). Hearing II. The physical basis of action in the cochlea. Proc. Roy. Soc. B135, 492-498.

15. Gold, T. (1989). Historical background to the proposal, 40 years ago, of an active model for cochlear frequency analysis. Ed. Wilson & Kemp. 299-305.

16. Grandori, F. (1983). Evoked otoacoustic emissions stimulus-response relationship. Revue Laryngol., Bordeaux 104, 153-155.

17. Hecox, K. and Galambos, R. (1974). Brain stem auditory evoked responses in human infants and adults. Arch Otolaryngol, 99, 30-33.

18. Horst, J.W., Wit, H.P. and Ritsma, R.J. (1983). Psychophysiological aspects of cochlear acoustic emissions ('Kemp echoes'). Hearing - Physiological bases and psychophysics. Ed. Klinke & Hartmann. 89-96.

19. Johnsen, N.J. and Elberling, C. (1982). Evoked acoustic emissions from the human ear, I. Equipment and response parameters. Scand. Audiol, 11, 3-12.

20. Johnsen, N.J. and Elberling, C. (1982). Evoked acoustic emissions from the human ear, II. Normative data in young adults and influence of posture. Scand. Audiol, 11, 69-77.

21. Johnsen, N.J., Bagi, P. and Elberling, C. (1983) Evoked acoustic emissions from the human ear, III. Findings in neonates. Scand. Audiol. 12, 17-24.

22. Johnstone, B.M. and Boyle, A.J.F. (1967). Basilar membrane vibration examined with the Mössbauer technique. Science, 389-390.

23. Kemp, D.T. (1978). Stimulated acoustic emissions from within the human auditory system, J. Acoust. Soc. Am, 64, 1386-1391.

24. Kemp, D.T. (1981). Cochlear echoes: implications for noise induced hearing loss. in New perspectives on noise induced hearing loss. Raven press.

25. Kemp, D.T. and Chum, R. (1980). Properties of the generator of stimulated acoustic emissions, Hearing Research, 2, 213-232.

26. Kemp, D.T., Bray, P.J., Alexander, L. and Brown, A.M. (1986). Acoustic emission cochleography -practical aspects. Scand. Audiol. suppl. 25, 71-94.

27. Kemp, D.T., Bray, P.J. and Alexander, L. (1986). Practical implementation of the cochlear echo test. Ann. de. Otorrinolaringologia, 1-2, 67-80.

28. Khanna, S.M. and Leonard, D.G.B. (1982). Basilar membrane tuning in the cat cochlea. Science 190, 1218-1221.

29. Kiang, N.Y.-S., Watenabe, T., Thomas, E.C. and Clark, L.F. (1965). Discharge patterns of single fibres in the cat auditory nerve. M.I.T. press, Cambridge, Mass.

30. Kim, D.O., Siegel, J.H. and Molnar, C.E. (1979). Cochlear nonlinearity phenomena in two-tone responses. Scand. Audiol. Suppl. 9, 64-81.

31. Kim, D.O. (1986). Active and nonlinear cochlear biomechanics and the role of outer hair cell subsystem in the mammalian auditory system. in Cellular mechanisms in hearing. Ed. Flock & Wersall.

32. Martin, J.A.M. (1982). Diagnosis and communicative ability in deaf children in the European community, Audiology, 21, 185-196.

33. Medical Research Council. Grant No. G8622310N, (Kemp,D.T., Bray, P.J. and Martin, J.A.M.).

34. Newton, V.E. (1985). Aetiology of bilateral sensori-neural hearing loss in young children. J. Laryngol. Otol. suppl. 10. 40-41

35. Probst, R., Coats, A.C., Martin, G.K. and Lonsbury-Martin, B.L. (1986). Spontaneous, click-, and toneburst-evoked otoacoustic emissions from normal ears. Hearing Research, 21, 261-275.

36. Rhode, W.S. (1971). Observations of the basilar membrane in squirrels monkeys using the Mössbauer technique. Science, 49, 1218-1231.

37. Russell, I.J. and Sellick, P.M. (1978). Intracellular studies of hair cells in the guinea pig cochlea. J. Physiol. (London) 284, 261-290.

38. Rutten, W.L.C. (1980). Evoked acoustic emissions from within the normal and abnormal human ears: comparison with audiometric and electrocochleographic findings. Hearing Research, 2,263-271.

39. Sellick, P.M., Patuzzi, R. and Johnstone, B.M. (1982). Measurements of basilar membrane motion in the guinea pig using the Mössbauer technique. J. Acoust. Soc. Am. 72, 131-141.

40. Spoendlin, H. (1972). Innervation densities of the cochlea. Acta. Otolar. 73, 235-248.

41. Stevens, J.C., and Ip, C.B. (1988). Click-evoked otoacoustic emissions in normal and hearing impaired adults. B.J.A. 22, 45-49.

42. Stevens, J.C., Webb, H.D., Hutchinson, J., Connell, J., Smith, M.F. and Buffin, J.T. (1989). Click evoked otoacoustic emission and the brain stem electric response as tests of hearing impairment in babies from a neonatal intensive care unit.

43. Wever, E.G and Bray, C.W. (1930). Action currents in the auditory nerve in response to acoustical stimulation. Proc. Nat. Acad. Sci. USA. 16, 344-350.

44. Wever, E.G. and Lawrence, M. (1949). The patterns of response in the cochlea. J. Acoust. Soc. Am. 21(2), 127-134.

45. Wilson, J.P. (1980). Evidence for a cochlear origin for acoustic re-emissions, threshold fine-structure and tonal tinnitus. Hearing Research, 2, 233-252.

46. Wilson, J.P. (1980). The combination tone, 2f1-f2, in psychophysics and ear canal recording. Psychophysical, physiological and behavioural studies in hearing. Ed. van den Brink & Bilsen.

47. Wit, H.P., Langevoort, J.C. and Ritsma, R.J. (1981). Frequency spectra of cochlear emissions. J. Acoust. Soc. Am. 70(2), 437-445.

48. Wit, H.P. and Ritsma, R.J. (1980). Evoked acoustical responses from the human ear: some experimental results, Hearing Research, 2, 253-261.

49. Wit, H.P. and Ritsma, R.J. (1979). Stimulated acoustic emissions from the human ear. J. Acoust. Soc. Am. 66(3), 911-913.

50. Zenner, H.P. (1980). Cytoskeletal and muscle like elements in cochlear hair cells. Arch. Otorhinolarngol. 230, 82-92.

51. Zenner, H.P., Zimmermann, U. and Schmitt, U. (1985). Reversible contraction of isolated mammalian cochlear hair cells. Hearing Res. 18, 127-133.

52. Zwicker, E. (1983). Delayed evoked otoacoustic emissions and their suppression by Gaussian-shaped pressure impulses. Hearing Research 2. 359-371.

53. Zwislocki, J. (1962). Analysis of the middle ear function, Part I: Input impedance. J. Acoust. Soc. Am. 34, 1514-1523.

Abbreviations

ADC	Analogue to digital converter
ALU	Arithmetic logic unit
BSER	Brain stem evoked response
CAD	Computer aided design
CM	Cochlear microphonic
CPU	Central processor unit
DAC	Digital to analogue converter
DPOAE	Distortion product otoacoustic emission
DVM	Digital voltage meter
ECoG	Electro-cochleagraphy
ERA	Evoked response audiometry
HL	Hearing level
IHC	Inner hair cell
ID	Internal diameter
IO	Input/output
IOHL	Inorganic hearing loss
MRC	Medical research council
NIHL	Noise induced hearing loss
OAE	Otoacoustic emission
OHC	Outer hair cell
PCB	Printed circuit board
PROM	Programmable read only memory
PST	Post stimulus time

RAM	Random access memory
RMS	Root mean square
SFOAE	Stimulus frequency otoacoustic emission
SOAE	Spontaneous otoacoustic emission
SPL	Sound pressure level
TEOAE	Transient evoked otoacoustic emission
TTS	Temporary threshold shift
VDU	Visual display unit

Component list

IC1	AD574
IC2	74HC32
IC3	74HC08
IC4	ZN439E
IC5	74HCT32
IC6	74HC00
IC7	74HC02
IC8	74HC32
IC9	74HCT688
IC10	74HCT125
IC11	74HC266
IC12	74HCT32
IC13	6116
IC14	74HC32
IC15	74HCT02
IC16	74LS245
IC17	74LS245
IC18	74LS245
IC19	6116
IC20	6116
IC21	74HC573
IC22	74HC573
IC23	74HC573
IC24	74HC573
IC25	74HC182
IC26	74HC181
IC27	74HC181
IC28	74HC181
IC29	74HC181
IC30	74S288
IC31	O515D
SW1	8-way DIL
SILR	8 commoned 8.2K
R1	4.7K
R2	4.7K
R3	4.7K
R4	82K
R5	2.2K
R6	8.2K
R7	8.2K
R8	5.6K
R9	1.6K
R10	4.7R
R11	4.7R
R12	4.7K (near IC17)
R13	4.7K (near IC16)
VR1	5K cermet trimmer
VR2	5K cermet trimmer
VR3	100R cermet trimmer
VR4	100R cermet trimmer
IDC	34-WAY IDC connector
DCON	9-WAY D-type plug (90 degree)
C1	100pF
C2	.47uF
C3	.01uF (near IC25)
C4	.01uF (near IC27)
C5	.01uF (near IC29)
C6	.01uF (near IC24)
C7	.01uF (near IC22)
C8	.01uF (near IC20)
C9	.01uF (near IC18)
C10	.01uF (near IC26)
C11	.01uF (near IC28)
C12	.01uF (near IC19)
C13	.01uF (near IC10)
C14	.01uF (near IC11)
C15	.01uF (near IC12)
C16	.1uF
C17	.1uF
C18	10uF
C19	.1uF
C20	10uF
C21	.47uF
C22	100uF

Component list

U2	74HCT244
U3	74HCT08
U4	74HCT04
U5	74HCT244
U6	74HCT02
U7	74HCT21
IC1	74HC02
IC2	74HC20
IC3	74HC08
IC4	74HCT573
IC5	74HCT573
IC6	74HCT688
IC7	6264
IC8	74HCT245
IC9	74HCT245
IC10	74HCT245
IC11	74HCT32
IC12	74HC02
IC13	74HCT245
IC14	6264
IC15	74HC00
IC16	74HC02
IC17	74HC02
IC18	74HC4017
IC19	74HC4024
IC20	74HC245
IC21	PXO-1000
IC22	74HC4024
IC23	74HC245
IC24	AD667
IC25	74HCT125
IC26	74HC02
IC27	74LS365
SW1	8-WAY DIL
SW2	2-WAY DIL
SILR	8 commoned 8.2K
R1	4.7K
R2	4.7K
R3	4.7K
R4	4.7K
R5	4.7K
R6	47R
R7	12R
VR1	100R cermet trimmer
VR2	100R cermet trimmer
IDC	34-WAY IDC connector
DCON	9-WAY D-type socket (90 degree)
C1	22pF
C2	.01uF (near IC21)
C3	.01uF (near IC19)
C4	.01uF (near IC20)
C5	.01uF (near IC14)
C6	.01uF (near IC17)
C7	.01uF (near IC16)
C8	.01uF (near IC13)
C9	.01uF (near IC7)
C10	.01uF (near IC8)
C11	.01uF (near IC9)
C12	.01uF (near IC2)
C13	.01uF (near IC3)
C14	.01uF (near U4)
C15	.01uF (near U6)
C16	.01uF (near U2)
C17	.01uF (near U3)
C18	10uF
C19	.1uF
C20	.1uF

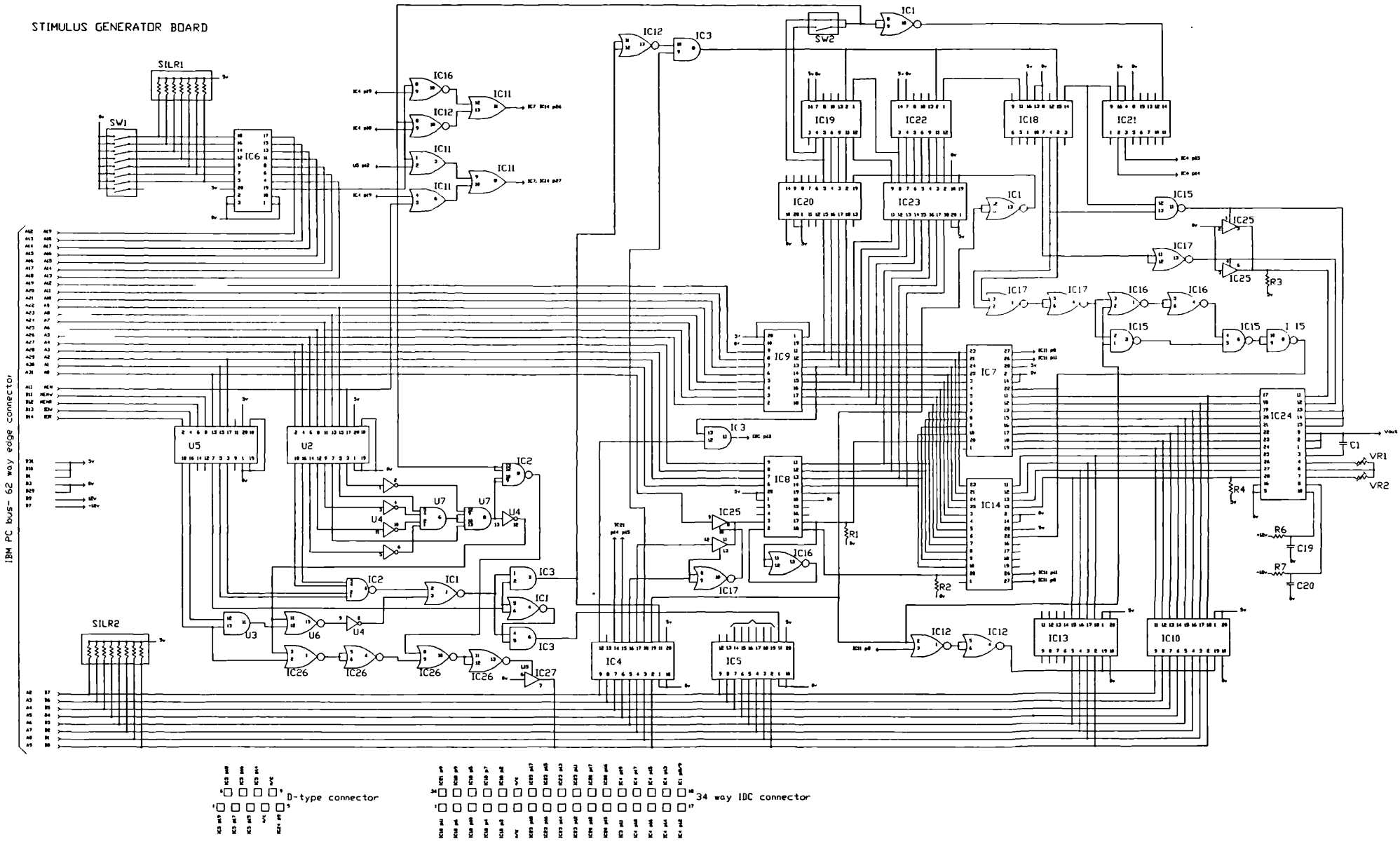
STIMULUS GENERATOR BOARD
IBM PC bus- 62 way edge connector
SW1
SW2
SILR1
SILR2
IC1
IC2
IC3
IC4
IC5
IC6
IC7
IC8
IC9
IC10
IC11
IC12
IC13
IC14
IC15
IC16
IC17
IC18
IC19
IC20
IC21
IC22
IC23
IC24
IC25
IC26
IC27
U1
U2
U3
U4
U5
U6
U7
R1
R2
R3
R4
R6
R7
C1
C19
C20
VR1
VR2
D-type connector
34 way IDC connector

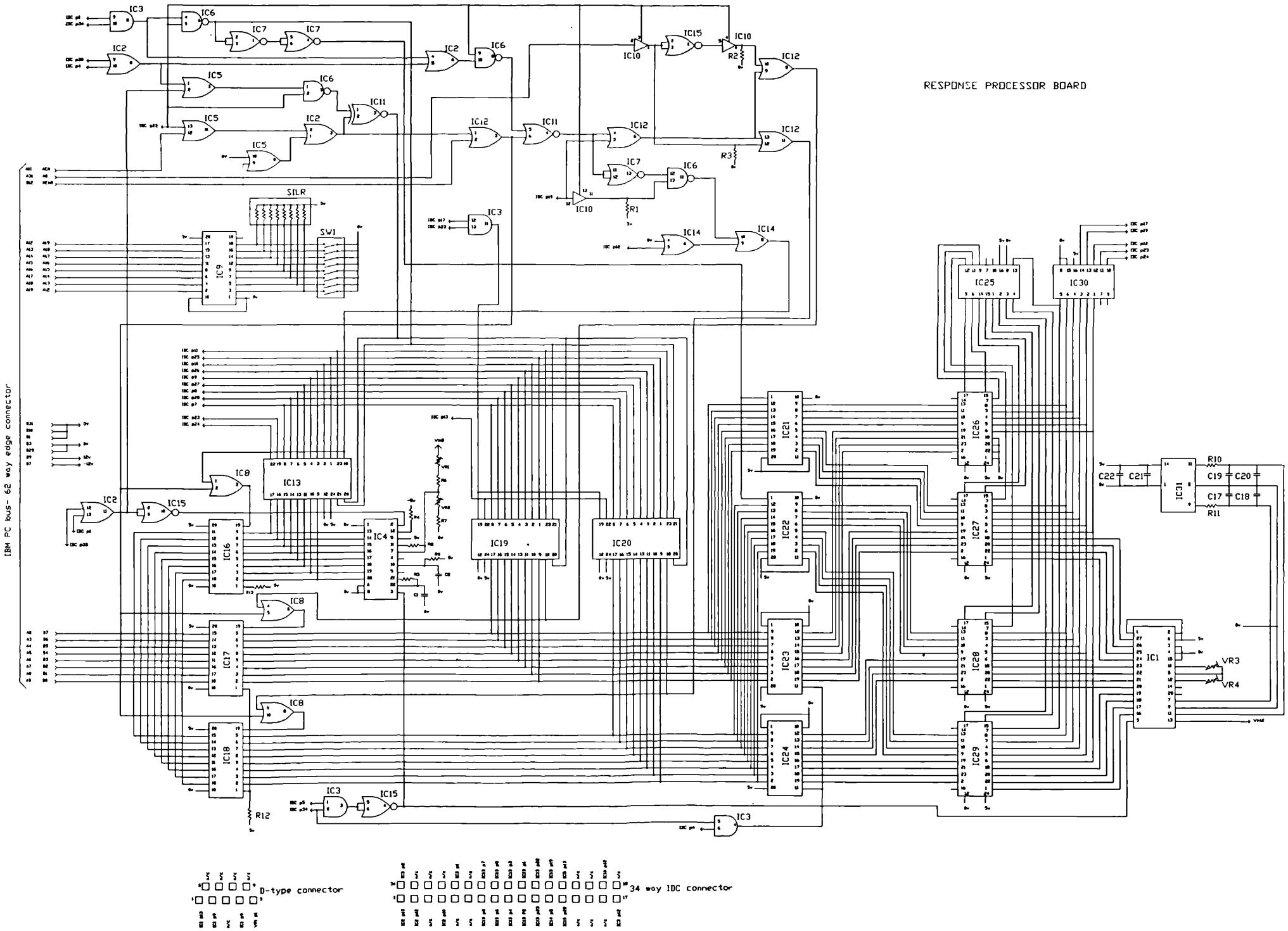
RESPONSE PROCESSOR BOARD
IBM PC bus- 62 way edge connector
D-type connector
34 way IDC connector

ANALOGUE CIRCUITS